ESD-TR-91-176

Technical Report
916

Volume 3: Appendix E

Multifrequency Measurements of Radar Ground Clutter at 42 Sites

Volume 1 contains Principal Results.
Volume 2 contains Appendices A through D.

J.B. Billingsley
J.F. Larrabee

15 November 1991

Lincoln Laboratory

MASSACHUSETTS INSTITUTE OF TECHNOLOGY

LEXINGTON, MASSACHUSETTS

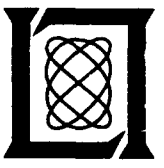

**Prepared for the Department of the Air Force
under Contract F19628-90-C-0002.**

Approved for pubiic release; distribution is unlimited.

This report is based on studies performed at Lincoln Laboratory, a center for research operated by Massachusetts Institute of Technology. The work was sponsored by the Department of the Air Force under Contract F19628-90-C-0002.

The ESD Public Affairs Office has reviewed this report, and it is releasable to the National Technical Information Service, where it will be available to the general public, including foreign nationals.

This technical report has been reviewed and is approved for publication.

FOR THE COMMANDER

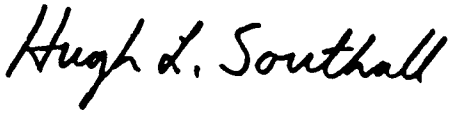

Hugh L. Southall, Lt. Col., USAF
Chief, ESD Lincoln Laboratory Project Office

Non-Lincoln Recipients

PLEASE DO NOT RETURN

Permission is given to destroy this document when it is no longer needed.

MASSACHUSETTS INSTITUTE OF TECHNOLOGY
LINCOLN LABORATORY

MULTIFREQUENCY MEASUREMENTS OF RADAR GROUND CLUTTER AT 42 SITES

J.B. BILLINGSLEY
Group 45
J.F. LARRABEE
Loral Aerospace

TECHNICAL REPORT 916
VOLUME 3: APPENDIX E

15 NOVEMBER 1991

LEXINGTON MASSACHUSETTS

APPENDIX E

TERRAIN DESCRIPTIVE INFORMATION AND CLUTTER MEASUREMENT RESULTS FOR EACH PHASE ONE SITE

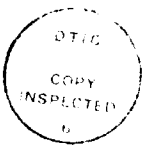

TABLE OF CONTENTS

LIST OF ILLUSTRATIONS

LIST OF ILLUSTRATIONS (Continued)

LIST OF ILLUSTRATIONS (Continued)

LIST OF ILLUSTRATIONS (Continued)

LIST OF ILLUSTRATIONS (Continued)

LIST OF ILLUSTRATIONS (Continued)

LIST OF ILLUSTRATIONS (Continued)

LIST OF ILLUSTRATIONS (Continued)

LIST OF TABLES

E.1 INTRODUCTION

In this appendix, we provide a package of site-specific terrain descriptive and clutter measurement background information for each Phase One measurement site. This information includes terrain photographs, a PPI clutter map showing the location of the repeat sector in the clutter map, a clutter amplitude histogram of a repeat sector measurement, and a plot of repeat sector mean clutter strength versus frequency for each Phase One site, as well as occasional additional information. This information is provided site by site within groups of similar terrain classes in the same order that results are discussed in Section 4 of this report. Thus, the information presented here may be readily kept in view as the discussions in Section 4 proceed. An alternative would have been to include the site-specific information of this appendix directly in Section 4. However, it was judged that to do so would overload Section 4 in that the volume of site-specific information would interfere too much with text continuity and assimilation and overwhelm the more important general information that Section 4 aims for. On the other hand, we believe it is necessary to include in this report some substantial sampling of site-specific information to illustrate the textual discussions and to indicate the scope of our measurement program and of the site-to-site variability of ground clutter. Thus, this relatively large volume of site-specific information is included in this separate appendix, as a companion volume, easily referable as discussions proceed in Section 4.

Table E-1 is a guide showing the site-by-site sequence in which the information is presented in this appendix. Table E-1 also includes the waveforms of the clutter map and the one or more clutter histograms shown for each site as a guide to readers who have interests in particular frequencies, polarizations, or resolutions. The three-letter waveform designation in Table E-1 is in order of frequency (VHF, UHF, L-, S-, or X-band), resolution (T = thin = 15 or 36 m, F = fat = 150 m), and polarization (V = vertical, H = horizontal). The following sections provide brief overview remarks concerning the various kinds of information presented here. The information is then presented in sequential figures following the text.

E.2 TERRAIN DISPLAYS

Terrain photos are provided in this appendix for almost every site. Where they are not provided here, they are provided in the main body of this report. Many of these photos include views of the Phase One measurement equipment on site and views of the terrain in the repeat sector. Also included are many views from the top of the Phase One antenna tower looking in the direction of the repeat sector.

Other terrain displays available are as follows: (1) aerial photography at 1:50,000 scale or our new CIR (Color Infra-Red) photography of repeat sectors at 1:10,000 scale; (2) terrain classification maps of both landform and land cover in repeat sectors, in 1 deg × 150 m cells, based on our new CIR aerial photos; (3) three-dimensional views of the terrain surface at an oblique aspect generated from DMA DTED (digital terrain elevation data); (4) terrain elevation profiles through the repeat sector, also based on DTED; and (5) large-scale topographic maps at 1:25,000 or 1:50,000 scale. Except for maps, examples of all of these kinds of terrain displays are provided in the main body of the report. In this appendix, besides terrain photos, the only other terrain displays we provide are aerial photos for Altona II, Orion, and Rosetown Hill.

TABLE E-1
Guide to Site-by-Site Sets of Figures in Appendix E

	PPI MAP (waveform)	SECTOR DISPLAY	HISTOGRAM(S) (waveform)	FIG. NO's.
URBAN				
Strathcona, Alta.	SFH	•	VTH,LTH	E.1-E.6
Lethbridge W., Alta.	XTH	-	LTH,STV	E.7-E.11
Altona II, Man.	XTH	-	LTH	E.12-E.17
Picture Butte II, Alta.	UFH	-	STV	E.18-E.21
Headingley, Man.	LFH	-	STH	E.22-E.26
MOUNTAINS				
Plateau Mt., Alta.	VTH	-	VTV	E.27-E.30
Waterton, Alta.	UTH	•	VTV	E.31-E.35
FOREST/HIGH-RELIEF (Terrain Slopes > 2°)				
a) High Depression Angle				
Blue Knob, Penna.	XFH	-	VFH	E.36-E.39
Scranton, Penna.	STH	•	VFH	E.40-E.44
b) Low Depression Angle				
Cold Lake, Alta.	VFH	-	UTV	E.45-E.48
Woking, Alta.	STH	•	UTV	E.49-E.53
Penhold II, Alta.	SFH	-	UTV	E.54-E.57
Peace River S.II, Alta.	UTH+5	-	UTV	E.58-E.63
FOREST/LOW-RELIEF (Terrain Slopes < 2°)				
a) High Depression Angle				
Puskwaskau, Alta.	LTH	-	VFH	E.64-E.67
Brazeau, Alta.	UTH	•	VTH,LFH	E.68-E.73
b) Intermediate Dep. Ang.				
Gull Lake W., Man.	See Sect. 2.2.2.1			
Wainwright, Alta.	XTH	•	SFV	E.74-E.78
Turtle Mt., Man.	XFH	-	XFH	E.79-E.82
Katahdin Hill, Mass.	LTH	-	SFV	E.83-E.85
Westlock, Alta.	LTH	-	XFV	E.86-E.89
c) Low Depression Angle				
Sandridge, Man.	XFH	-	XFH	E.90-E.93
Dundurn, Sask.	XFH	-	XFH	E.94-E.97

Continued ...

TABLE E-1 (Continued)
Guide to Site-by-Site Sets of Figures in Appendix E

	PPI MAP (waveform)	SECTOR DISPLAY	HISTOGRAM(S) (waveform)	FIG. NO's.
AGRICULTURAL/HIGH-RELIEF (Terrain Slopes > 2°)				
Plateau Mt., Alta.	VFH	-	LFH	E.98-E.100
Polonia, Man.	LFH	-	LFH	E.101-E.104
Neepawa, Man.	XFH	•	LFH	E.105-E.109
AGRICULTURAL/LOW-RELIEF				
a) Moderately Low-Relief (1° < Terrain Slopes < 2°)				
Beulah, N.D.	UTH	-	VTV	E.110-E.113
Magrath, Alta.	XTH	•	UFV,LFH	E.114-E.118
Beiseker, Alta.	XTH	-	VTV,UTH, LFH,SFH	E.119-E.126
b) Very Low-Relief (Terrain Slopes < 1°)				
Orion, Alta.	LTH	-	LTH	E.127-E.130
Wolseley, Sask.	XTH	-	LTH	E.131-E.134
Rosetown Hill, Sask.	LTH	•	LTH	E.135-E.140
Pakowki Lake, Alta.	XTH	-	LTH,XTV	E.141-E.144
Shilo, Man.	XFH	-	LFH	E.145-E.148
Corinne, Sask.	XFH	-	LTH,SFV	E.149-E.152
DESERT, MARSH, OR GRASSLAND (Few Discretes)				
a High Depression Angle				
Booker Mt., Nev.	XFH	-	UFV	E.153-E.156
Vananda E., Mont.	XTH	•	UFV	E.157-E.161
b) Low Depression Angle				
Knolls, Utah	XTH	-	UFV	E.162-E.165
Big Grass Marsh, Man.	XTH	•	UFV,SFH	E.166-E.171
FOUR REPEAT SECTORS				
Wachusett Mt., Mass.	UTH	•	SFH	E.172-E.175
Cochrane, Alta.	UTH	-	LTV	E.176-E.179
Suffield, Alta.	XTH	-	LFH	E.180-E.183
Spruce Home, Sask.	XTH	-	LFH,XTV	E.184-E.188

Concluded.

E.3 CLUTTER SPATIAL DISPLAYS

Our main display showing how clutter varies spatially is the PPI clutter map, which is a polar display showing cells in which clutter strength exceeds a specified threshold. A PPI clutter map is provided in this appendix for every site (except Gull Lake West, for which see Section 2.2.2.1), for a selected maximum range (usually less than the maximum range to which clutter was recorded), for a selected clutter strength threshold (not necessarily near the noise level), and for a selected set of radar measurement parameters (viz., frequency, pulse length, and polarization). The clutter map is shown in red, and the spatial boundary of the repeat sector in this map is shown as a black outline. The red clutter map is generated from Phase One survey data, usually obtained in 90-deg sectors. These sectors are pieced together on the computer to form the map. At some sites, not all sectors are available (e.g., Shilo, Figure E-46). At other sites, sectors were recorded to different maximum ranges (e.g., Waterton, Figure E-32). Occasionally sector boundaries or data gaps between sectors (e.g., Dundurn, data gap from 45 to 66 deg, Figure E-95) are visible in the red clutter maps. The gaps that occur within the area of the repeat sector itself (e.g., Picture Butte II, Figure E-19) do not represent gaps in the repeat sector experiments upon which this report is based. In the clutter maps, usually red indicates the existence of signal strength above threshold, and white indicates signal strength below threshold; however, occasionally white means above threshold, and red means below. The maps do not discriminate between clutter and noise, so cells in which system noise level,* normalized to $\sigma^\circ F^4$ space, exceeds threshold can also show as clutter. This is usually of little consequence for the maps and thresholds shown; but, for example, see Altona II, Figure E-15. However, in a few clutter maps, spurious rings of clutter (or partial rings in an individual 90-deg experiment) are indicated in the first few range gates around the origin (e.g., Westlock, Figure E-87; Pakowki Lake, Figure E-141). This artifact results from high noise levels at close ranges sometimes occurring when STC dynamic attenuation is used (see Appendix A).

Our other method for showing how clutter varies spatially is as an A-scope sector display, in which mean clutter strength is shown as a function of range through the repeat sector, range gate by range gate, averaged over a specified azimuth interval (usually, the full interval) of the repeat sector. An example of a five-frequency sector display is provided in this appendix for most terrain categories (12 figures in total, see Table E-1). These sector displays are corrected for elevation gain variation on the vertical beam of the antenna, range gate by range gate, using the DTED terrain elevation information along the center azimuth of the repeat sector (recall that antenna boresight is always fixed to be locally horizontal at the Phase One setup position). Where the correction is too great (i.e., too far down on the beam) to be reliable, we delete indicating clutter strength there. When this occurs, it is usually at X- or S-band (i.e., narrow vertical beams, see Table A-6) for relatively high sites and close ranges.†

In the body of this report, for Suffield we show five X-band sector displays for five individual 1-deg beam positions in which no azimuth averaging occurs (see Figure 95). That is, these data show results cell by cell in which the only averaging that occurs is over the 1024 pulses recorded at each cell position.

---

* The noise level depends upon the number of pulses coherently integrated in each cell. In our partially integrated data base, from which these PPI clutter maps were generated, the number of pulses integrated is ≤ 32.

† But see also Figure E-33 (Waterton) for unusual situation where high mountains at farther ranges rise *above* beam.

We utilize these Suffield results as a probe to indicate the presence of a large discrete building on what is otherwise prairie grassland terrain.

E.4 CLUTTER AMPLITUDE DISTRIBUTIONS

In the package of information provided for each site in this appendix, we include one or more examples of histograms of measured clutter strengths over each site's repeat sector. These histograms are discussed in Section 2.2.2.1 of this report. We would need to show 20 such histograms for each site's repeat sector to cover our radar parameter matrix of available measurements. In addition, we typically repeated each of our 20 measurements four times during the time on site. As a result, the totality of repeat sector histograms upon which this report is based constitutes 4465 measured histograms, stored on three magnetic tapes (see Section 6.1). A major purpose of our Phase One clutter measurement program was to measure many such histograms. Thus, we take the opportunity here to show 52 examples of measured clutter strength histograms from repeat sectors. These examples illustrate the large degree of variability that exists among such histograms. This variability reflects the specific nature of the underlying terrain. Our purpose is to reach beyond such specificity to general parametric trends occurring in these histograms. However, the 52 histograms shown here may be regarded as fairly basic examples of what actually occurs at the level of raw clutter strength, for those who would like to see examples from our measurements in relatively unreduced form.

Elsewhere in our studies we have shown clutter amplitude statistics as cumulative distributions rather than histograms. Cumulative distributions have the benefit that a number of them can be shown on one set of axes, that percentile levels in the distribution can be read directly off the ordinate, and that the closeness-of-fit to standard distributions such as Weibull or lognormal can be estimated by the degree of linearity of the distribution when plotted against the corresponding nonlinear ordinate. Here, however, we are not attempting to illustrate that clutter distributions are often Weibull-like or occasionally lognormal-like (although Weibull and lognormal regression coefficients and goodness-of-fit quantities are provided in the table of numbers above each histogram plot for the shadowed histogram including noise samples in the fourth column of numbers and for the shadowless histogram excluding noise samples in the fifth column of numbers). Rather, we choose to concentrate on histograms in the belief that a histogram is a more intuitively meaningful plot and that showing many different histograms together constitutes a useful catalog illustrating how these histograms vary with important parameters characterizing the radar, the geometry, and the terrain. We do have cumulative distribution plots available for all of our histograms both on Weibull and lognormal scales (they are part of our standard clutter patch plot package), but we do not include them in this appendix. We do show several examples of cumulative distributions in the main body of this report (see Figures 57, 58, and 75).

In the histogram plots of clutter amplitude statistics in this appendix, the abscissa, marked "reflectivity (dB)," is more specifically $\sigma^{o}F^{4}$ in units of m^2/m^2, converted to decibels. The total number of samples in the histogram, shown just above and to the right of the histogram box, is the number of range/azimuth resolution cells in the repeat sector times the number of pulse groups per cell from our partially integrated data base (in most of our repeat sector experiments, the total number of pulses per cell is 1024, and the number of integrated pulses within a pulse group in our partially integrated data is ≤ 32, see Appendix A).

In the plotted histograms, noise contamination is shown as black. More specifically, in each 1-dB $\sigma^{\circ}F^4$ bin, noise samples are first accumulated as black, above which the valid clutter samples are binned as white, with the sum of the two comprising the total number of samples in the bin. In addition, bins with 15 percent or more noise samples are doubly underlined; bins containing one or more saturated samples are triply underlined. The noise level in each range gate is determined on the basis of the measured data by means of an algorithm based on 128-point FFT processing in which Doppler cells well removed from the near-zero-Doppler ground clutter regime and which pass criteria for proper Rayleigh-like noise behavior are combined to establish a system noise level in that gate (see Appendix A). Usually, the black noise samples accumulate in the histogram as a well-behaved, roughly bell-shaped distribution; where they do not so accumulate, but instead show a complicated or multimoded distribution (e.g., Cochrane, Figure E-178), is often indicative of data collected with STC attenuation.

The numbers that are in the table at the top of each histogram will now be defined. The second line in the table is terrain classification information [see Section 2.3; also, TC = tree cover,* DA = depression angle (deg), DAC = depression angle correction (dB)]. Below that, in the first three columns of numbers on the left, the first four numbers in each column are the moments of the distribution, i.e., mean, standard deviation, and coefficients of skewness (COS) and kurtosis (COK, see Appendix C). The following two numbers in each column are derivative quantities depending on the moments. The moments are shown computed three ways in the first three columns, as shadowed upper bounds in the first column (black noise samples get the measured noise-level values), shadowed lower bounds in the second column (black noise samples get zero power values), and shadowless in the third column (black noise samples are left out of the computation). The next two columns of numbers show regression and goodness-of-fit coefficients to Weibull and lognormal distributions. The last column of numbers on the right shows the maximum and minimum values of clutter strength in the histogram [SIG(MAX) and SIG(MIN)], as well as the maximum and minimum values of saturated samples [SAT(MAX) and SAT(MIN)] and noise samples [NOI(MAX) and NOI(MIN)] in the histogram (default = 999). Below that are percentile levels in the histogram, 50 (or median), 70, 90, and 99, first in the shadowed histogram including noise samples and second in the shadowless histogram excluding noise samples. Almost all of the clutter strength attributes, including moments and percentiles, in the table above each histogram plot are based on computations in which clutter strengths are in linear units of m^2/m^2, but each attribute after computation is subsequently converted to decibels (see Appendix C). Exceptions to this are the bottom four numbers in the first and third columns of numbers, which are the first four moments of the shadowed and shadowless distributions, respectively, when each individual sample of clutter strength is kept in decibels units throughout the computations of moments; such nonlinear (i.e., logarithmic) adjunct information is occasionally useful when treating the distributions as lognormal.

The most important attribute of each histogram shown in this appendix is the shadowed upper bound mean strength in the histogram, shown as the topmost number in the far left column of numbers and indicated in the plot as a vertical dashed line. Although many of our histograms appear to show a large number of black noise samples, their effect on mean strength is usually beyond the second decimal place.

---

* TC = 0, 8, 1, 2, 3, 4, 5 corresponds to the percent of tree cover = 0, 1 to 3, 4 to 10, 11 to 30, 31 to 50, >50, unknown, respectively.

The true mean lies between our upper bound approximation to the mean, i.e., top number in the first or far left column of numbers, and our lower bound approximation to the mean, i.e., top number in the second column of numbers. These bounds are usually identical to two decimal places, not only for the mean but for the other moments as well. Most of our clutter computations in this report (see Appendices C and D) were made on the basis of 128-pulse integration, not the ≤ 32-pulse integration for which it is convenient to show plotted histograms from our repeat sector clutter patch tapes in this appendix; the additional integration usually resulted in considerably fewer noise samples. We largely disregard the shadowless mean strength (top number in the third column of numbers) of the distribution excluding noise samples in this report because it is dependent on radar sensitivity. A radar of theoretically infinite sensitivity would give a single value of mean strength somewhere between our shadowed upper and lower bounds. However, the shadowless mean may be used to compute the total percent of noise samples in the histogram (otherwise not shown in the histogram plots here) as: shadowless mean in decibels minus lower bound mean in decibels is equal to $10 \log_{10} (N/N_c)$, where N is the total number of samples in the histogram, N_c is the number of samples above radar noise level, so the percent of noise samples in the histogram is $100 (N-N_c)/N$ (see Appendix C).

We have shown that the mean strength in the shadowed histogram including noise samples, plotted as a vertical dashed line, is not dependent or degraded by the black noise contamination in the histogram. The 50-, 70-, 90-, and 99-percentile levels in the shadowed distribution including noise samples are also shown plotted in the histogram as vertical dotted lines proceeding, respectively, left to right. To the extent that these dotted percentile levels in the shadowed distribution occur to the right of the black noise contamination, they also are unaffected by the noise because they only indicate the relative number of samples above or below their level. If noise does exist at or to the right of a percentile level, then that percentile level constitutes an upper bound to the true percentile level in the histogram that would be measured by a radar of infinite sensitivity. Percentile levels in the shadowless distribution excluding noise samples are very dependent on the amount of noise contamination and are not indicated in the histogram.

E.5 MEAN CLUTTER STRENGTH VERSUS FREQUENCY

We include in this appendix a plot of mean clutter strength versus frequency as measured by Phase One at each measurement site. The mean strengths shown in these plots are applicable for one selected spatial macroregion or patch at each site, our so-called repeat sector patch. The boundaries of the repeat sector patch at each site are shown in the clutter map included in the information presented for each site in this appendix. For each site, the plot of mean strength versus frequency typically includes 20 different data points, one for each combination of radar parameters across our 20-element radar parameter matrix (i.e., five frequencies, two polarizations, two resolutions). Each of these 20 data points comes from its own histogram of repeat sector measured clutter strengths, one or more examples of which are included for each site. Thus, each data point plotted in our plots of mean clutter strength versus frequency comes from a well-calibrated, repeatable measurement (i.e., each measurement is centrally selected from four or more repetitions), unaffected by sensitivity limitations or radar noise contamination (i.e., tight upper and lower bounds to mean strength, usually identical to two decimal places).

As these plots of mean clutter strength versus frequency in this appendix are perused, it is usually observed that the manner in which mean strength varies with frequency is relatively complex and quite specific to each site. Depending on which site we are at, we may observe mean clutter strength to decrease strongly with increasing frequency (e.g., Waterton, Figure E-35), to increase strongly with increasing frequency (e.g., Corinne, Figure E-152), or to show very little variation at all with changes in frequency (e.g., Wainwright, Figure E-78). The major purpose of this report is to attempt to make some general sense of these highly site-specific variations. The variation of mean clutter strength versus frequency for the repeat sector at each Phase One measurement site, as plotted here, is discussed and interpreted in Section 4 in this report. Also embedded in these plots of mean strength versus frequency are variations with polarization and pulse length. As with frequency, these variations with polarization and pulse length are complex, highly site-specific, and difficult to generalize or easily comprehend. We also at least bring some statistical order to variations with polarization and pulse length in the main body of this report. It is clear from these plots of multifrequency mean strength that clutter measurements at any one site or frequency are insufficient to fully understand ground clutter, and one value of having many plots is to indicate how variable ground clutter is and why its proper characterization has required a major multisite measurement exercise.

The mean strengths plotted in the figures of mean strength versus frequency in this appendix are identical to those tabulated in Tables D-2 through D-6 in Appendix D. Almost all of these results are based on 128-point coherent integration in our pulse-by-pulse data; whereas, the example histograms in this appendix are based on ≤ 32-point coherent integration in our partially integrated data. Thus, there may be occasional minor differences between the histogram value of mean strength and the corresponding value plotted in the multifrequency mean strength figure, although these differences are usually $<<$ 1 dB. Occasionally, there are missing data points in the mean strength versus frequency figures in this appendix. Comments in the captions of the figures provide some information on missing data and other caveats. More information on missing data is provided in Tables D-2 through D-6 and in Table A-25, which indicate how individual sites fit chronologically into sequences of sites with particular hardware problems. In these plots of mean strength versus frequency, sites that were revisited to establish seasonal variations (see Table D-1) show mean strengths for each visit, in which visit number is indicated by numerical superscript.

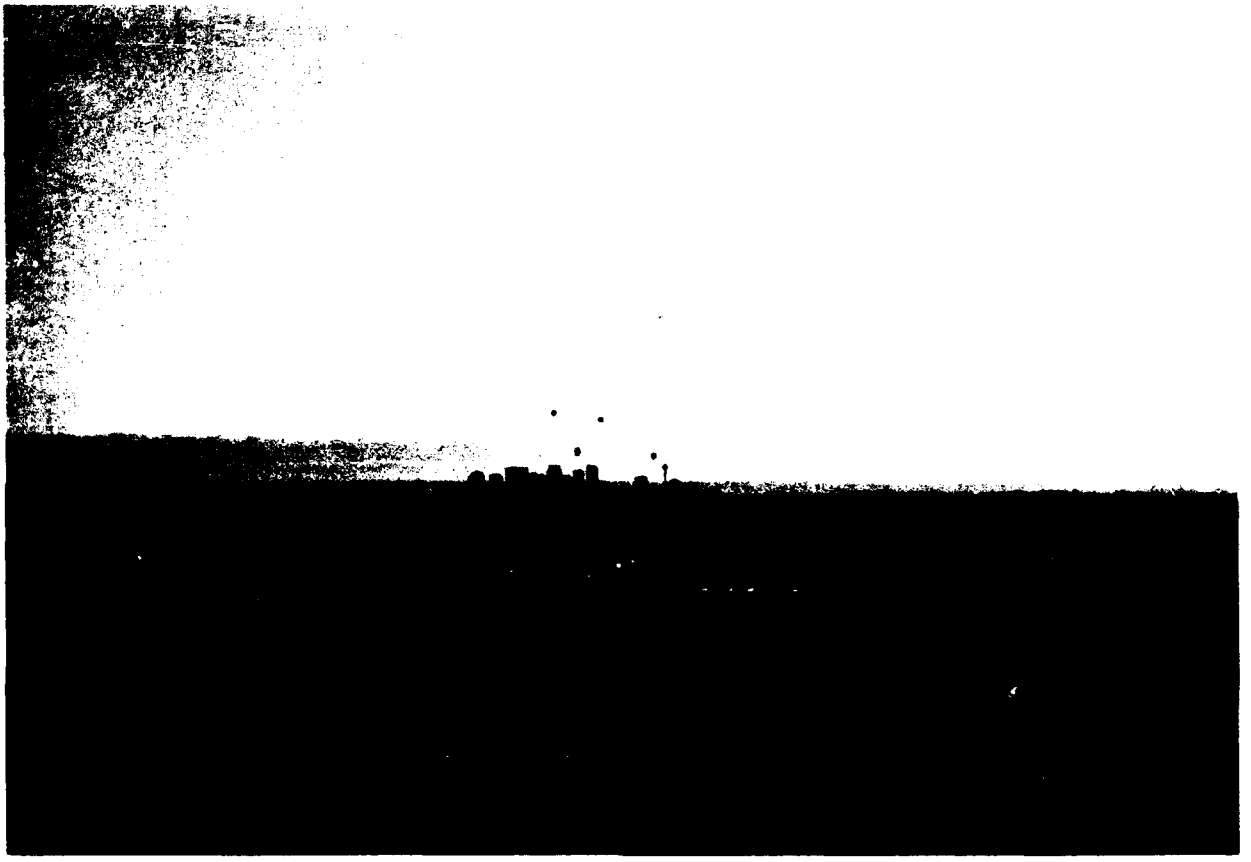

Figure E-1 Strathcona repeat sector. View into repeat sector from site center, down grassy 5-deg slope to city center of Calgary

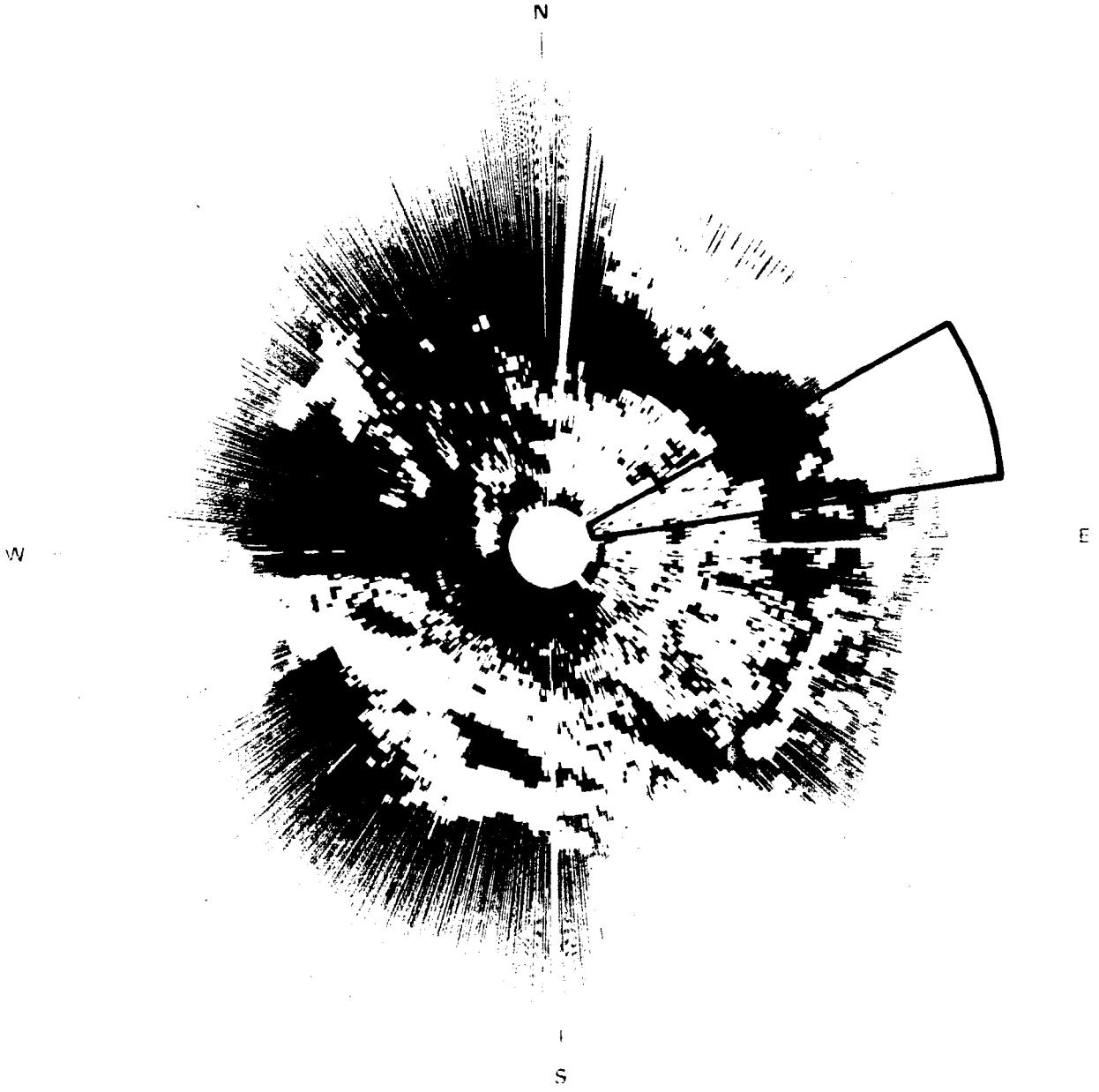

Figure E-2. PPI clutter map and repeat sector at Strathcona. Repeat sector is outlined in black. Maximum range = 11 km; S-band, 150-m pulse, horizontal polarization; nominally, cells with $\sigma^{o}F^{4} \geq -50$ dB are white, but precise threshold is unknown due to uncertain calibration in these particular data.

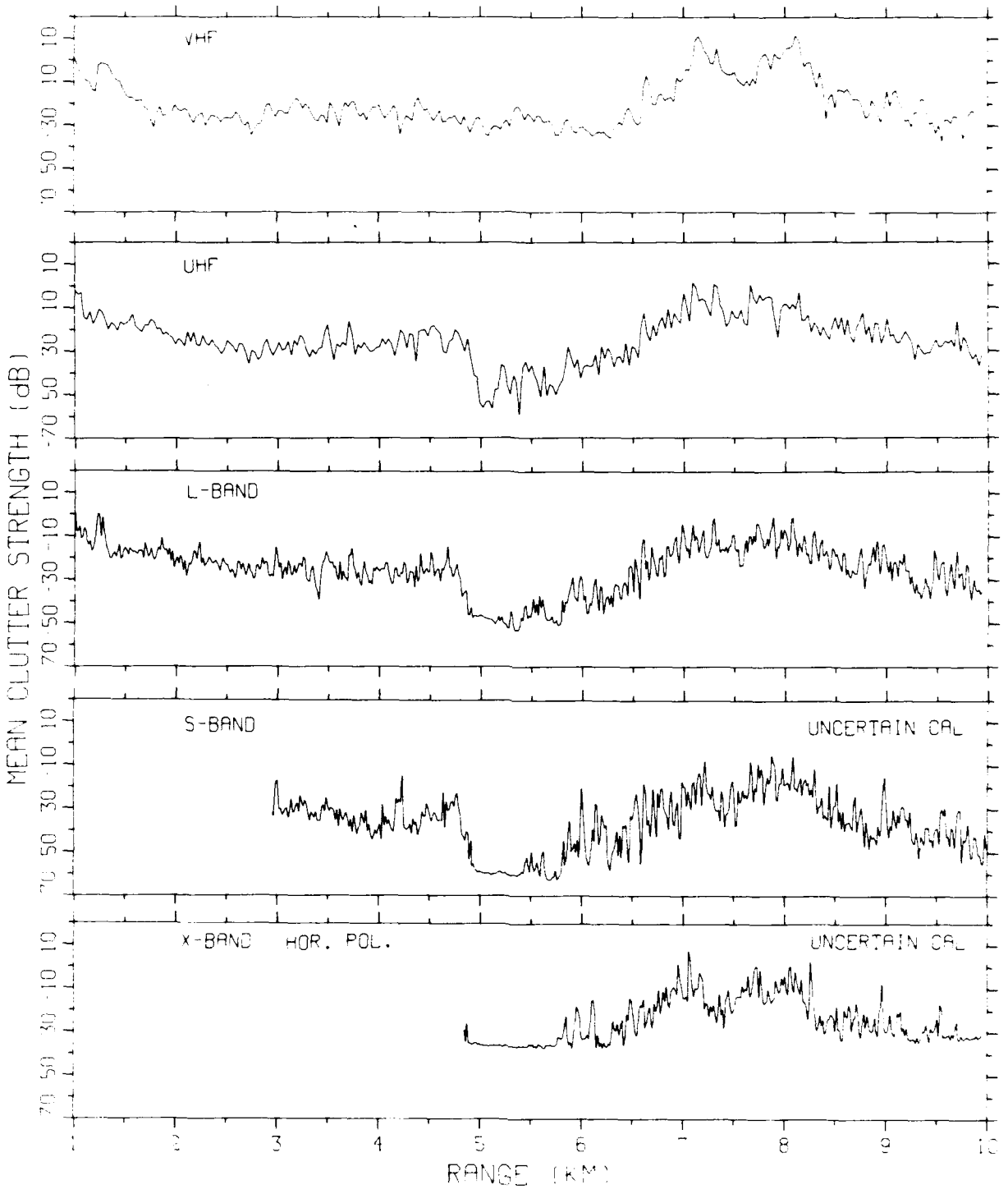

Figure E-3. Mean clutter strength versus range at Strathcona. Repeat sector data. Vertical polarization except X-band. 15/36-m pulse length. Data shown range gate by range gate, averaged in azimuth over 20 deg.

SITE = STRATHCONA RDF = RVTH02.RDF;1

LC = 11 12 51 LF = 3 2 TC = 1 DA = 1.51 DAC = 0.0 PN = R99 DATE = \~ < &

-I-

	SHOWUB	SHOWLB	SHOLSS		SHOW	SHOLSS			
MEAN	-0.77	-0.78	1.93	WEIB0	0.411E+00	0.276E+00	SIG(MAX)		18
SD	6.73	6.73	8.02	WEIB1	0.194E-01	0.256E-01	NOI(MAX)		-15
COS	9.93	9.92	8.55	WEIR2	0.993E+00	0.996E+00	SAT(MAX)		999
COK	20.63	20.63	17.94	WEISS	0.707E-02	0.634E-02	SIG(MIN)		-52
SPOL	-999.00	-999.00	-999.00	LOGB0	0.104E+01	0.775E+00	NOI(MIN)		-64
SPOR	8.21	8.22	7.05	LOGB1	0.454E-01	0.534E-01	SAT(MIN)		999
DBME	-20.52		-12.34	LOGR2	0.977E+00	0.987E+00	50	-23.0	-15.0
DBSD	12.58		10.89	LOGSS	0.130E+00	0.106E+00	70	-17.0	-8.0
DBCOS	0.69		0.67				90	-2.0	4.0
DBCOK	3.28		2.81				99	13.0	15.0

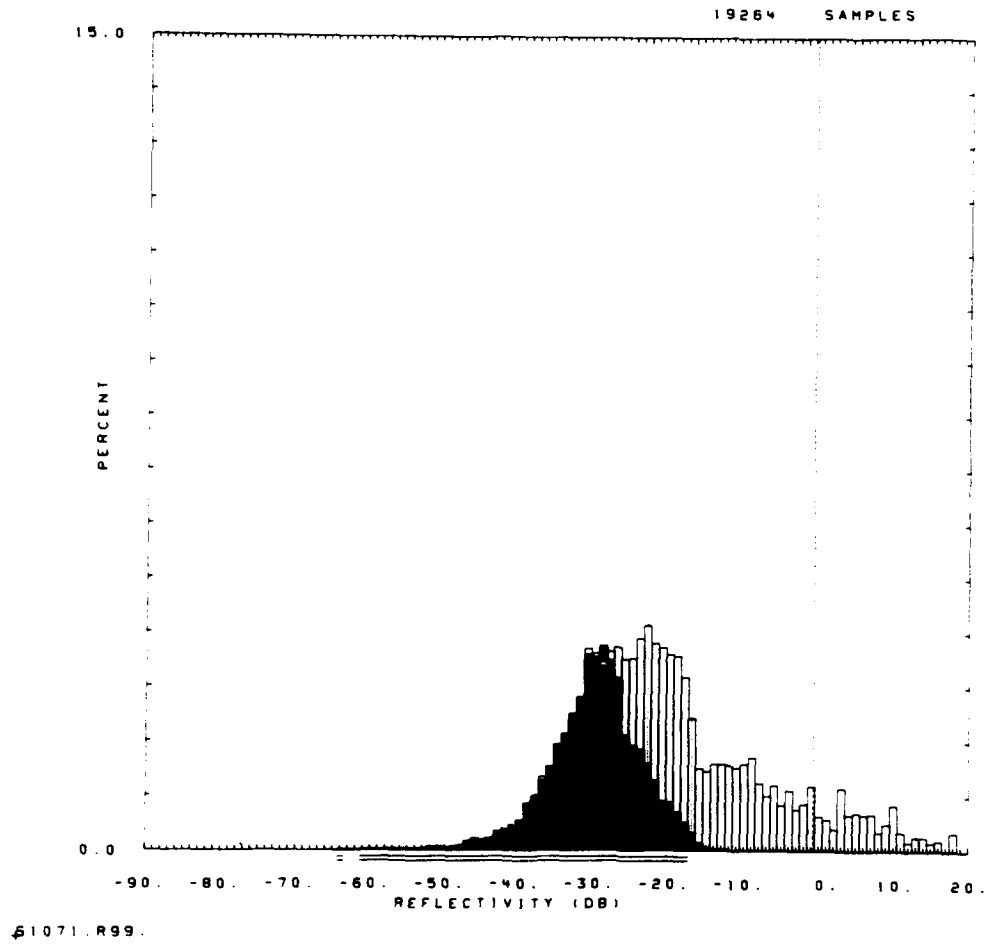

Figure E-4. Clutter strength histogram for Strathcona repeat sector, VHF, 36-m pulse, horizontal polarization.

SITE = STRATHCONA RDF = RLTH10.RDF;1

LC = 11 12 51 LF = 3 2 TC = 1 DA = 1.50 DAC = 0.68 PN = R99 DATE = 13-SEP-

	SHDWUB	SHDWLB	SHDLSS		SHDW	SHDLSS			
MEAN	-13.55	-13.55	-12.83	WEIB0	0.735E+00	0.730E+00	SIG(MAX)		13
SD	-3.29	-3.29	-2.93	WEIB1	0.252E-01	0.275E-01	NOI(MAX)		-33
COS	13.90	13.90	13.54	WEIR2	0.993E+00	0.988E+00	SAT(MAX)		999
COK	28.81	28.81	28.10	WEISS	0.160E-01	0.330E-01	SIG(MIN)		-71
SPDL	-999.00	-999.00	-999.00	LOGB0	0.176E+01	0.173E+01	NOI(MIN)		-80
SPDR	10.65	10.65	10.32	LOGB1	0.538E-01	0.567E-01	SAT(MIN)		999
DBME	-31.31		-28.45	LOGR2	0.999E+00	0.999E+00	50	-32.0	-30.0
DBSD	11.84		10.34	LOGSS	0.939E-02	0.711E-02	70	-26.0	-24.0
DBCOS	0.34		0.64				90	-15.0	-14.0
DBCOK	3.01		3.08				99	-2.0	-1.0

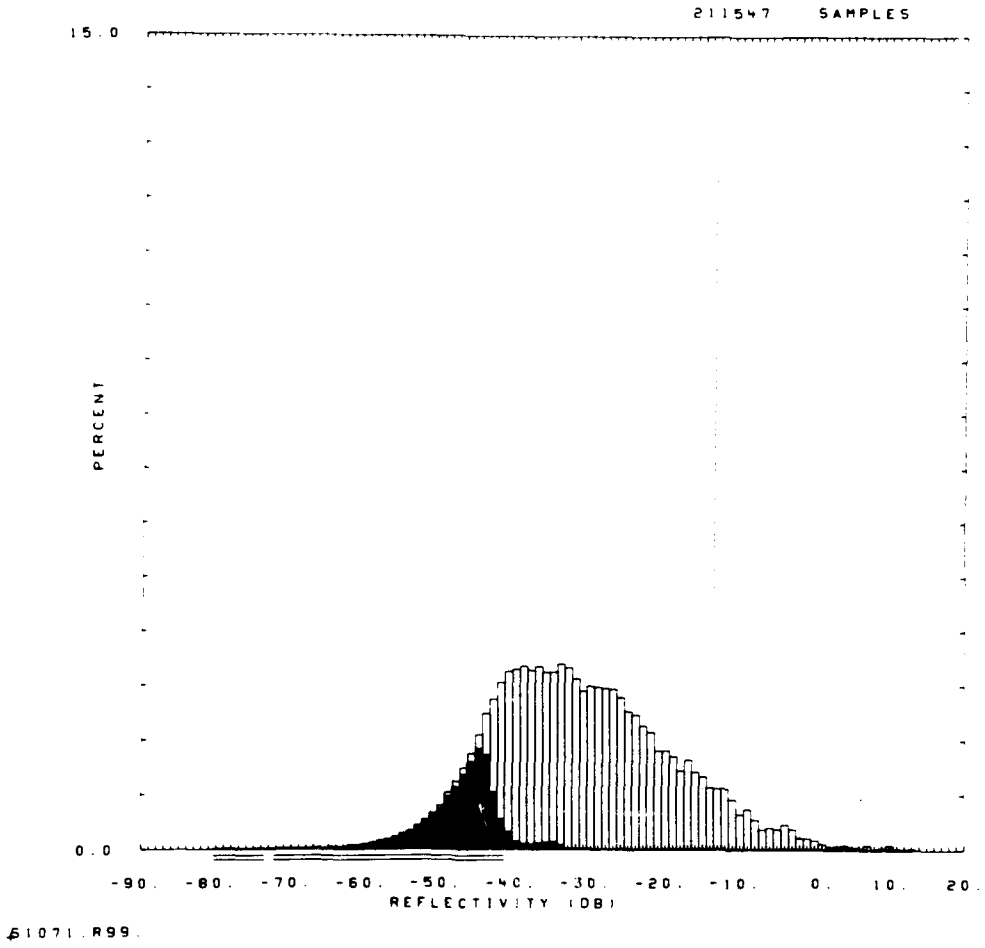

S1071.R99.

Figure E-5. Clutter strength histogram for Strathcona repeat sector, L-band, 15-m pulse, horizontal polarization.

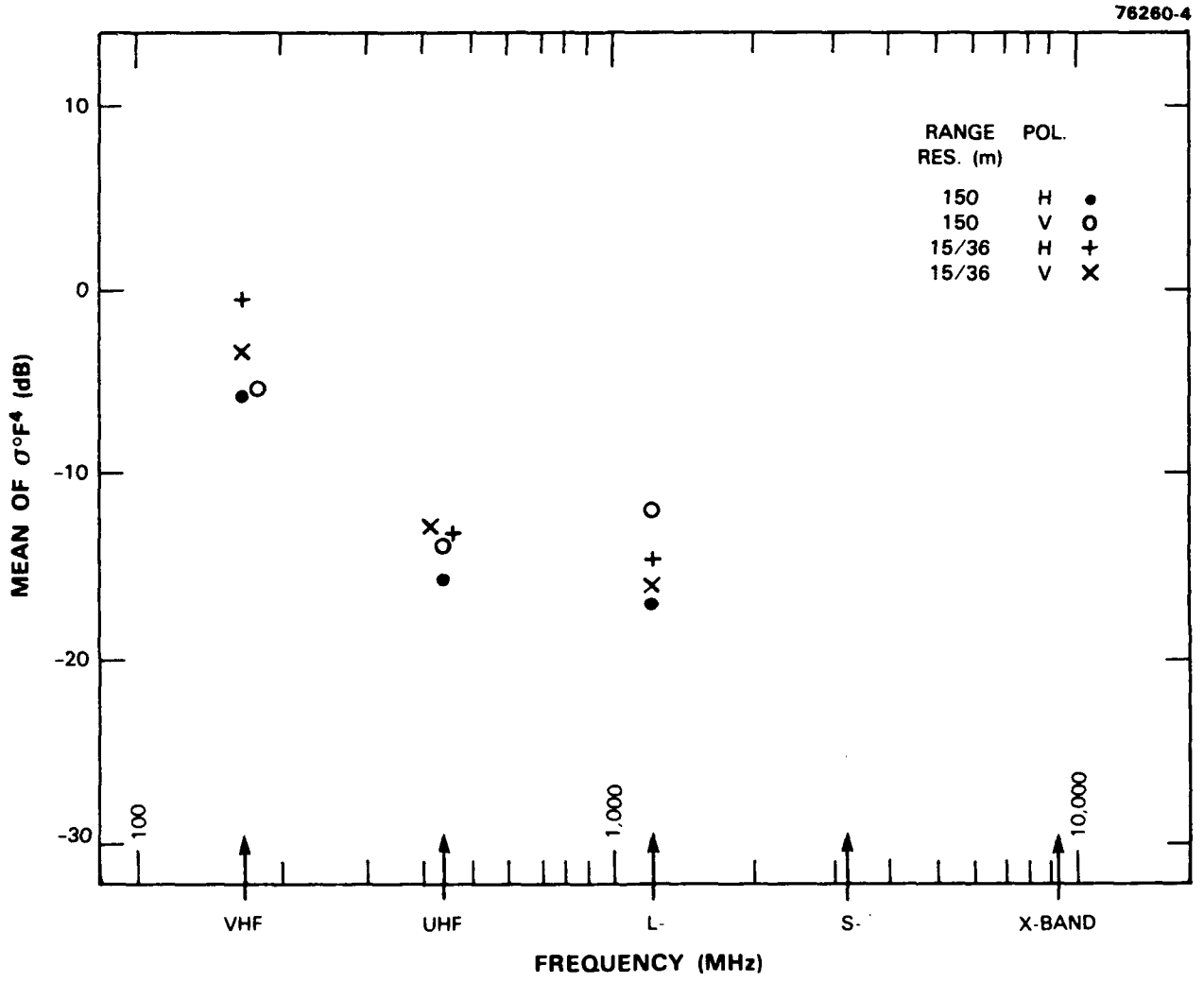

Figure E-6. Mean clutter strength versus frequency at Strathcona. For the Strathcona repeat sector, depression angle = 1.5 deg, landform = 3-2, land cover = 11-12-51, range = 1 to 10 km, azimuth = 62 to 82 deg. Comment: Hardware problems precluded useful data collection at both X- and S-bands.

ESE

(a)

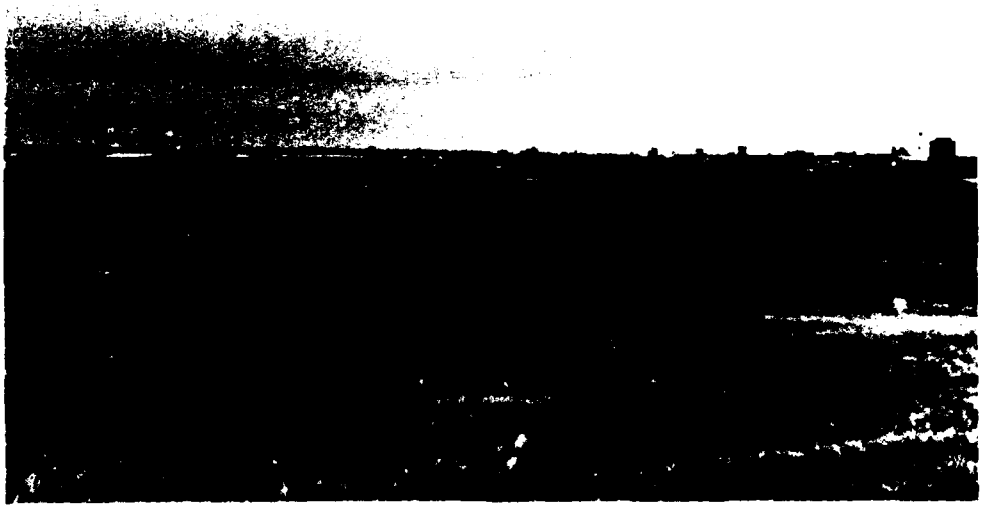

(b)

Figure F-7. Repeat sector at Lethbridge West: (a) Tower-top view looking ESE into repeat sector. Buildings of Lethbridge visible on distant horizon and (b) beginning of repeat sector at 7 km range looking east across steep gullied slopes of Oldman River to outskirts of Lethbridge.

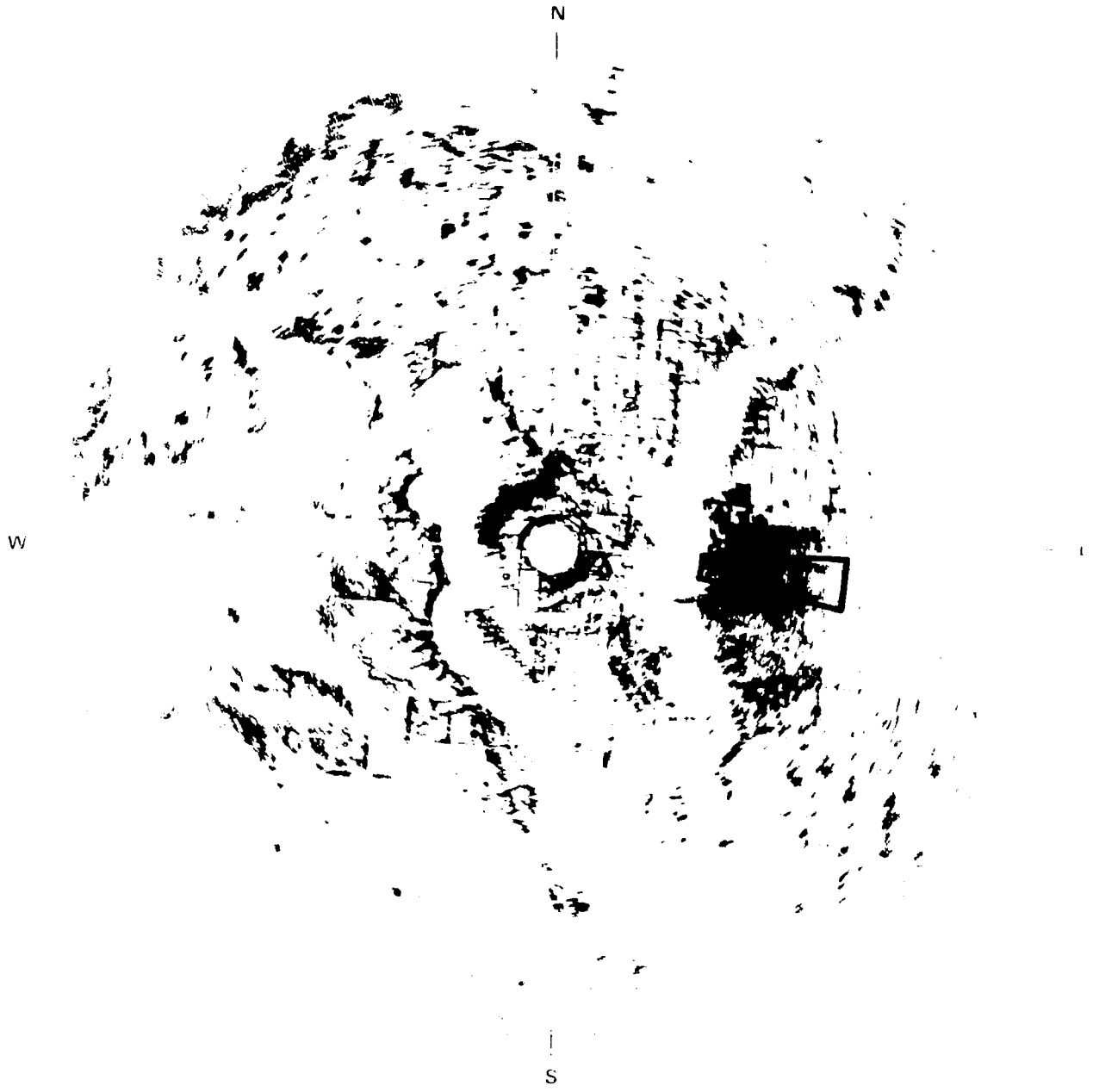

Figure E-8. PPI clutter map and repeat sector at Lethbridge West. Repeat sector is outlined in black. Maximum range = 20 km; X-band, 15-m pulse, horizontal polarization; cells with $\sigma^{\circ}F^{4} \geq -40$ dB are red.

SITE = LETHBRIDGE WEST RDF = RLTH10A.RDF:1

LC = 11 12 21 LF = 3 8 TC = 0 DA = 0.23 DAC = 0.01 PN = R99 DATE = 12-MAY-83

	SHDWUB	SHDWLB	SHDLSS		SHDW	SHDLSS			
MEAN	-5.17	-5.18	-1.77	WEI80	0.593E+00	0.484E+00	SIG(MAX)		24
SD	7.88	7.88	9.58	WEI81	0.183E-01	0.250E-01	NOI(MAX)		-20
COS	15.58	15.58	13.87	WEIR2	0.969E+00	0.941E+00	SAT(MAX)		999
COK	31.57	31.57	28.16	WEISS	0.325E-01	0.116E+00	SIG(MIN)		-67
SPOL	-999.00	-999.00	-999.00	LOGBO	0.148E+01	0.123E+01	NOI(MIN)		-81
SPOR	13.26	13.27	11.66	LOGB1	0.452E-01	0.541E-01	SAT(MIN)		999
DBME	-26.09		-17.39	LOGR2	0.986E+00	0.976E+00	50	-27.0	-19.0
DBSD	10.98		8.58	LOGSS	0.892E-01	0.215E+00	70	-21.0	-15.0
DBCOS	0.36		0.59				90	-13.0	-6.0
DBCOK	3.80		5.50				99	4.0	8.0

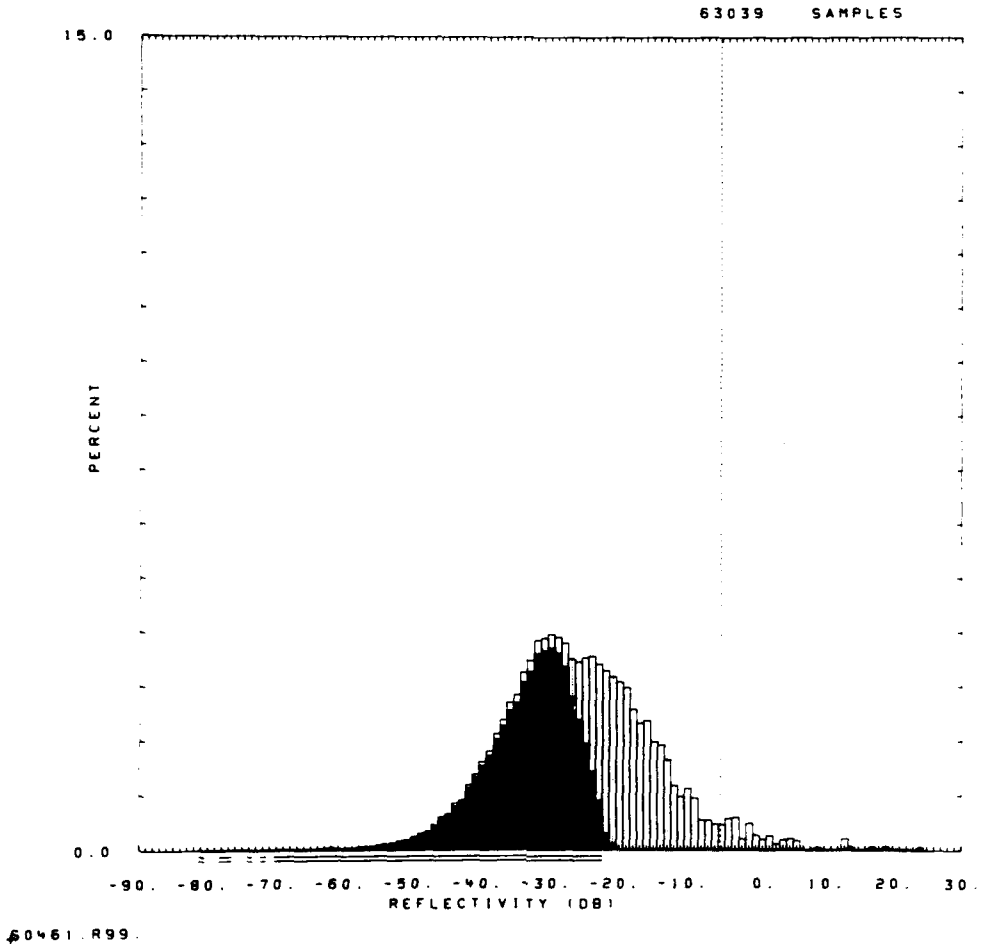

Figure E-9. Clutter strength histogram for Lethbridge West repeat sector. L-band, 15-m pulse, horizontal polarization. RF preamplifier bypassed to avoid excessive saturation. Three tower sections.

SITE = LETHBRIDGE WEST RDF = RSTV13A.RDF;1

LC = 11 12 21 LF = 3 8 TC = 0 DA = 0.28 DAC = 0.07 PN = R99 DATE = 05-MAY-83

	SHDWUB	SHDWLB	SHDLSS		SHDW	SHDLSS			
MEAN	-10.03	-10.03	-6.27	WEIB0	0.649E+00	0.552E+00	SIG(MAX)		16
SD	1.04	1.04	2.90	WEIB1	0.157E-01	0.221E-01	NOI(MAX)		-26
COS	13.70	13.70	11.82	WEIR2	0.977E+00	0.947E+00	SAT(MAX)		999
COK	28.08	28.08	24.32	WEISS	0.226E-01	0.106E+00	SIG(MIN)		-74
SPDL	-999.00	-999.00	-999.00	LOGB0	0.162E+01	0.136E+01	NOI(MIN)		-85
SPOR	11.39	11.39	9.66	LOGB1	0.387E-01	0.474E-01	SAT(MIN)		999
DBME	-32.38		-22.97	LOGR2	0.989E+00	0.980E+00	50	-34.0	-24.0
DBSD	11.23		9.74	LOGSS	0.649E-01	0.174E+00	70	-28.0	-20.0
DBCOS	0.68		0.63				90	-18.0	-11.0
DBCOK	4.25		5.12				99	3.0	7.0

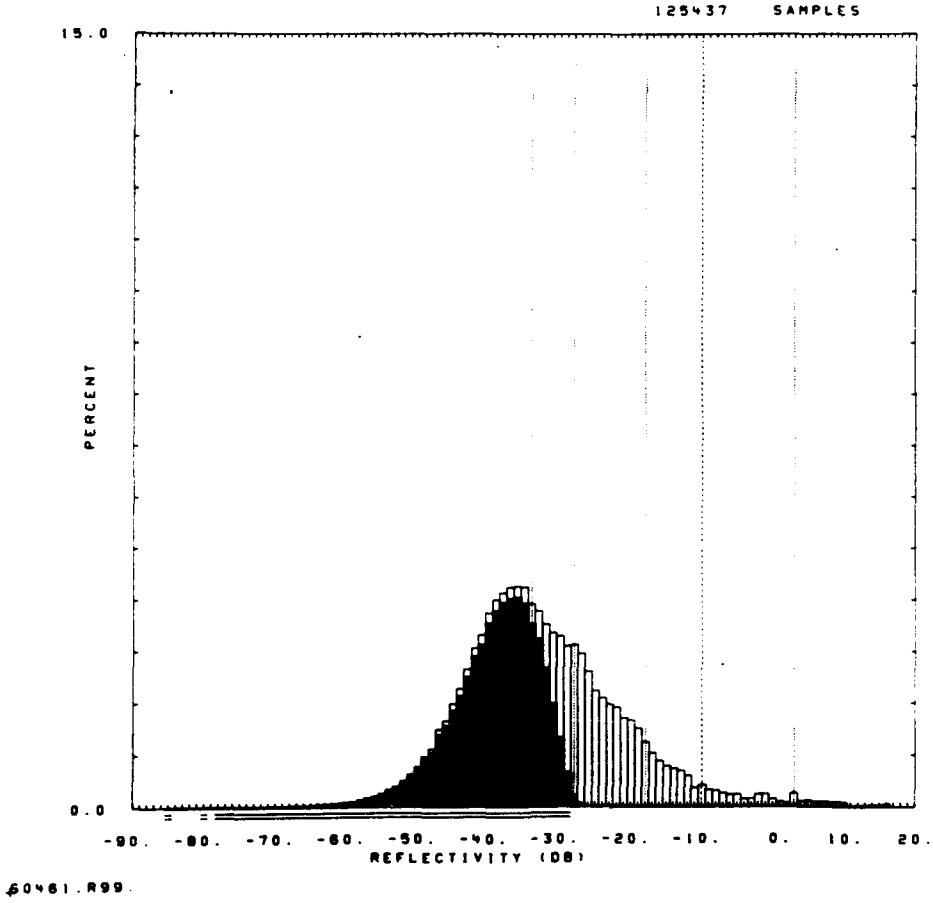

Figure E-10. Clutter strength histogram for Lethbridge West repeat sector. S-band, 15-m pulse, vertical polarization. RF preamplifier bypassed to avoid excessive saturation. Three tower sections.

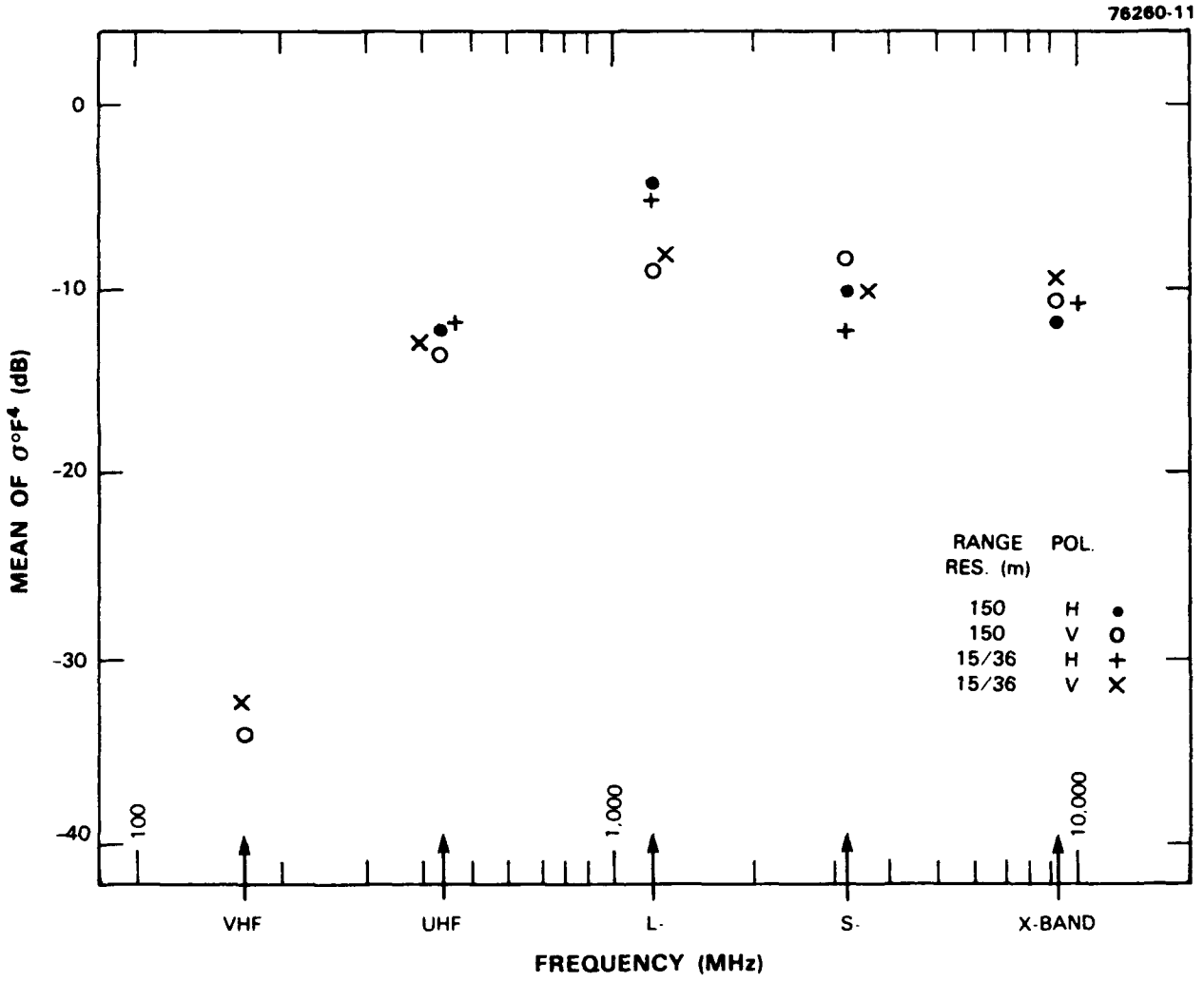

Figure E-11. Mean clutter strength versus frequency at Lethbridge West. For the Lethbridge West repeat sector, depression angle = 0.3 deg, landform = 3-8, land cover = 11-12-21, range = 6 to 11.9 km, azimuth = 92 to 102 deg. Comments: (1) VHF data limited to vertical polarization because of stuck polarization switch. (2) Interference may have slightly affected VHF data shown.

Figure I-12. Altona II repeat-sector. Looking west from Phase One 106 ft tower. Set up in village of Horndean visible in foreground. Grain elevators in village of Plum Coulee in repeat sector at 8 km range visible on horizon.

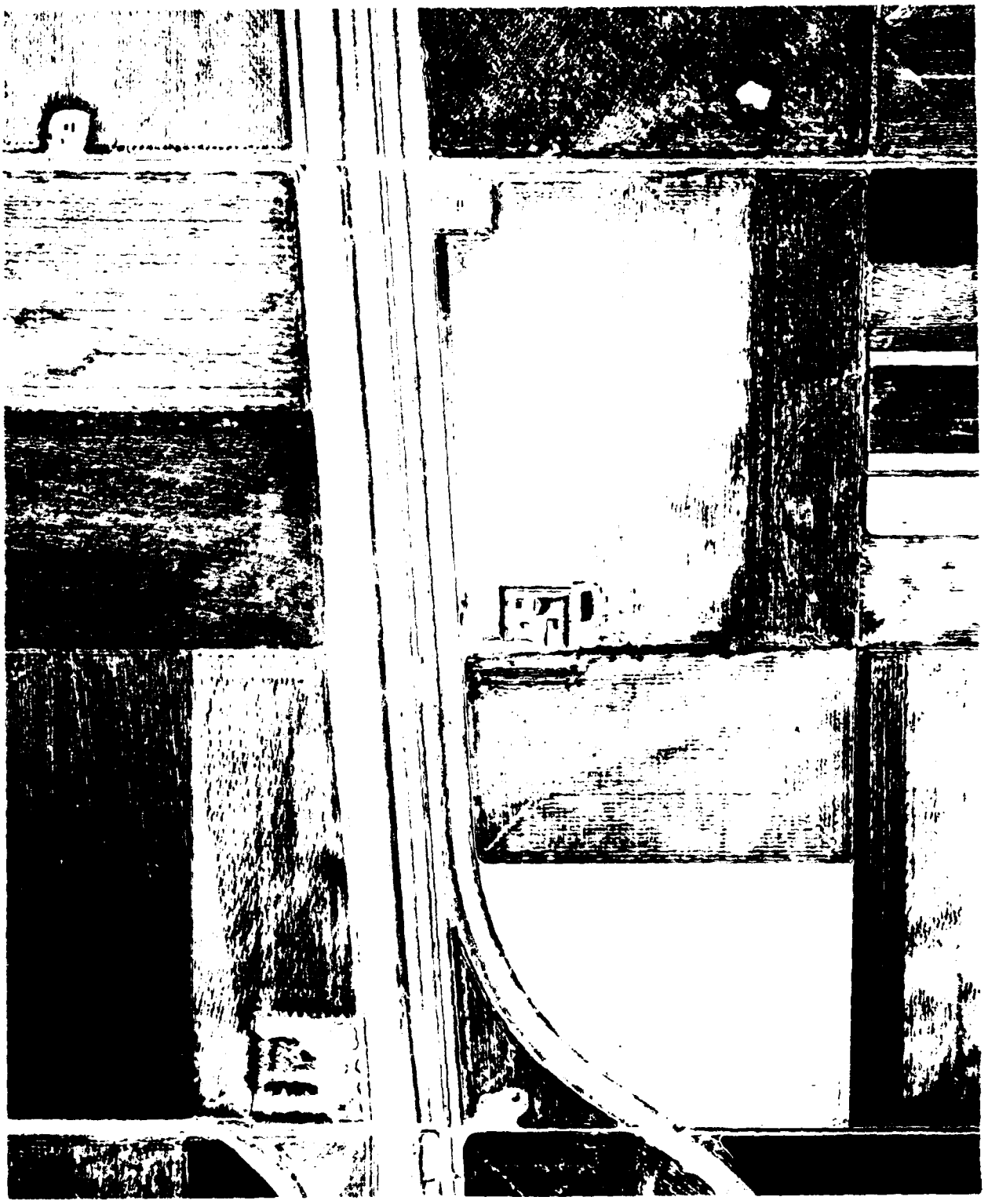

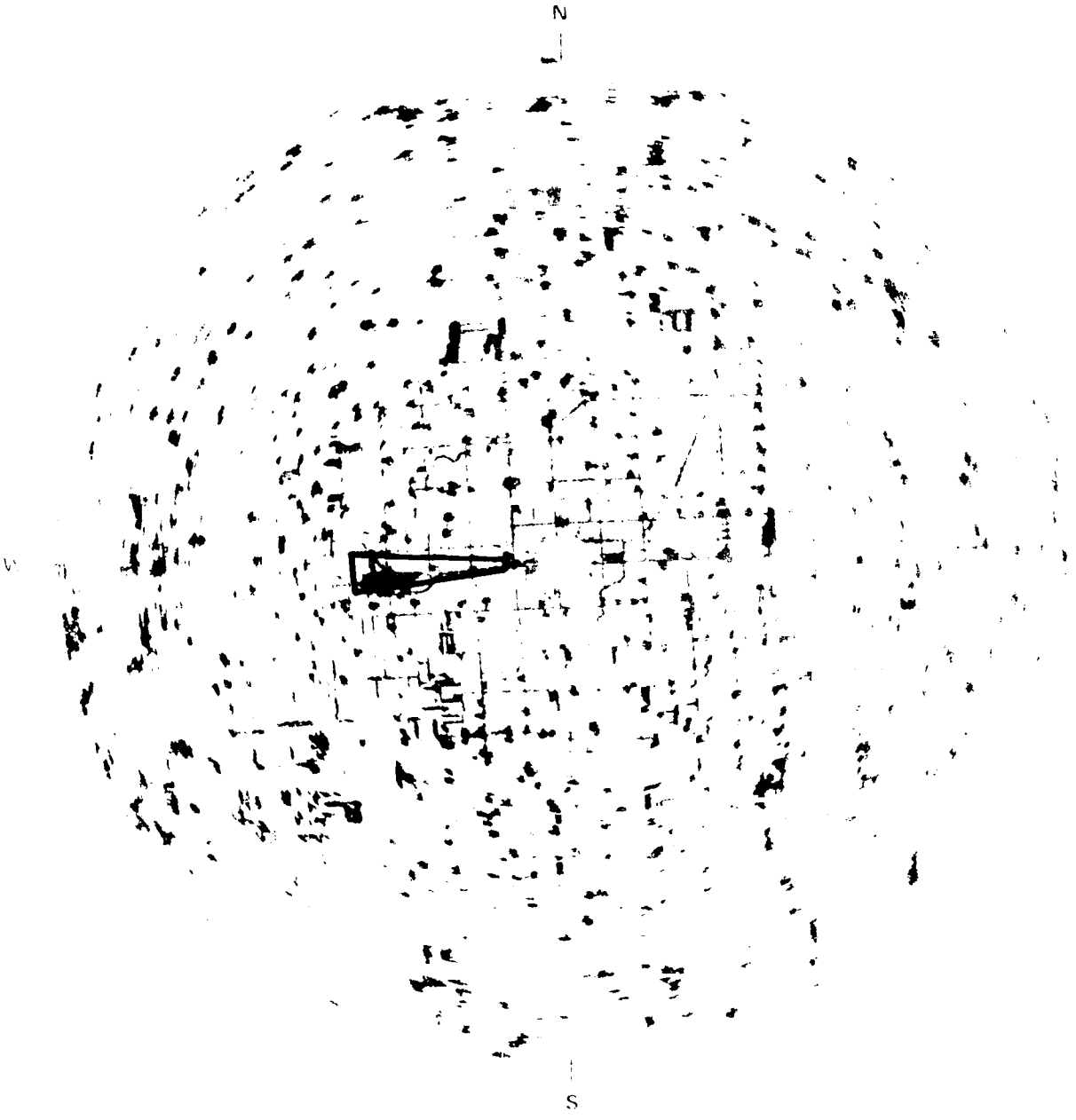

Figure E-15. PPI clutter map and repeat sector at Altona II. Repeat sector is outlined in black. Maximum range = 20 km; X-band, 15-m pulse, horizontal polarization; cells with $\sigma^{\circ}F^{4} \geq -45$ dB are red.

SITE = ALTONA II RDF = RLTH10.RDF;1

LC = 21 11 14 LF = 1 0 TC = 0 DA = 0.21 DAC = 0.01 PN = R99 DATE = 14-JAN-84

	SHDWUB	SHDWLB	SHDLSS		SHDW	SHDLSS			
MEAN	-10.35	-10.35	-7.56	WEIB0	0.670E+00	0.628E+00	SIG(MAX)		11
SD	-0.38	-0.38	0.99	WEIB1	0.157E-01	0.237E-01	NOI(MAX)		-44
COS	10.58	10.58	9.14	WEIR2	0.958E+00	0.909E+00	SAT(MAX)		999
COK	21.41	21.41	18.57	WEISS	0.142E+00	0.738E+00	SIG(MIN)		-81
SPDL	-999.00	-999.00	-999.00	LOGB0	0.164E+01	0.148E+01	NOI(MIN)		-85
SPDR	10.38	10.38	9.12	LOGB1	0.343E-01	0.436E-01	SAT(MIN)		999
DBME	-42.54		-31.42	LOGR2	0.979E+00	0.963E+00	50	-46.0	-32.0
DBSD	15.23		12.16	LOGSS	0.334E+00	0.970E+00	70	-35.0	-26.0
DBCOS	0.68		0.71				90	-22.0	-16.0
DBCOK	3.29		4.17				99	1.0	9.0

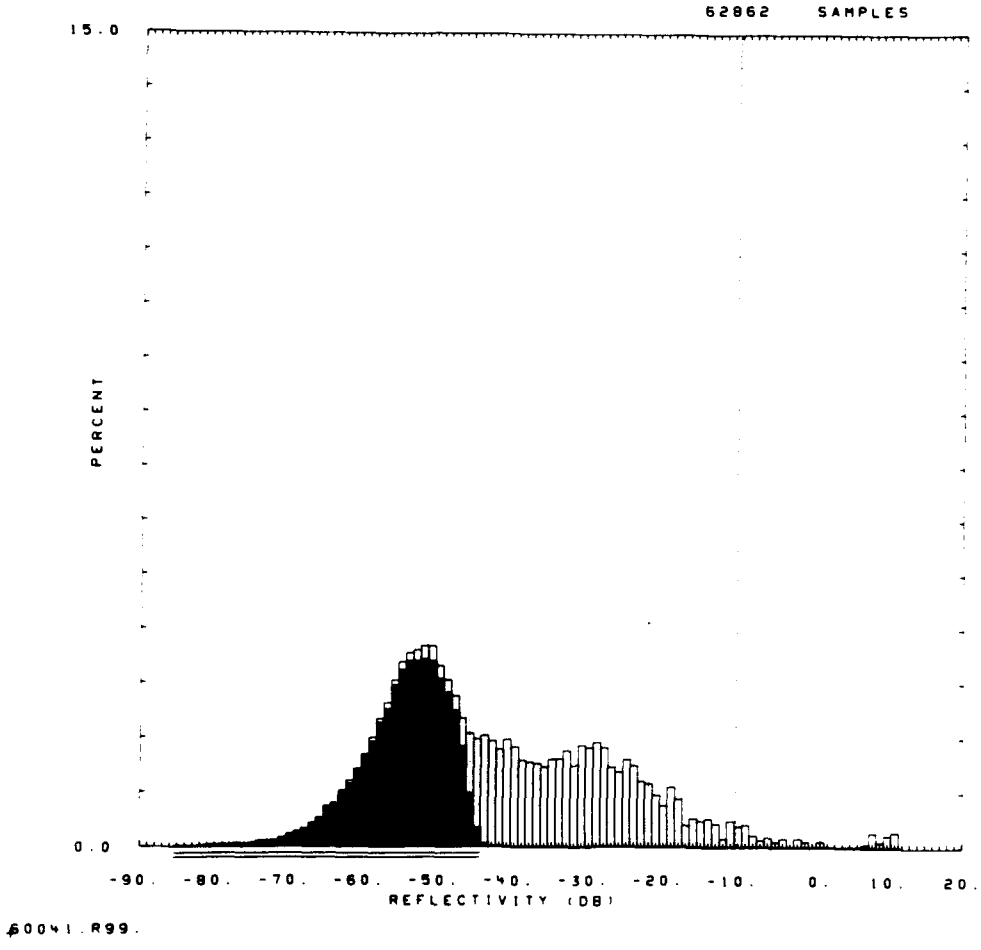

Figure E-16. Clutter strength histogram for Altona II repeat sector. L-band, 15-m pulse, horizontal polarization.

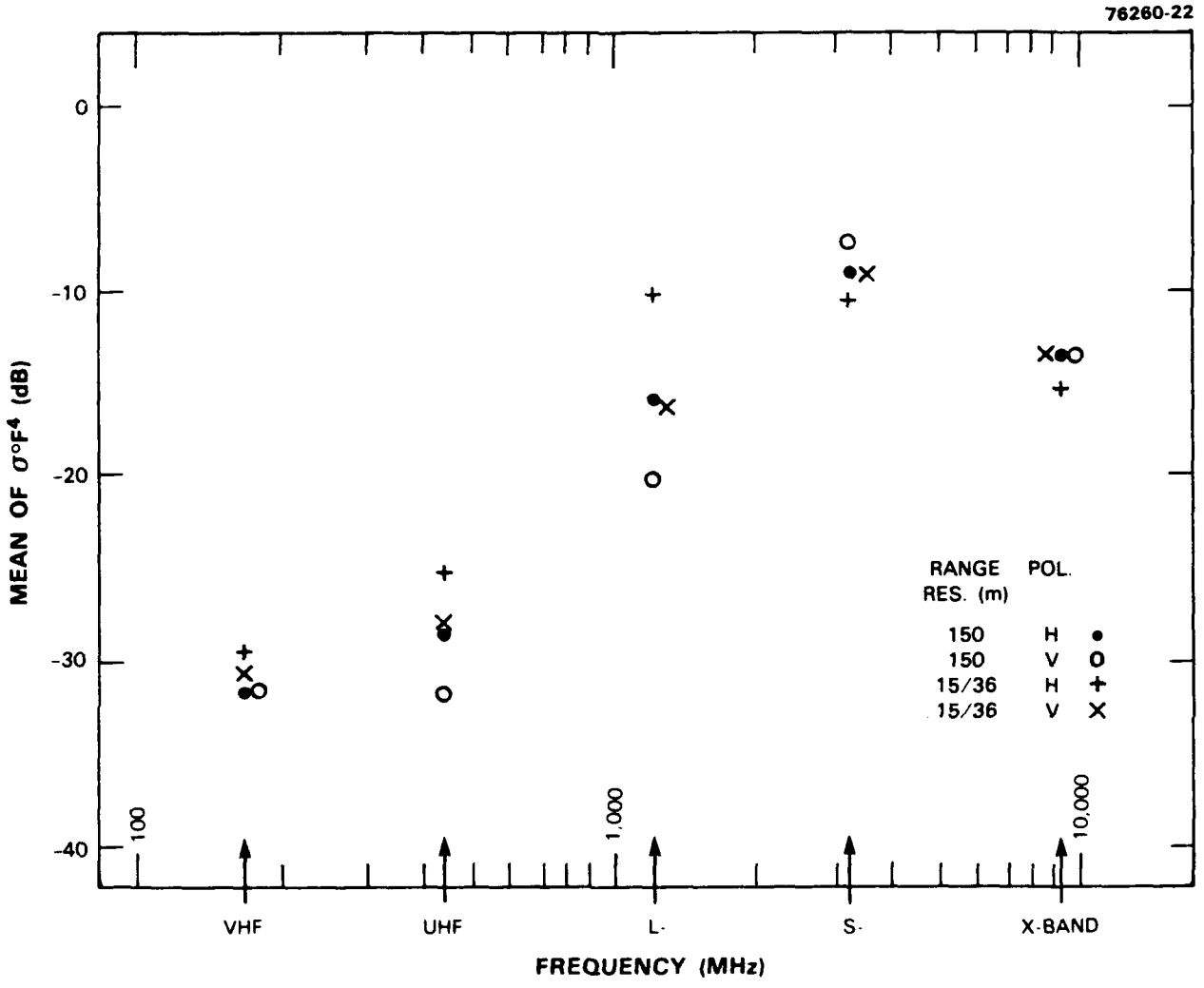

Figure E-17. Mean clutter strength versus frequency at Altona II. For the Altona II repeat sector, depression angle = 0.2 deg, landform = 1, land cover = 21-11-14, range = 2.5 to 8.4 km, azimuth = 262 to 272 deg. Comment: UHF data may have been affected by interference from nearby Perimeter Acquisition Radar.

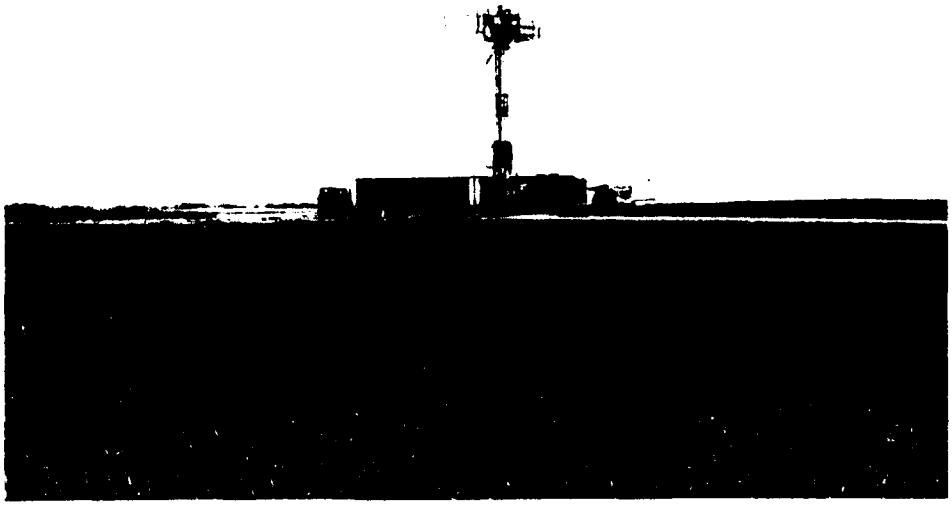

(a)

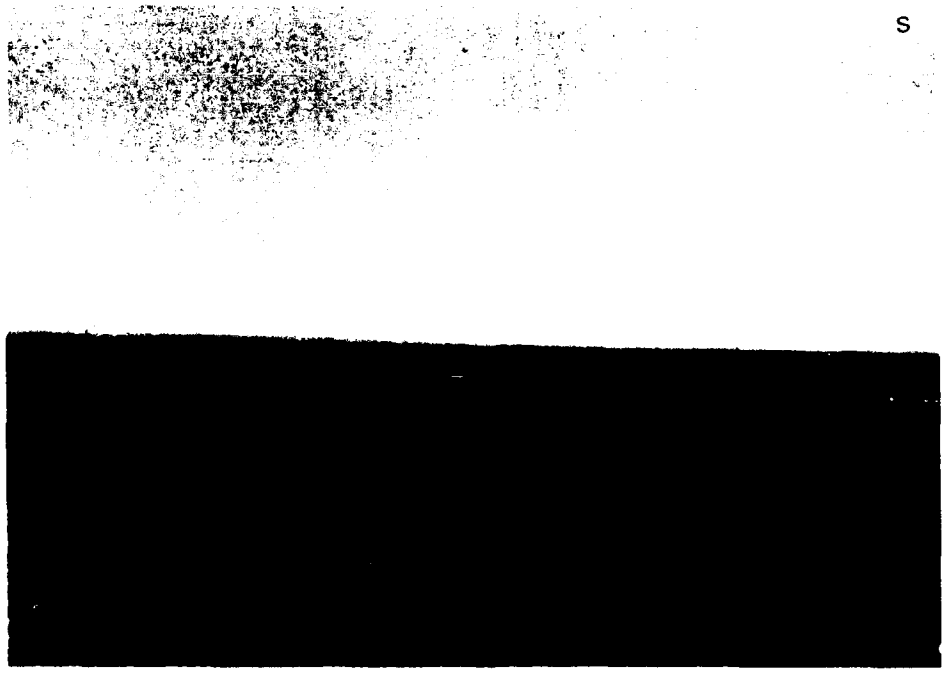

(b)

Figure E-18 Phase One at Picture Butte II. (a) Equipment on site. Looking SSE to town of Picture Butte and (b) tower-top view looking south into repeat sector to city of Lethbridge on far horizon.

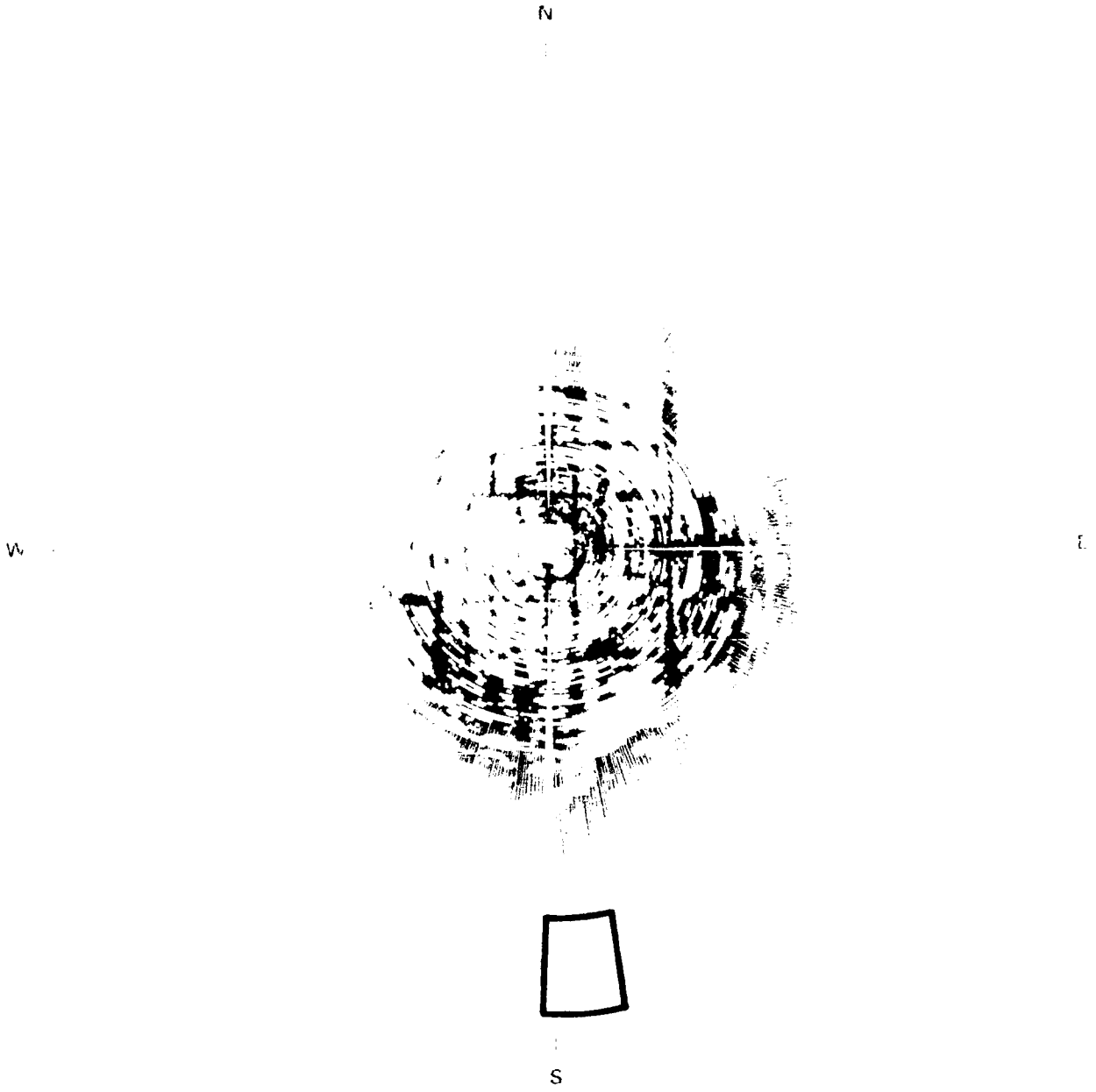

Figure E-19. PPI clutter map and repeat sector at Picture Butte II. Repeat sector is outlined in black. Maximum range = 30 km; UHF, 150-m pulse, horizontal polarization; cells with $\sigma^{o}F^{4} \geq -45$ dB are red.

SITE = PICTURE BUTTE II RDF = RSTV13.RDF;1

LC = 11 12 0 LF = 3 8 TC = 8 DA = 0.10 DAC = 0.01 PN = R99 DATE = 01-AUG-33

	SHDWUB	SHDWLB	SHDLSS		SHDW	SHDLSS			
MEAN	-9.92	-9.92	-7.40	WEIB0	0.683E+00	0.637E+00	SIG(MAX)		20
SD	3.38	3.[illegible]	4.64	WEIB1	0.182E-01	0.247E-01	NOI(MAX)		-36
COS	15.82	15.82	14.56	WEIR2	0.985E+00	0.952E+00	SAT(MAX)		999
COK	32.03	32.03	29.50	WEISS	0.375E-01	0.232E+00	SIG(MIN)		-82
SPDL	-999.00	-999.00	-999.00	LOGB0	0.169E+01	0.154E+01	NOI(MIN)		-85
SPDR	13.50	13.50	12.30	LOGB1	0.418E-01	0.498E-01	SAT(MIN)		999
DBME	-36.36		-28.02	LOGR2	0.998E+00	0.992E+00	50	-38.0	-30.0
DBSO	13.01		10.89	LOGSS	0.255E-01	0.160E+00	70	-31.0	-24.0
DBCOS	0.61		0.62				90	-19.0	-13.0
DBCOK	3.49		4.19				99	-1.0	2.0

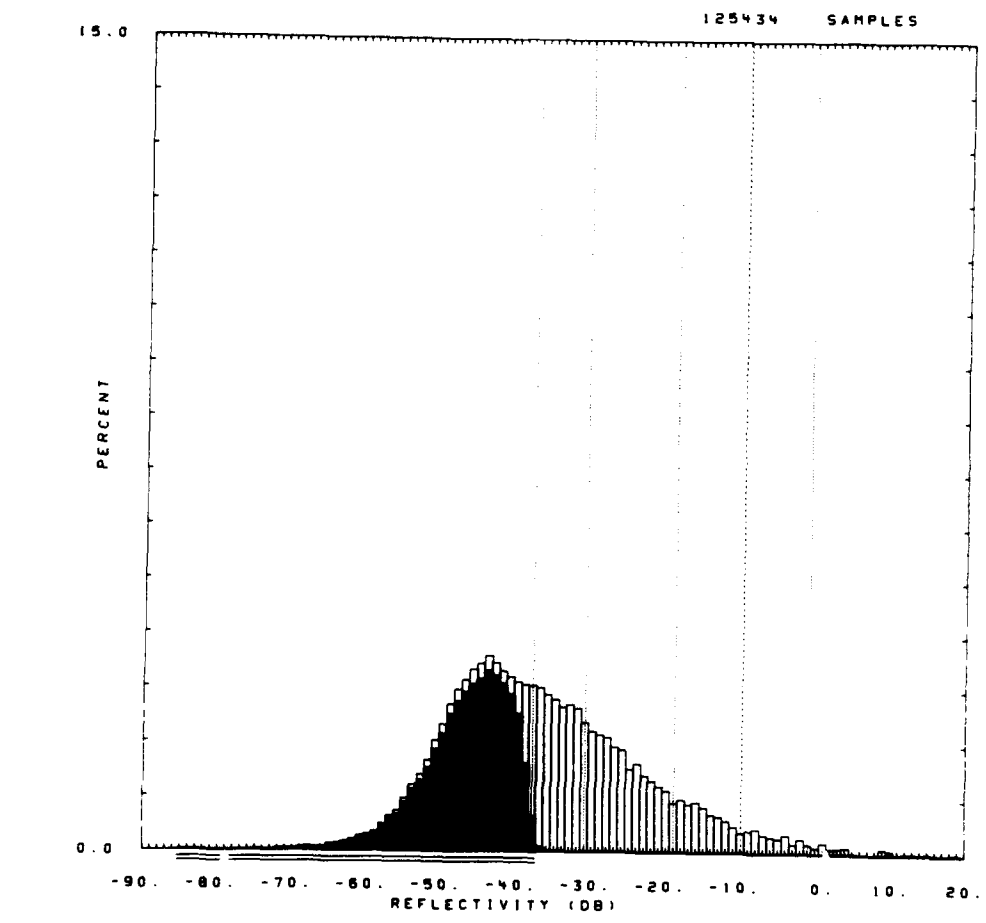

Figure E-20. Clutter strength histogram for Picture Butte II repeat sector. S-band, 15-m pulse, vertical polarization.

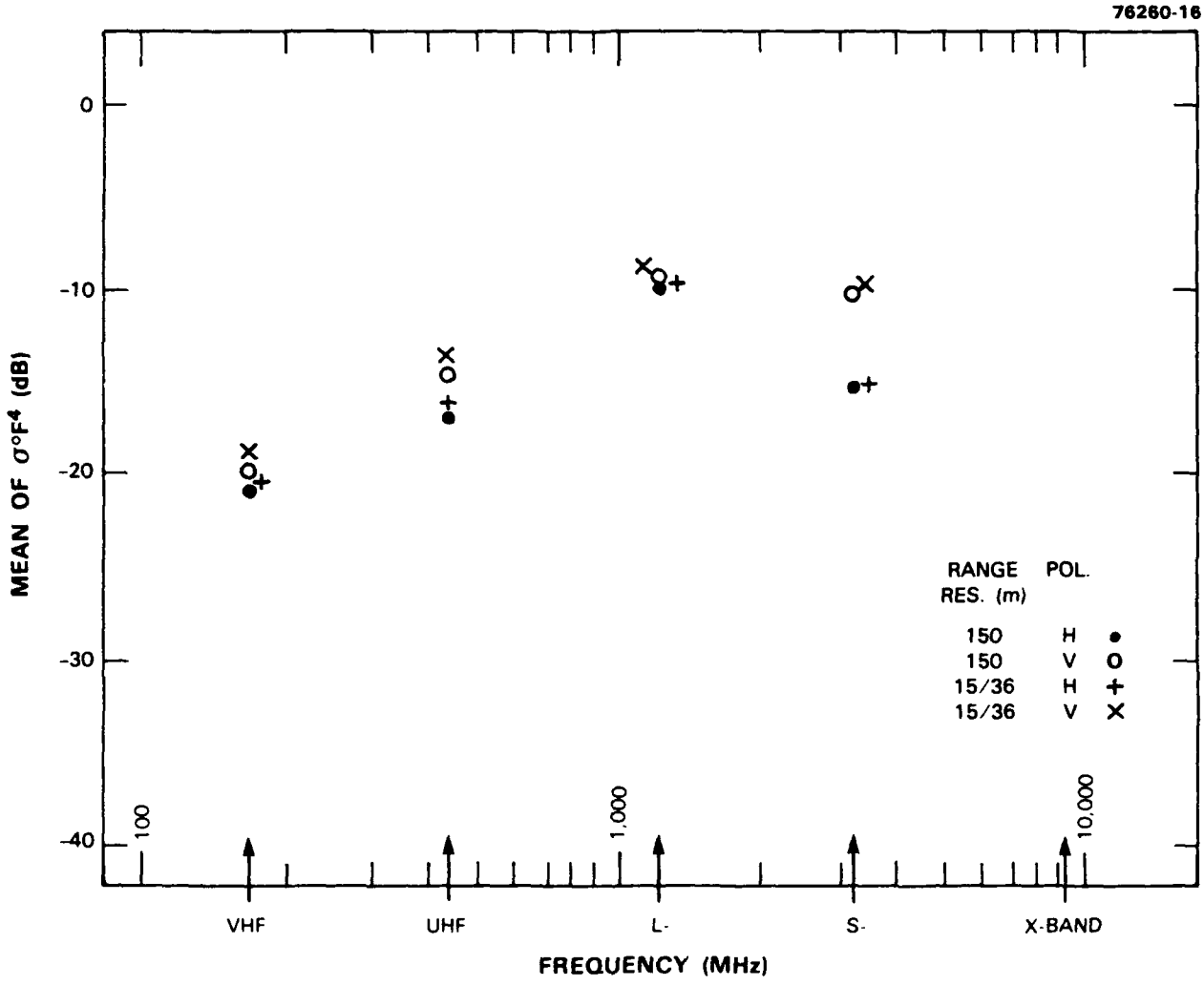

Figure E-21. Mean clutter strength versus frequency at Picture Butte II. For the Picture Butte II repeat sector, depression angle = 0.1 deg, landform = 3-8, land cover = 11-12, range = 22 to 27.9 km, azimuth = 172 to 182 deg. Comment: X-band transmitter inoperable at this site.

(a)

(b)

Figure E-22. Phase One at Headingley: (a) Equipment on site and (b) tower top view south from site.

(a)

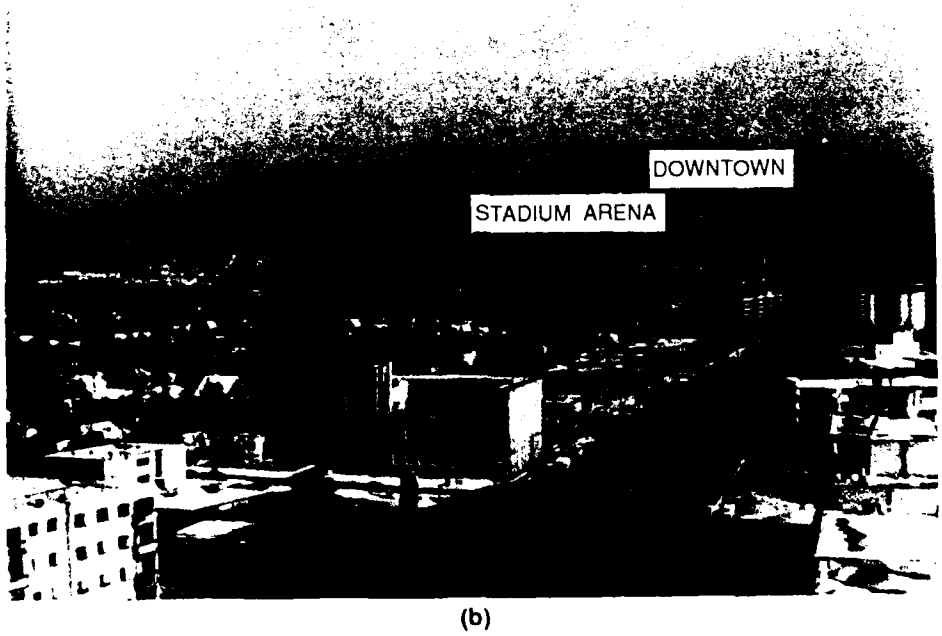

(b)

Figure E-23. Repeat sector at Headingley: (a) Lower top view looking east to Winnipeg city center in repeat sector in haze on horizon at 18.5 km range and (b) looking east to Winnipeg city center from near beginning of repeat sector at 12-km range

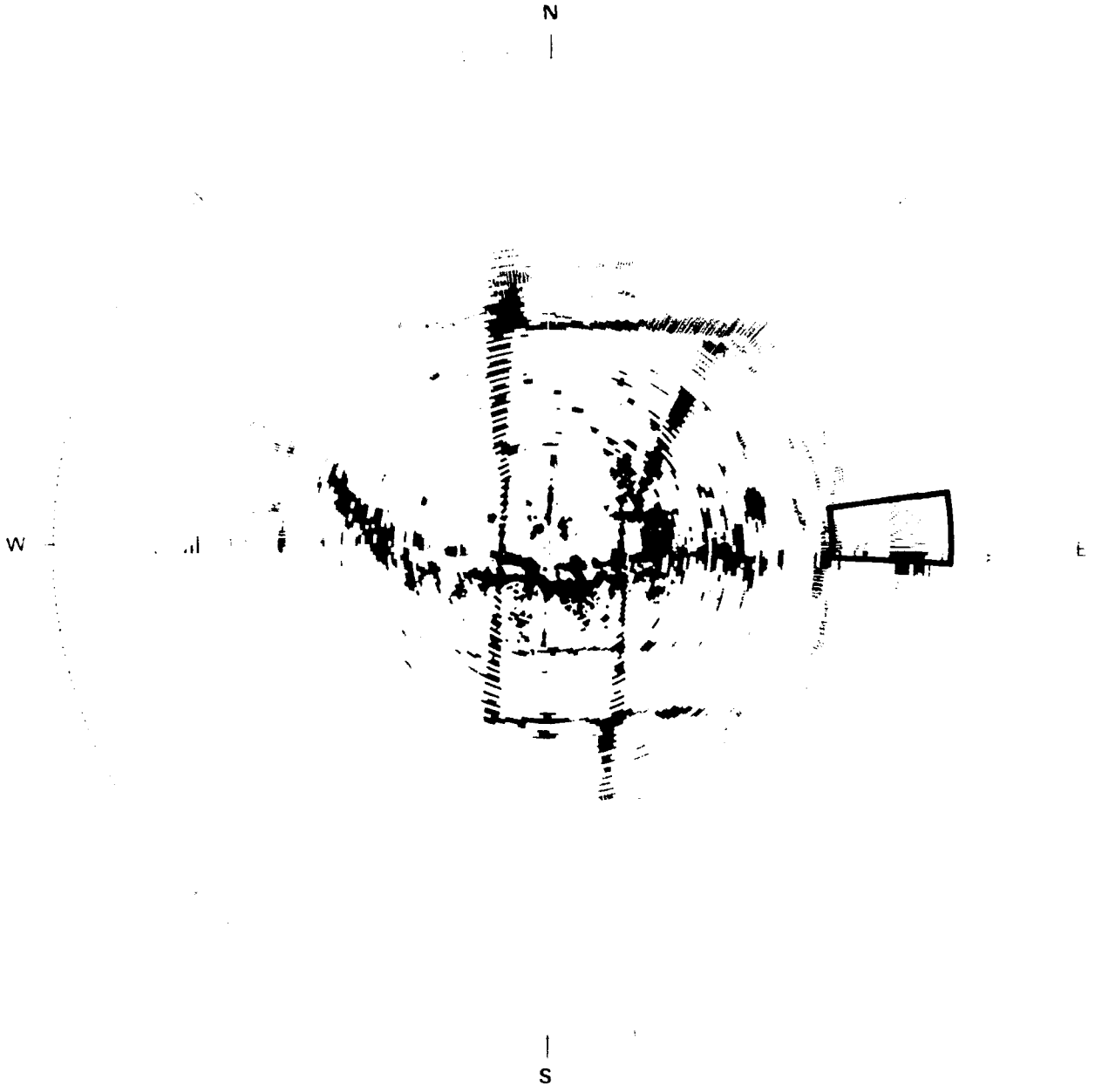

Figure E-24. PPI clutter map and repeat sector at Headingley. Repeat sector is outlined in black. Maximum range = 24.7 km; L-band, 150-m pulse, horizontal polarization; cells with $\sigma^{\circ}F^{4} \geq -40$ dB are red.

SITE = HEADINGLEY RDF = RSTH14A.RDF;1

LC = 11 12 41 LF = 1 0 TC = 2 DA = 0.04 DAC = 0.09 PN = R99 DATE = 15-DEC-83

	SHDHUB	SHDHLB	SHDLSS		SHDH	SHDLSS			
MEAN	-17.09	-17.09	-11.79	WEIB0	0.765E+00	0.703E+00	SIG(MAX)		11
SD	-4.31	-4.31	-1.68	WEIB1	0.128E-01	0.221E-01	NOI(MAX)		-44
COS	14.90	14.90	12.24	WEIR2	0.999E+00	0.979E+00	SAT(MAX)		999
COK	30.11	30.11	24.81	WEISS	0.890E-03	0.973E-01	SIG(MIN)		-85.
SPDL	-999.00	-999.00	-999.00	LOGB0	0.191E+01	0.165E+01	NOI(MIN)		-85
SPDR	13.00	13.00	10.52	LOGB1	0.317E-01	0.436E-01	SAT(MIN)		999
DBME	-51.41		-36.10	LOGR2	0.993E+00	0.998E+00	50	-55.0	-37.0
DBSD	13.80		14.64	LOGSS	0.654E-01	0.339E-01	70	-49.0	-30.0
DBCOS	1.28		0.21				90	-31.0	-16.0
DBCOK	4.85		3.17				99	-7.0	1.0

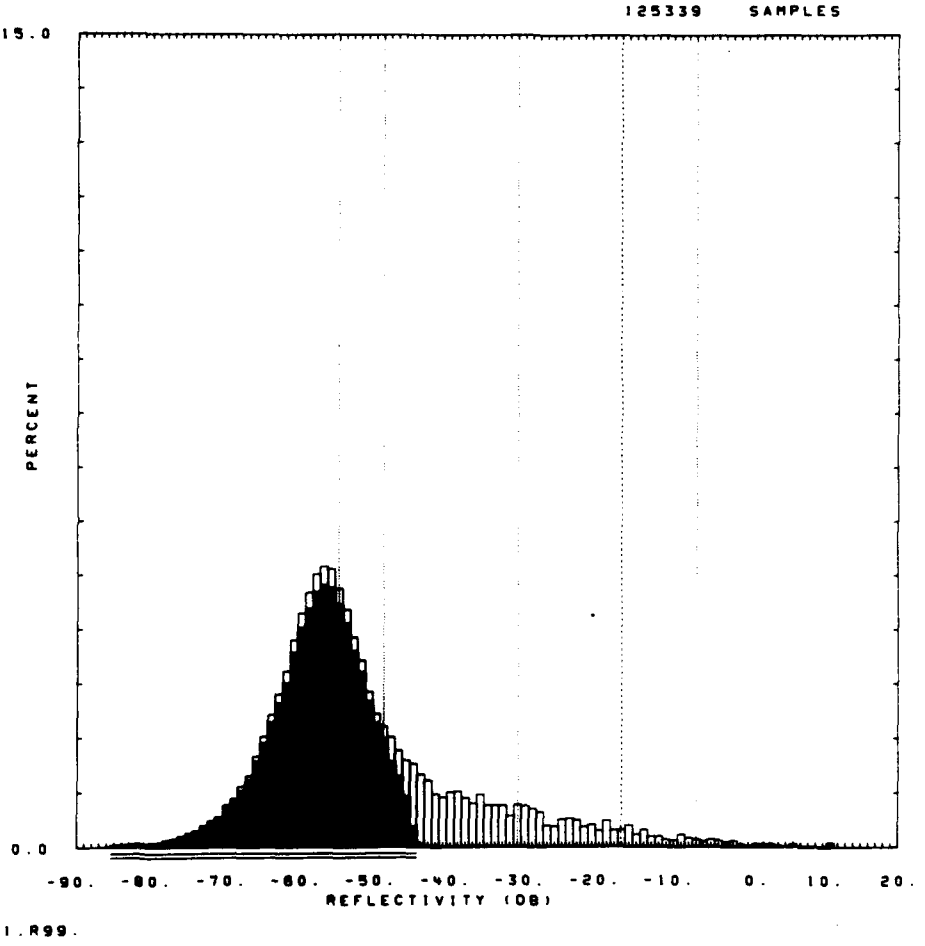

Figure E-25. Clutter strength histogram for Headingley repeat sector. S-band, 15-m pulse, horizontal polarization. No attenuation. RF preamplifier on.

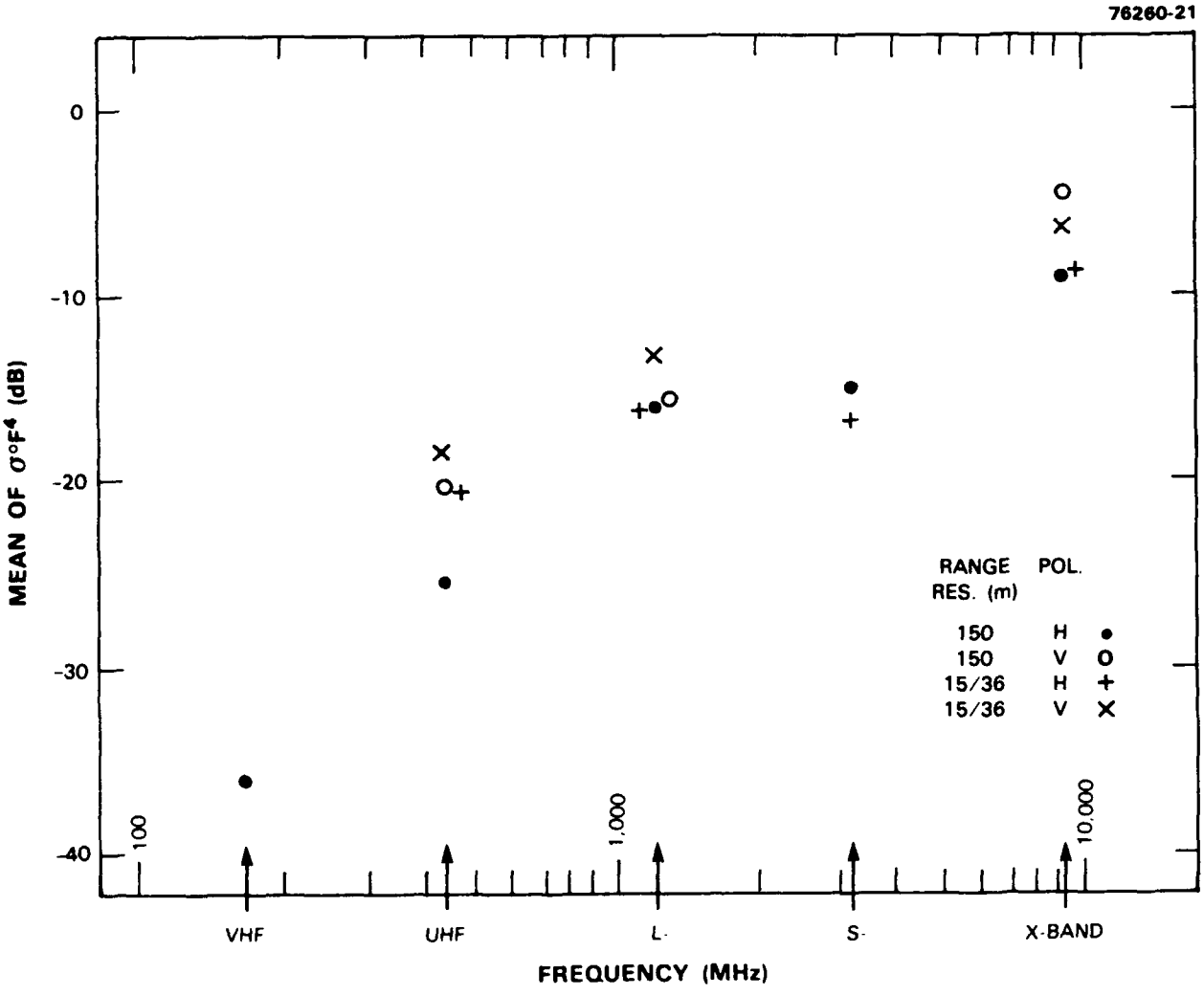

Figure E-26. Mean clutter strength versus frequency at Headingley. For the Headingley repeat sector, depression angle = 0.04 deg, landform = 1, land cover = 11-12-41, range = 14 to 19.9 km, azimuth = 82 to 92 deg. Comments: (1) At VHF, only repeat sector experiment is low resolution/horizontal polarization because of severe weather and hardware problems. (2) At S-band, only vertical polarization data collected for same reasons.

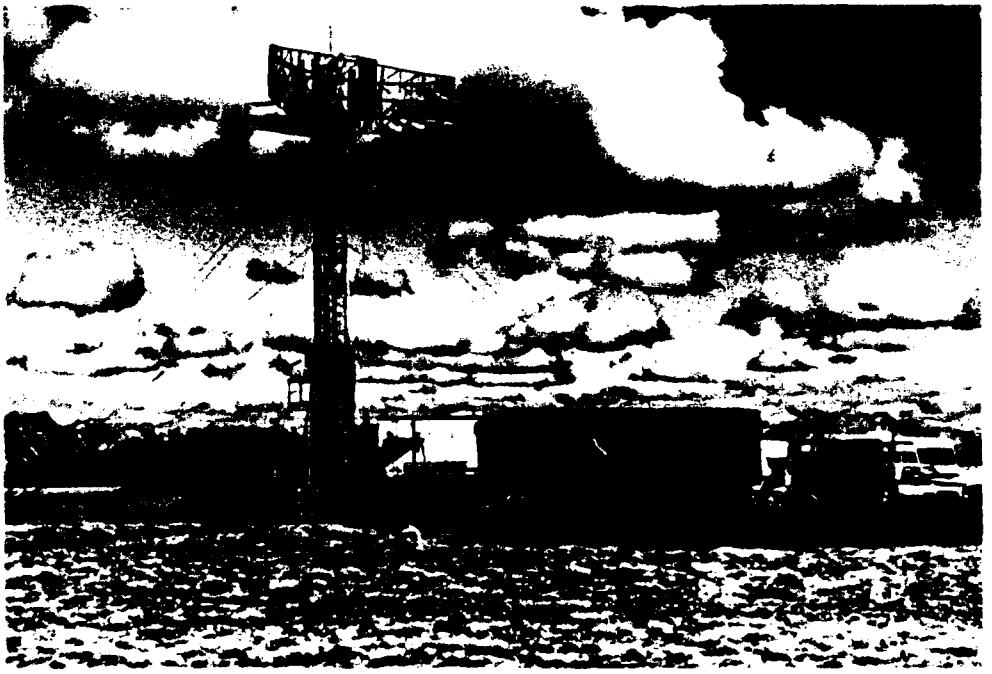

(a)

(b)

Figure E-27. Phase One at Plateau Mountain: (a) Equipment on site and (b) view west into repeat sector. Far peaks at 15- to 20-km range.

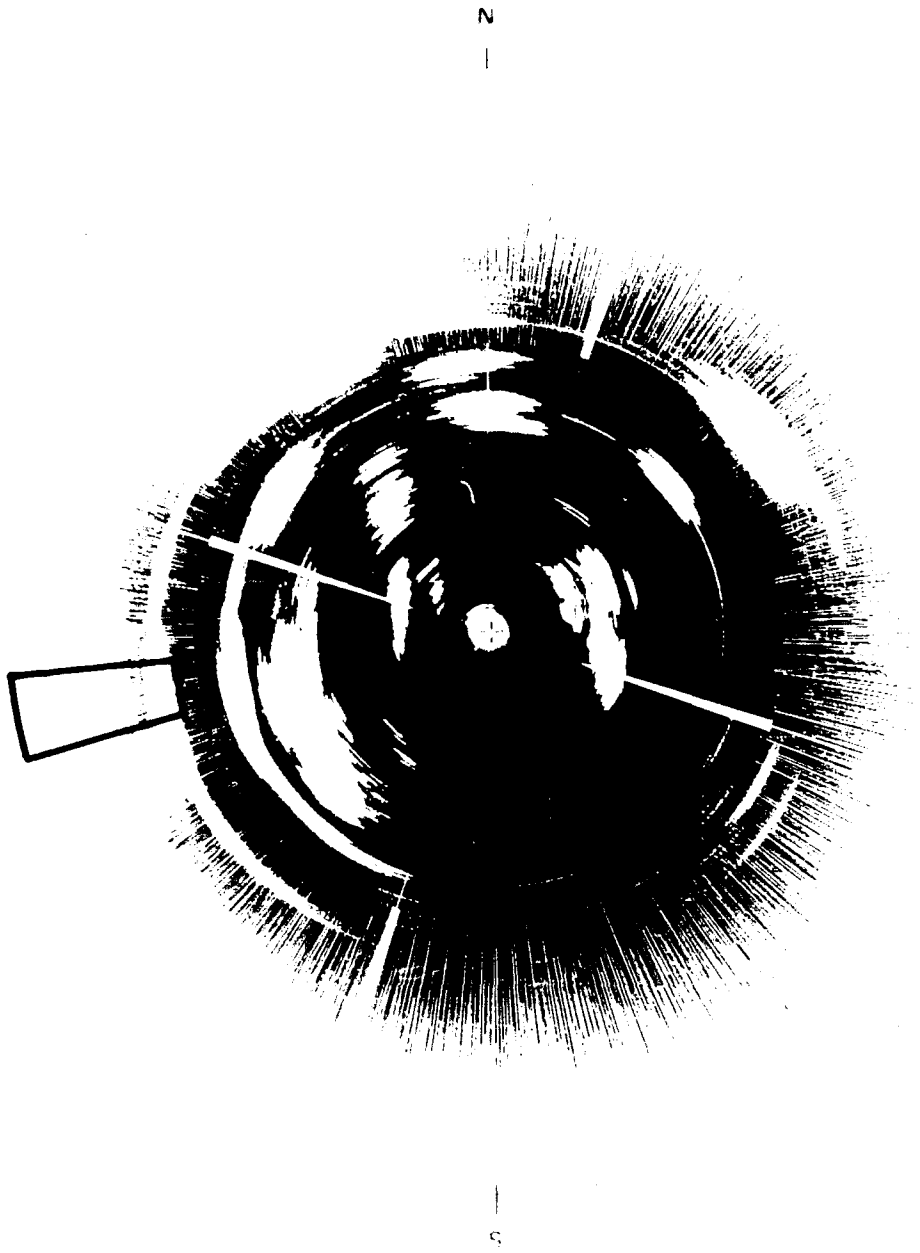

Figure E-28. PPI clutter map and repeat sector (b) at Plateau Mountain. Repeat sector is outlined in black. Maximum range = 20 km; VHF, 36-m pulse, horizontal polarization; cells with $\sigma^{\circ}F^{4} \geq -40$ dB are white.

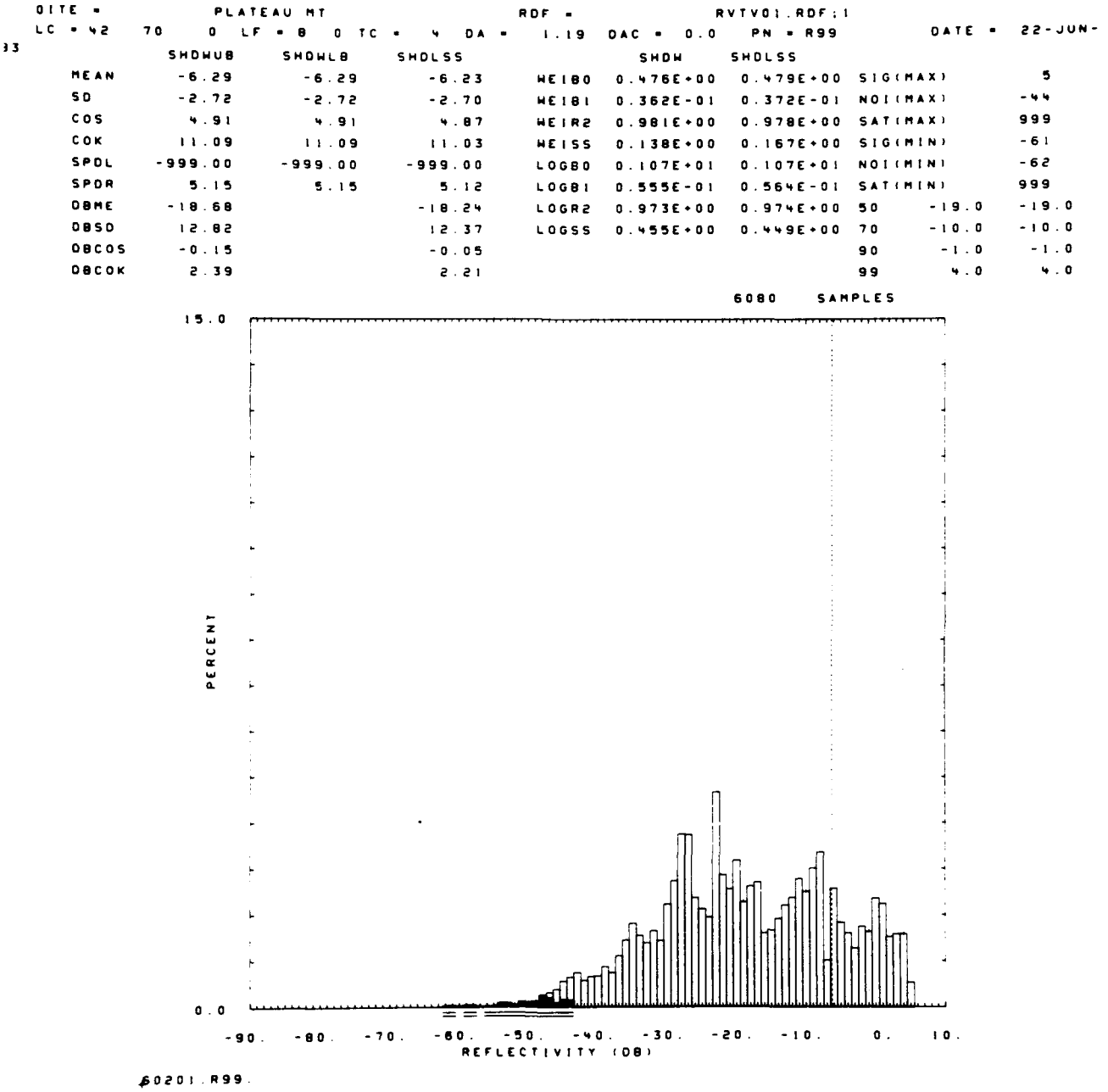

Figure E-29. Clutter strength histogram for Plateau Mountain (b) repeat sector. VHF, 36-m pulse, vertical polarization.

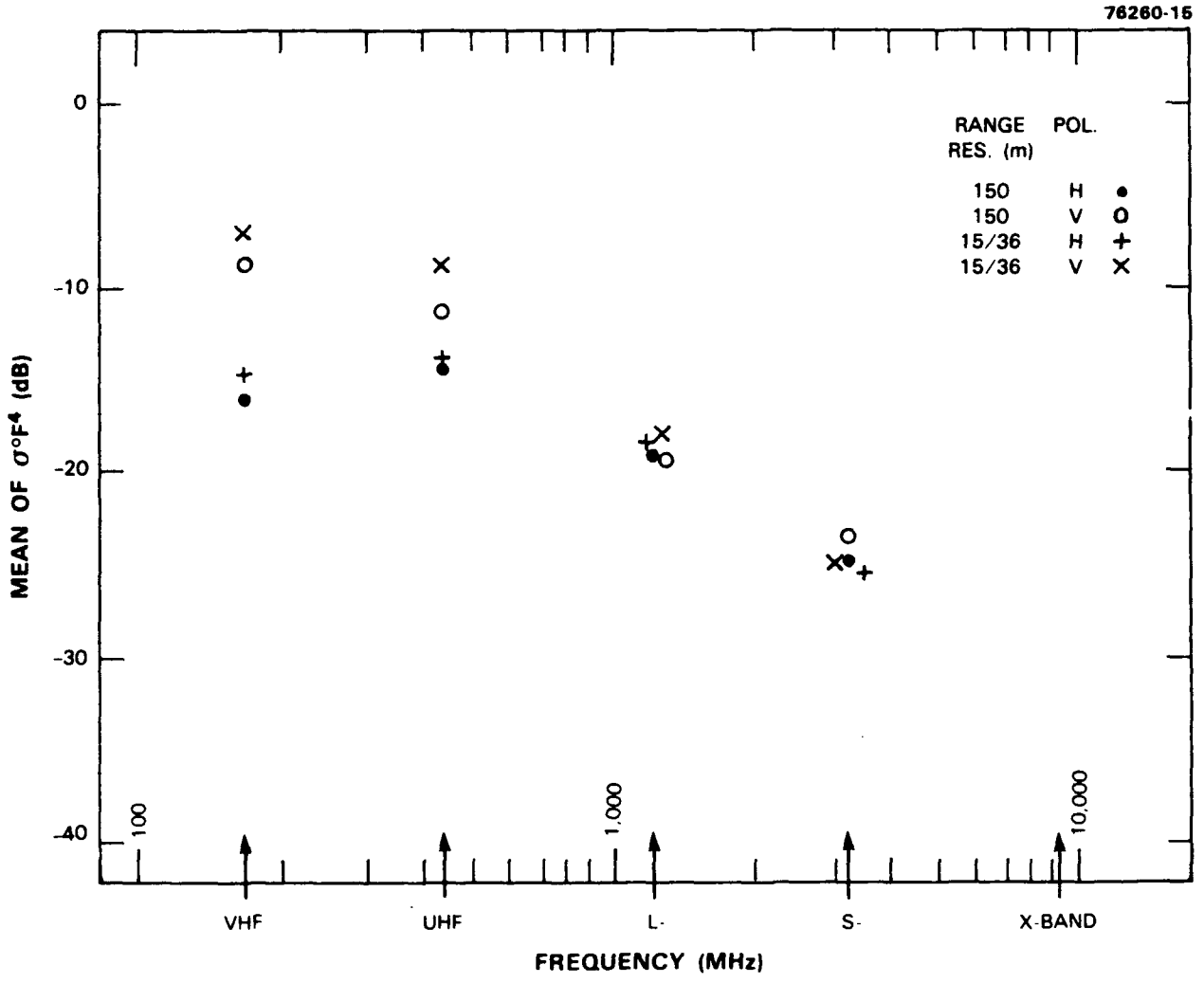

Figure E-30. Mean clutter strength versus frequency at Plateau Mountain (b). For the Plateau Mountain (b) repeat sector, depression angle = 1.2 deg, landform = 8, land cover = 42-7, range = 11 to 16.7 km, azimuth = 255 to 265 deg. Comment: X-band transmitter failed; no data collected.

(a)

(b)

Figure E-31. Phase One at Waterton. (a) Equipment on site and (b) view south into repeat sector from 7-km range.

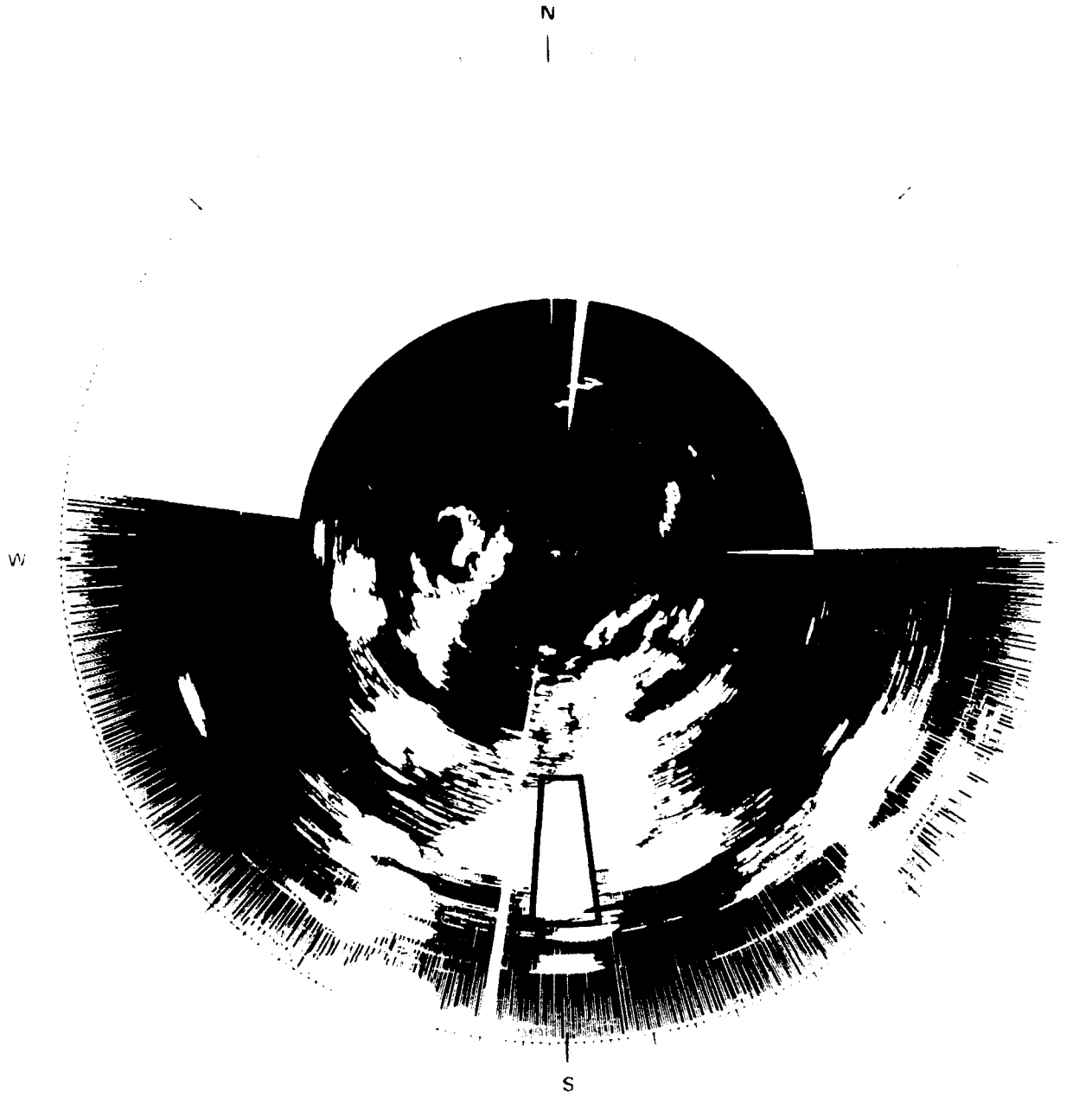

Figure E-32. PPI clutter map and repeat sector at Waterton. Repeat sector is outlined in black. Maximum range = 20 km; UHF, 36-m pulse, horizontal polarization; cells with $\sigma^{o}F^{4} \geq -40$ dB are white.

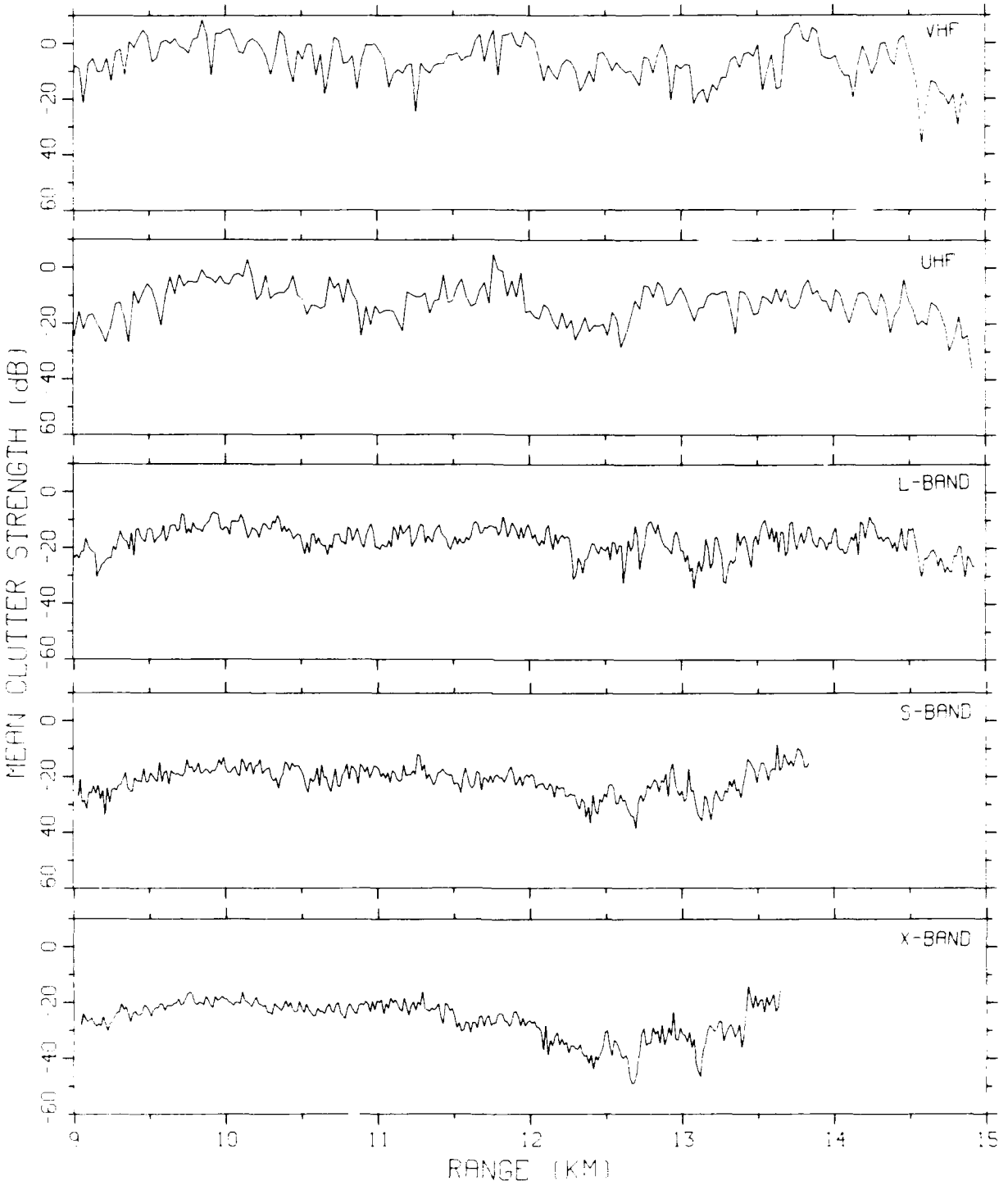

Figure E-33. Mean clutter strength versus range at Waterton. Repeat sector data. Vertical polarization. 15/36-m pulse length. Data shown range gate by range gate, averaged in azimuth over 10 deg.

SITE = WATERTON RDF = RVTV01.RDF;1
LC = 42 70 41 LF = 8 7 TC = 4 DA = -1.78 DAC = 0.0 PN = R99 DATE = 12-JUN-33

	SHOWUB	SHOWLB	SHOLSS		SHOW	SHOLSS			
MEAN	-2.91	-2.91	-2.90	WEIB0	0.316E+00	0.315E+00	SIG(MAX)		10
SD	-0.84	-0.84	-0.84	WEIB1	0.677E-01	0.680E-01	NOI(MAX)		-25
COS	5.66	5.66	5.65	WEIR2	0.995E+00	0.995E+00	SAT(MAX)		999
COK	13.85	13.85	13.84	WEISS	0.339E-01	0.358E-01	SIG(MIN)		-41
SPOL	-999.00	-999.00	-999.00	LOGB0	0.899E+00	0.898E+00	NOI(MIN)		-44
SPOR	4.17	4.17	4.17	LOGB1	0.109E+00	0.109E+00	SAT(MIN)		999
DBME	-7.70		-7.63	LOGR2	0.981E+00	0.981E+00	50	-7.0	-7.0
DBSD	7.42		7.28	LOGSS	0.336E+00	0.332E+00	70	-3.0	-3.0
DBCOS	-0.63		-0.49				90	1.0	1.0
DBCOK	4.12		3.53				99	6.0	6.0

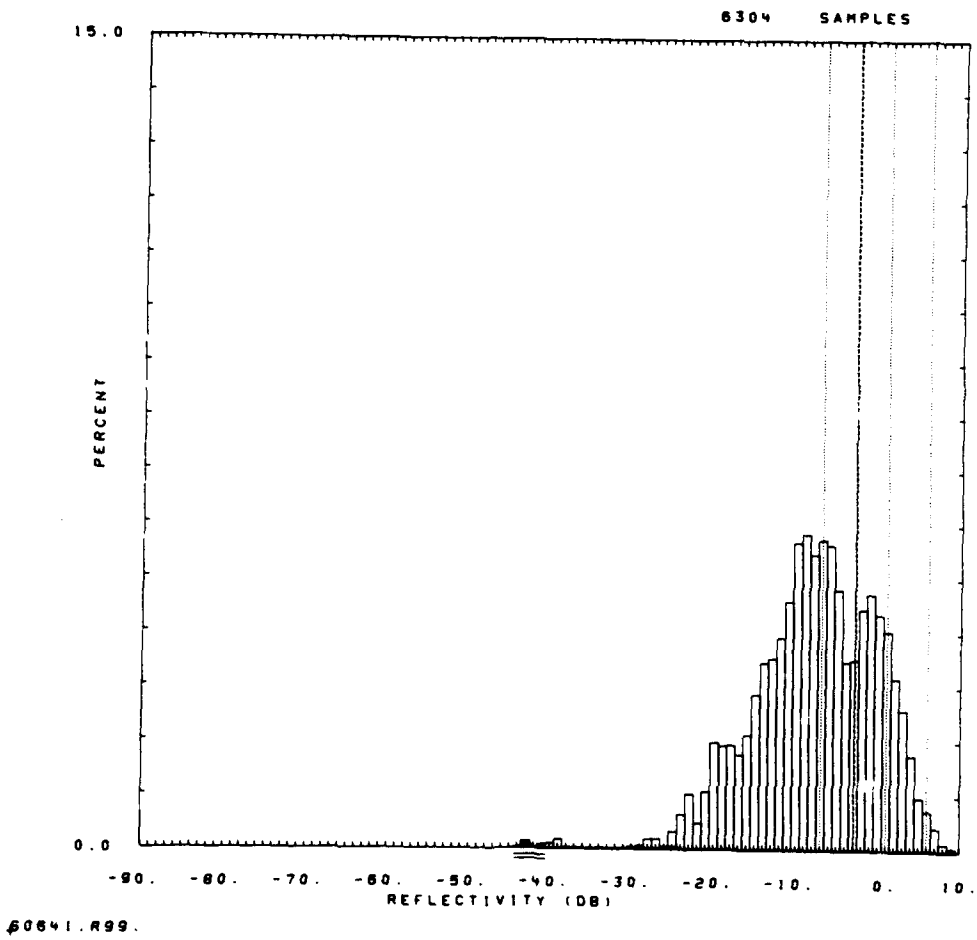

Figure E-34. Clutter strength histogram for Waterton repeat sector. VHF, 36-m pulse, vertical polarization.

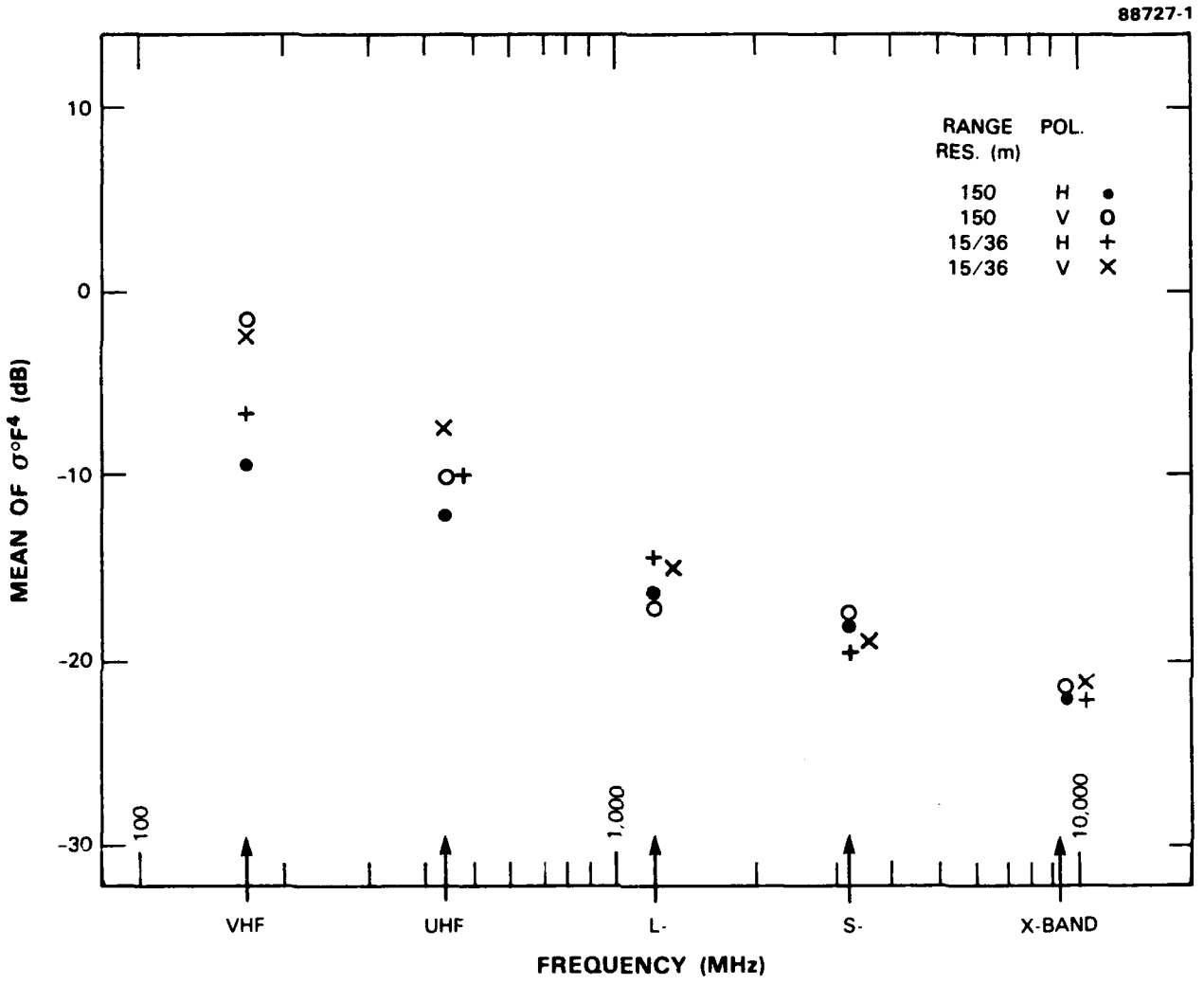

Figure E-35. Mean clutter strength versus frequency at Waterton. For the Waterton repeat sector, depression angle = -1.8 deg, landform = 8-7, land cover = 42-7-41, range = 9 to 14.9 km, azimuth = 175 to 185 deg.

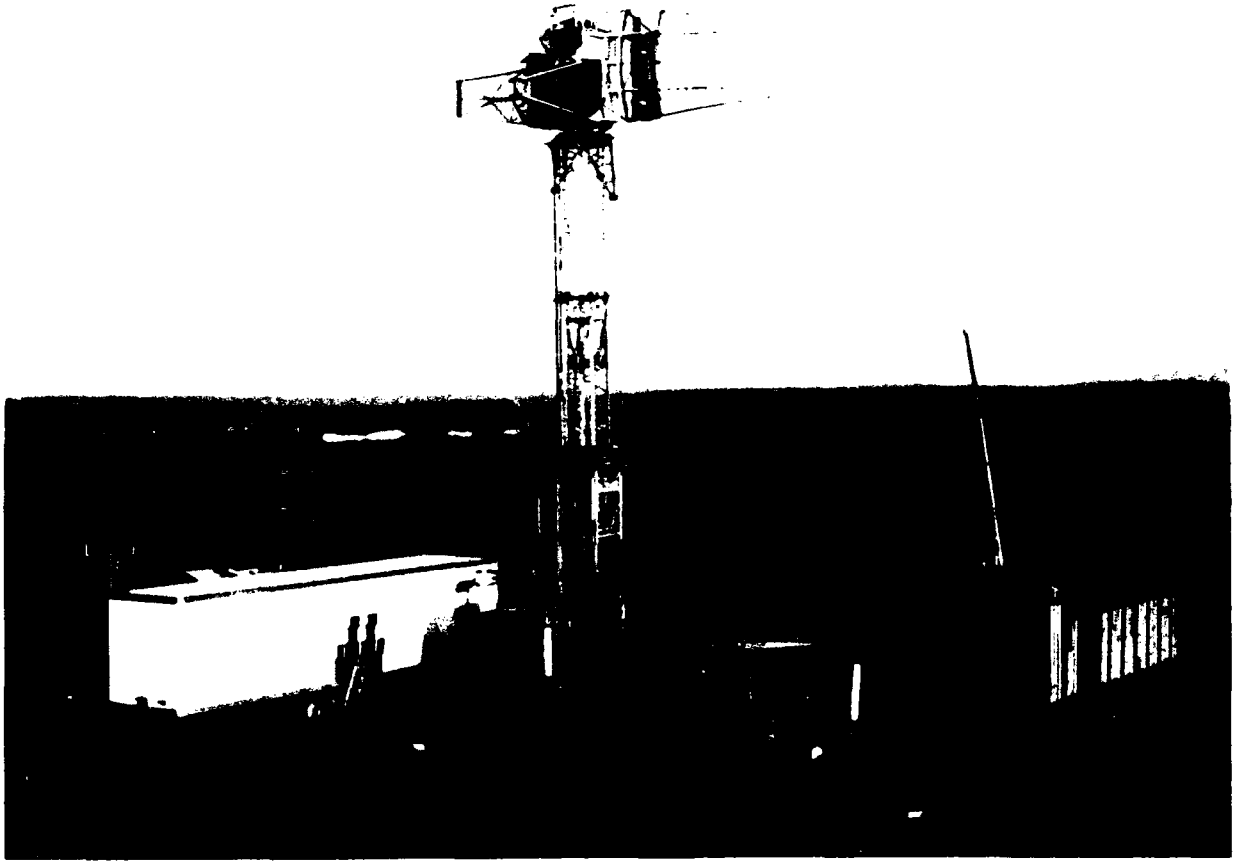

Figure E-36. Phase One at Blue Knob.

Figure E-37. PPI clutter map and repeat sector at Blue Knob. Repeat sector is outlined in black. Maximum range = 48.4 km; X-band, 150-m pulse, horizontal polarization; cells with $\sigma^{\circ}F^{4} \geq -40$ dB are red

SITE = BLUE KNOB RDF = RVFH04.RDF;1

LC = 21 43 11 LF = 4 0 TC = 1 DA = 1.55 DAC = 0.0 PN = R99 DATE = 15-SEP-34

	SHDWUB	SHDWLB	SHDLSS		SHDW	SHDLSS			
MEAN	-10.83	-10.83	-10.83	WEIB0	0.724E+00	0.724E+00	SIG(MAX)		0
SD	-8.33	-8.33	-8.33	WEIB1	0.526E-01	0.526E-01	NOI(MAX)		999
COS	6.00	6.00	6.00	WEIR2	0.988E+00	0.988E+00	SAT(MAX)		999
COK	13.52	13.52	13.52	WEISS	0.886E-01	0.886E-01	SIG(MIN)		-54
SPDL	-999.00	-999.00	-999.00	LOGB0	0.148E+01	0.148E+01	NOI(MIN)		-999
SPOR	4.44	4.44	4.44	LOGB1	0.803E-01	0.803E-01	SAT(MIN)		999
DBME	-17.54		-17.54	LOGR2	0.958E+00	0.958E+00	50	-15.0	-15.0
DBSD	9.61		9.61	LOGSS	0.769E+00	0.769E+00	70	-10.0	-10.0
DBCOS	-0.56		-0.56				90	-7.0	-7.0
DBCOK	2.58		2.58				99	0.0	0.0

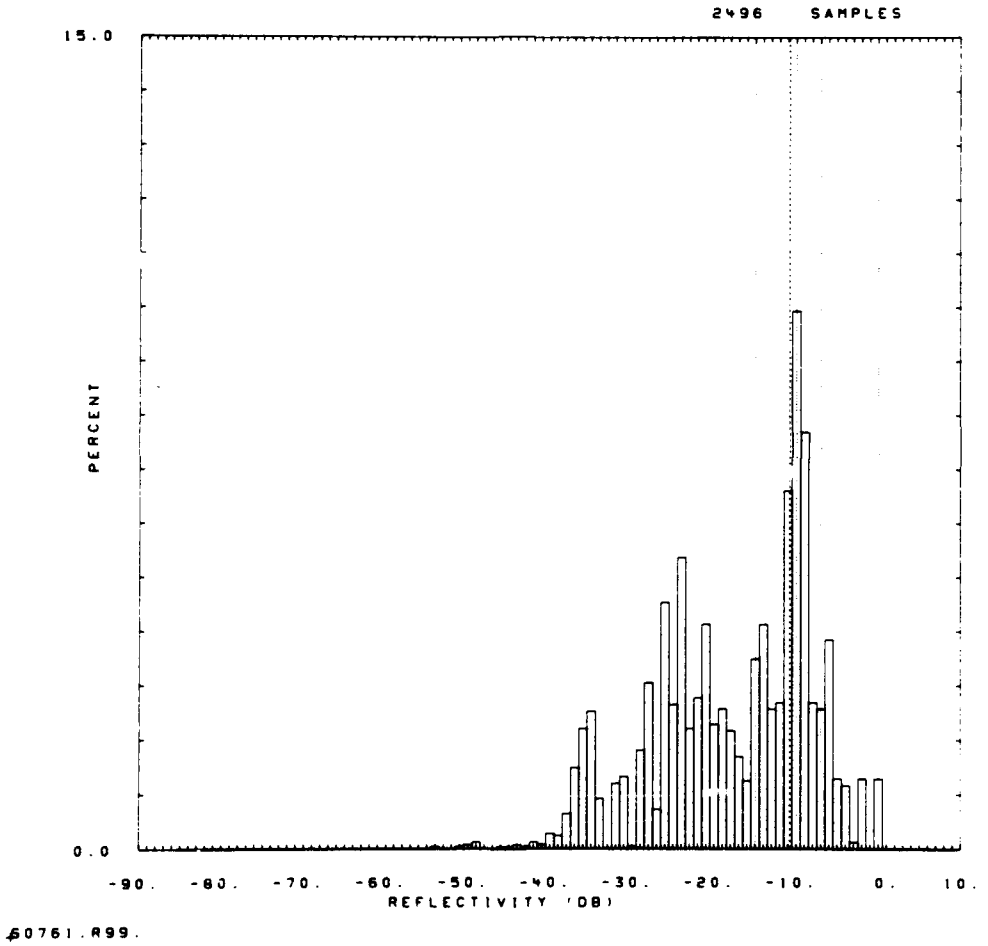

Figure E-38. Clutter strength histogram for Blue Knob repeat sector. VHF, 150-m pulse, horizontal polarization.

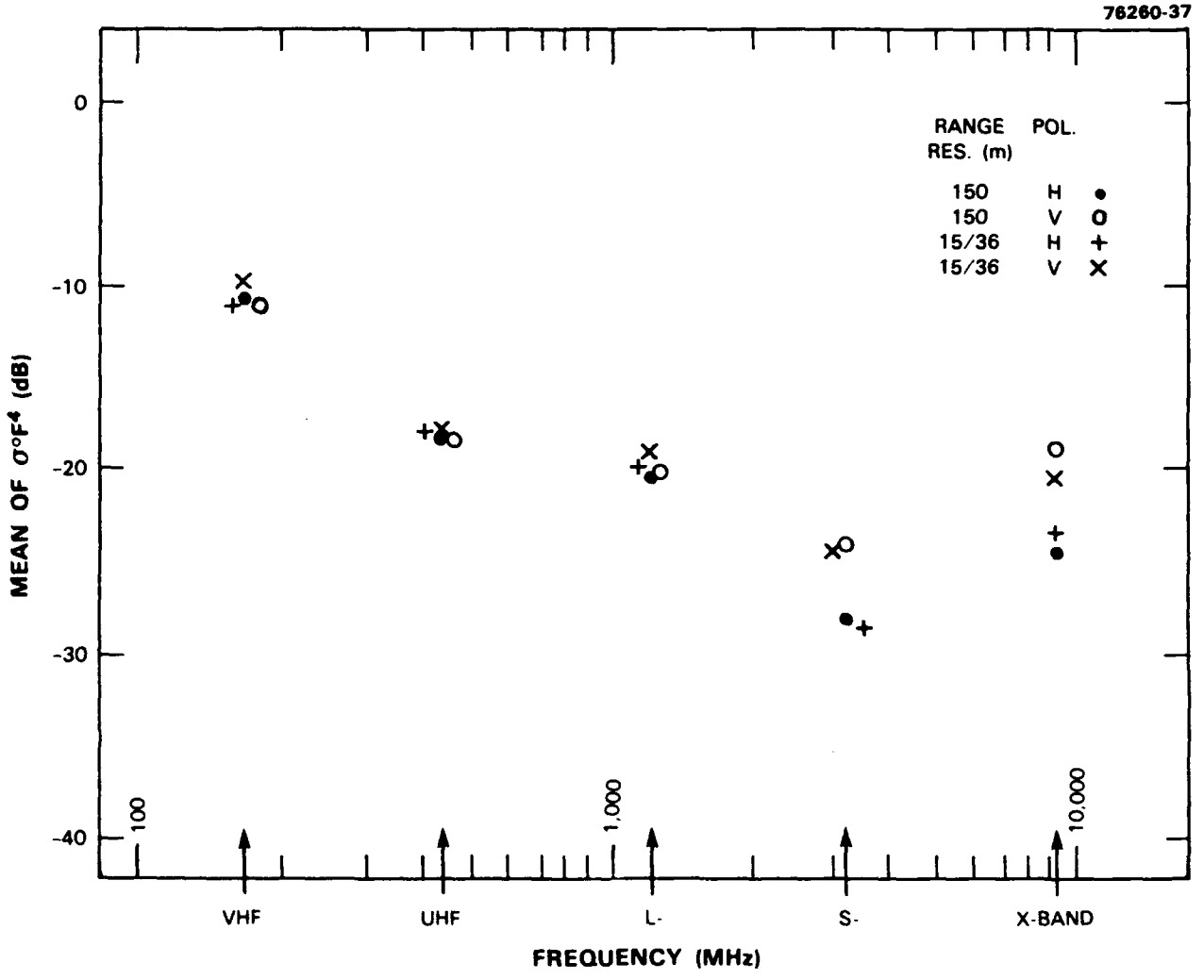

Figure E-39. Mean clutter strength versus frequency at Blue Knob. For the Blue Knob repeat sector, depression angle = 1.6 deg, landform = 4, land cover = 21-43-11, range = 16 to 21.9 km, azimuth = 80 to 100 deg.

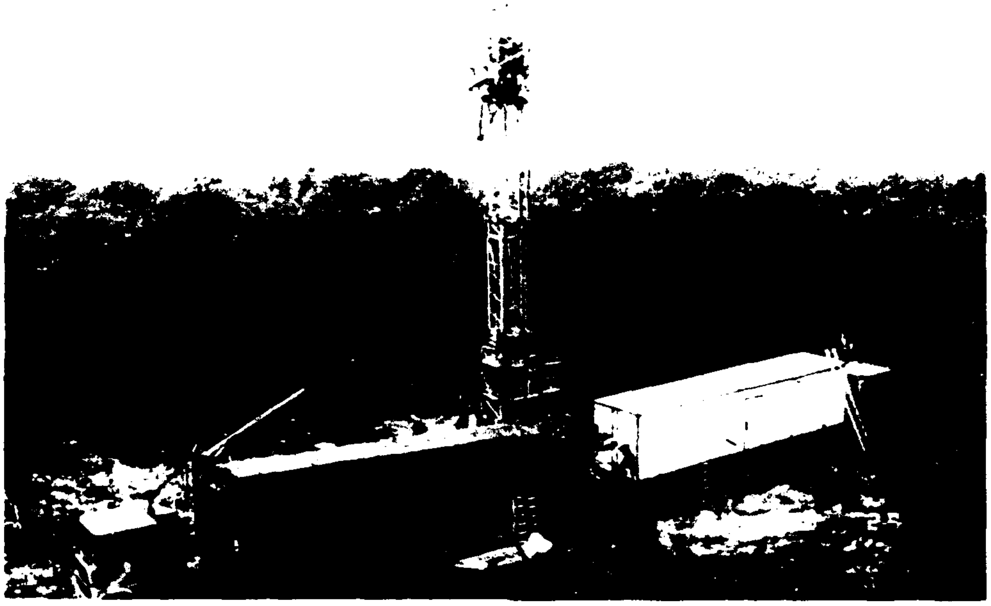

(a)

NW

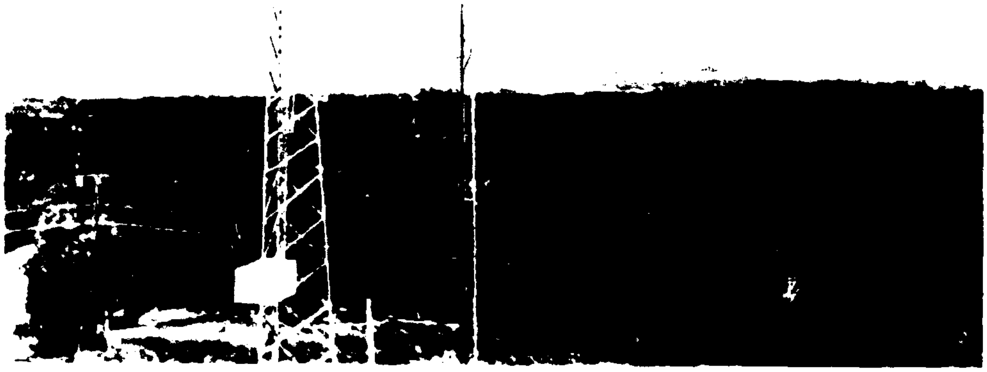

(b)

Figure F-40. Phase One at Scranton: (a) Equipment on site and [illegible] view looking NW [illegible]

Figure E-41. PPI clutter map and repeat sector at Scranton. Repeat sector is outlined in black. Maximum range = 20 km, S band, 15-m pulse, horizontal polarization, cells with $\sigma^{o}F^{4} \geq -40$ dB are red

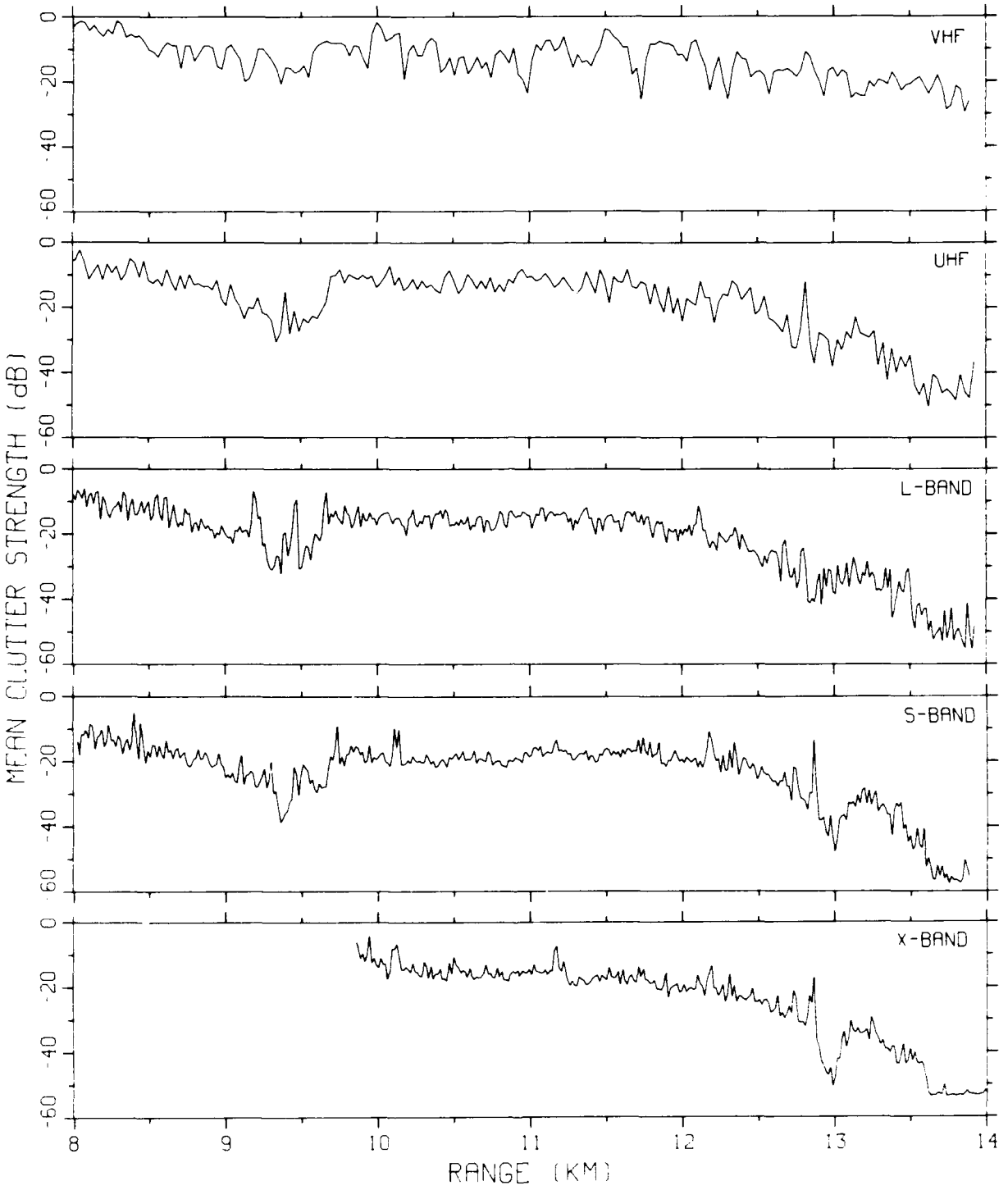

Figure E-42. Mean clutter strength versus range at Scranton. Repeat sector data. Vertical polarization, 15/36-m pulse length. Data shown range gate by range gate, averaged in azimuth over 20 deg.

SITE = SCRANTON RDF = [RVFH04.RDF;1]

LC = 43 12 11 LF = 7 4 TC = 4 DA = 0.93 DAC = 0.0 PN = R99 DATE = 10-SEP-84

	SHDWUB	SHDWLB	SHDLSS		SHDW	SHDLSS			
MEAN	-10.38	-10.38	-10.34	WEIB0	0.686E+00	0.690E+00	SIG(MAX)		3
SD	-5.89	-5.89	-5.88	WEIB1	0.490E-01	0.498E-01	NOI(MAX)		-46
COS	7.32	7.32	7.30	WEIR2	0.986E+00	0.986E+00	SAT(MAX)		999
COK	15.52	15.52	15.47	WEISS	0.119E+00	0.127E+00	SIG(MIN)		-47
SPDL	-999.00	-999.00	-999.00	LOGB0	0.147E+01	0.148E+01	NOI(MIN)		-79
SPDR	5.81	5.81	5.79	LOGB1	0.778E-01	0.786E-01	SAT(MIN)		999
DBME	-18.59		-18.24	LOGR2	0.988E+00	0.988E+00	50	-17.0	-17.0
DBSD	10.04		9.44	LOGSS	0.273E+00	0.261E+00	70	-14.0	-14.0
DBCOS	-0.76		-0.49				90	-7.0	-7.0
DBCOK	4.09		3.16				99	2.0	2.0

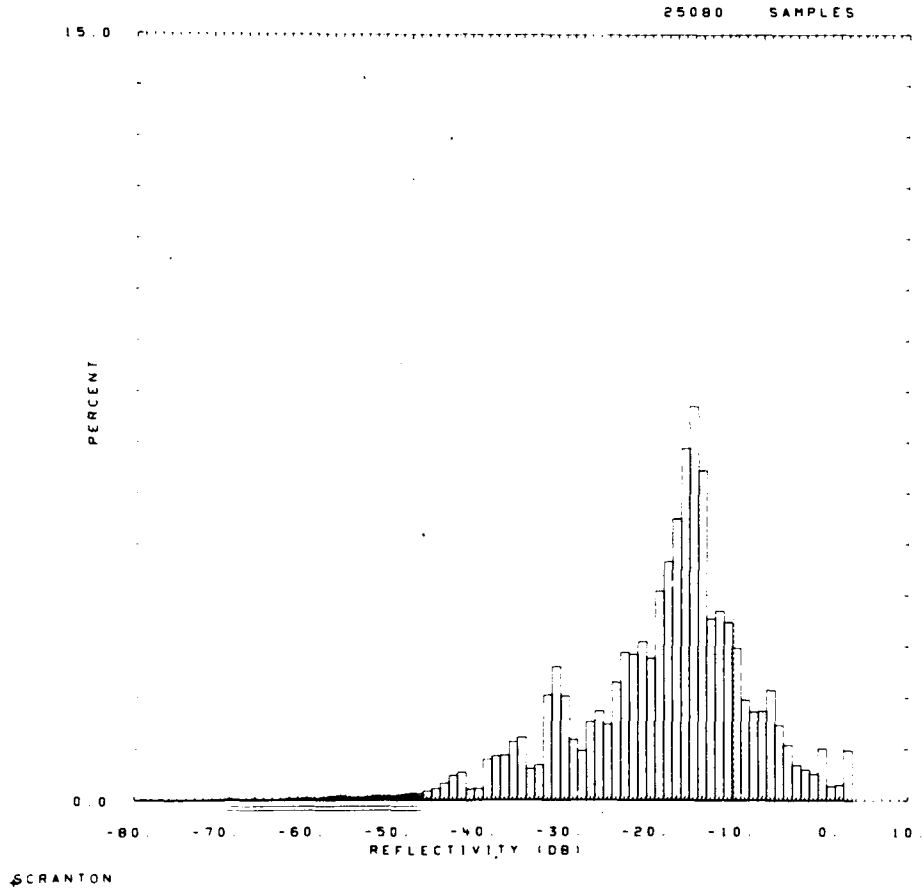

Figure E-43. Clutter strength histogram for Scranton repeat sector. VHF, 150-m pulse, horizontal polarization. Slow scan, 0.125 deg/s, experiment type 3, see Appendix C.

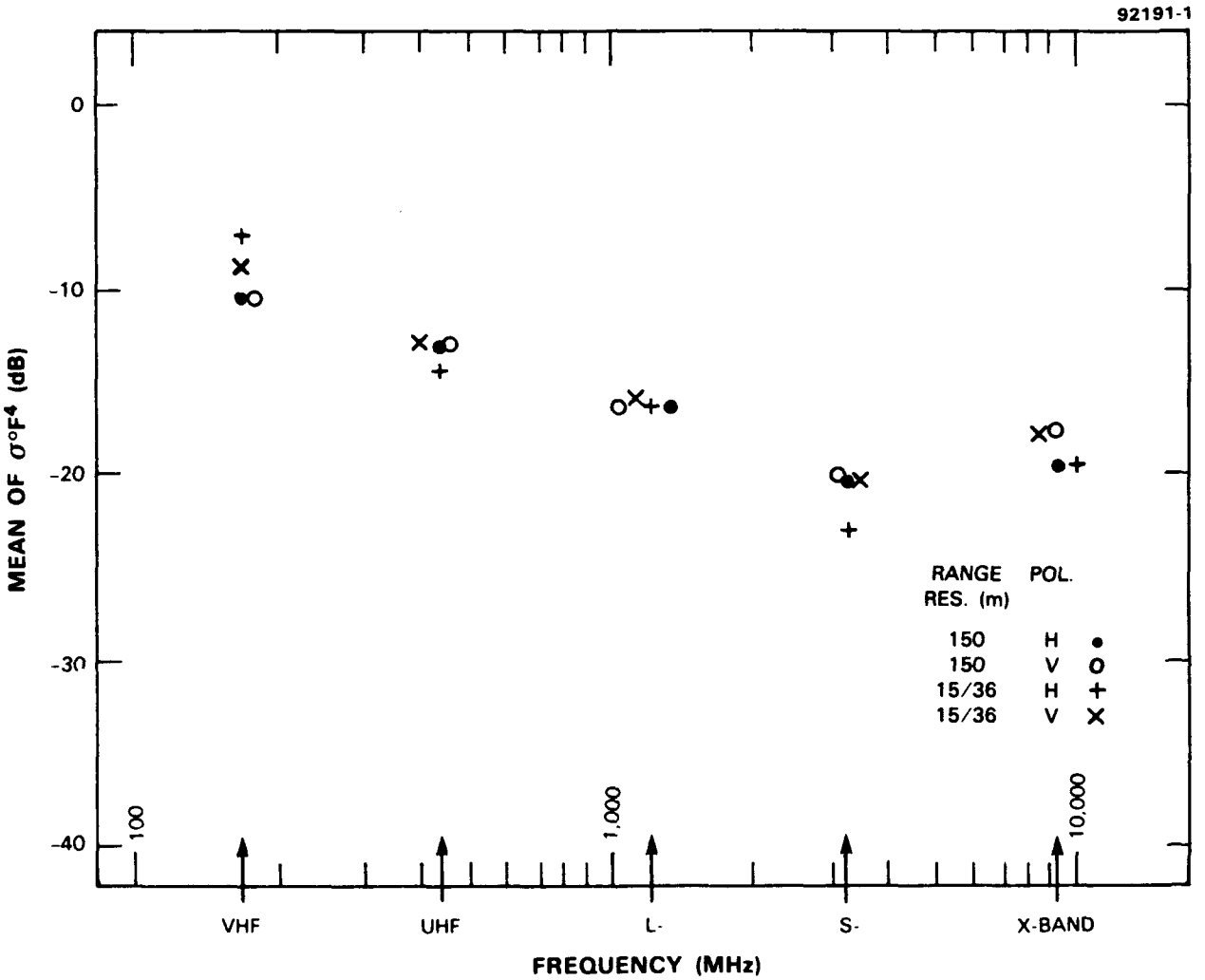

Figure E-44. Mean clutter strength versus frequency at Scranton. For the Scranton repeat sector, depression angle = 1.0 deg, landform = 7-4-3, land cover = 43-12-11, range = 8 to 13.9 km, azimuth = 300 to 320 deg.

(a)

(b)

Figure E 45. Phase One at Cold Lake (a) Phase One erected beside L-band (search) and S-band (height-finder) radars, Cold Lake Station, Pine Tree Line and (b) from a point well out in repeat sector, looking SE to treed ridge farther out

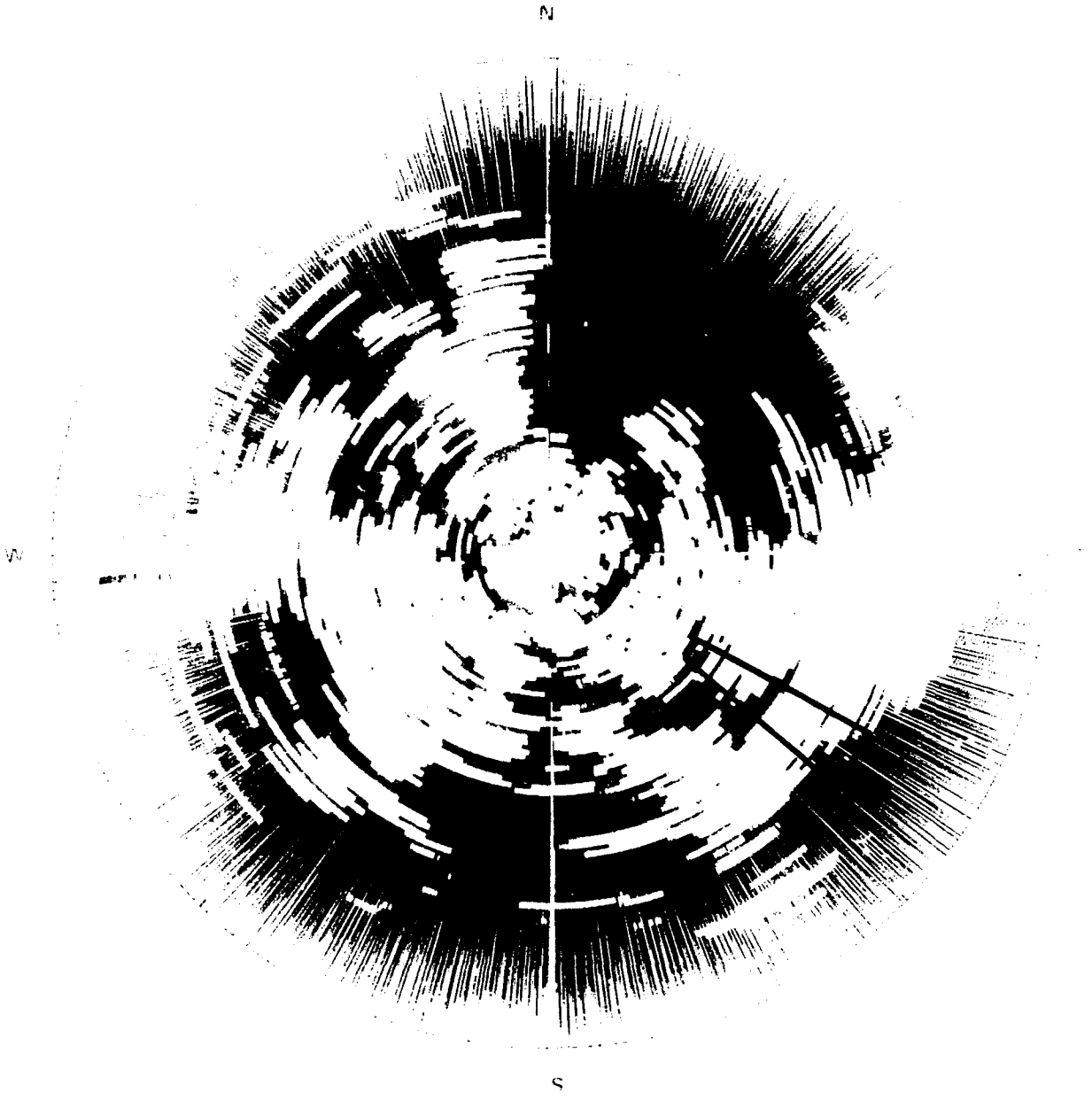

Figure E-46 PPI clutter map and repeat sector at Cold Lake. Repeat sector is outlined in black. Maximum range = 15 km. VHF, 150-m pulse, horizontal polarization; cells with $\sigma^{o}F^{4} \geq -40$ dB are white.

SITE = COLD LAKE RDF = RUTV05.RDF;1

LC = 43 21 0 LF = 3 7 TC = 4 DA = 0.19 DAC = 0.04 PN = R99 DATE = 06-DEC-82

	SHDWUB	SHDWLB	SHDLSS		SHDW	SHDLSS			
MEAN	-15.88	-15.88	-15.84	WEIB0	0.831E+00	0.837E+00	SIG(MAX)		-2
SD	-11.72	-11.72	-11.70	WEIB1	0.356E-01	0.361E-01	NOI(MAX)		-56
COS	6.30	6.30	6.28	WEIR2	0.983E+00	0.982E+00	SAT(MAX)		999
COK	14.01	14.01	13.97	WEISS	0.141E+00	0.158E+00	SIG(MIN)		-62
SPDL	-999.00	-999.00	-999.00	LOGB0	0.166E+01	0.166E+01	NOI(MIN)		-79
SPDR	5.57	5.57	5.56	LOGB1	0.560E-01	0.564E-01	SAT(MIN)		999
DBME	-29.07		-28.81	LOGR2	0.974E+00	0.975E+00	50	-29.0	-29.0
DBSD	13.17		12.87	LOGSS	0.545E+00	0.538E+00	70	-21.0	-21.0
DBCOS	-0.15		-0.07				90	-11.0	-11.0
DBCOK	2.44		2.29				99	-4.0	-4.0

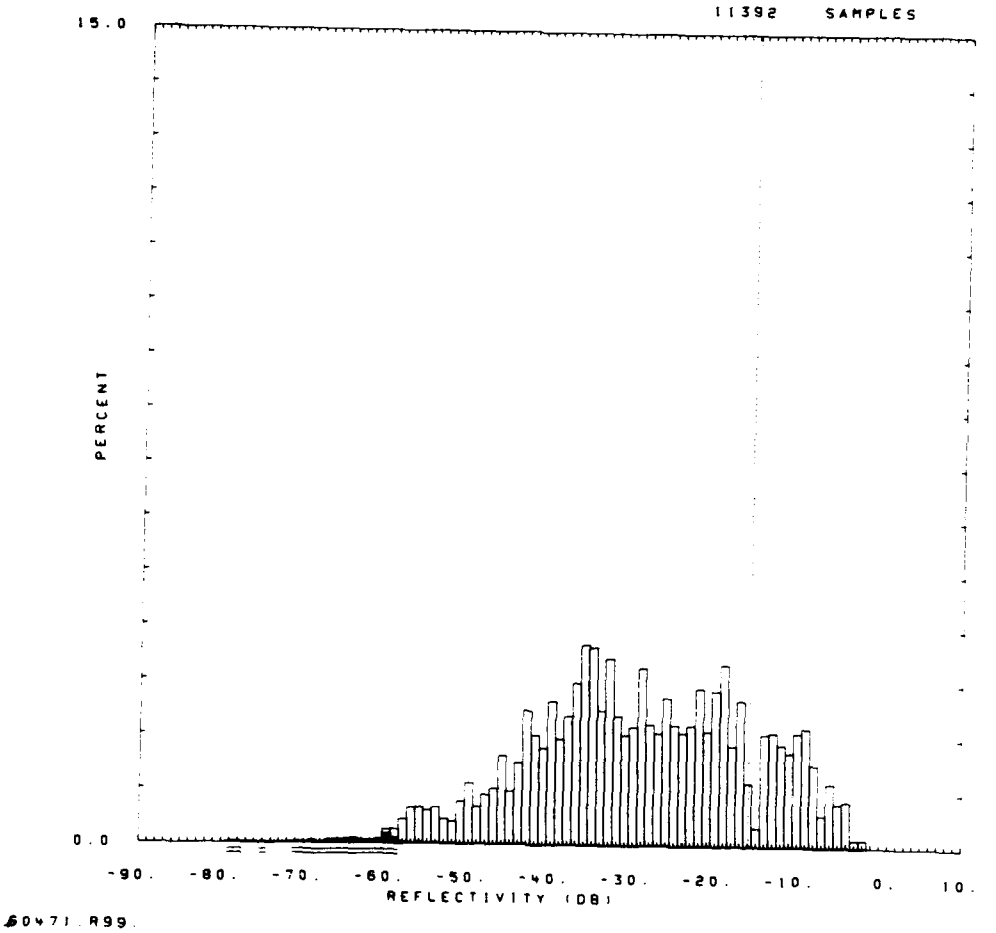

Figure E-47. Clutter strength histogram for Cold Lake repeat sector. UHF, 36-m pulse, vertical polarization.

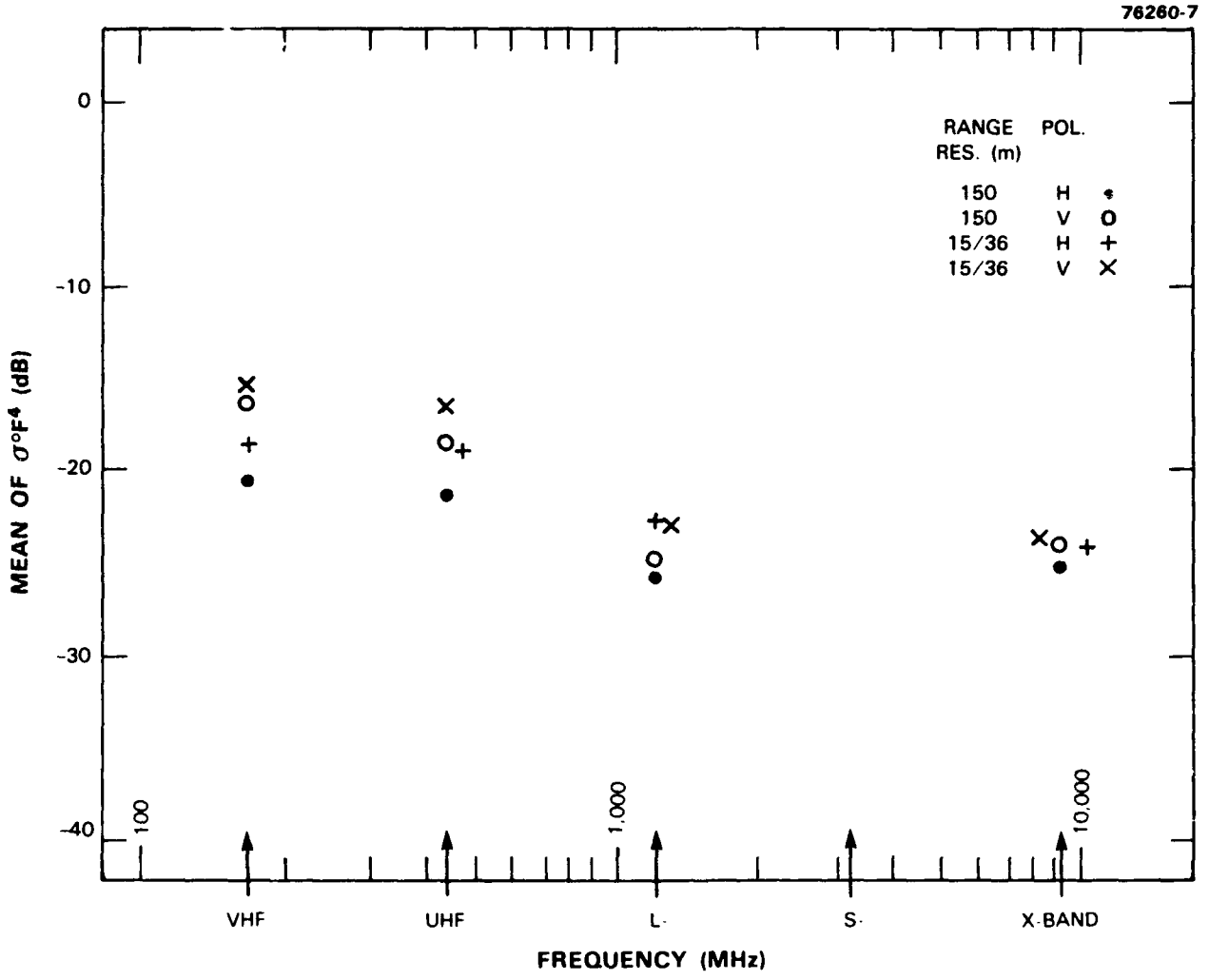

Figure E-48. Mean clutter strength versus frequency at Cold Lake. For the Cold Lake repeat sector, depression angle = 0.2 deg, landform = 3-7, land cover = 43-21, range = 5 to 10.9 km, azimuth = 120 to 130 deg. Comment: hardware problems precluded useful data collection at S-band.

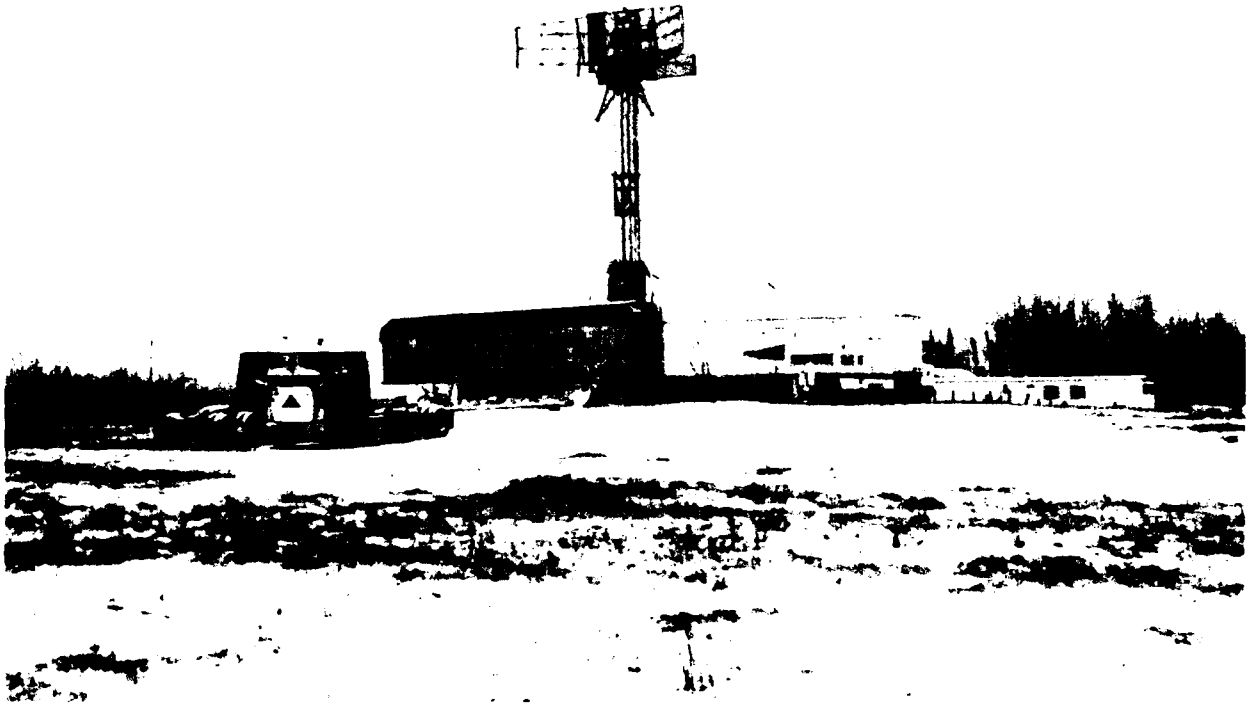

Figure E-49. Phase One at Woking. Equipment on site

Figure E-50. PPI clutter map and repeat sector at Woking. Repeat sector is outlined in black. Maximum range = 20 km. S-band, 15-m pulse, horizontal polarization; cells with $\sigma^{\circ}F^{4} \geq -40$ dB are red

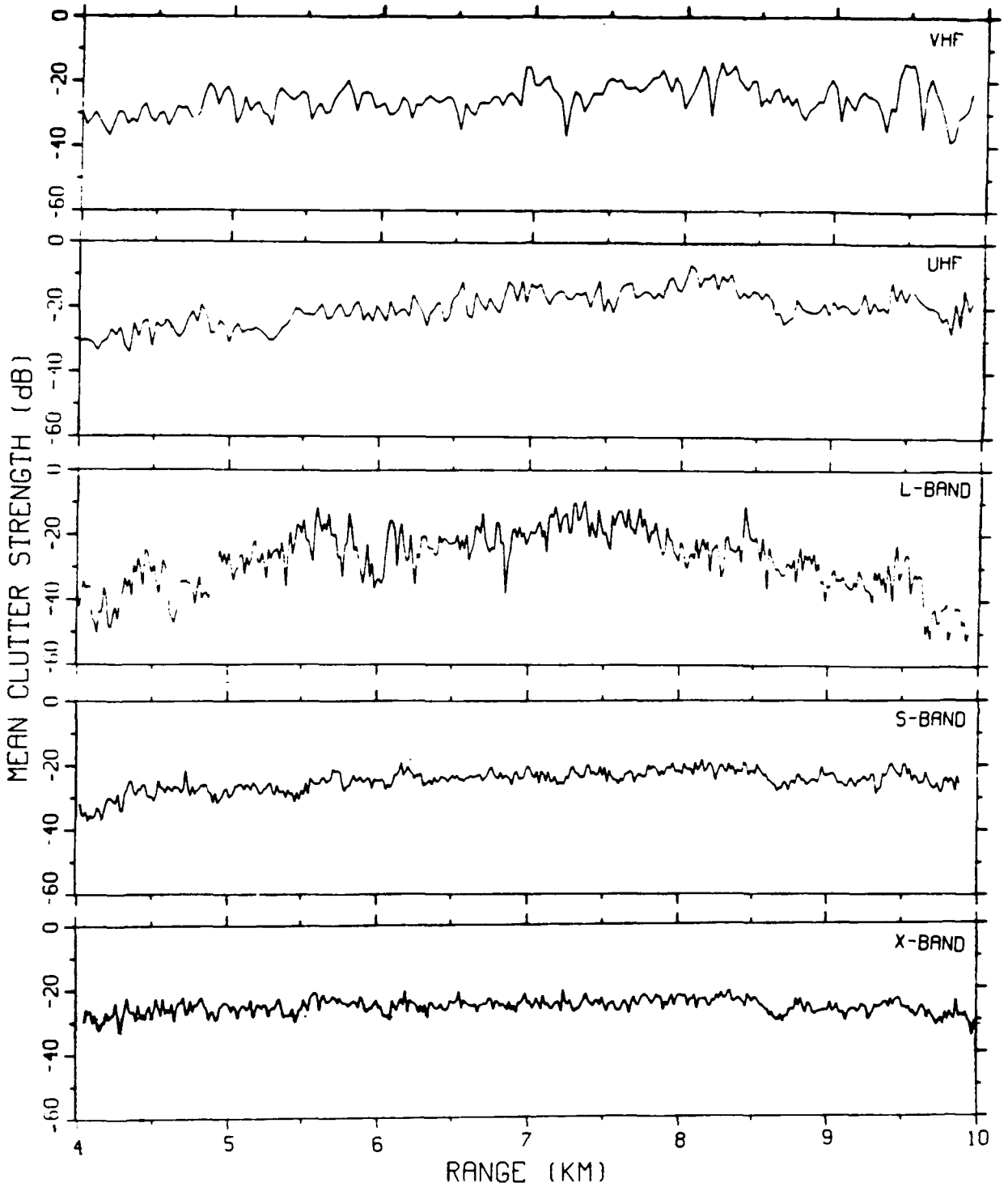

Figure E-51. Mean clutter strength versus range at Woking. Repeat sector data. Vertical polarization, 15/36-m pulse length. Data shown range gate by range gate, averaged in azimuth over 18 deg.

SITE = WOKING RDF = RUTV05.RDF;1

LC = 43 0 0 LF = 2 7 TC = 4 DA = 0.18 DAC = 0.04 PN = R99 DATE = 10-NOV-83

	SHOWU8	SHOWL8	SHOLSS		SHOW	SHOLSS			
MEAN	-16.27	-16.27	-16.26	WEIB0	0.105E+01	0.104E+01	SIG(MAX)		-1
SD	-12.04	-12.04	-12.04	WEIB1	0.548E-01	0.545E-01	NOI(MAX)		-53
COS	8.37	8.37	8.36	WEIR2	0.990E+00	0.989E+00	SAT(MAX)		999
COK	18.09	18.09	18.07	WEISS	0.846E-01	0.783E-01	SIG(MIN)		-54
SPDL	-999.00	-999.00	-999.00	LOGB0	0.209E+01	0.210E+01	NOI(MIN)		-68
SPDR	5.62	5.62	5.61	LOGB1	0.887E-01	0.897E-01	SAT(MIN)		999
DBME	-23.10		-22.98	LOGR2	0.995E+00	0.995E+00	50	-22.0	-22.0
DBSD	8.74		8.51	LOGSS	0.110E+00	0.906E-01	70	-18.0	-18.0
DBCOS	-0.54		-0.38				90	-13.0	-13.0
DBCOK	3.66		3.07				99	-5.0	-5.0

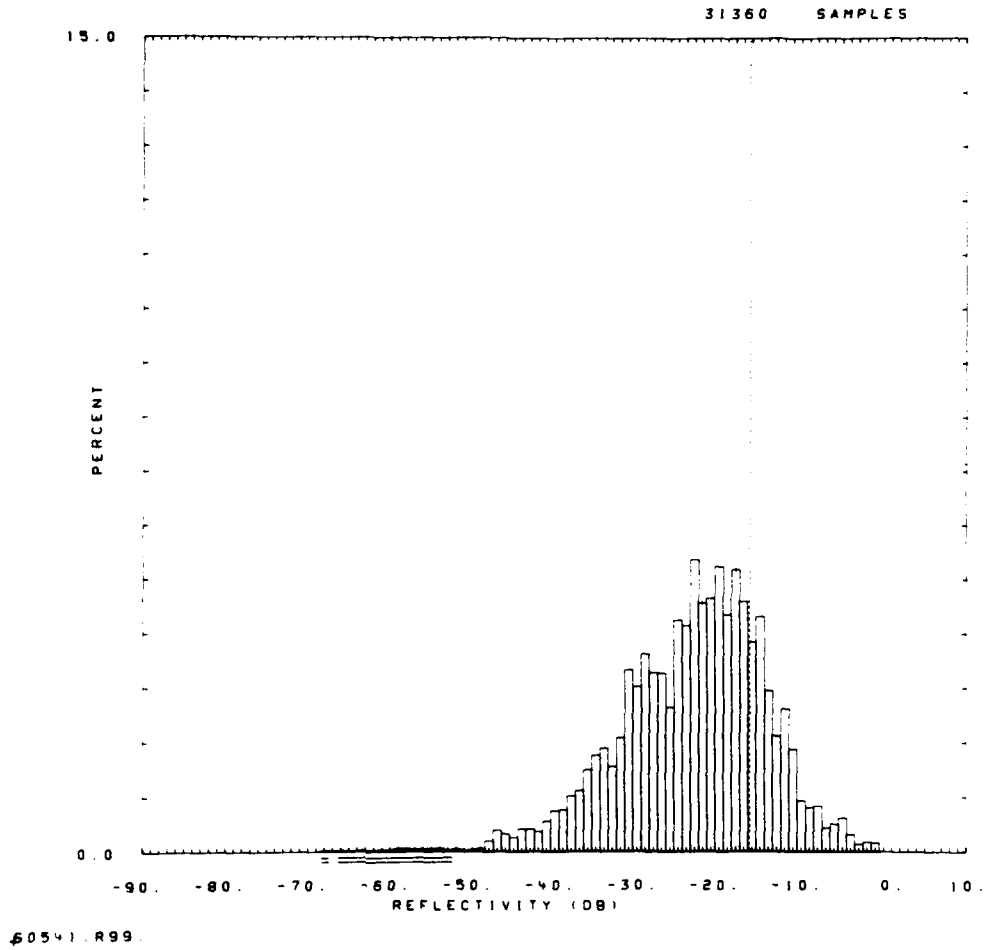

Figure E-52. Clutter strength histogram for Woking repeat sector. UHF, 36-m pulse, vertical polarization.

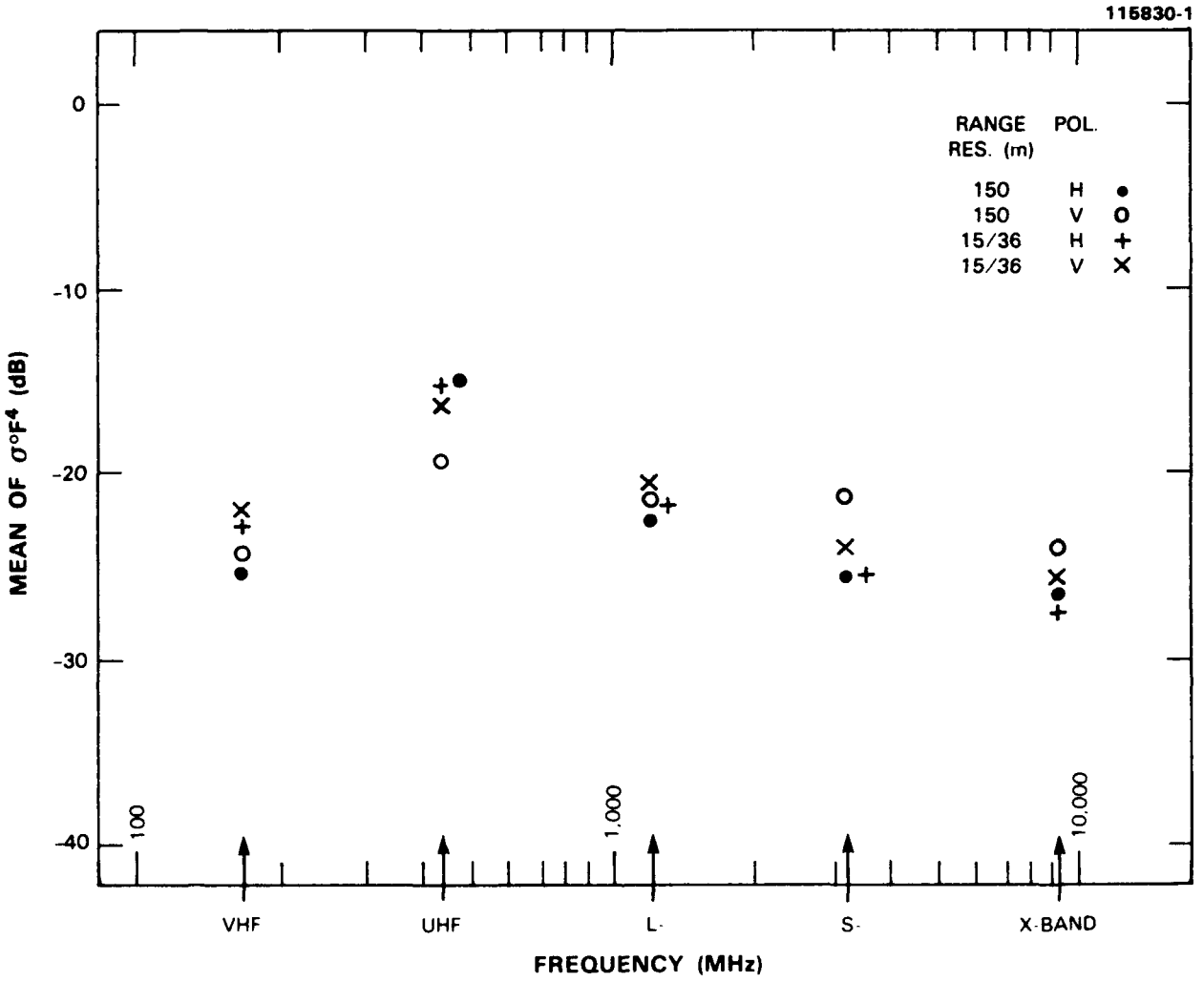

Figure E-53. Mean clutter strength versus frequency at Woking. For the Woking repeat sector, depression angle = 0.2 deg, landform = 2-7, land cover = 43, range = 4 to 9.9 km, azimuth = 118 to 136 deg.

(a)

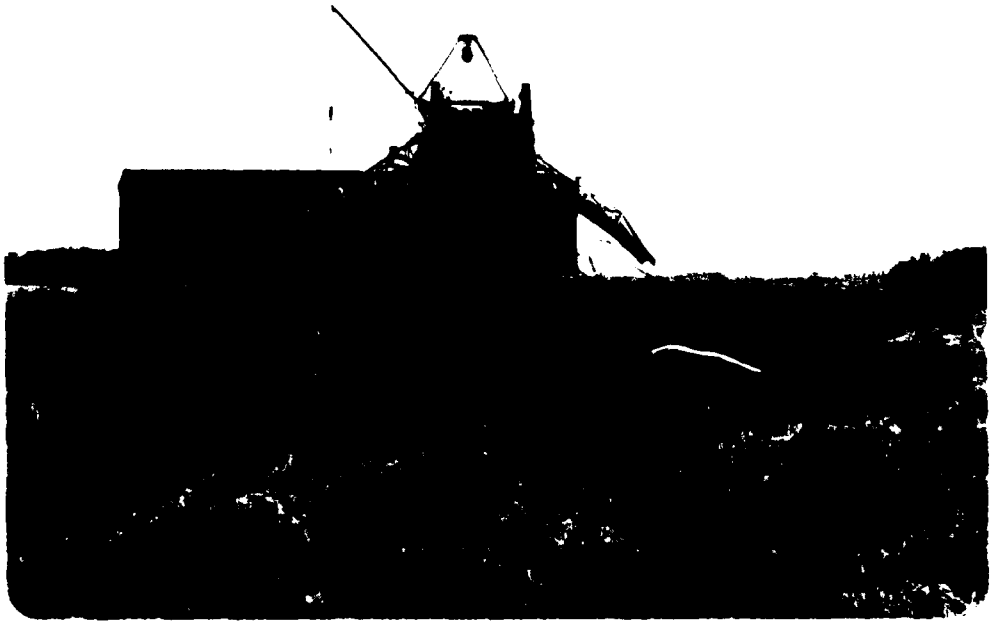

(b)

Figure E-54. Penhold II site photos. (a) Cropland with trees on rising slopes in far distance and (b) assembling antenna reflectors in muddy field

Figure E-55. PPI clutter map and repeat sector at Penhold II. Repeat sector is outlined in black. Maximum range = 25 km; S-band, 150-m pulse, horizontal polarization; nominally, cells with $\sigma^{o}F^{4} \geq -50$ dB are red, but precise threshold is unknown due to uncertain calibration.

SITE = PENHOLD II RDF = RUTV05.RDF;1

LC = 21 41 11 LF = 4 2 TC = 2 DA = 0.08 DAC = 0.03 PN = R99 DATE = 14-OCT-12

	SHDWUB	SHDWLB	SHDLSS		SHDW	SHDLSS			
MEAN	-13.91	-13.91	-13.59	WEIB0	0.723E+00	0.742E+00	SIG(MAX)		5
SD	-7.71	-7.71	-7.55	WEIB1	0.300E-01	0.329E-01	NOI(MAX)		-45
COS	9.70	9.70	9.55	WEIR2	0.995E+00	0.987E+00	SAT(MAX)		999
COK	20.84	20.84	20.53	WEISS	0.365E-01	0.119E+00	SIG(MIN)		-73
SPDL	-999.00	-999.00	-999.00	LOGB0	0.160E+01	0.160E+01	NOI(MIN)		-84
SPDR	7.14	7.14	7.00	LOGB1	0.523E-01	0.551E-01	SAT(MIN)		999
DBME	-29.91		-28.05	LOGR2	0.987E+00	0.991E+00	50	-30.0	-28.0
DBSD	13.90		12.57	LOGSS	0.287E+00	0.224E+00	70	-22.0	-21.0
DBCOS	-0.01		0.16				90	-11.0	-11.0
DBCOK	2.40		2.25				99	-1.0	-1.0

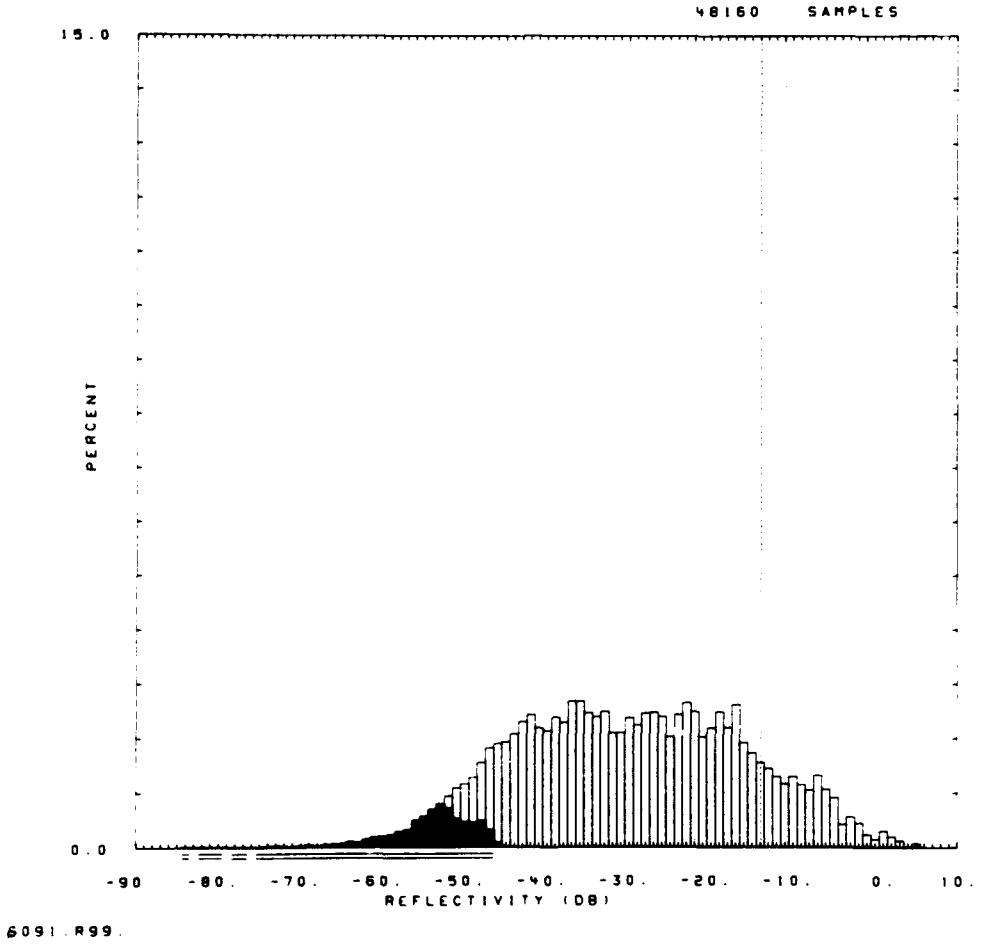

Figure E-56. Clutter strength histogram for Penhold II repeat sector. UHF, 36-m pulse, vertical polarization.

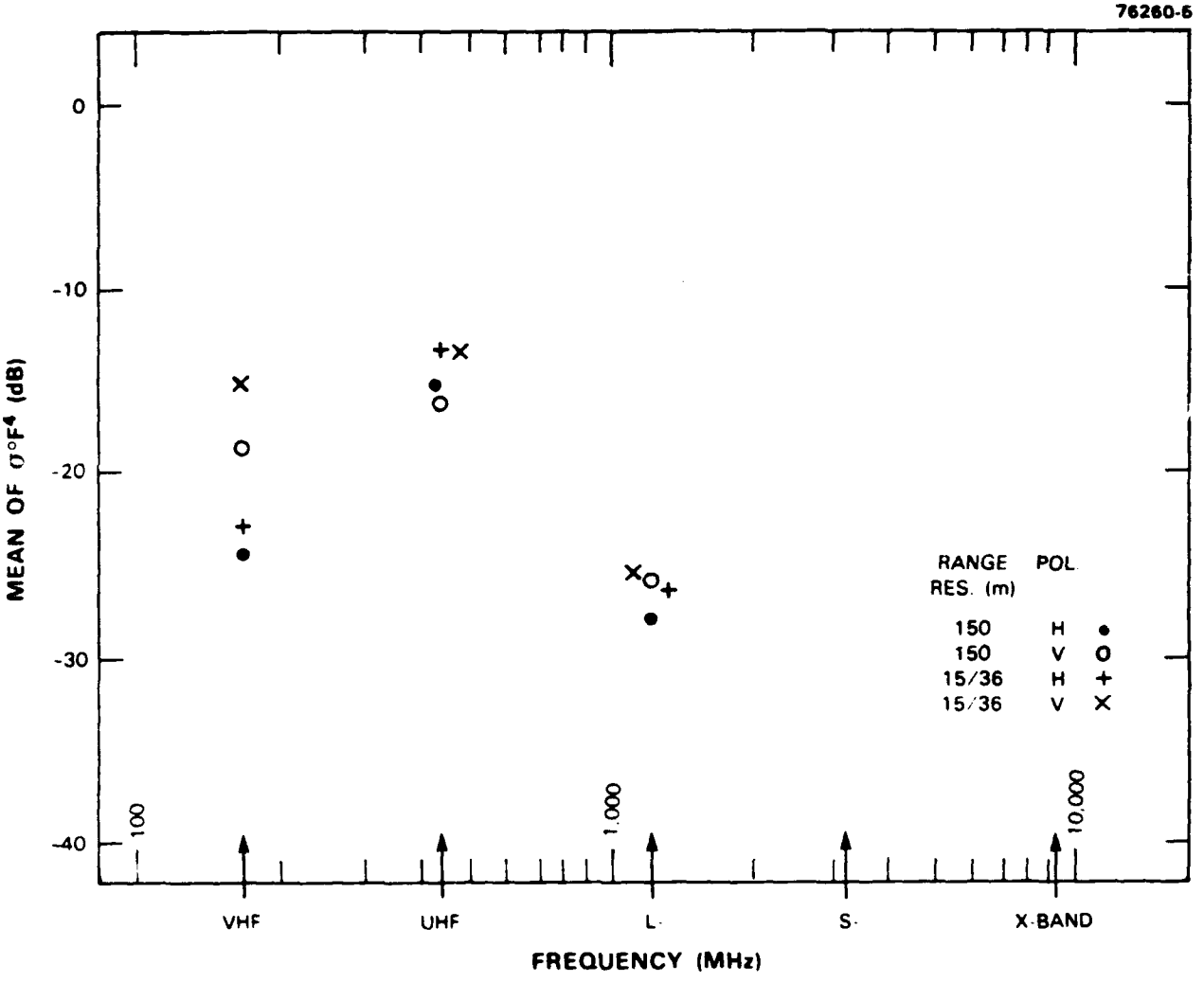

Figure E-57. Mean clutter strength versus frequency at Penhold II. For the Penhold II repeat sector, depression angle = 0.1 deg, landform = 4-2, land cover = 21-41-11, range = 15 to 24 km, azimuth = 54 to 74 deg. Comment: hardware problems precluded useful data collection at both X- and S-bands.

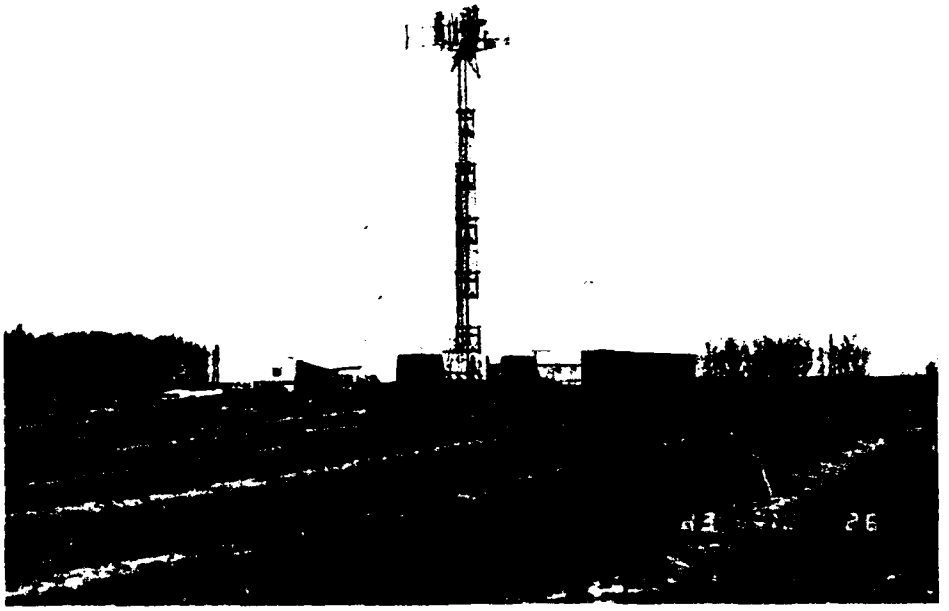

(a)

NNW

(b)

Figure F-58. Phase One at Peace River South II tail. Looking west to equipment on site and across valley of Peace River and sky tower top view NNW to repeat sector across valley beginning at 12 km range at far right.

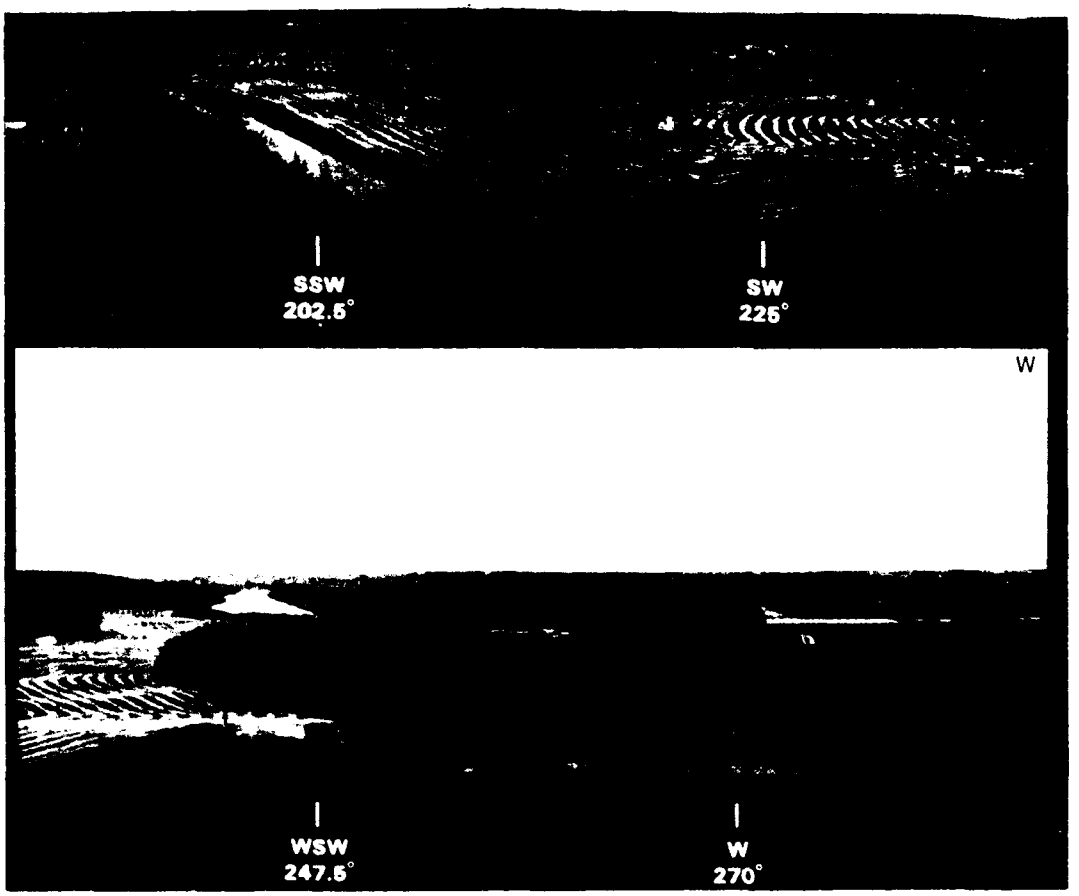

Figure E-59. Terrain panorama to the south and west at Peace River, Alberta

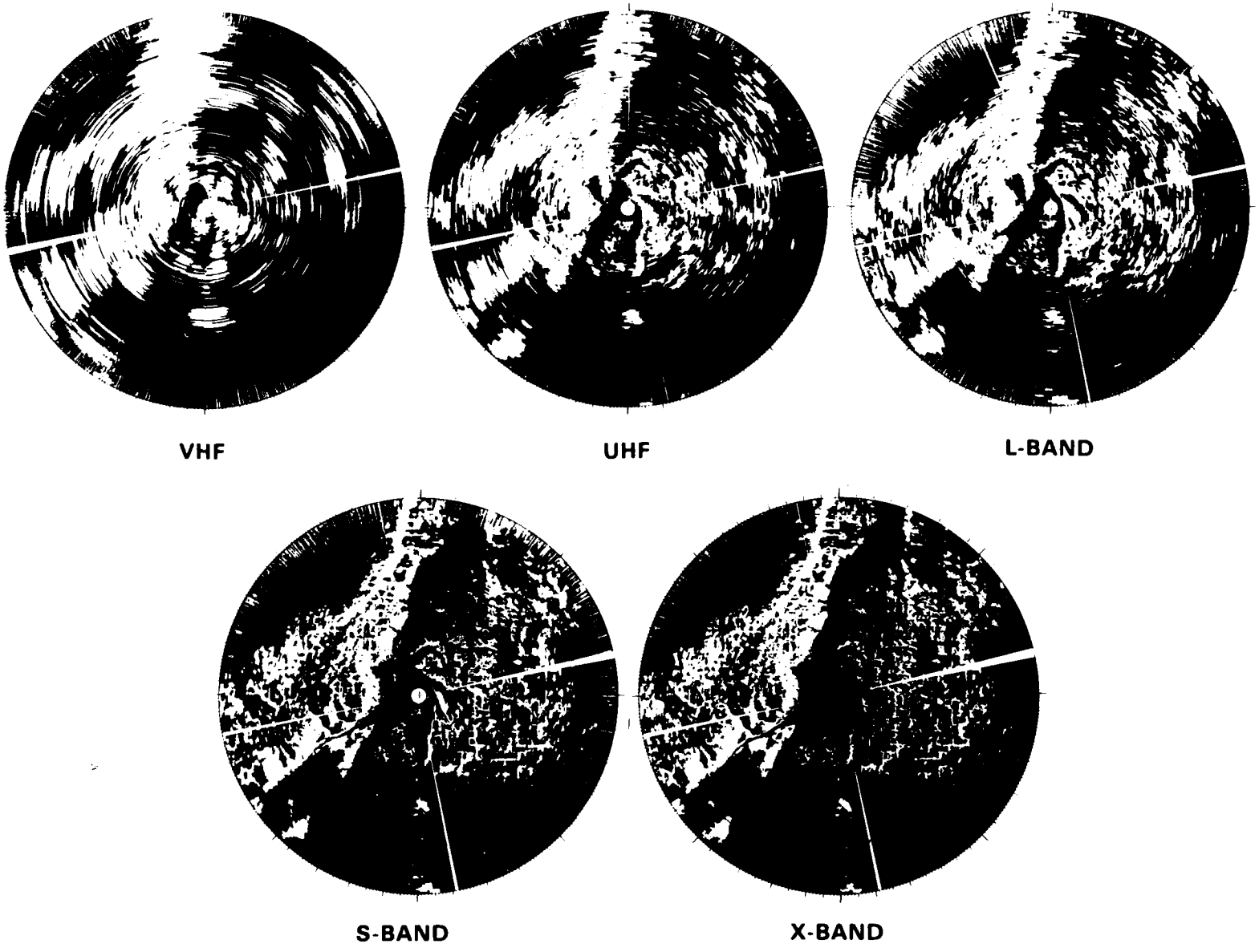

Figure E-60. Multifrequency ground clutter maps at Peace River South II. $\sigma^{\circ}F^{4} \geq -40$ dB, 23-km maximum range.

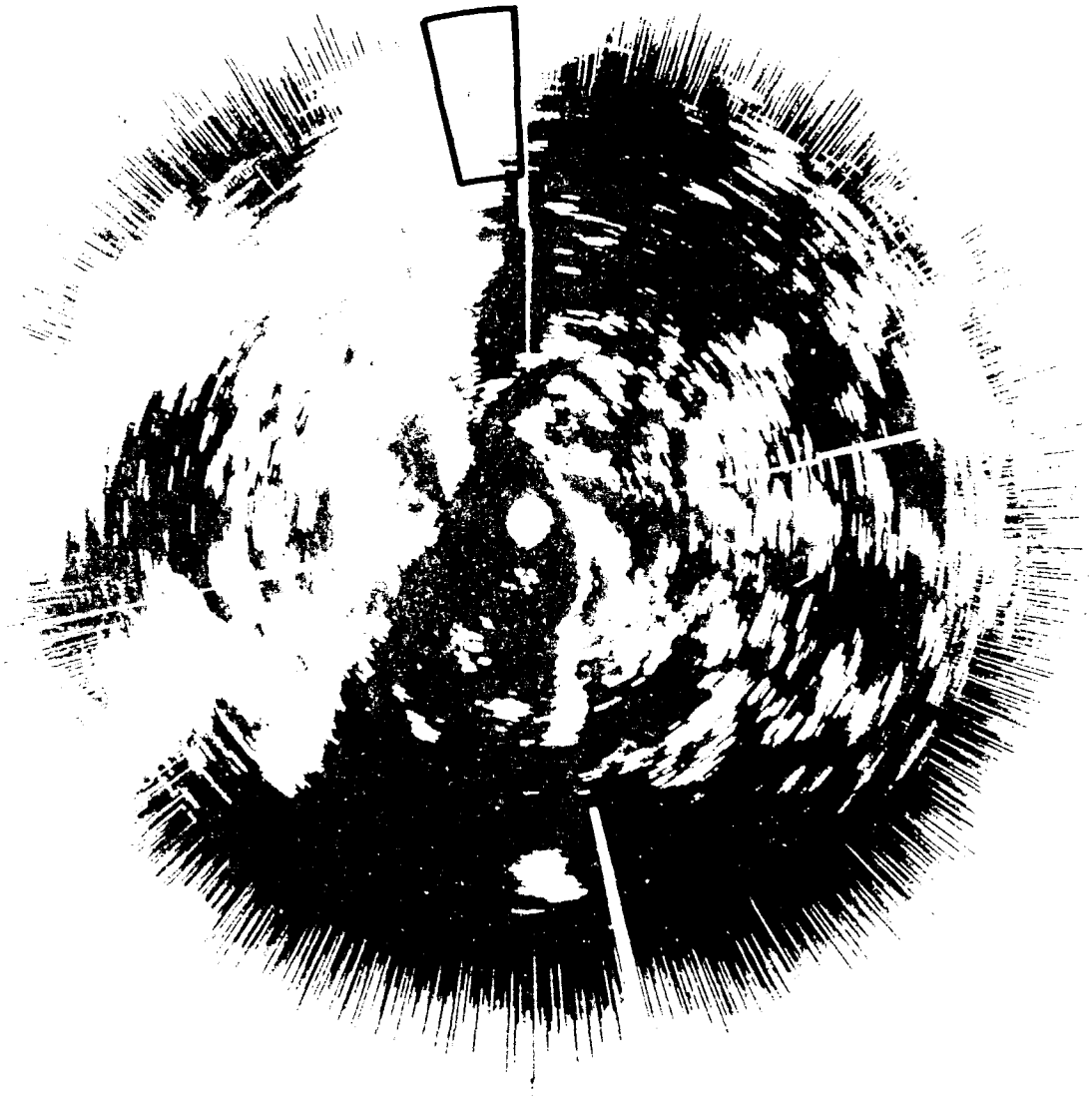

Figure E.61 PPI clutter map and repeat sector at Peace River South II. Repeat sector is outlined in black. Maximum range = 20 km. UHF, 36 m pulse, horizontal polarization, cells with $\sigma^{0}F^{4} \geq 40$ dB are white.

SITE = PEACE RIVER STH II RDF = RUTV05.RDF;1

LC = 21 41 0 LF = 2 7 TC = 2 DA = -0.11 DAC = 0.00 PN = R99 DATE = 18-OCT-83

	SHOWUB	SHOWLB	SHOLSS
MEAN	-15.62	-15.62	-15.62
SD	-11.44	-11.44	-11.44
COS	7.05	7.05	7.05
COK	15.34	15.34	15.34
SPOL	-999.00	-999.00	-999.00
SPOR	5.58	5.58	5.58
DBME	-24.69		-24.68
DBSD	10.05		10.04
DBCOS	-0.17		-0.17
DBCOK	2.64		2.62

	SHOW	SHOLSS
WEIB0	0.928E+00	0.929E+00
WEIB1	0.462E-01	0.462E-01
WEIR2	0.984E+00	0.984E+00
WEISS	0.138E+00	0.138E+00
LOGB0	0.187E+01	0.187E+01
LOGB1	0.744E-01	0.744E-01
LOGR2	0.992E+00	0.992E+00
LOGSS	0.164E+00	0.164E+00

SIG(MAX)		-2
NOI(MAX)		-56
SAT(MAX)		999
SIG(MIN)		-55
NOI(MIN)		-58
SAT(MIN)		999
50	-24.0	-24.0
70	-19.0	-19.0
90	-11.0	-11.0
99	-5.0	-5.0

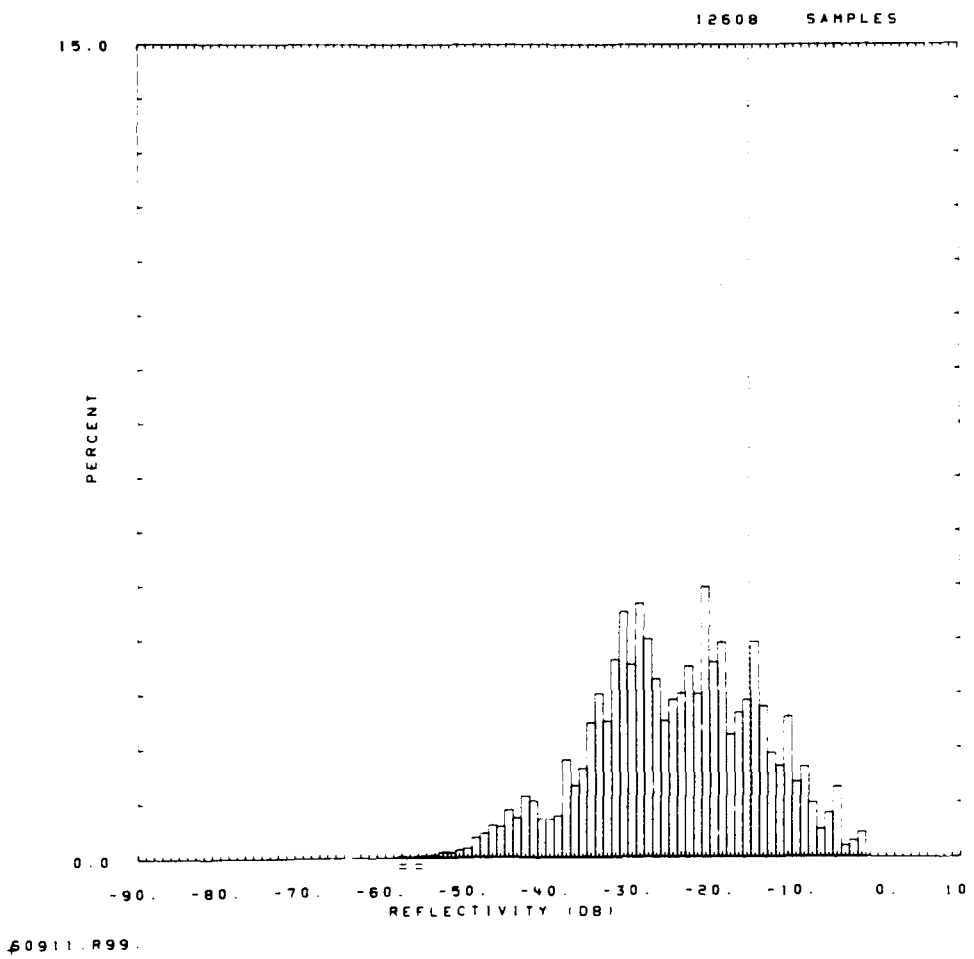

Figure E-62. Clutter strength histogram for Peace River South II repeat sector. UHF, 36-m pulse, vertical polarization.

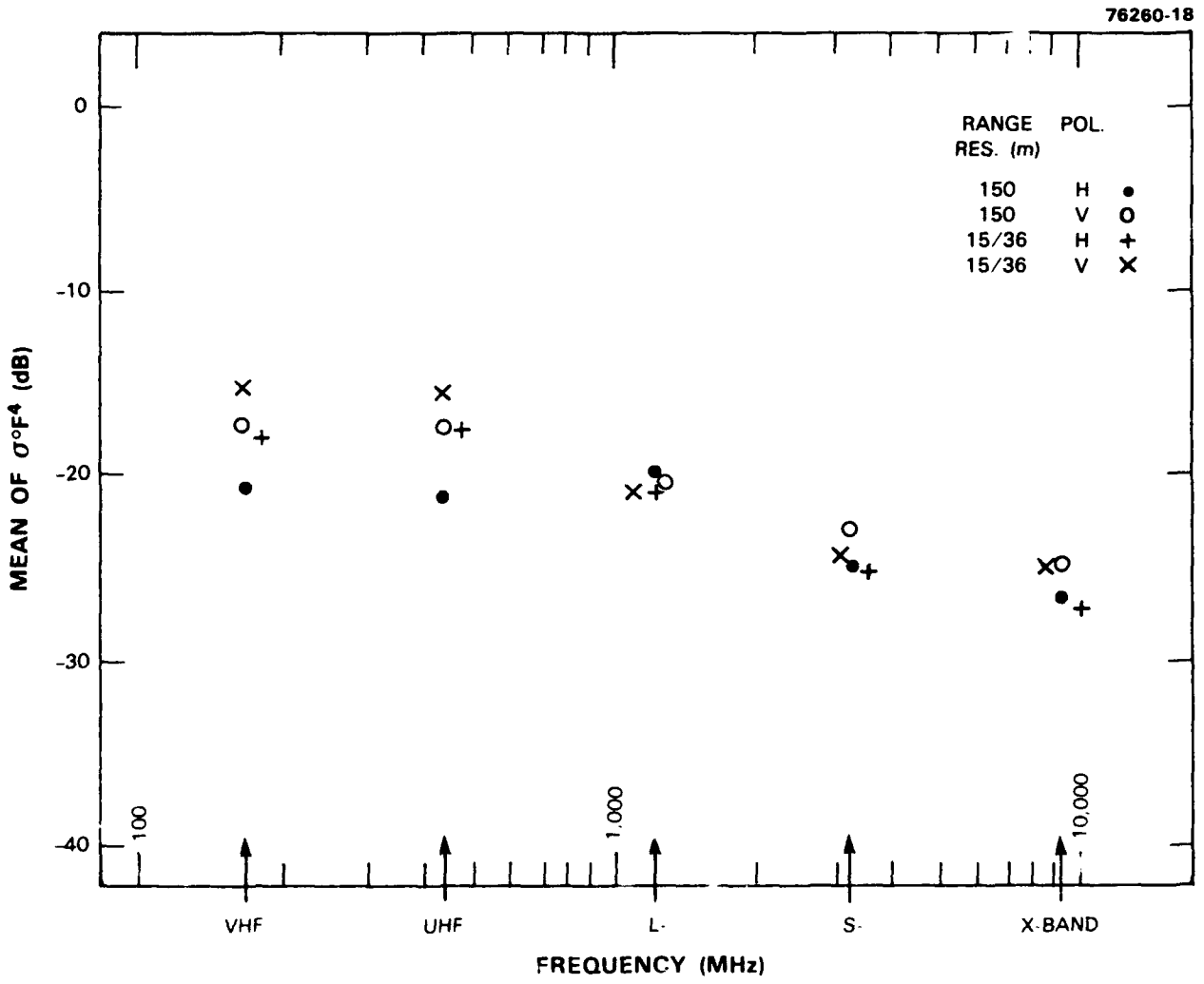

Figure E-63. Mean clutter strength versus frequency at Peace River South II. For the Peace River South II repeat sector, depression angle = -0.1 deg, landform = 2-7, land cover = 21-41, range = 12 to 17.9 km, azimuth = 348 to 358 deg.

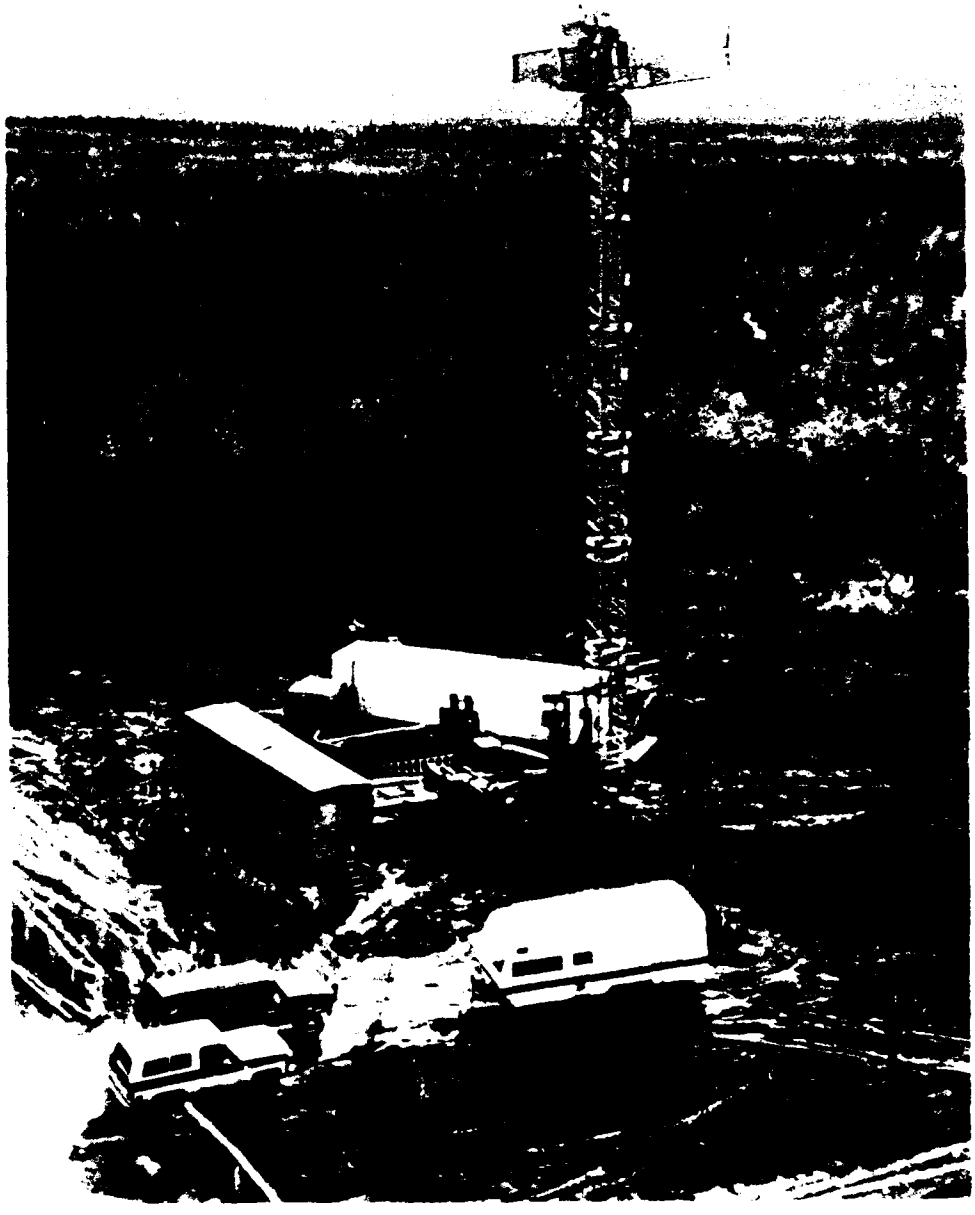

Figure E-64. Phase One at Puskwaskau. Antenna tower erected to 100 ft, October 1985.

Figure E-65. PPI clutter map and repeat sector at Puskwaskau. Repeat sector is outlined in black. Maximum range = 20 km, L band, 15-m pulse, horizontal polarization, cells with $\sigma^{\circ}F^{4} \geq 40$ dB are white.

SITE = PUSKWASKAU RDF = RVFH24.RDF;1

LC = 43 0 0 LF = 2 0 TC = 4 DA = 2.08 DAC = 0.0 PN = R99 DATE = 08-OCT-83

	SHDWUB	SHDWLB	SHDLSS		SHDW	SHDLSS			
MEAN	-15.12	-15.12	-15.12	WEIB0	0.844E+00	0.844E+00	SIG(MAX)		0
SD	-9.72	-9.72	-9.72	WEIB1	0.405E-01	0.405E-01	NOI(MAX)		999
COS	8.06	8.06	8.06	WEIR2	0.981E+00	0.981E+00	SAT(MAX)		999
COK	16.73	16.73	16.73	WEISS	0.122E+00	0.122E+00	SIG(MIN)		-56
SPDL	-999.00	-999.00	-999.00	LOGB0	0.182E+01	0.182E+01	NOI(MIN)		-999
SPDR	6.50	6.50	6.50	LOGB1	0.707E-01	0.707E-01	SAT(MIN)		999
DBME	-24.91		-24.91	LOGR2	0.986E+00	0.986E+00	50	-25.0	-25.0
DBSD	9.88		9.88	LOGSS	0.270E+00	0.270E+00	70	-19.0	-19.0
DBCOS	-.874E-02		-.874E-02				90	-12.0	-12.0
DBCOK	2.68		2.68				99	-2.0	-2.0

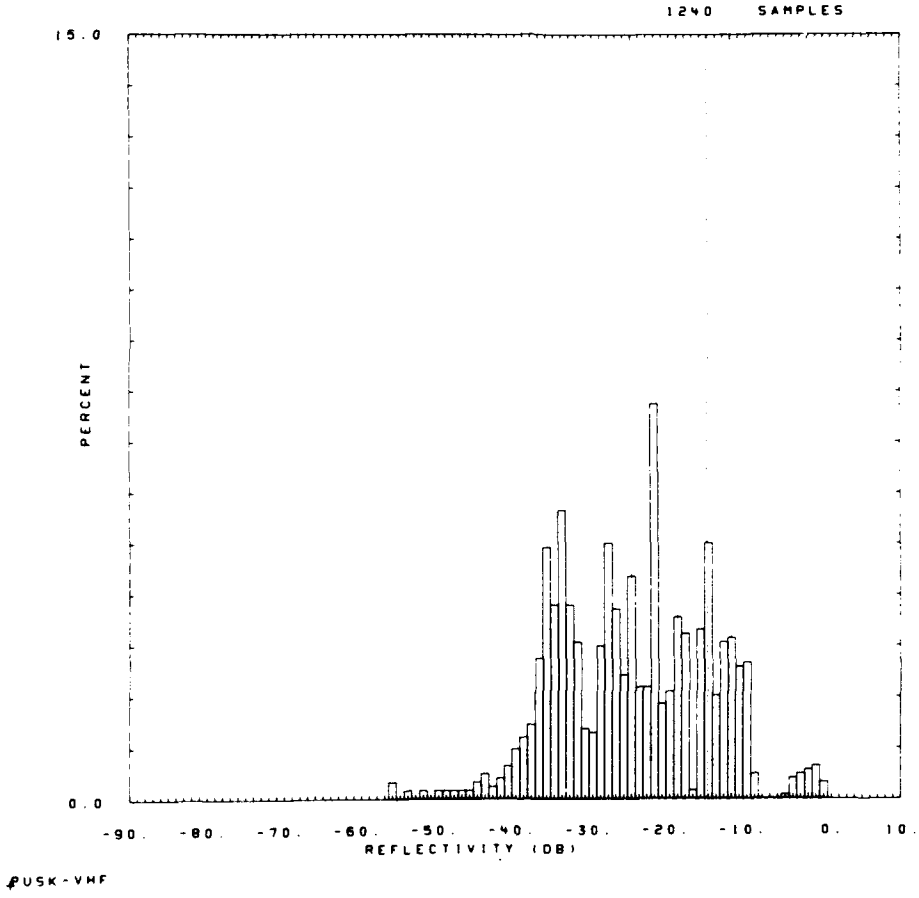

Figure E-66. Clutter strength histogram for Puskwaskau repeat sector. VHF, 150-m pulse, horizontal polarization. Scan mode, 2.0 deg/s.

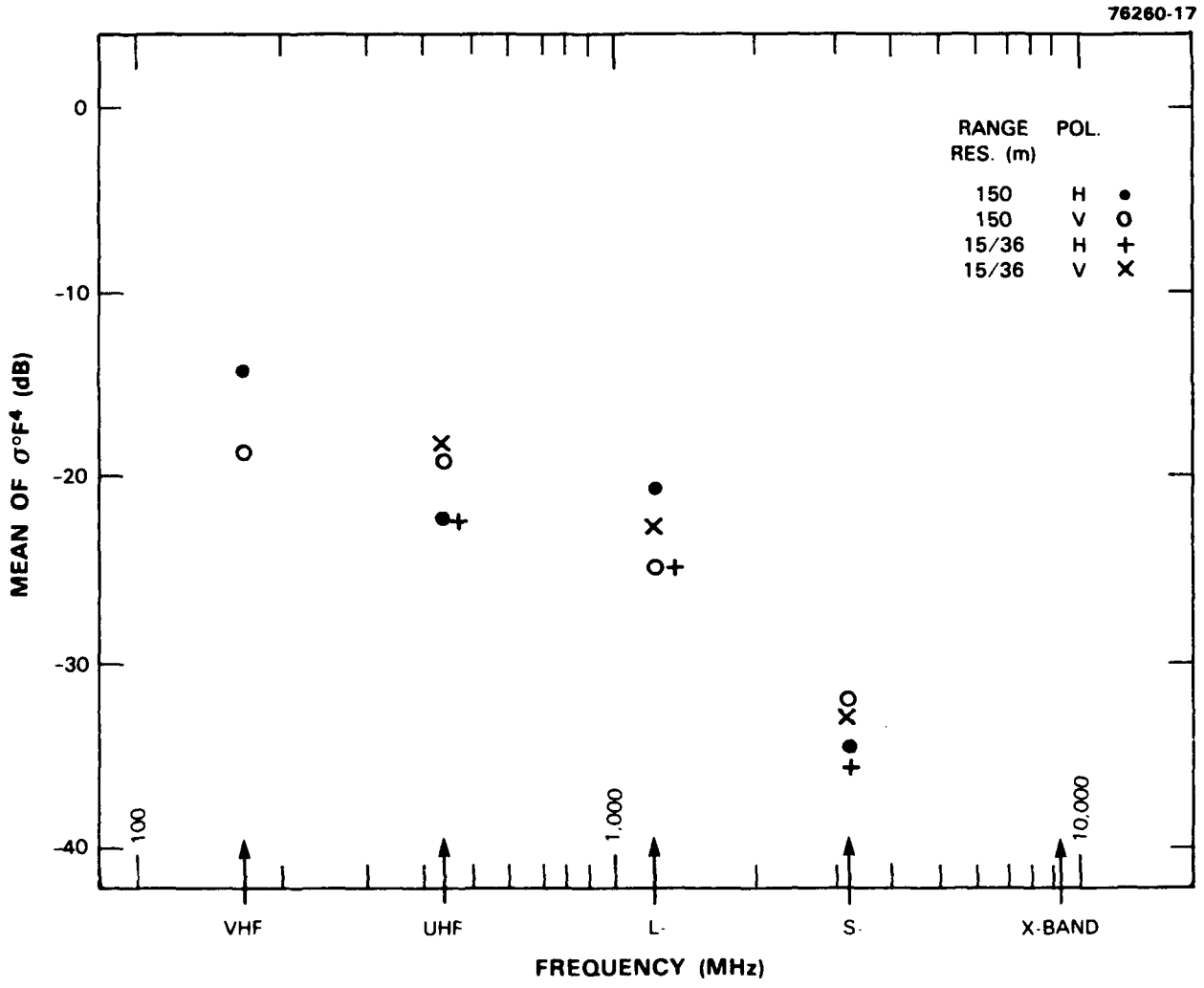

Figure E-67. Mean clutter strength versus frequency at Puskwaskau. For the Puskwaskau repeat sector, depression angle = 2.1 deg, landform = 2, land cover = 43, range = 1 to 6.9 km, azimuth = 230 to 240 deg. Comments: (1) VHF interference precluded high resolution data. (2) X-band transmitter inoperable at this site.

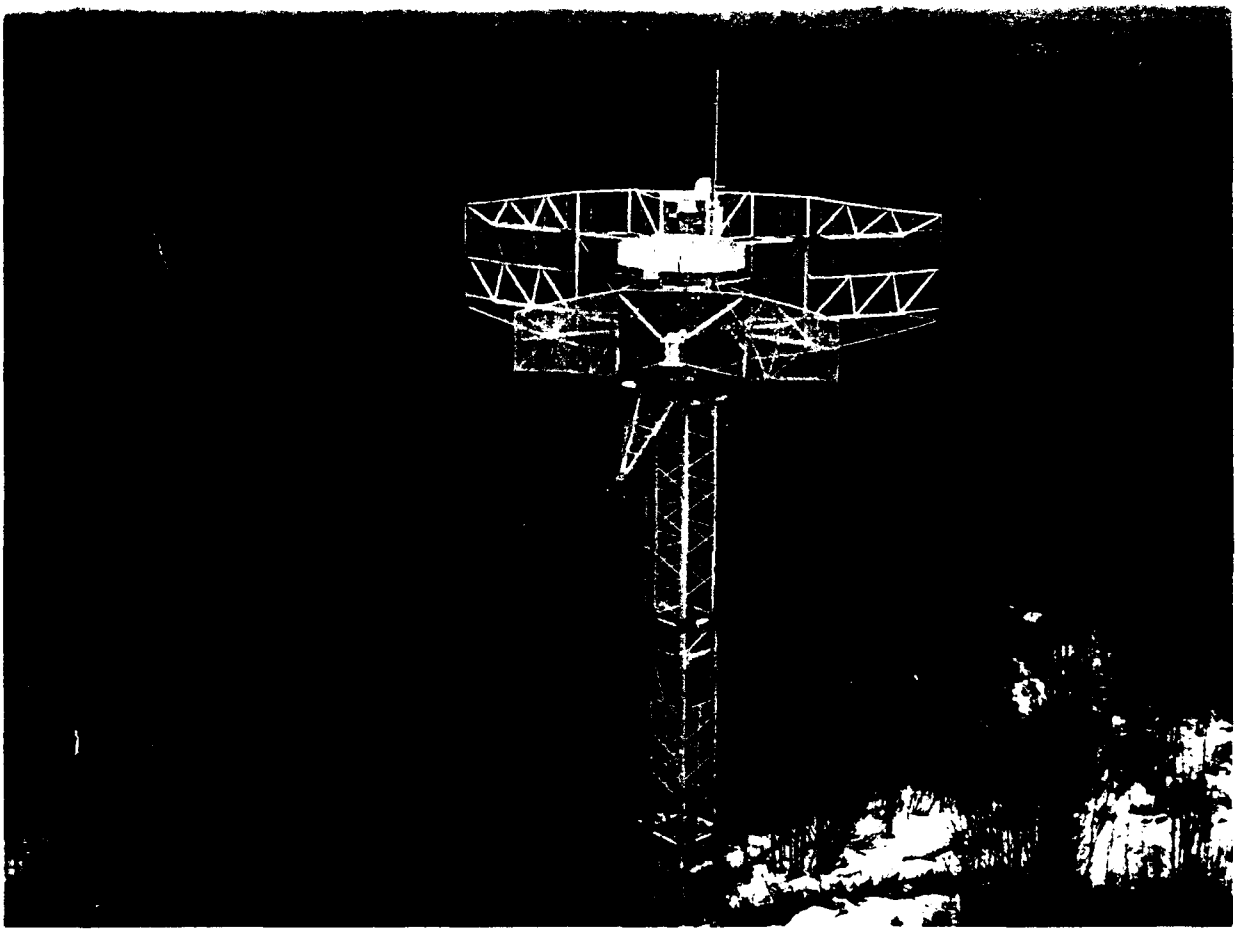

Figure F-68 Phase One at Brazeau April 1983

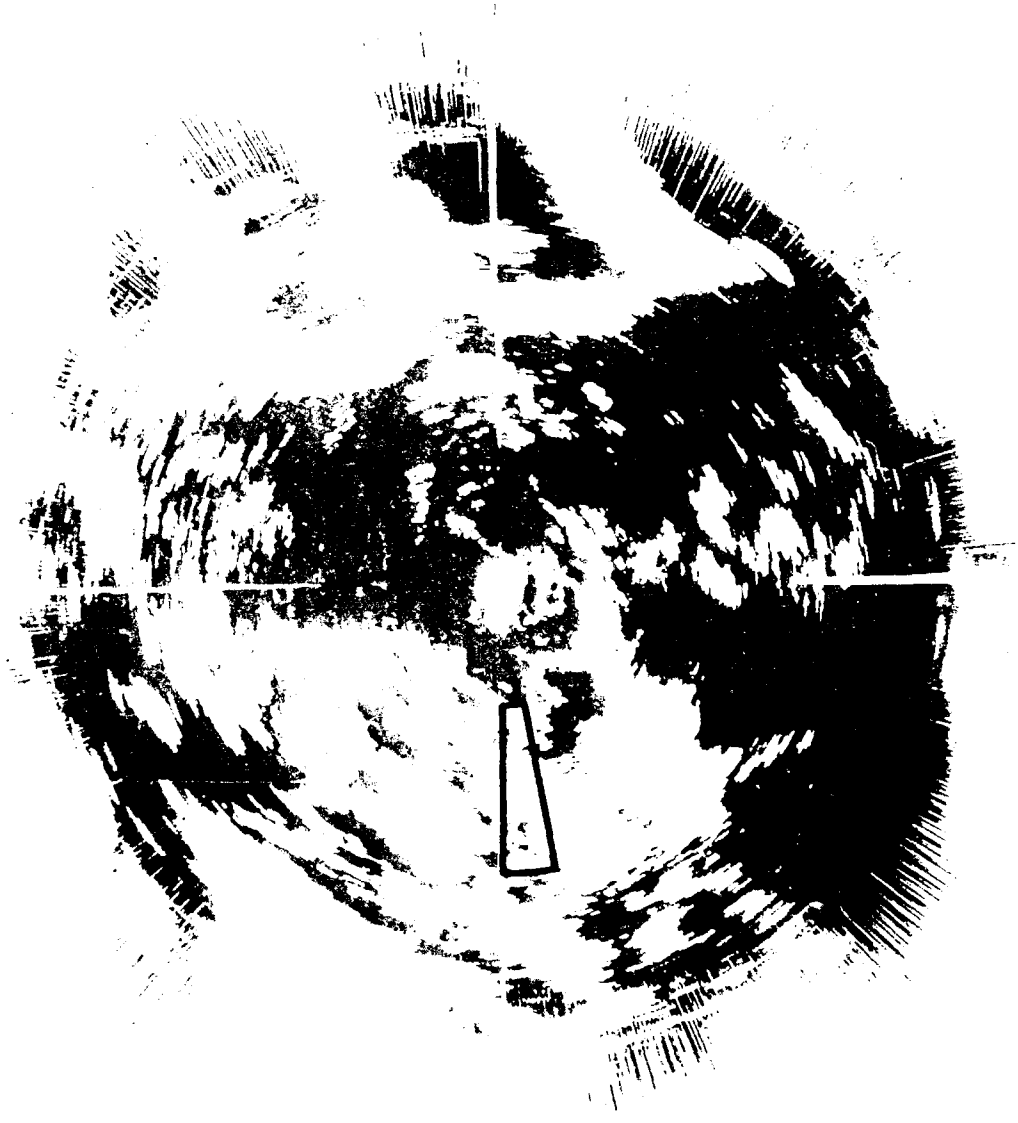

Figure E-59. PPI clutter map and repeat sector at Brazeau. Repeat sector is outlined in black. Maximum range = 20 km, UHF, 36 m pulse, horizontal polarization, cells with $\sigma^{\circ}F^{4} \geq -40$ dB are white. First visit.

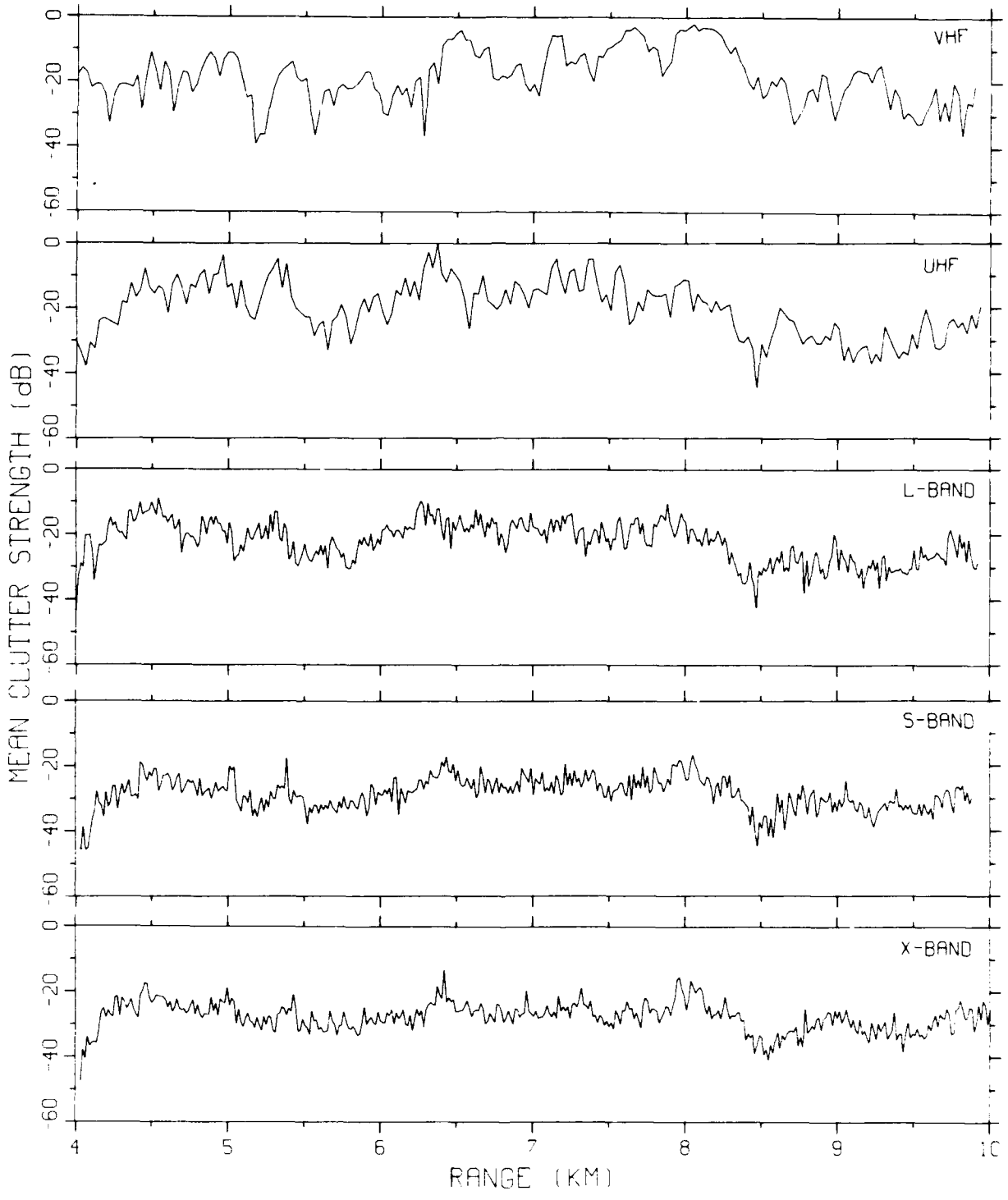

Figure E-70. Mean clutter strength versus range at Brazeau. Repeat sector data. Vertical polarization, 15/36-m pulse length. Data shown range gate by range gate, averaged over 10 deg.

SITE = BRAZEAU RDF = RVTH02.RDF;1

LC = 42 62 41 LF = 3 0 TC = 4 DA = 1.20 DAC = 0.0 PN = R99 DATE = 10-APR-83

	SHDWUB	SHDWLB	SHDLSS		SHDW	SHDLSS			
MEAN	-11.55	-11.55	-11.54	WEIB0	0.773E+00	0.775E+00	SIG(MAX)		-1
SD	-8.97	-8.97	-8.97	WEIB1	0.531E-01	0.533E-01	NOI(MAX)		-52
COS	4.89	4.89	4.88	WEIR2	0.994E+00	0.993E+00	SAT(MAX)		999
COK	11.54	11.54	11.53	WEISS	0.412E-01	0.424E-01	SIG(MIN)		-50
SPDL	-999.00	-999.00	-999.00	LOGB0	0.158E+01	0.156E+01	NOI(MIN)		-63
SPDR	4.49	4.49	4.49	LOGB1	0.824E-01	0.826E-01	SAT(MIN)		999
DBME	-18.43		-18.33	LOGR2	0.972E+00	0.972E+00	50	-17.0	-17.0
DBSD	9.44		9.25	LOGSS	0.439E+00	0.435E+00	70	-13.0	-13.0
DBCOS	-0.60		-0.49				90	-7.0	-7.0
DBCOK	3.29		2.81				99	-1.0	-1.0

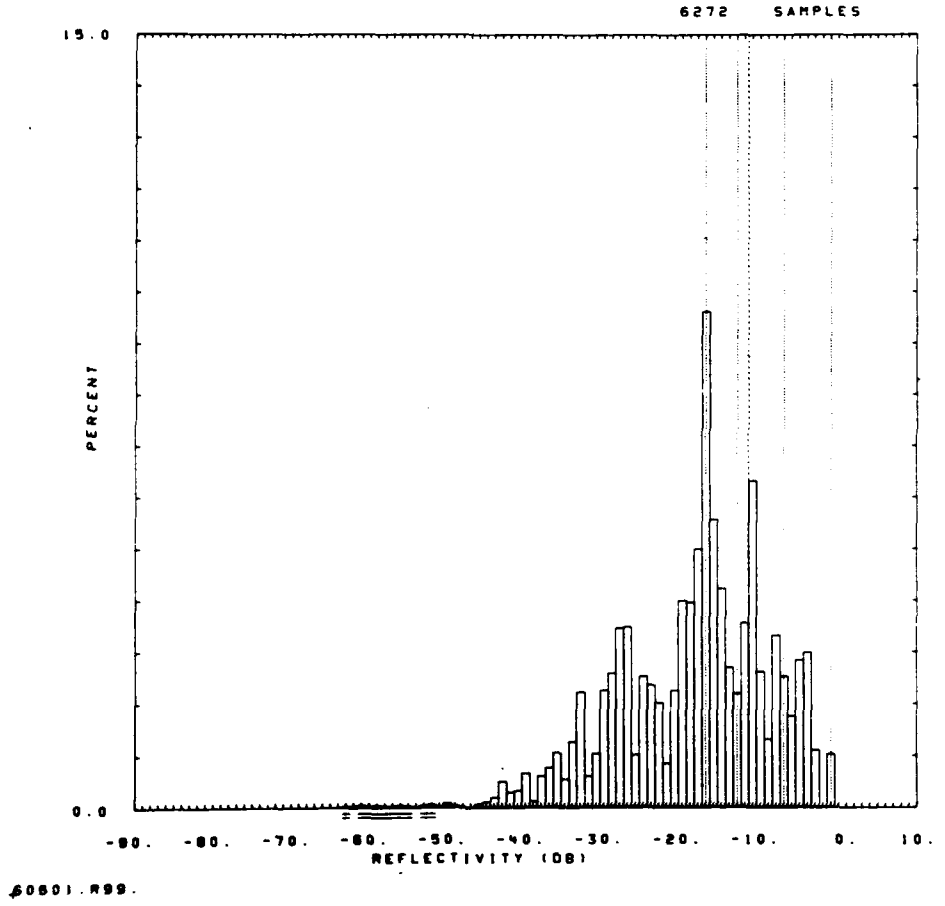

Figure E-71. Clutter strength histogram for Brazeau repeat sector. VHF, 36-m pulse, horizontal polarization. First visit.

SITE = BRAZEAU RDF = RLFH12.RDF;1

LC = 42 62 41 LF = 3 0 TC = 4 DA = 1.18 DAC = 0.59 PN = R99 DATE = 09-APR-83

	SHDWUB	SHDWLB	SHDLSS
MEAN	-22.11	-22.11	-22.08
SD	-18.38	-18.38	-18.37
COS	7.99	7.99	7.98
COK	17.39	17.39	17.37
SPDL	-999.00	-999.00	-999.00
SPDR	5.26	5.26	5.25
DBME	-29.23		-29.03
DBSD	9.59		9.24
DBCOS	-0.73		-0.56
DBCOK	3.73		3.14

	SHDW	SHDLSS
WEIB0	0.131E+01	0.132E+01
WEIB1	0.523E-01	0.528E-01
WEIR2	0.995E+00	0.994E+00
WEISS	0.464E-01	0.507E-01
LOGB0	0.258E+01	0.258E+01
LOGB1	0.864E-01	0.869E-01
LOGR2	0.981E+00	0.982E+00
LOGSS	0.466E+00	0.453E+00

SIG(MAX)		-8
NOI(MAX)		-61
SAT(MAX)		999
SIG(MIN)		-61
NOI(MIN)		-74
SAT(MIN)		999
50	-28.0	-28.0
70	-24.0	-23.0
90	-18.0	-18.0
99	-11.0	-11.0

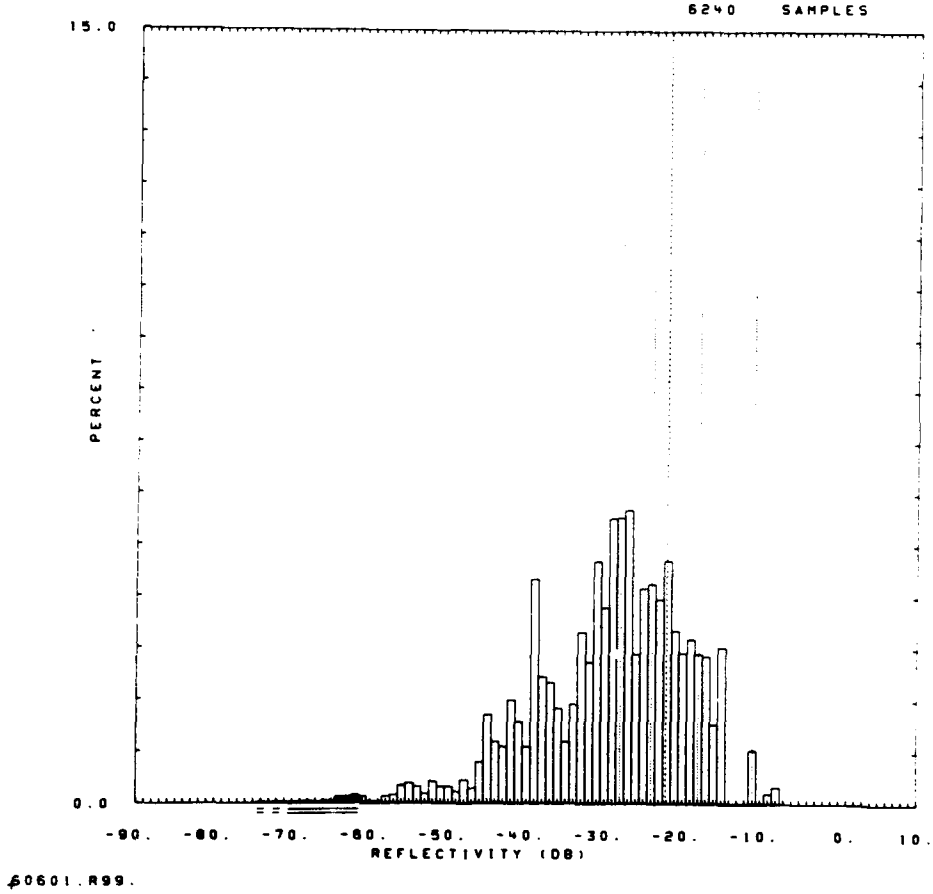

60601.R99.

Figure E-72. Clutter strength histogram for Brazeau repeat sector. L-band, 150-m pulse, horizontal polarization. First visit.

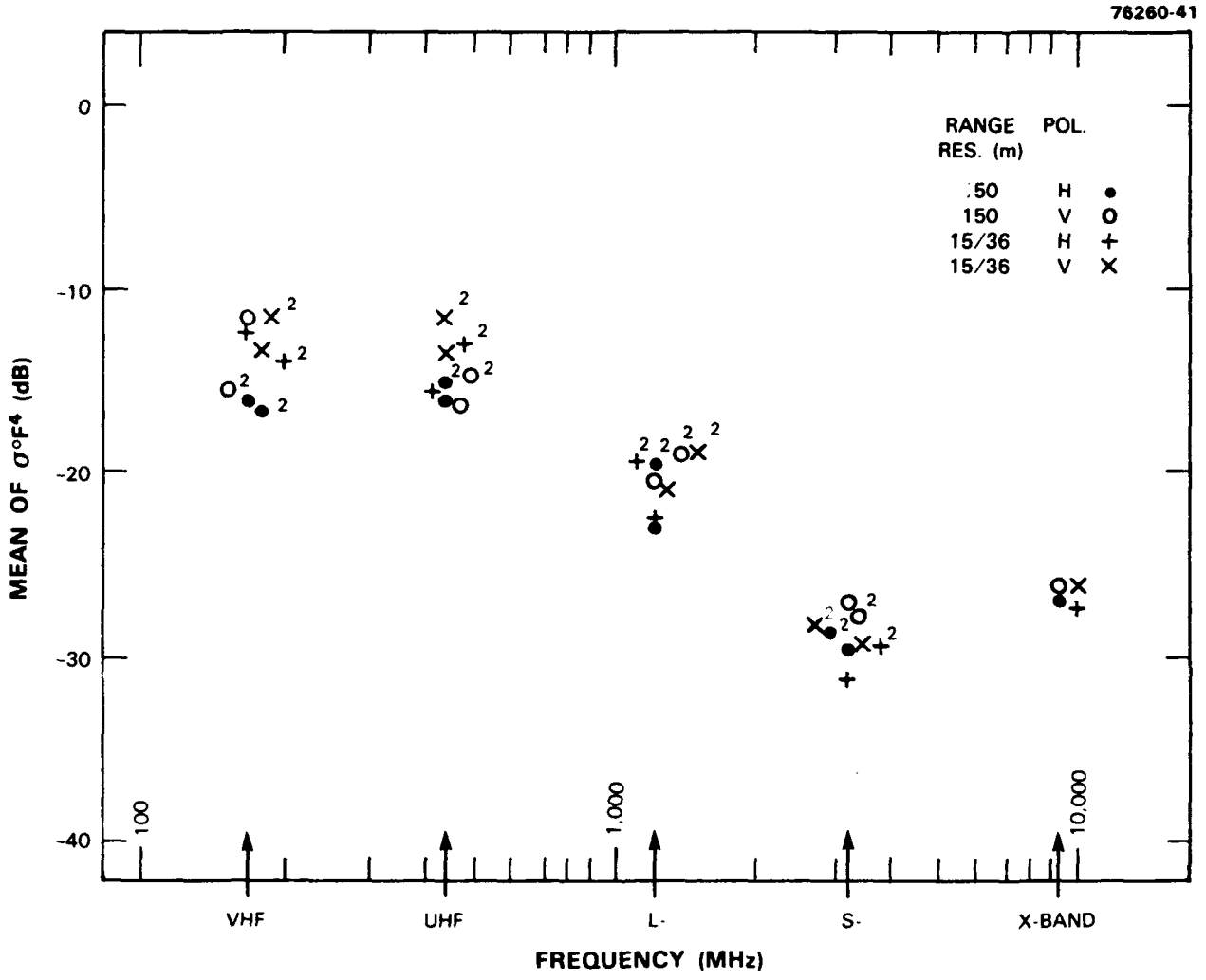

Figure E-73. Mean clutter strength versus frequency at Brazeau. For the Brazeau repeat sector, depression angle = 1.2 deg, landform = 3, land cover = 42-62-41, range = 4 to 9.9 km, azimuth = 170 to 180 deg. Comments: (1) There were two Phase One visits to Brazeau, with the second visit results indicated by 2's. (2) For the second visit, hardware problems precluded data collection at X-band.

Figure F-74. Repeat sector at Wainwright. DND bulldozer hauling Phase One tractor-trailers onto site. Repeat sector visible to SE.

Figure E-75. PPI clutter map and repeat sector at Wainwright. Repeat sector is outlined in black. Maximum range = 20 km; X-band, 15-m pulse, horizontal polarization; cells with $\sigma^{\circ}F^{4} \geq -40$ dB are red

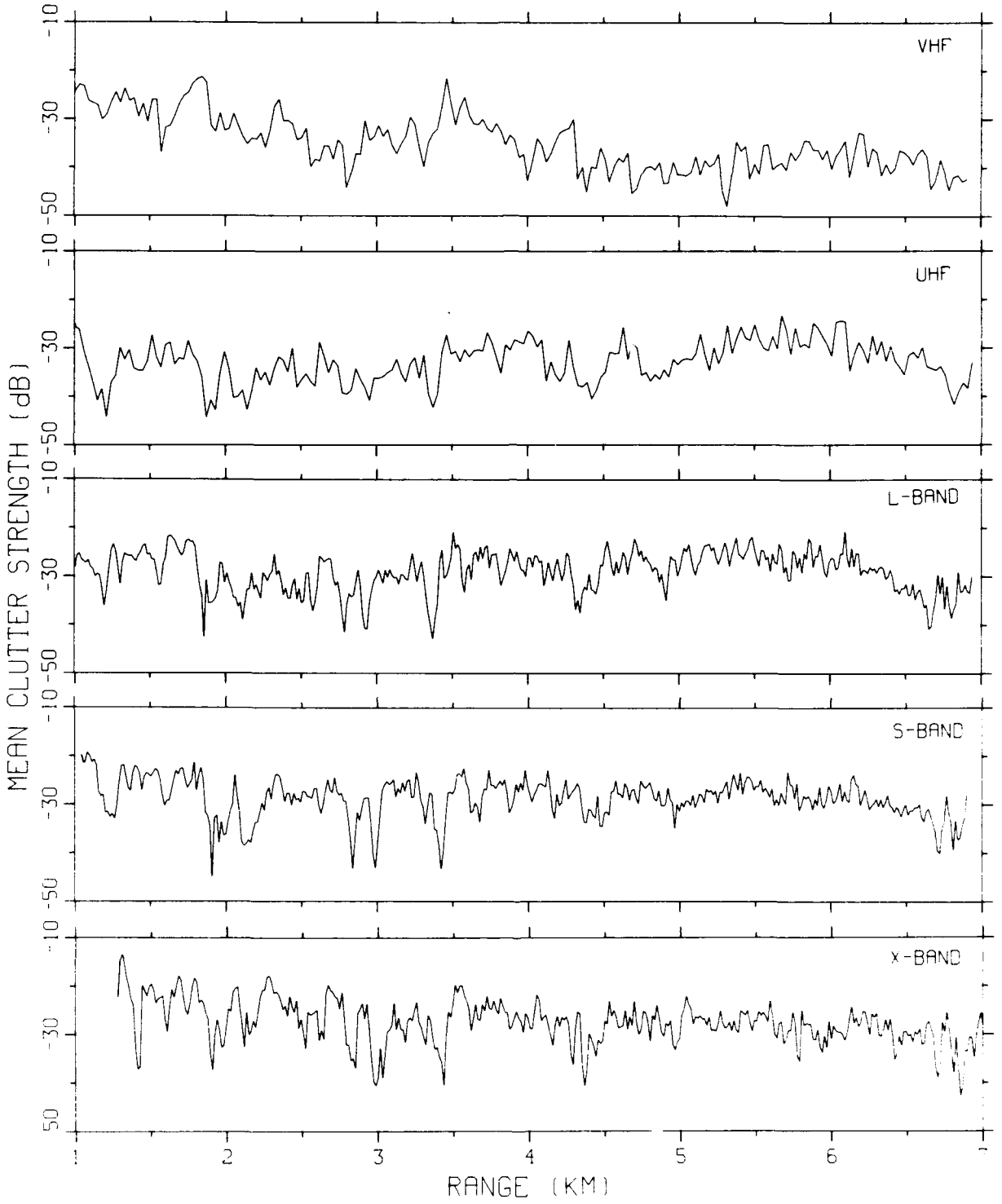

Figure E-76. Mean clutter strength versus range at Wainwright. Repeat sector data. Vertical polarization, 15/36-m pulse length. Data shown range gate by range gate, averaged in azimuth over 30 deg.

SITE = WAINWRIGHT RDF = RSFV15.RDF;1

LC = 33 41 0 LF = 5 3 TC = 2 DA = 0.55 DAC = 0.24 PN = R99 DATE = 24-MAR-

	SHOWUB	SHOWLB	SHOLSS		SHOW	SHOLSS			
MEAN	-29.48	-29.48	-29.45	WEIB0	0.162E+01	0.164E+01	SIG(MAX)		-14
SD	-26.02	-26.02	-26.00	WEIB1	0.489E-01	0.497E-01	NOI(MAX)		-68
COS	7.90	7.90	7.89	WEIR2	0.100E+01	0.100E+01	SAT(MAX)		999
COK	17.91	17.91	17.89	WEISS	0.353E-02	0.164E-02	SIG(MIN)		-77
SPDL	-999.00	-999.00	-999.00	LOGB0	0.293E+01	0.298E+01	NOI(MIN)		-85
SPDR	5.08	5.08	5.06	LOGB1	0.767E-01	0.786E-01	SAT(MIN)		999
DBME	-37.61		-37.33	LOGR2	0.966E+00	0.969E+00	50	-36.0	-36.0
DBSD	11.05		10.60	LOGSS	0.795E+00	0.702E+00	70	-31.0	-31.0
DBCOS	-0.85		-0.72				90	-25.0	-25.0
DBCOK	3.58		3.17				99	-19.0	-19.0

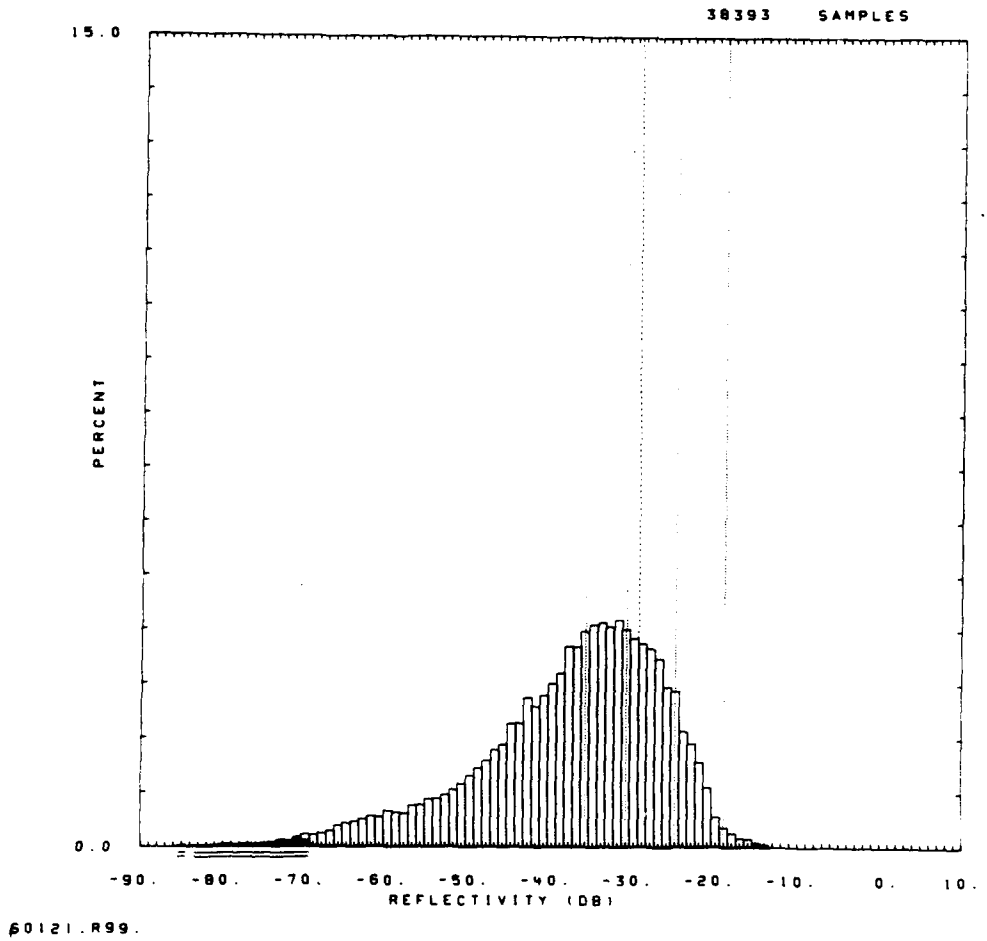

Figure E-77. Clutter histogram for Wainwright repeat sector. S-band, 150-m pulse, vertical polarization.

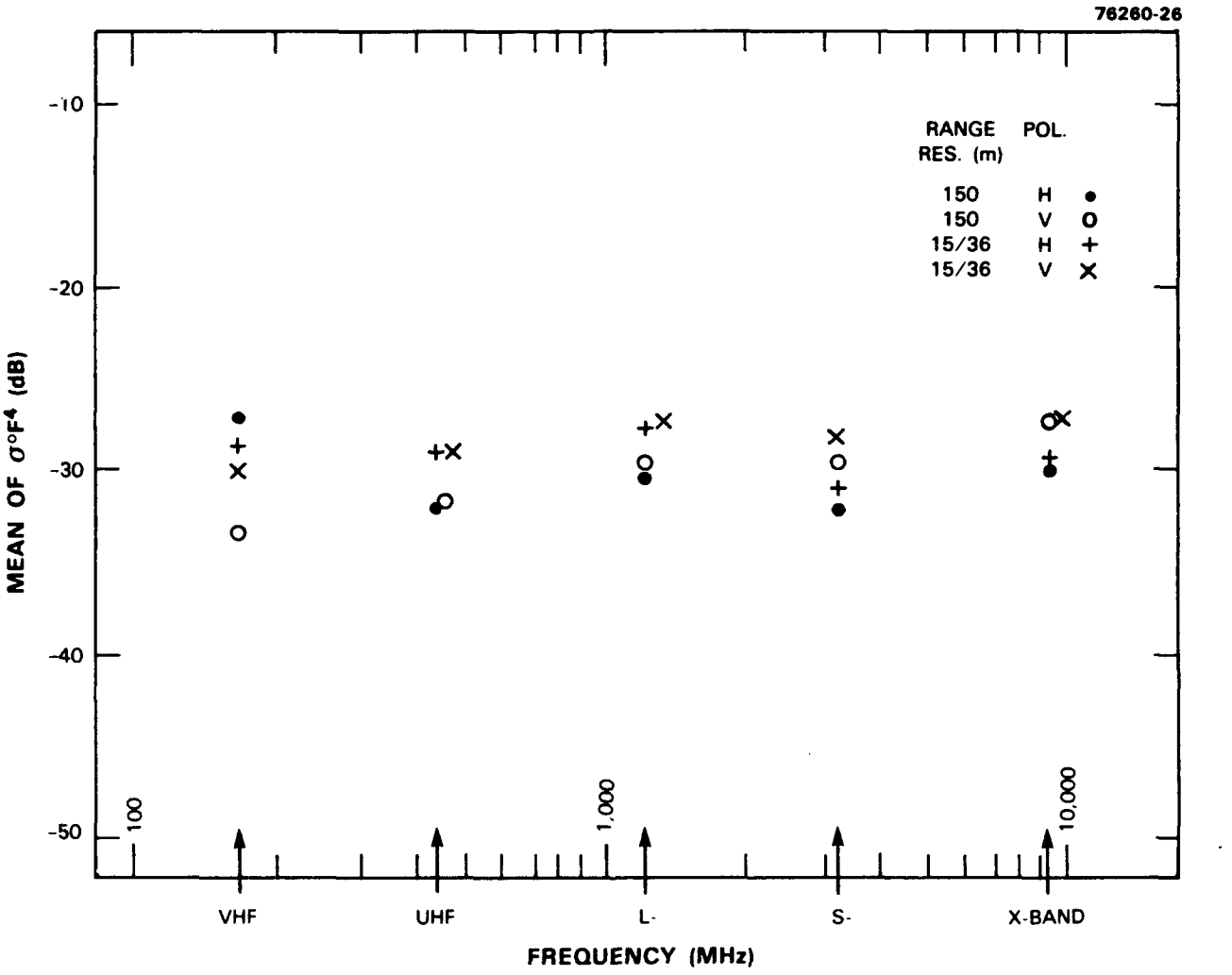

Figure E-78. Mean clutter strength versus frequency at Wainwright. For the Wainwright repeat sector, depression angle = 0.6 deg, landform = 5-3, land cover = 41-32-31, range = 1 to 6.9 km, azimuth = 120 to 150 deg.

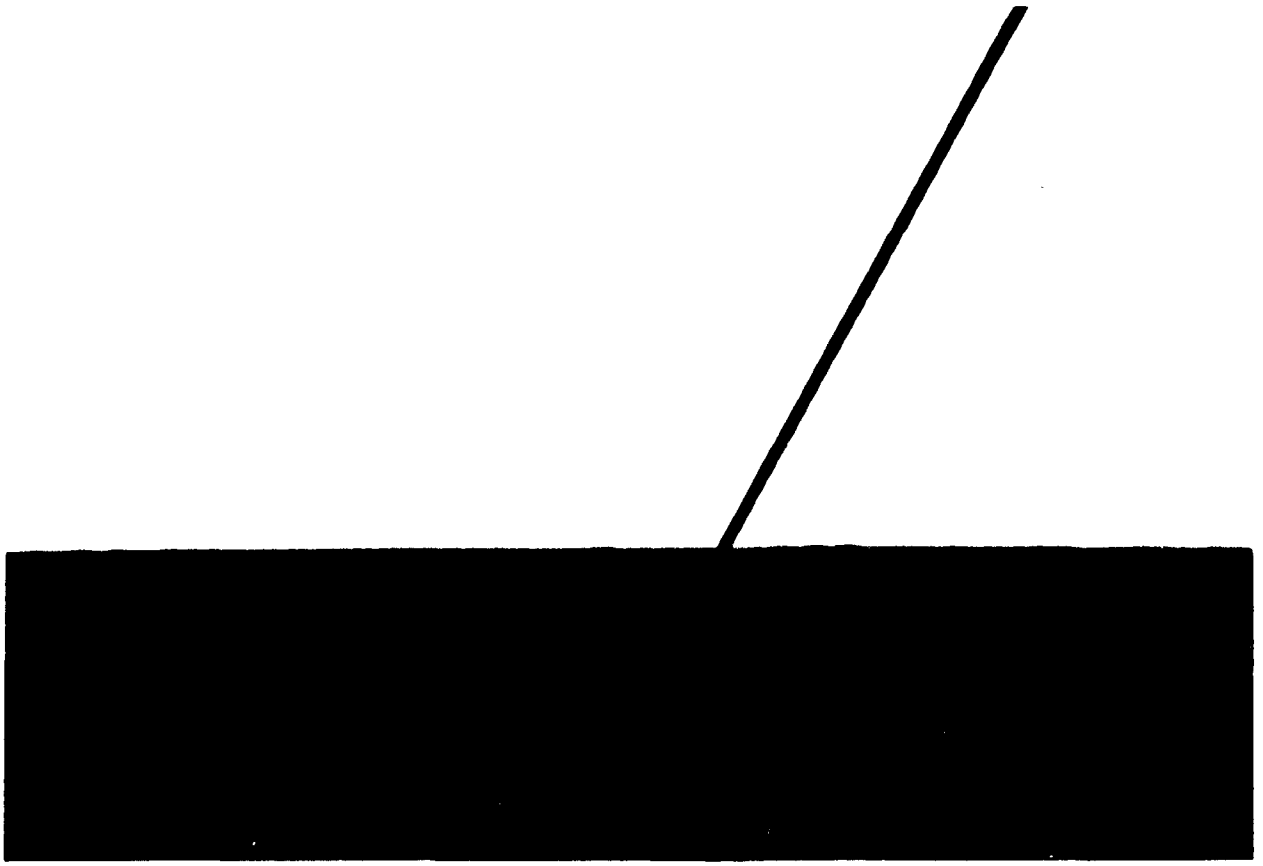

Figure E-79. Phase One at Turtle Mountain. View from Phase One tower ESE into repeat sector

Figure E-80. PPI clutter map and repeat sector at Turtle Mountain. Repeat sector is outlined in black. Maximum range = 8.5 km; X-band, 150-m pulse, horizontal polarization; cells with $\sigma^{o}F^{4} \geq -40$ dB are red

SITE = TURTLE MT RDF = RXFM20.RDF:1

LC = 41 52 0 LF = 5 0 TC = 4 DA = 0.50 DAC = 1.33 PN = R99 DATE = 01-JUN-84

	SHDWUB	SHDWLB	SHDLSS		SHDW	SHDLSS			
MEAN	-29.94	-29.94	-29.57	WE80	0.110E+01	0.115E+01	SIG(MAX)		-14
SD	-26.14	-26.14	-25.99	WE181	0.282E-01	0.306E-01	NOI(MAX)		-57
COS	6.91	6.91	6.73	WEIR2	0.958E+00	0.968E+00	SAT(MAX)		-17
COK	15.86	15.86	15.55	WEISS	0.171E+00	0.152E+00	SIG(MIN)		-85
SPDL	-999.00	-999.00	-999.00	LOGB0	0.229E+01	0.232E+01	NOI(MIN)		-85
SPDR	5.31	5.31	5.16	LOGB1	0.509E-01	0.534E-01	SAT(MIN)		-30
DBME	-47.27		-44.52	LOGR2	0.894E+00	0.905E+00	50	-43.0	-41.0
DBSD	18.81		17.01	LOGSS	0.151E+01	0.148E+01	70	-33.0	-32.0
DBCOS	-0.37		-0.46				90	-25.0	-25.0
DBCOK	1.86		2.04				99	-19.0	-19.0

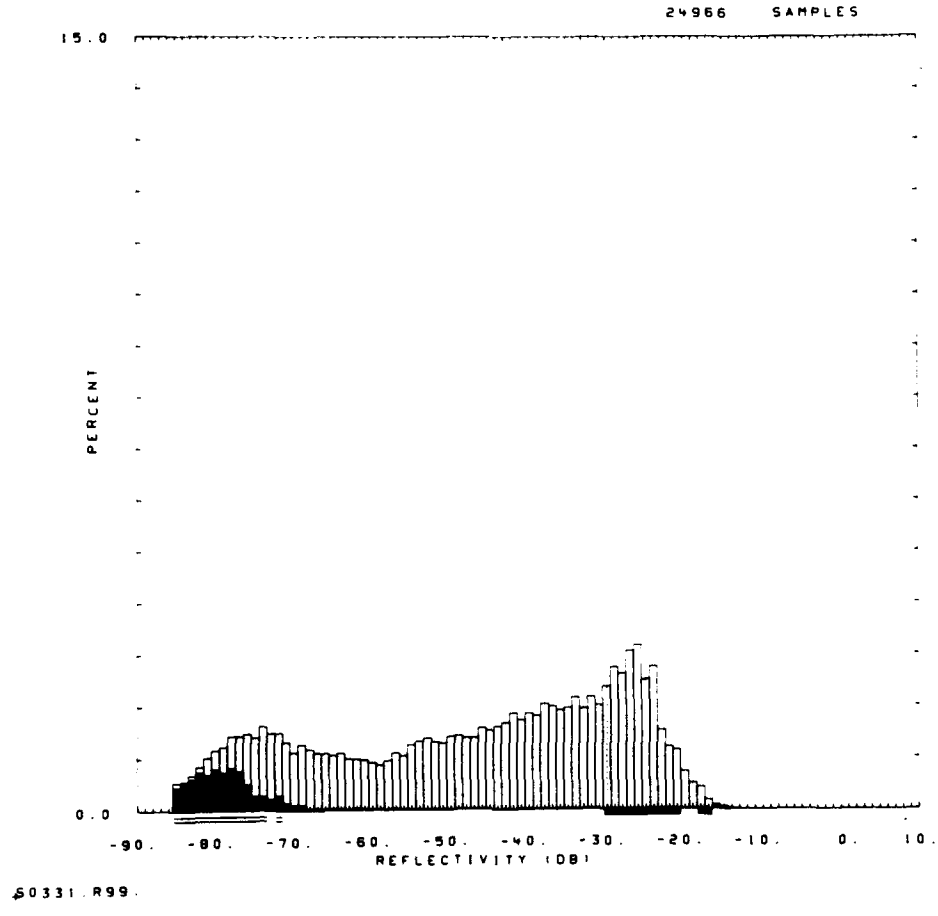

Figure E-81. Clutter strength histogram for Turtle Mountain repeat sector. X-band, 150-m pulse, horizontal polarization. One percent saturations.

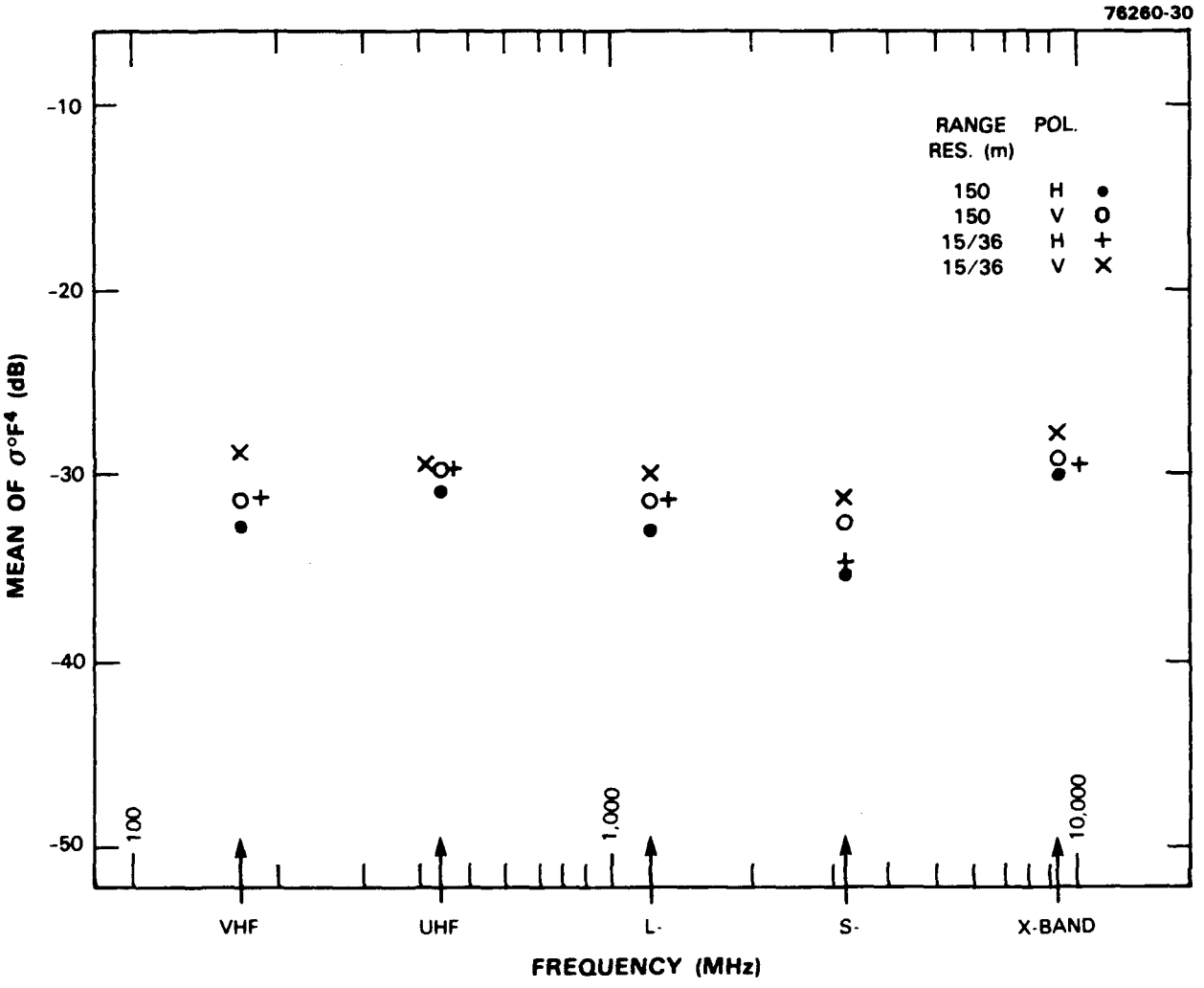

Figure E-82. Mean clutter strength versus frequency at Turtle Mountain. For the Turtle Mountain repeat sector, depression angle = 0.5 deg, landform = 5, land cover = 41-52, range = 2 to 7.9 km, azimuth 102 to 122 deg.

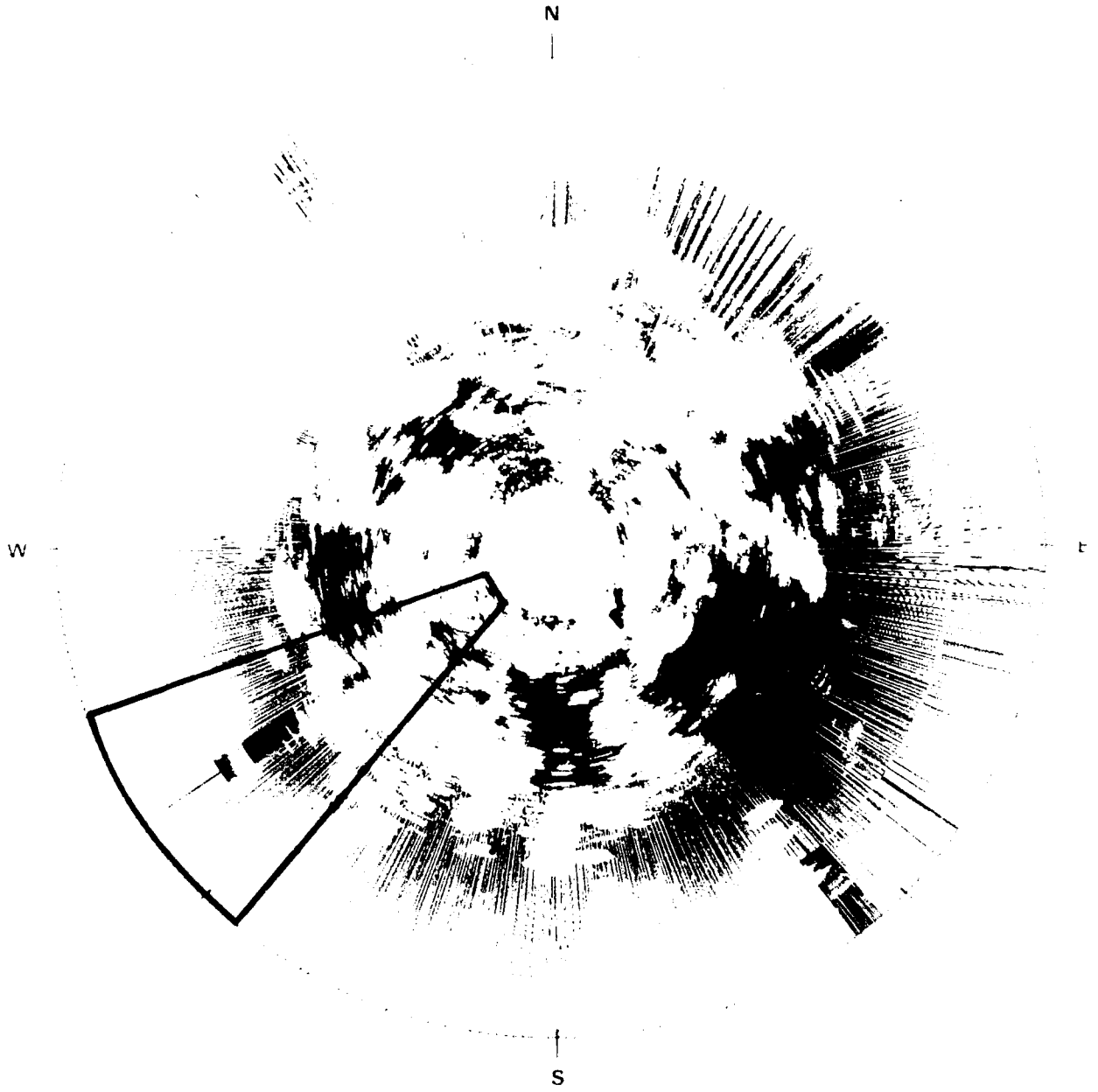

Figure E-83. PPI clutter map and repeat sector at Katahdin Hill. Repeat sector is outlined in black. Maximum range = 7 km; L-band, 15-m pulse, horizontal polarization; cells with $\sigma^{\circ} F^4 > -45$ dB are white

SITE = KATAHDIN HILL RDF = RSFV15A.RDF;1

LC = 43 21 0 LF = 5 4 TC = 4 DA = 0.42 DAC = 0.16 PN = R99 DATE = 12-OCT-84

	SHOWUB	SHOWLB	SHOLSS		SHOW	SHOLSS			
MEAN	-30.02	-30.02	-28.02	WEIB0	0.106E+01	0.128E+01	SIG(MAX)		-14
SD	-25.32	-25.32	-24.47	WEIB1	0.254E-01	0.377E-01	NOI(MAX)		-52
COS	7.12	7.11	6.08	WEIR2	0.965E+00	0.995E+00	SAT(MAX)		999
COK	15.84	15.84	13.98	WEISS	0.836E-01	0.277E-01	SIG(MIN)		-85
SPOL	-999.00	-999.00	-999.00	LOGB0	0.234E+01	0.248E+01	NOI(MIN)		-85
SPOR	5.97	5.97	5.14	LOGB1	0.501E-01	0.634E-01	SAT(MIN)		999
DBME	-47.92		-38.98	LOGR2	0.915E+00	0.954E+00	50	-50.0	-37.0
DBSD	15.79		12.66	LOGSS	0.833E+00	0.685E+00	70	-37.0	-30.0
DBCOS	0.18		-0.41				90	-26.0	-23.0
DBCOK	1.85		2.47				99	-18.0	-18.0

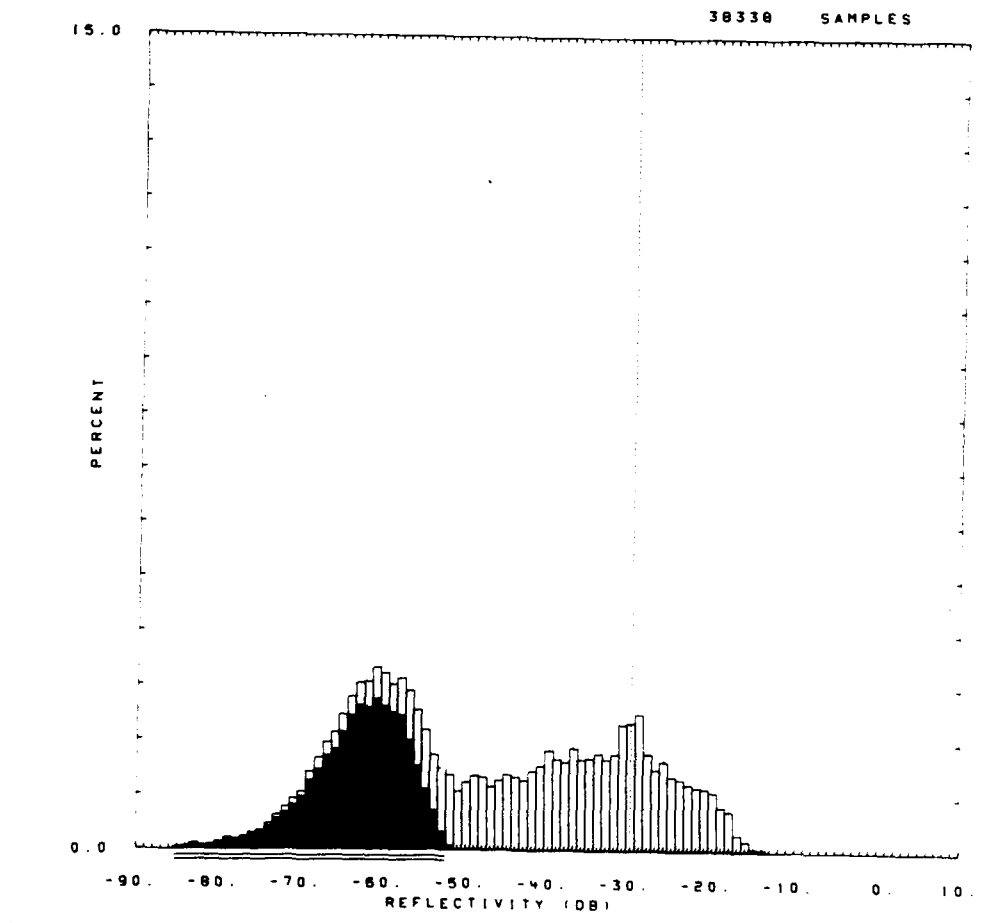

Figure E-84. Clutter strength histogram for Katahdin Hill repeat sector. S-band, 150-m pulse, vertical polarization. Second visit. RF preamplifier bypassed.

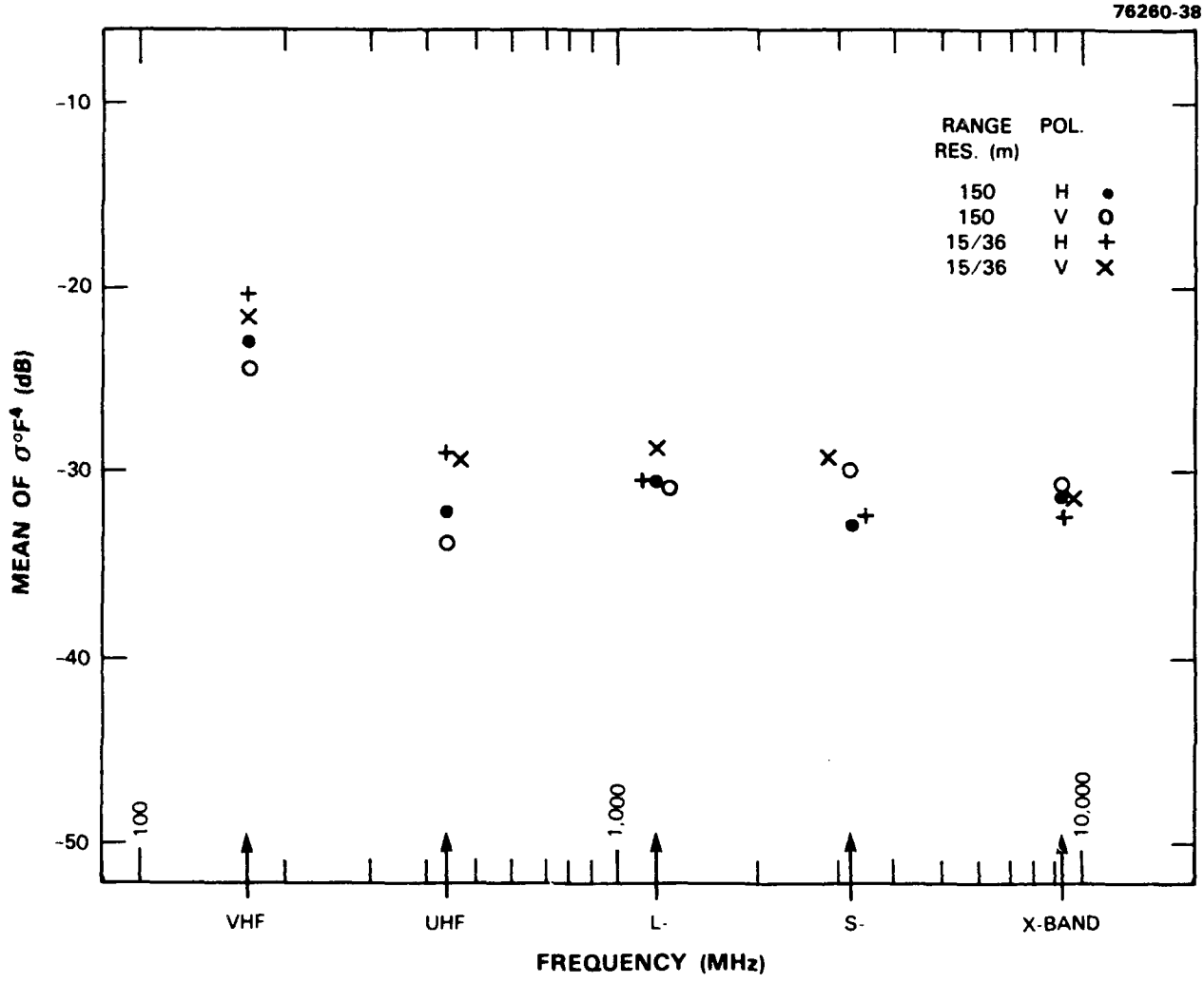

Figure E-85. Mean clutter strength versus frequency at Katahdin Hill. For the Katahdin Hill repeat sector, depression angle = 0.4 deg, landform = 5-4, land cover = 43-21-52, range = 1 to 6.9 km, azimuth = 220 to 250 deg.

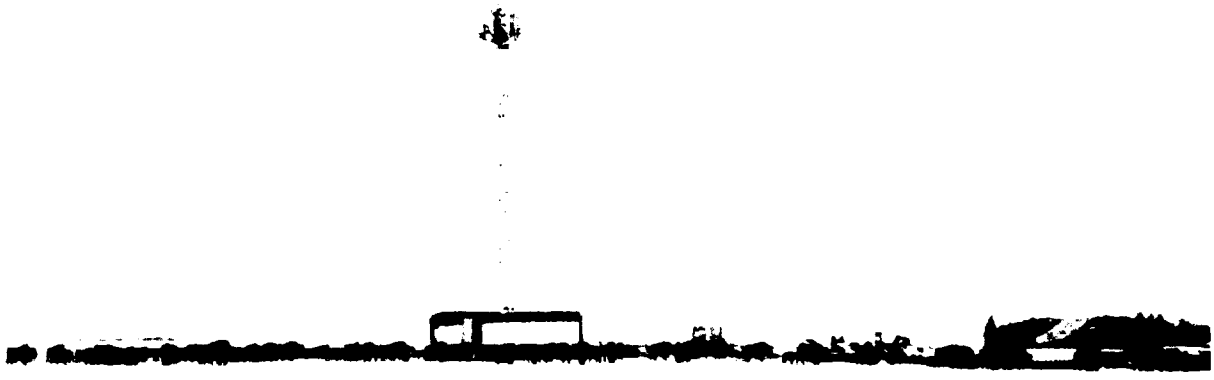

Figure E-86. Phase One at Westlock. Set up in buffalo pasture.

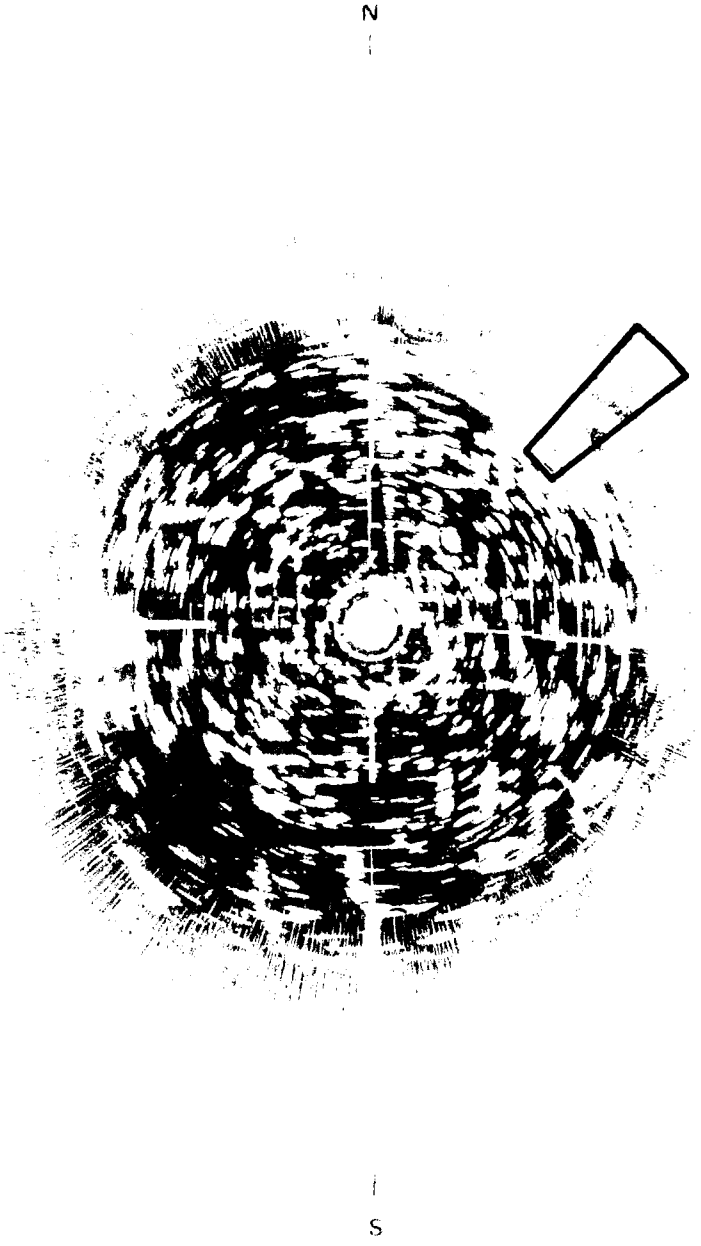

Figure E-87. PPI clutter map and repeat sector at Westlock. Repeat sector is outlined in black. Maximum range = 20 km; L-band, 15-m pulse, horizontal polarization; cells with $\sigma^{o}F^{4} \geq -40$ dB are white.

SITE = WESTLOCK RDF = RXFV19.RDF;1

LC = 43 21 52 LF = 3 5 TC = 4 DA = 0.36 DAC = 2.16 PN = R99 DATE = 23-NOV-

2

	SHDWUB	SHDWLB	SHDLSS		SHDW	SHDLSS			
MEAN	-28.83	-28.83	-28.34	WEIB0	0.131E+01	0.143E+01	SIG(MAX)		-15
SD	-24.61	-24.61	-24.40	WEIB1	0.377E-01	0.434E-01	NOI(MAX)		-52
COS	7.33	7.33	7.09	WEIR2	0.994E+00	0.997E+00	SAT(MAX)		999
COK	15.89	15.89	15.43	WEISS	0.328E-01	0.186E-01	SIG(MIN)		-82
SPDL	-999.00	-999.00	-999.00	LOGB0	0.263E+01	0.272E+01	NOI(MIN)		-85
SPDR	5.61	5.61	5.41	LOGB1	0.659E-01	0.715E-01	SAT(MIN)		999
DBME	-40.27		-37.19	LOGR2	0.962E+00	0.974E+00	50	-38.0	-36.0
DBSD	13.46		10.51	LOGSS	0.664E+00	0.527E+00	70	-31.0	-30.0
DBCOS	-0.60		-0.29				90	-25.0	-25.0
DBCOK	2.75		2.32				99	-17.0	-17.0

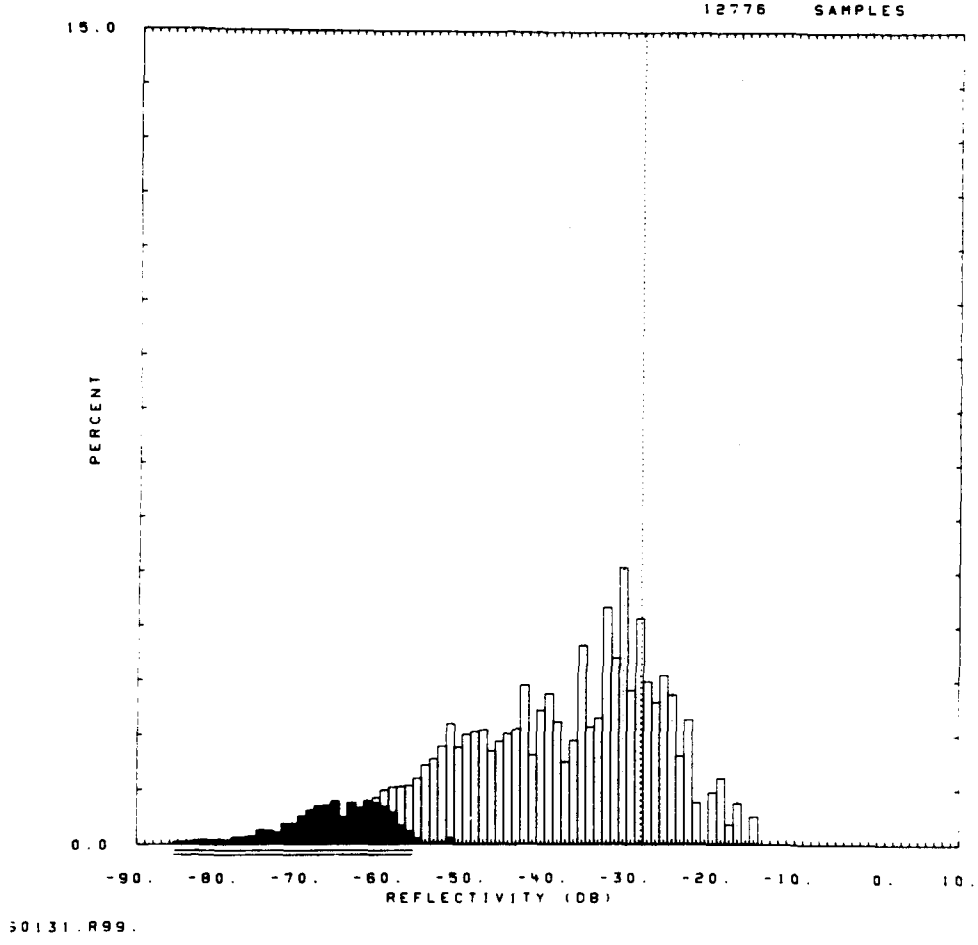

Figure E-88. Clutter strength histogram for Westlock repeat sector. X-band, 150-m pulse, vertical polarization.

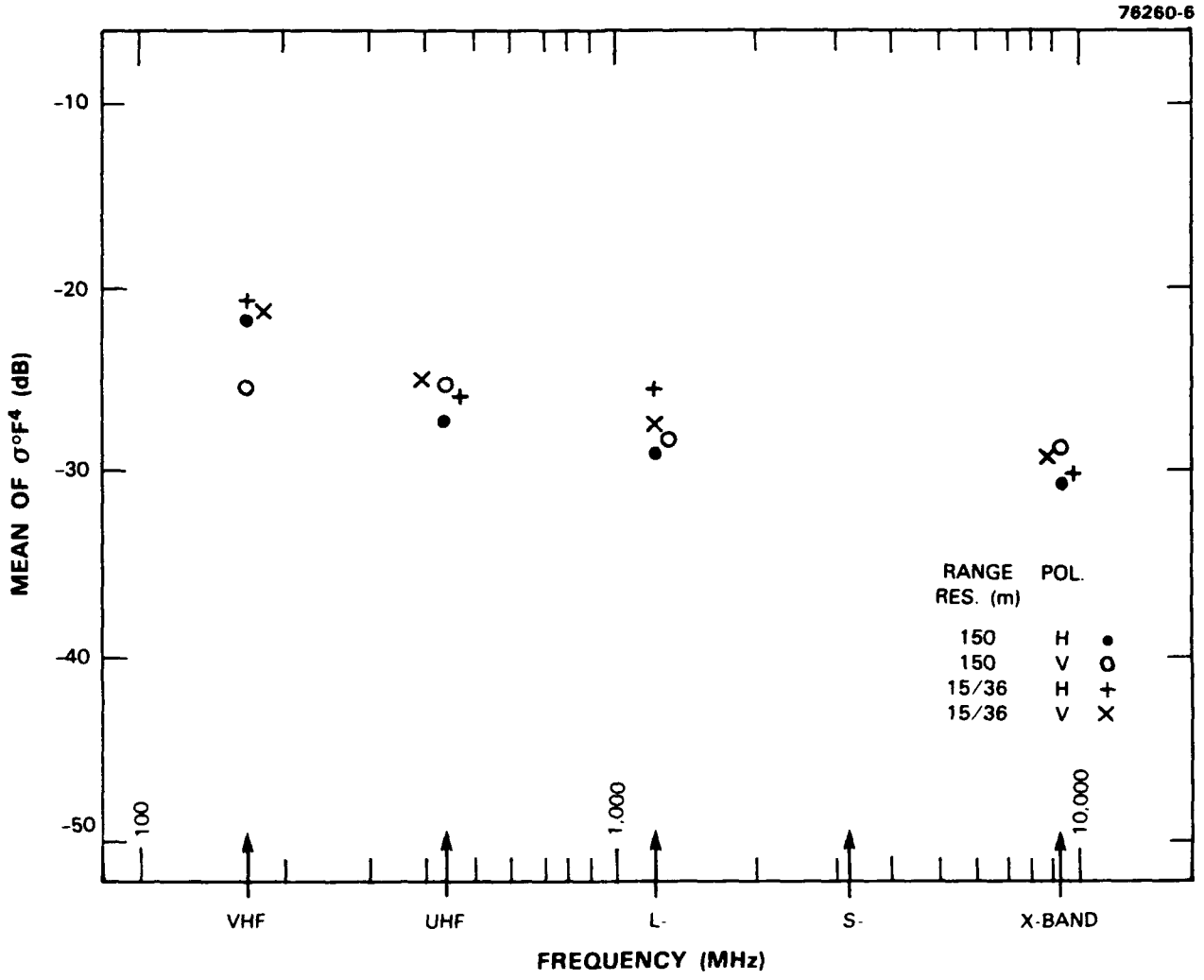

Figure E-89. Mean clutter strength versus frequency at Westlock. For the Westlock repeat sector, depression angle = 0.4 deg, landform = 3, land cover = 43-21-62, range = 8 to 13.9 km, azimuth = 42 to 52 deg. Comment: hardware problems precluded useful data collection at S-band.

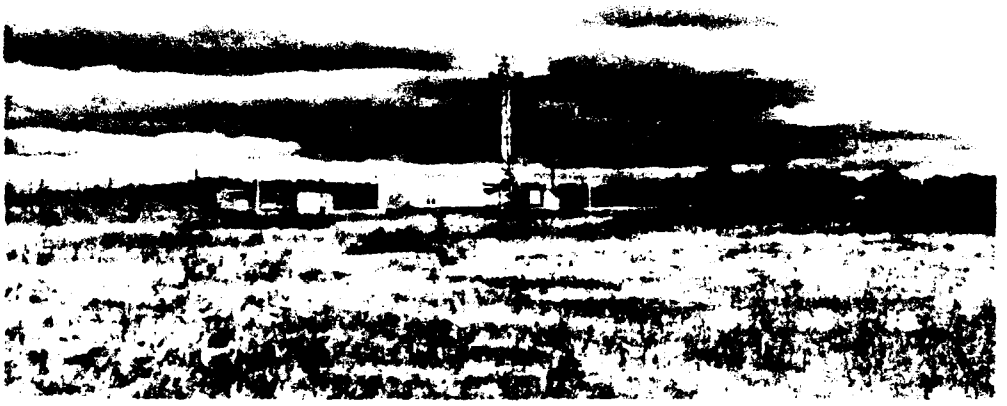

(a)

(b)

Figure E-90. Phase One at Sandridge: (a) Looking east to equipment on site and (b) view from remote weather station in repeat sector. Aspen and maple with scattered stands of taller spruce (none visible here) and occasional bur oak.

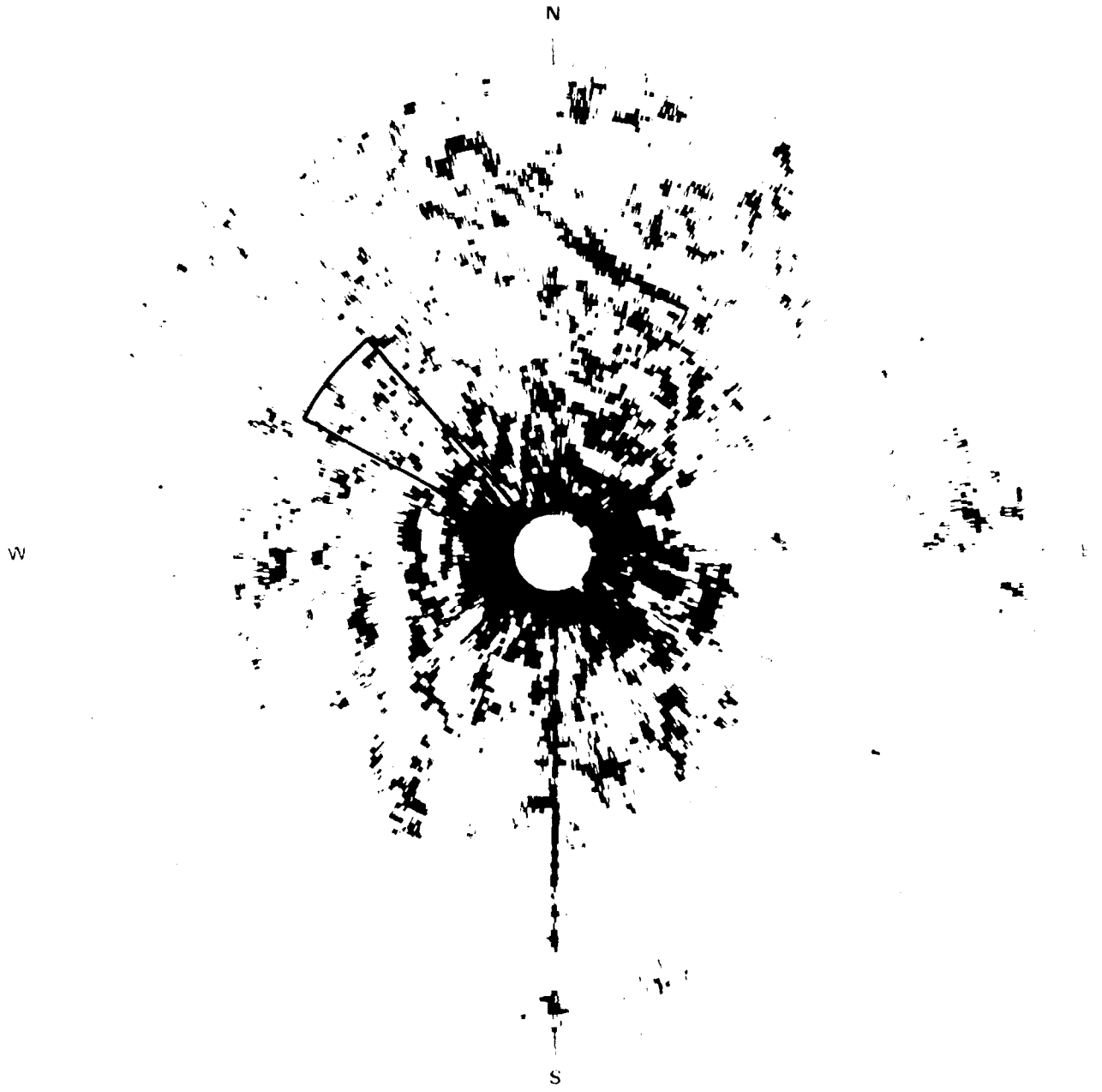

Figure E-91. PPI clutter map and repeat sector at Sandridge. Repeat sector is outlined in black. Maximum range = 12 km; X-band, 150-m pulse, horizontal polarization; cells with $\sigma^{\circ}F^{4} \geq -40$ dB are red.

SITE = SANDRIDGE RDF = RXFM28.RDF;1 DATE = 19-MAY-

LC = 91 62 22 LF = 1 0 TC = 4 DA = 8.28 DAC = 0.83 PN = R98

	SHDMUB	SHDMLB	SHDLSS
MEAN	-35.80	-35.80	-35.67
SD	-32.23	-32.23	-32.18
COS	7.00	7.00	6.94
COK	15.80	15.80	15.69
SPOL	-999.00	-999.00	-959.00
SPOR	5.16	5.16	5.10
DBME	-48.38		-45.42
DBSD	13.38		12.38
DBCOS	-0.72		-0.66
DBCOK	2.84		2.79

	SHDM	SHDLSS
MEI80	0.185E+01	0.170E+01
MEI81	0.401E-01	0.419E-01
MEIR2	0.994E+00	0.998E+00
MEISS	0.394E-01	0.268E-01
LOG80	0.309E+01	0.313E+01
LOG81	0.668E-01	0.692E-01
LOGR2	0.951E+00	0.955E+00
LOGSS	0.970E+00	0.918E+00

SIG(MAX)		-28
MOI(MAX)		-61
SAT(MAX)		-23
SIG(MIN)		-85
MOI(MIN)		-85
SAT(MIN)		-27
50	-44.0	-43.0
70	-37.0	-37.0
90	-31.0	-31.0
99	-25.0	-25.0

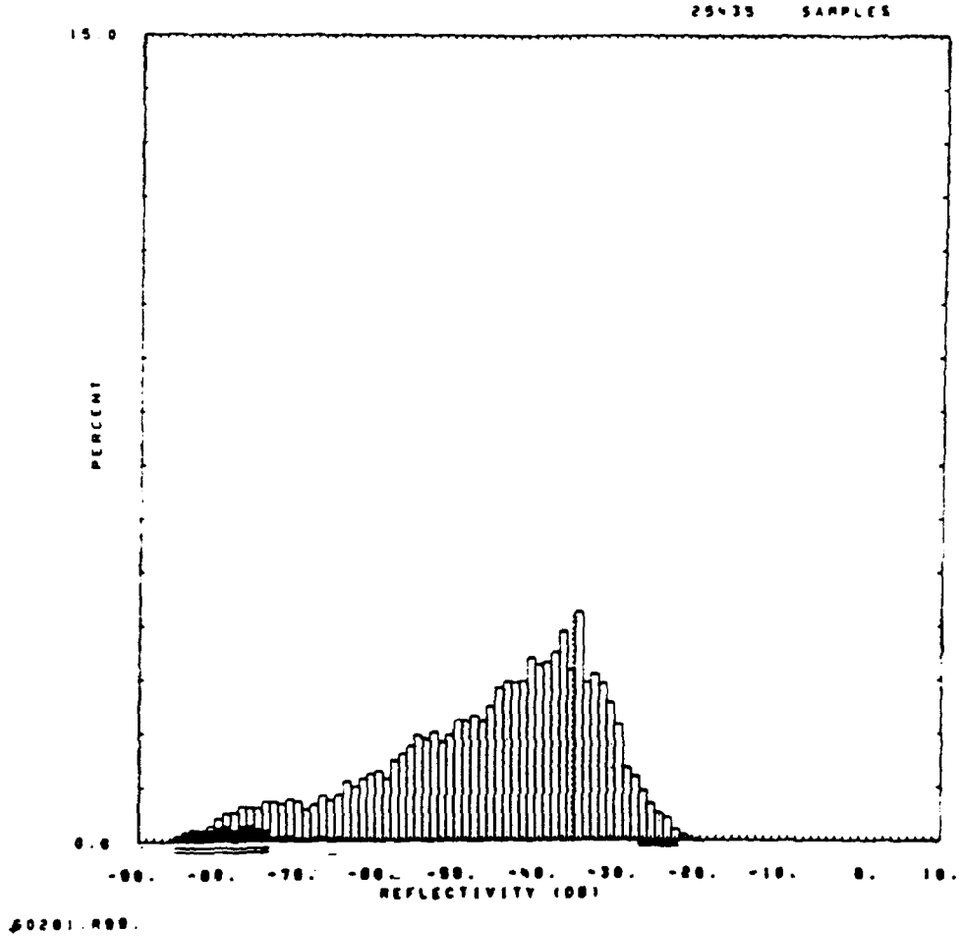

Figure E-92. Clutter strength histogram for Sandridge repeat sector. X-band, 150-m pulse, horizontal polarization.

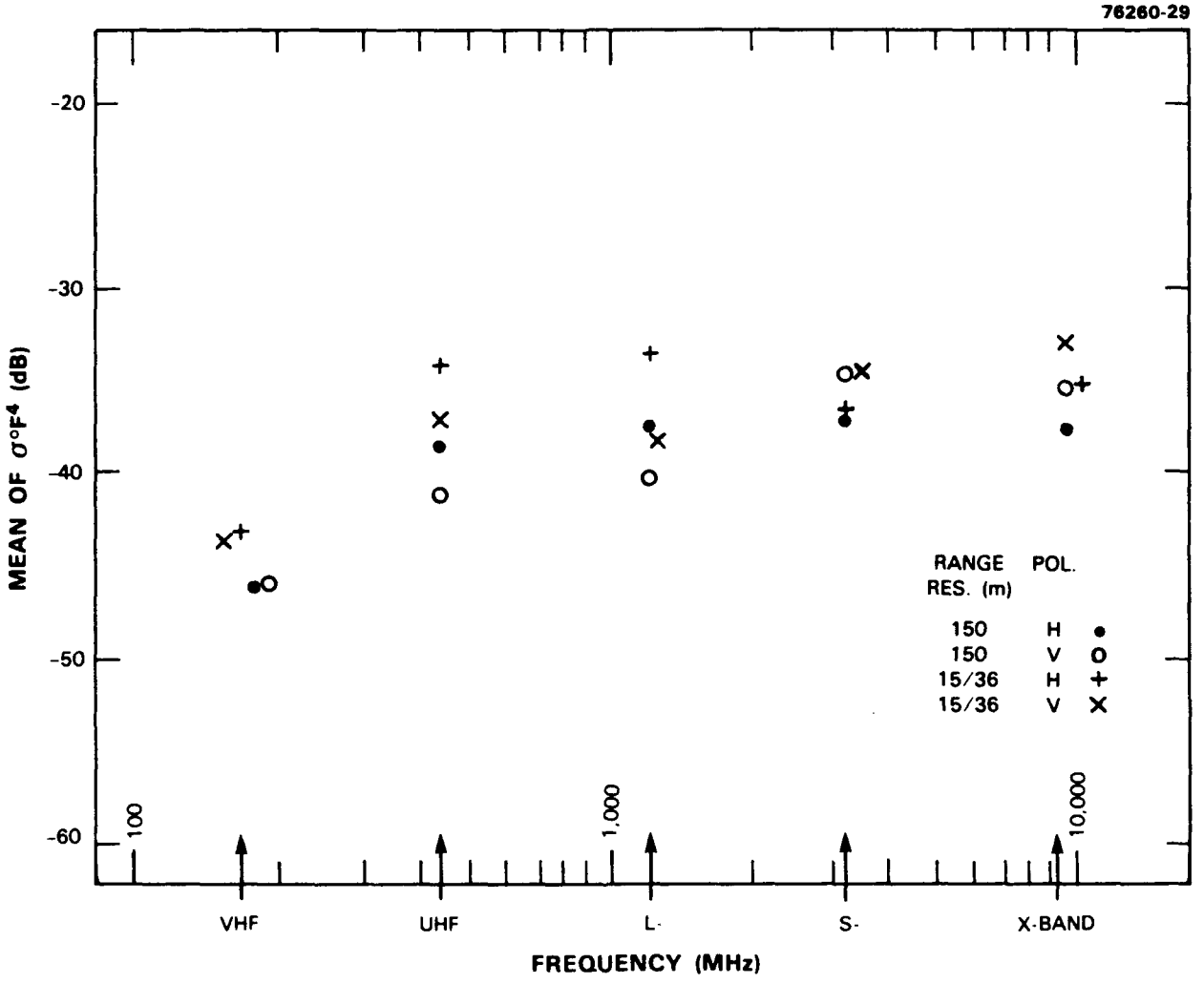

Figure E-93. Mean clutter strength versus frequency at Sandridge. For the Sandridge repeat sector, depression angle = 0.3 deg, landform = 1, land cover = 41-62-22, range = 1 to 6.9 km, azimuth = 298 to 318 deg.

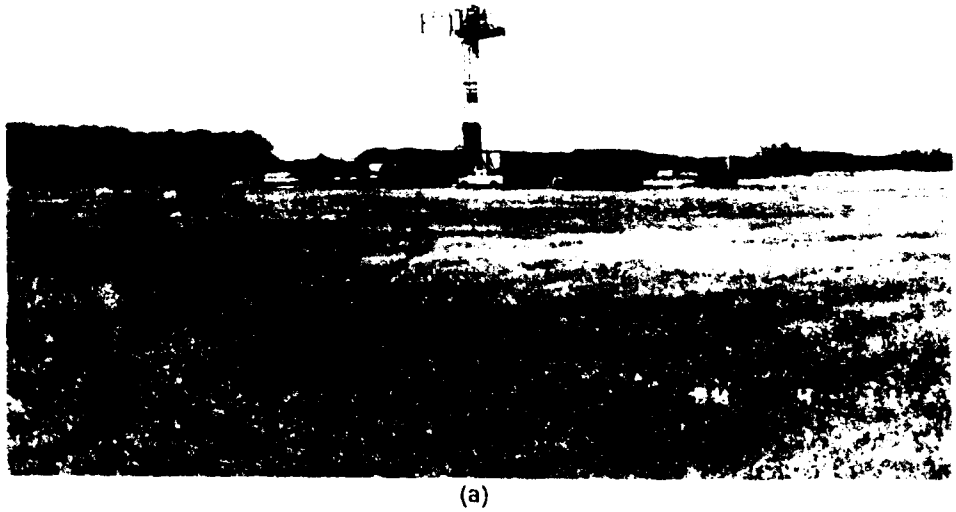

(a)

NW

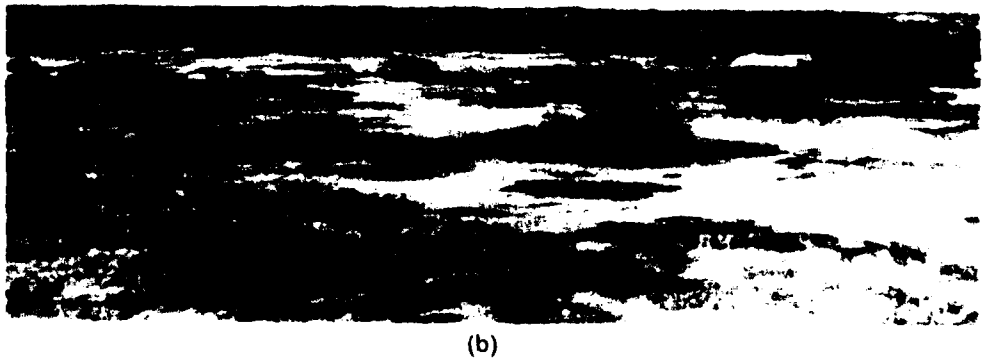

(b)

Figure E-91. Phase One at Dundurn, sat Looking NW beyond equipment erected on airstrip to hammocky sand dunes of repeat sector beyond and (b) tower top view looking NW into repeat sector

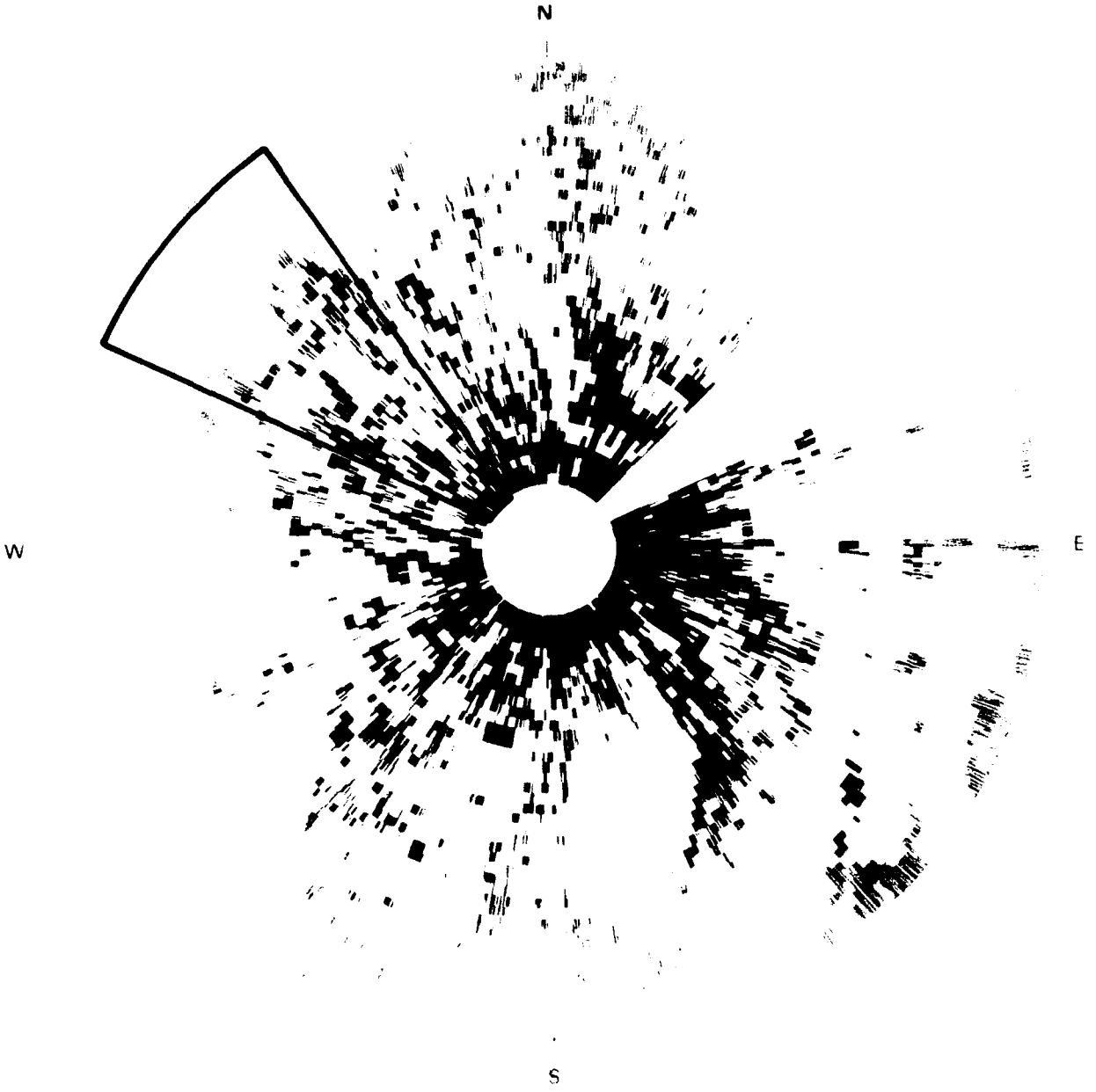

Figure E-95 PPI clutter map and repeat sector at Dundurn. Repeat sector is outlined in black. Maximum range = 7 km; X-band, 150-m pulse, horizontal polarization; cells with $\sigma^{\circ}F^{4} \geq -45$ dB are red.

SITE = DUNDURN RDF = RXFH20.RDF;1

LC = 32 41 0 LF = 5 0 TC = 2 DA = 0.19 DAC = 0.68 PN = R99 DATE = 11-APR-

	SHDWUB	SHDWLB	SHDLSS		SHDW	SHDLSS			
MEAN	-36.05	-36.05	-35.59	WEIB0	0.129E+01	0.140E+01	SIG(MAX)		-17
SD	-30.32	-30.32	-30.11	WEIB1	0.274E-01	0.314E-01	NOI(MAX)		-70
COS	10.05	10.05	9.83	WEIR2	0.993E+00	0.993E+00	SAT(MAX)		-21
COK	21.59	21.59	21.16	WEISS	0.487E-01	0.598E-01	SIG(MIN)		-85
SPDL	-999.00	-999.00	-999.00	LOGB0	0.258E+01	0.267E+01	NOI(MIN)		-85
SPDR	6.76	6.76	6.56	LOGB1	0.478E-01	0.516E-01	SAT(MIN)		-31
DBME	-53.07		-50.37	LOGR2	0.952E+00	0.965E+00	50	-52.0	-50.0
DBSD	15.60		14.05	LOGSS	0.106E+01	0.900E+00	70	-43.0	-41.0
DBCOS	-0.03		-0.02				90	-32.0	-32.0
DBCOK	1.95		1.99				99	-25.0	-25.0

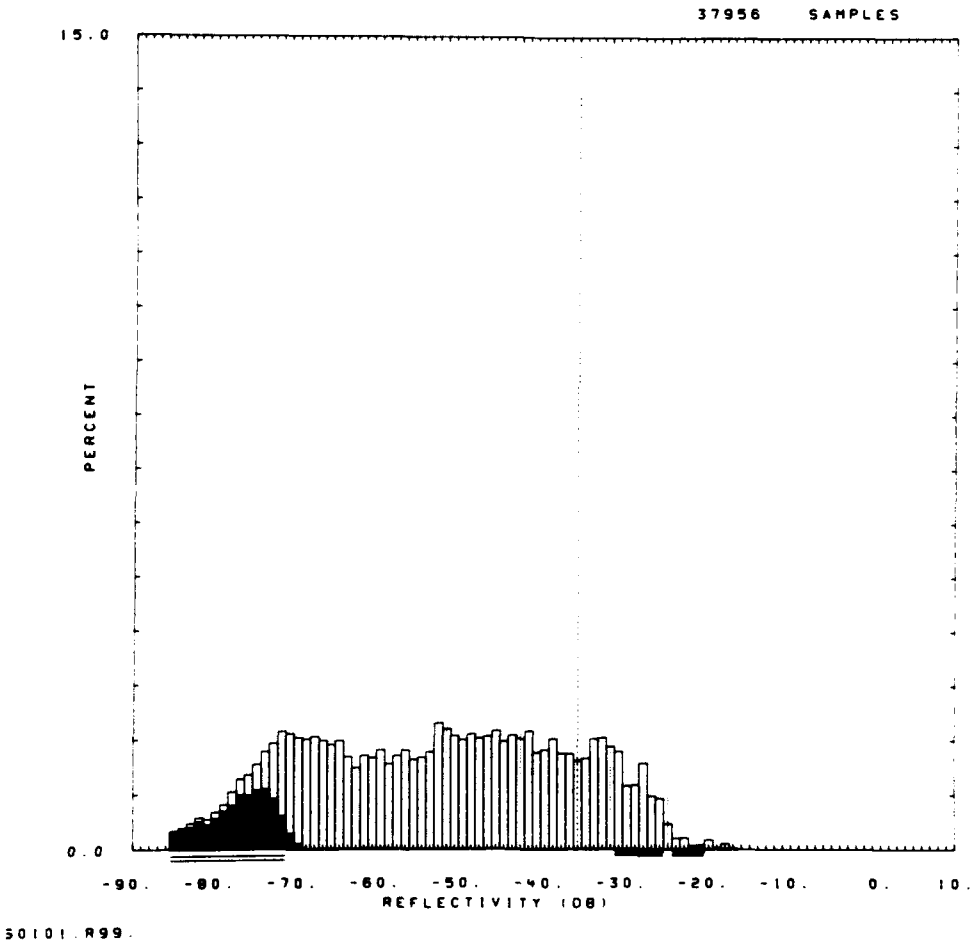

Figure E-96. Clutter strength histogram for Dundurn repeat sector. X-band, 150-m pulse, horizontal polarization.

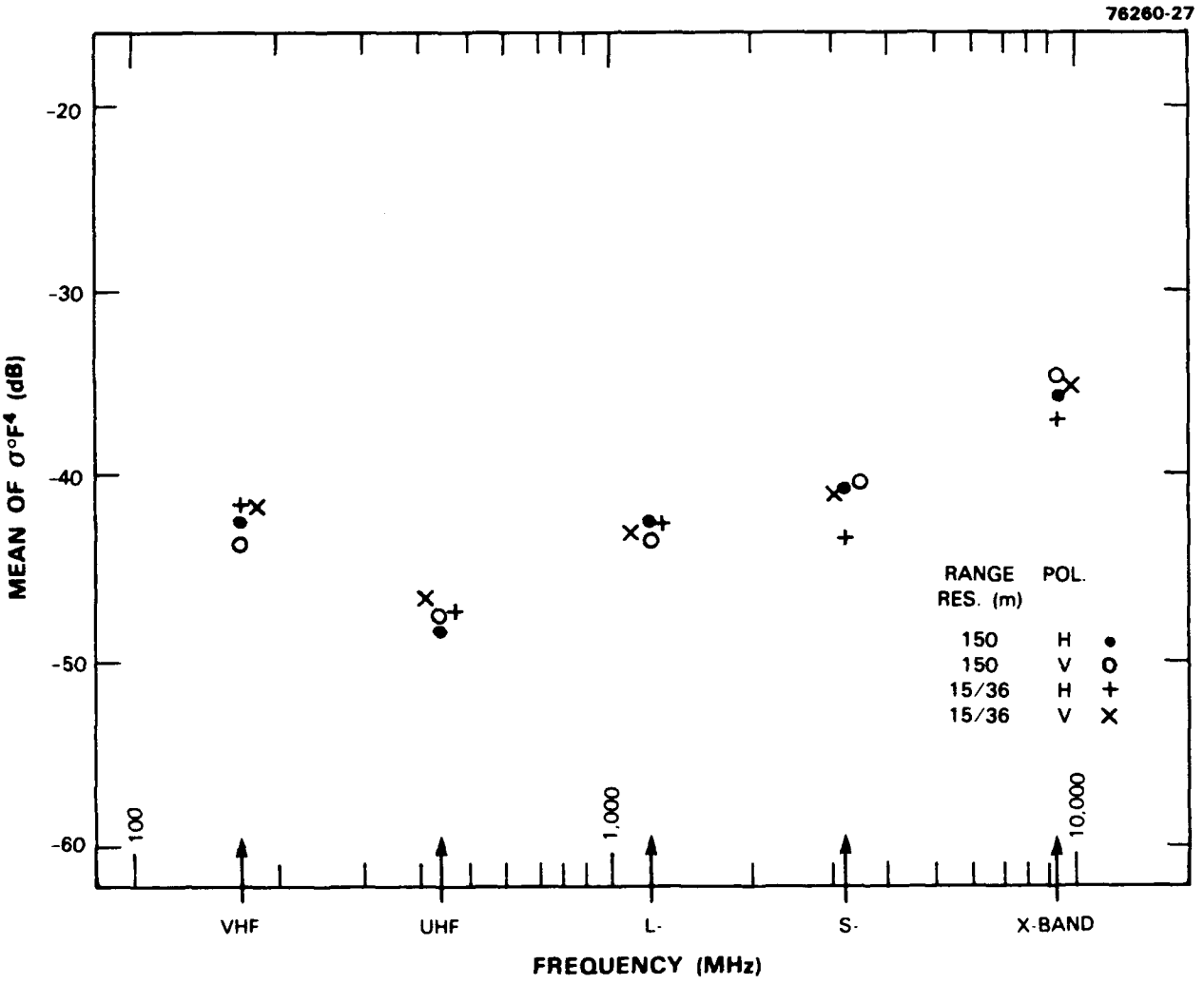

Figure E-97. Mean clutter strength versus frequency at Dundurn. For the Dundurn repeat sector, depression angle = 0.2 deg, landform = 5, land cover = 32-41-31, range = 1 to 6.9 km, azimuth = 295 to 325 deg.

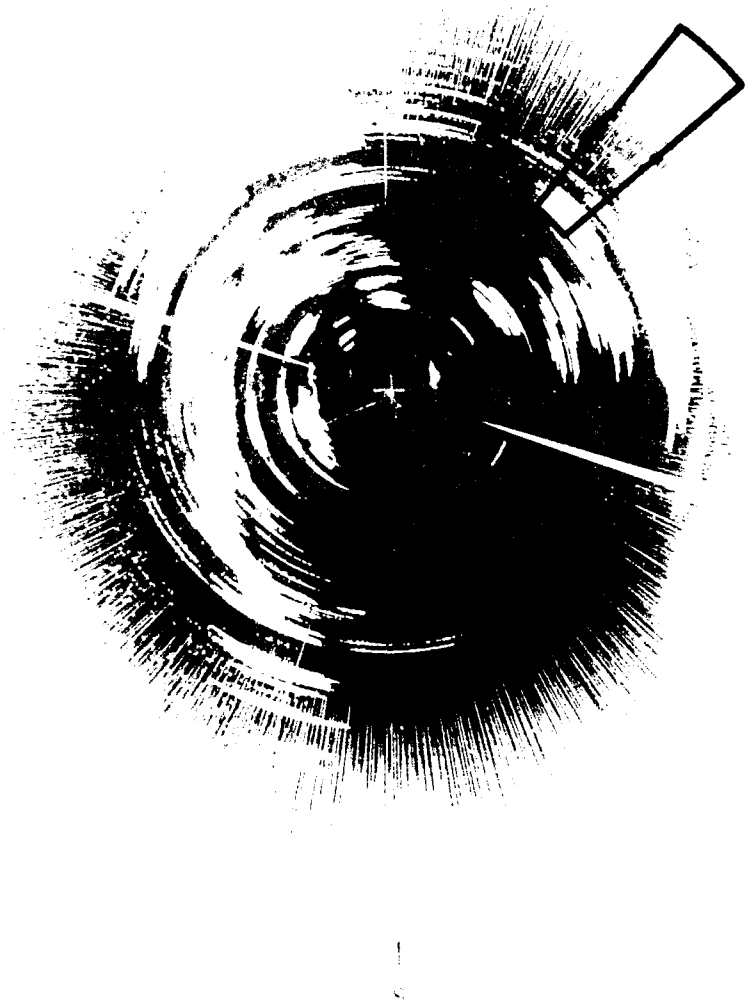

Figure E-98. PPI clutter map and repeat sector (a) at Plateau Mountain. Repeat sector is outlined in black. Maximum range = 48.4 km; VHF, 150-m pulse, horizontal polarization; cells with $\sigma^{\circ}E^{4} \geq -40$ dB are white.

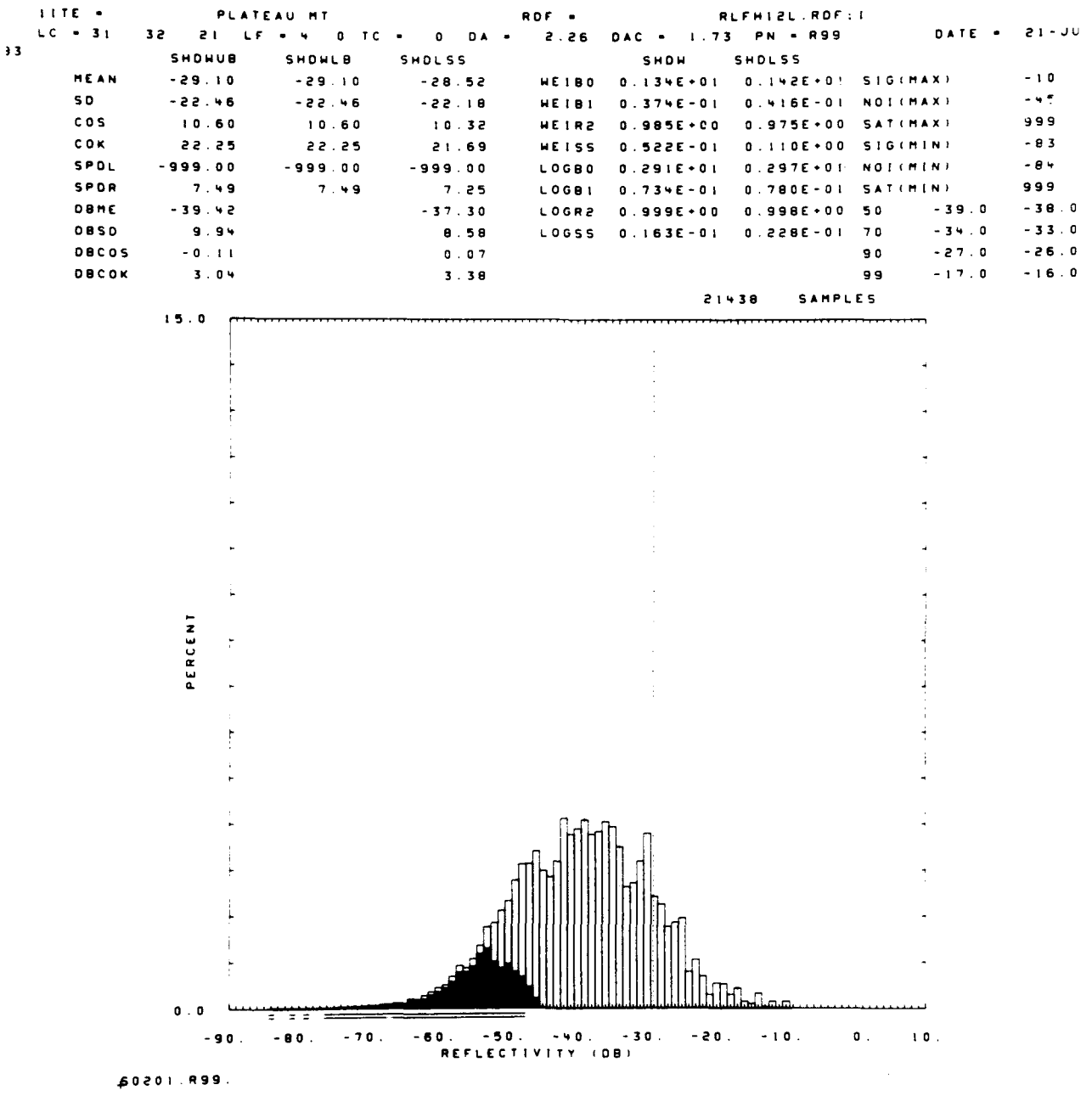

Figure E-99. Clutter strength histogram for Plateau Mountain (a) repeat sector. L-band, 150-m pulse, horizontal polarization.

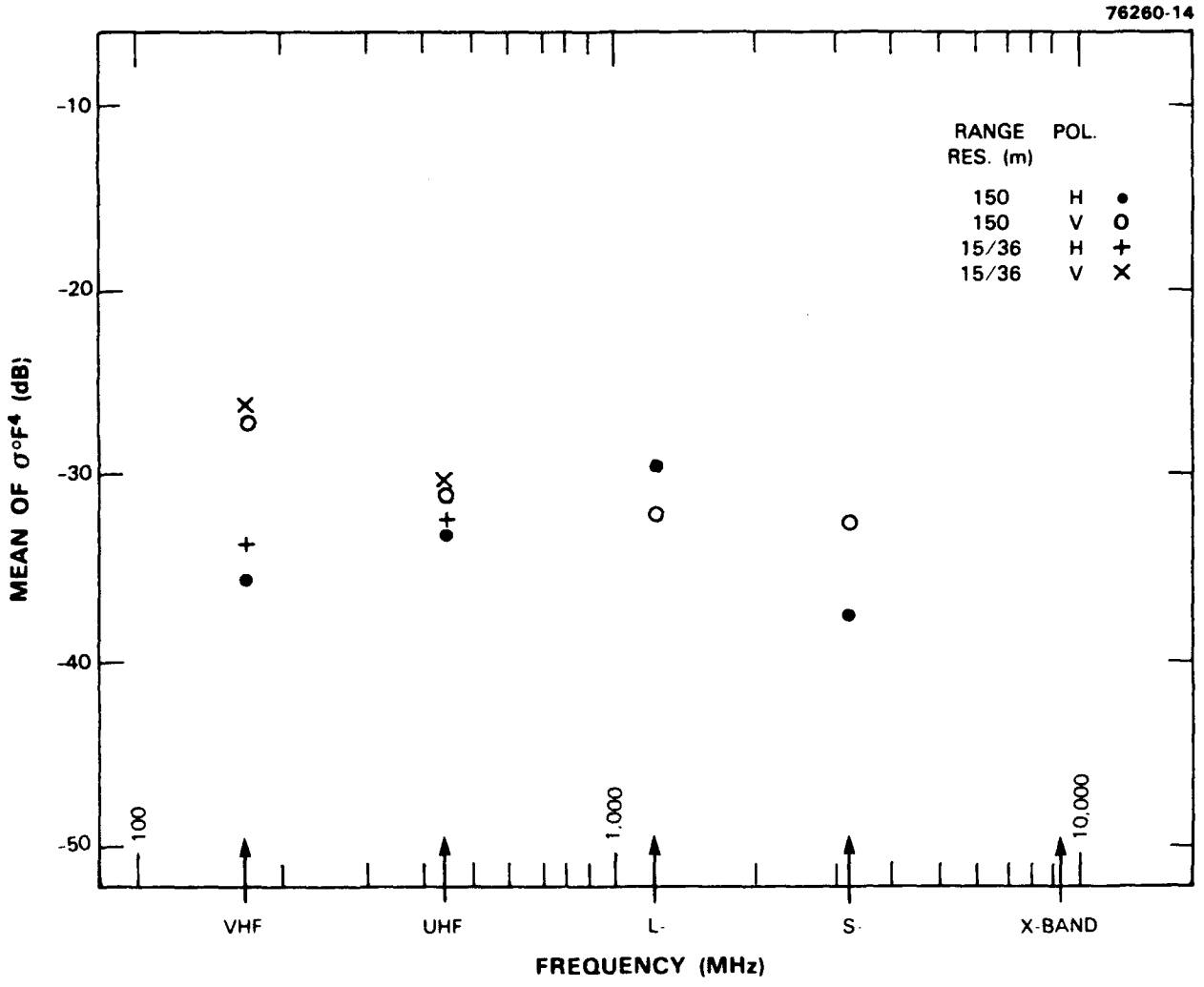

Figure E-100. Mean clutter strength versus frequency at Plateau Mountain (a). For the Plateau Mountain (a) repeat sector, depression angle = 2.3 deg, landform = 4, land cover = 31-32-21, range = 20 to 40 km, azimuth = 40 to 50 deg. Comments: (1) X-band transmitter failed; no data collected. (2) High resolution data were not collected at L- and S-bands.

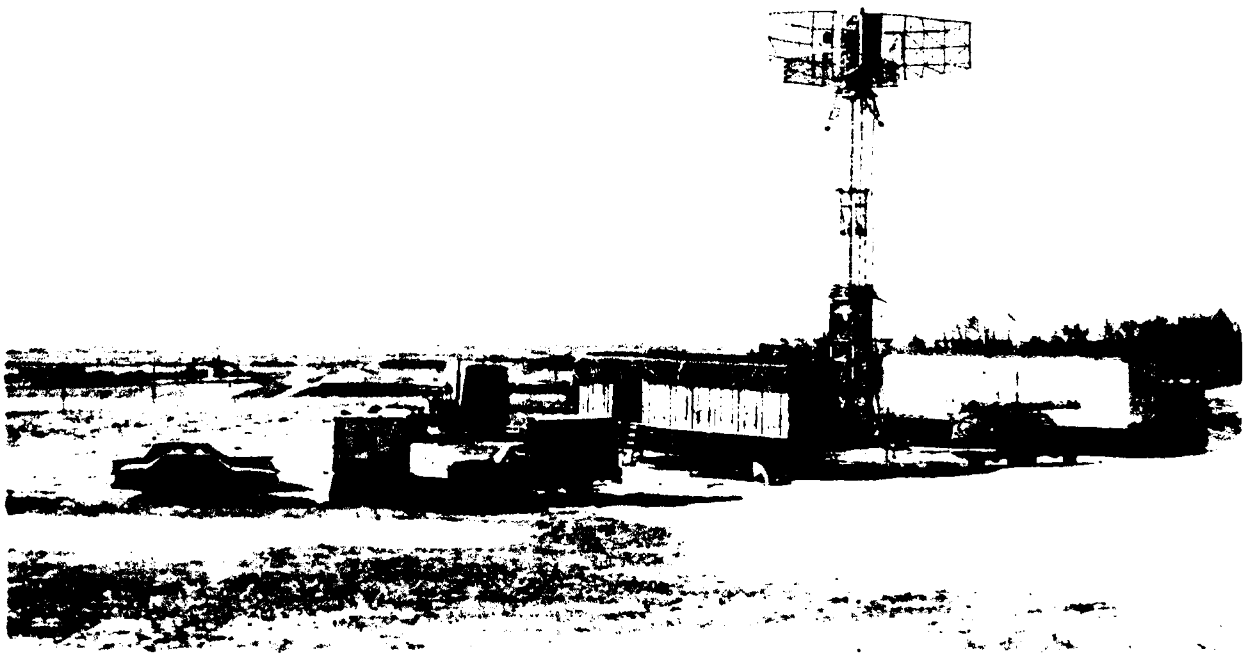

Figure E.107. Phase One at Polovra Lookout with past equipment and down Ruby Mountain escarpment. Antenna tower erected to 60 ft. March 1982

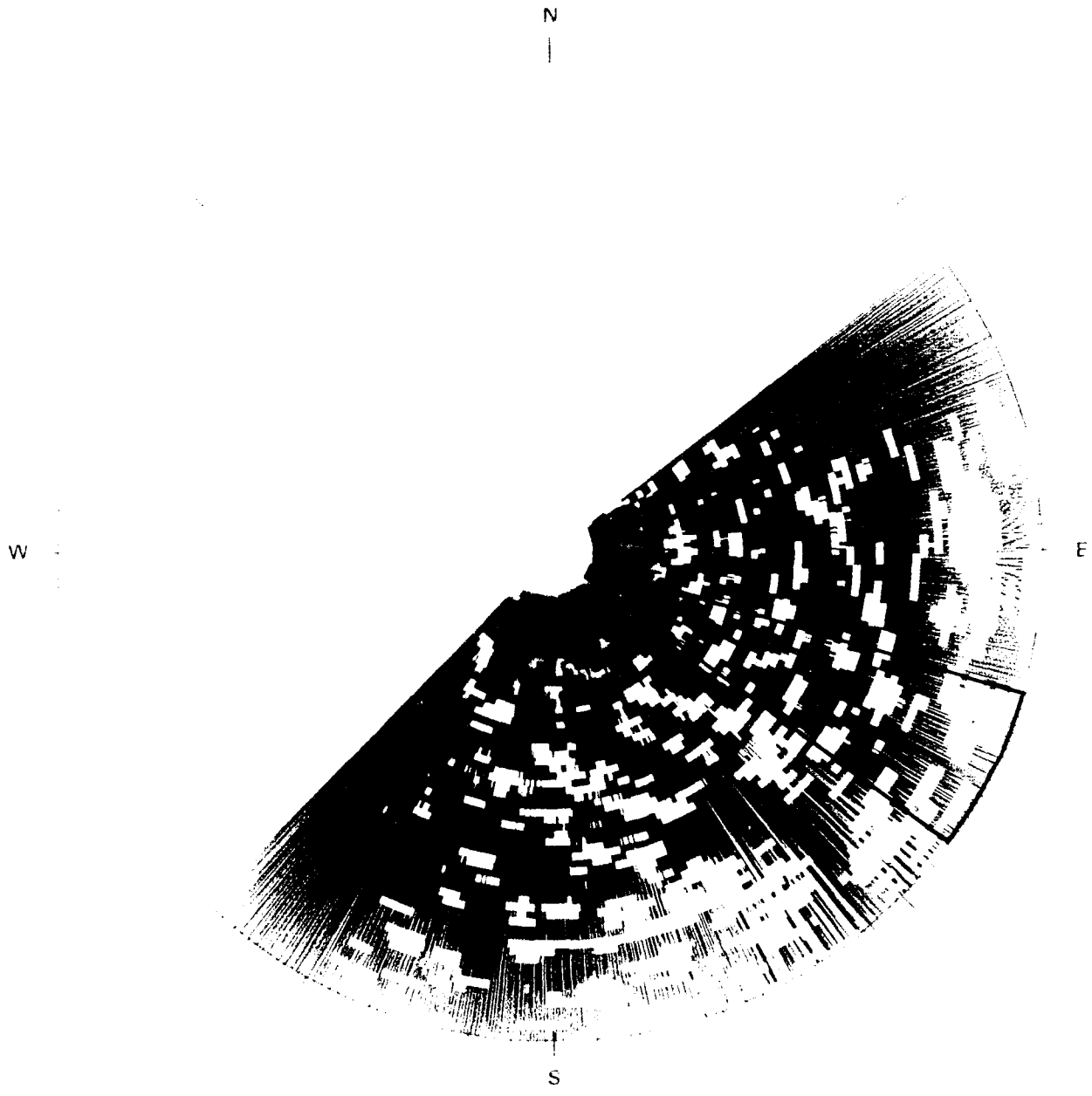

Figure E-102. PPI clutter map and repeat sector at Polonia. Repeat sector is outlined in black. Maximum range = 10 km; L-band, 150-m pulse, horizontal polarization; cells with $\sigma^{o}F^{4} \geq -40$ dB are white.

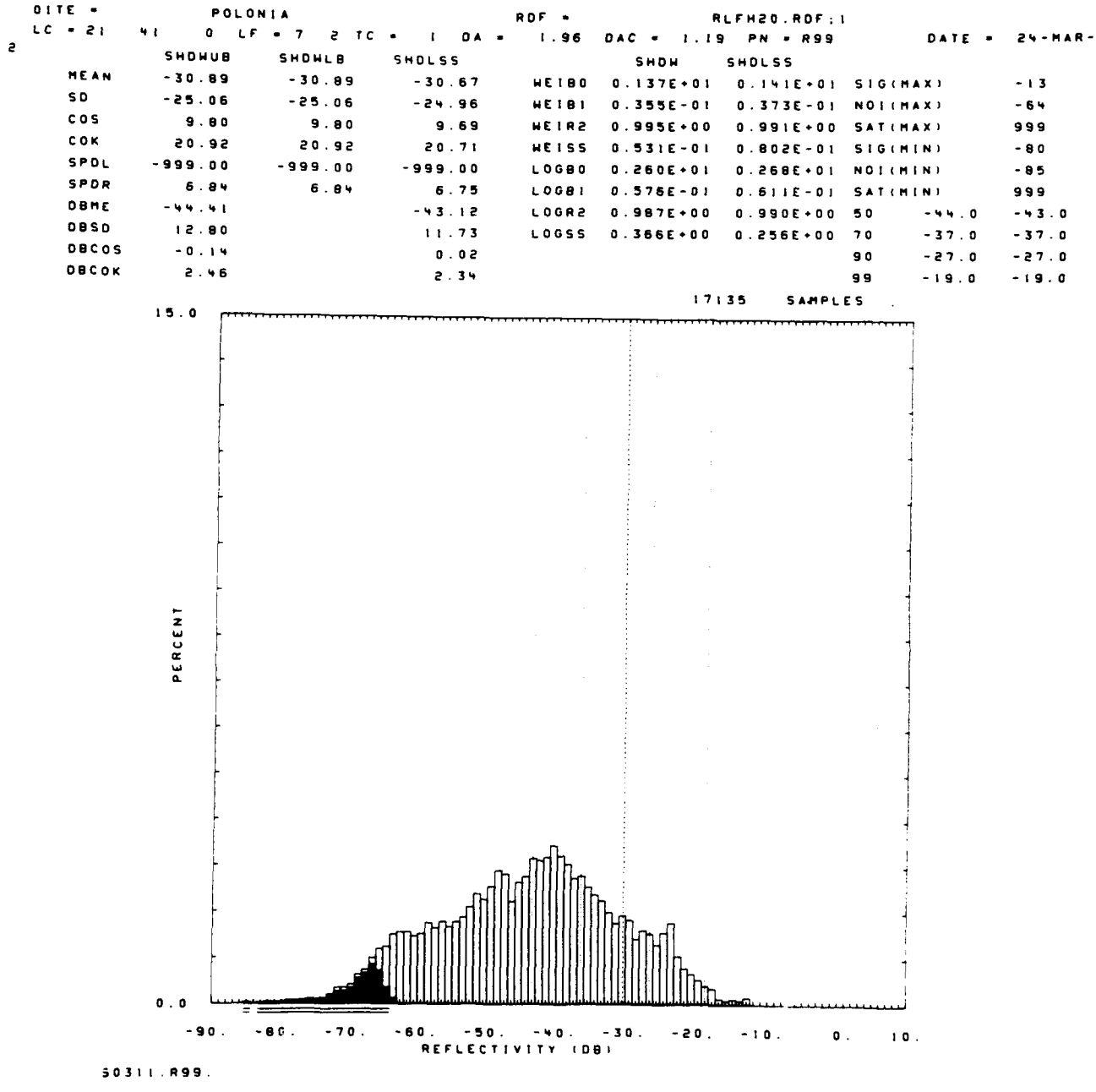

Figure E-103. Clutter strength histogram for Polonia repeat sector. L-band, 150-m pulse, horizontal polarization.

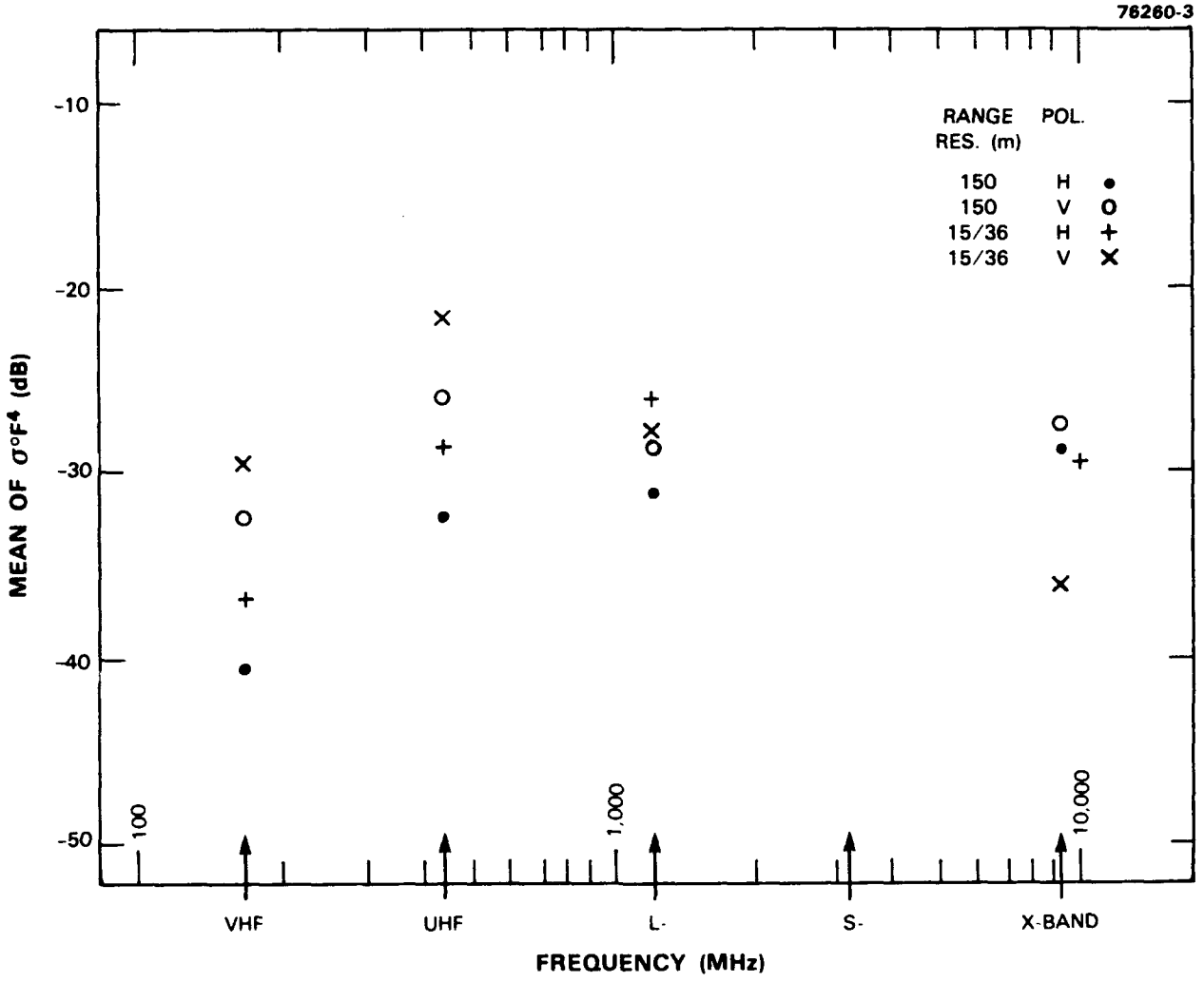

Figure E-104. Mean clutter strength versus frequency at Polonia. For the Polonia repeat sector, depression angle = 2.0 deg, landform = 7-2, land cover = 21-41, range = 1 to 10 km, azimuth = 107 to 127 deg. Comment: S-band was not yet installed at Polonia.

(a)

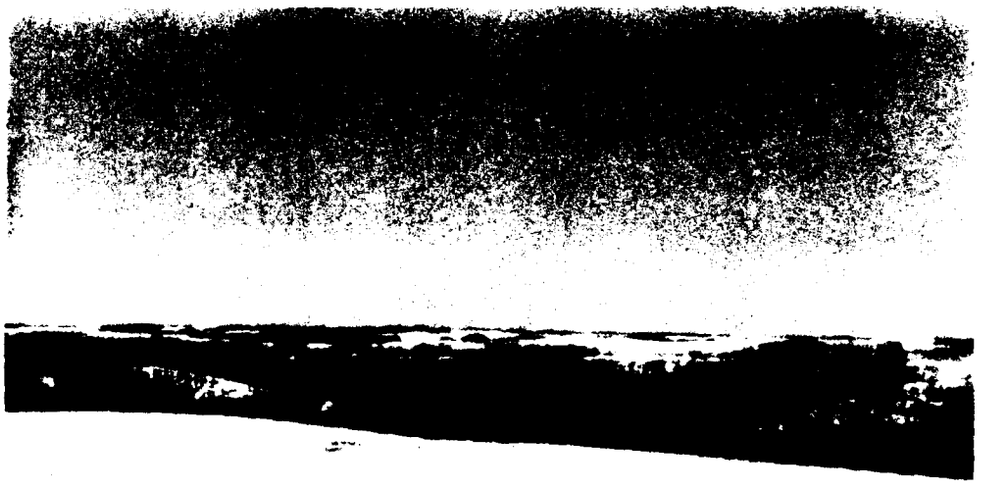

(b)

Figure F-105. Neapaia repeat sector: (a) Looking WNW and (b) looking NNW, mixed gully running across cropland

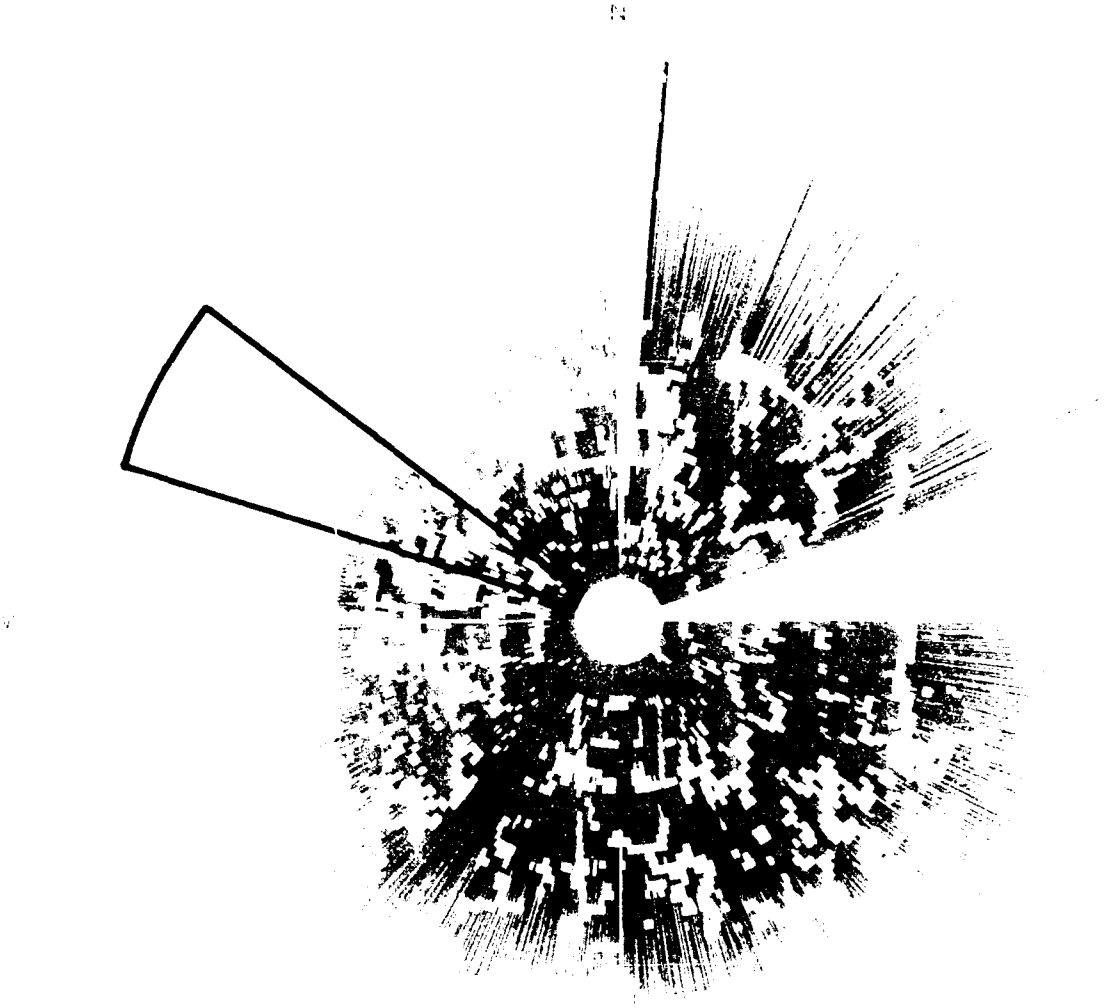

Figure E-106. PPI clutter map and repeat sector at Neepawa. Repeat sector is outlined in black. Maximum range = 11 km, X-band, 150-m pulse, horizontal polarization; cells with $\sigma^{\circ}F^{-4} \geq -45$ dB are white.

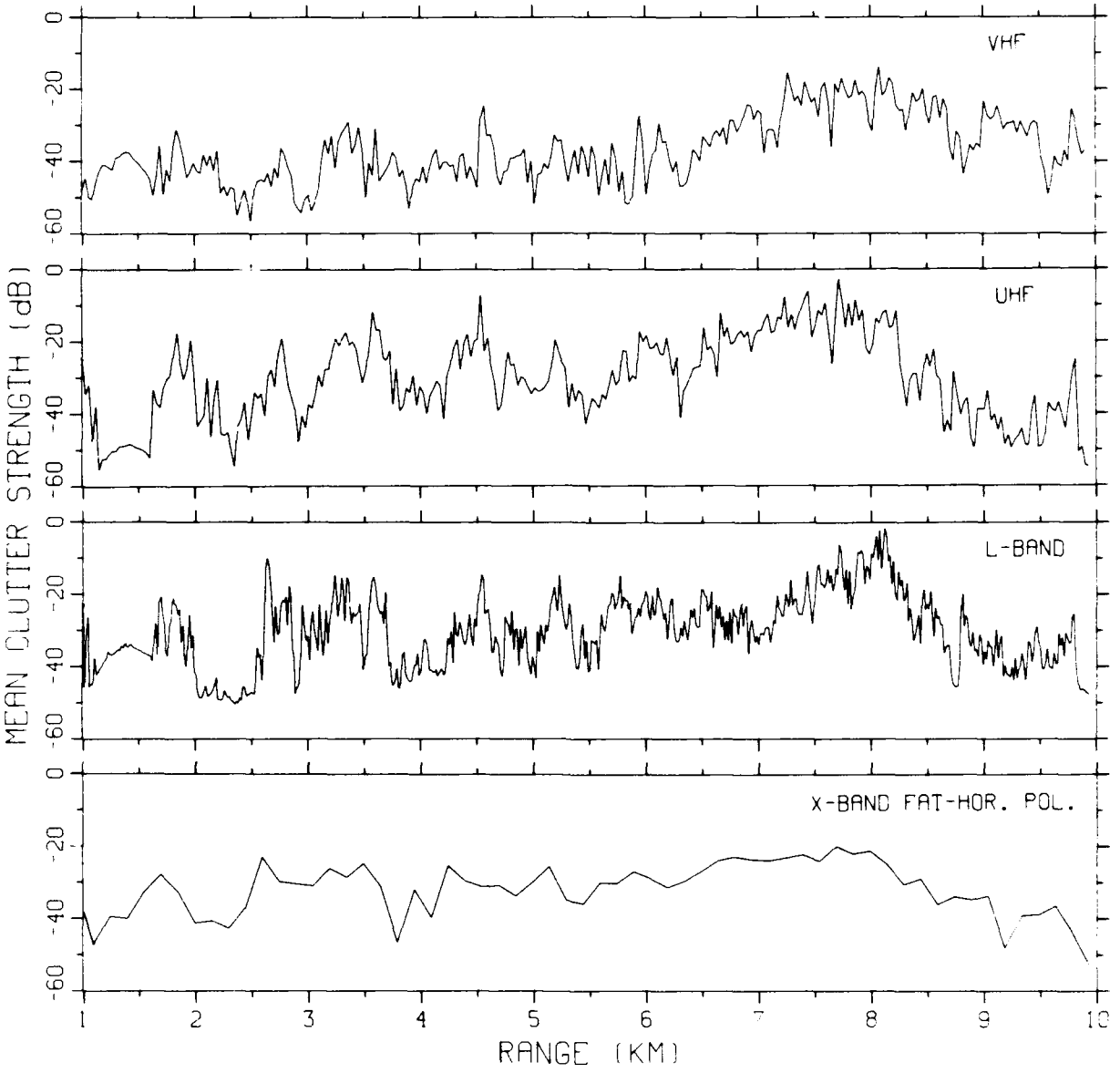

Figure E-107. Mean clutter strength versus range at Neepawa. Repeat sector data. Vertical polarization, 15/36-m pulse length except X-band (horizontal polarization, 150-m pulse length). Data shown range gate by range gate, averaged in azimuth over 20 deg.

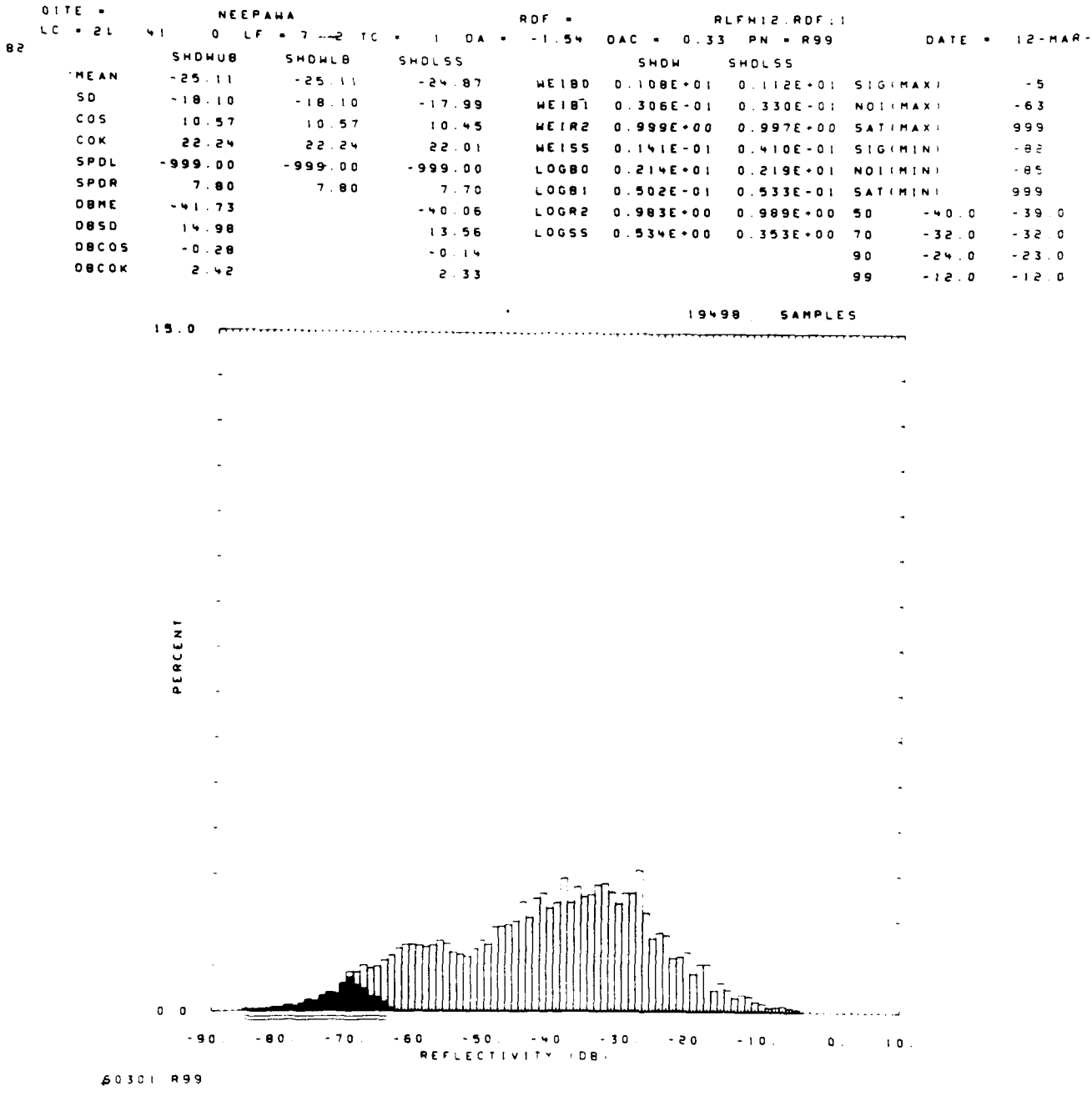

Figure E-108. Clutter strength histogram for Neepawa repeat sector. L-band, 150-m pulse, horizontal polarization.

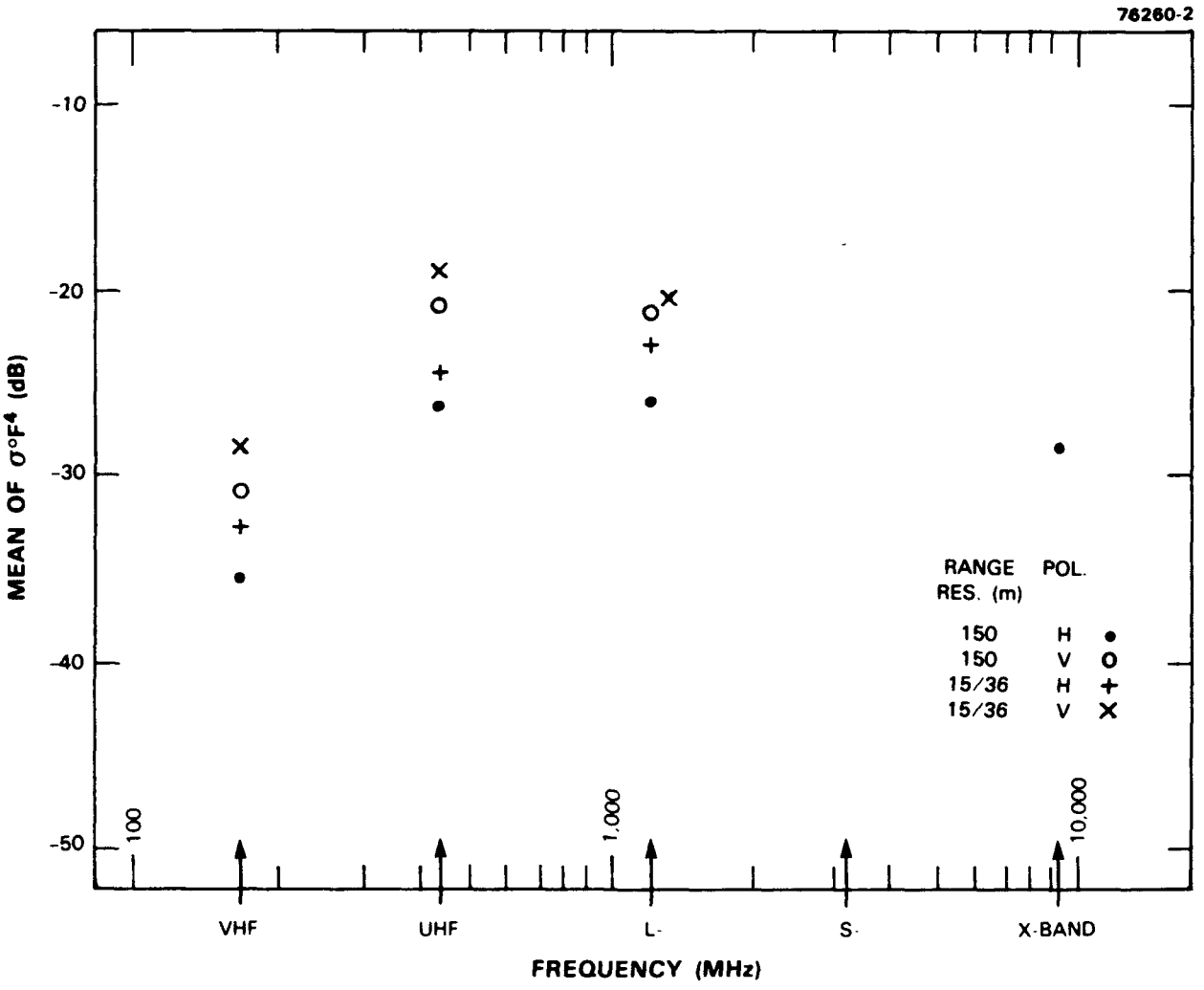

Figure E-109. Mean clutter strength versus frequency at Neepawa. For the Neepawa repeat sector, depression angle = -0.9 deg, landform = 7-2, land cover = 21-41, range = 1 to 10 km, azimuth = 287 to 307 deg. Comments: (1) X-band data collected only at low resolution/horizontal polarization. (2) S-band was not yet installed at Neepawa.

Figure E-110. Repeat sector at Beulah. Tower-top view looking across strip mine spoil piles to agricultural repeat sector beyond.

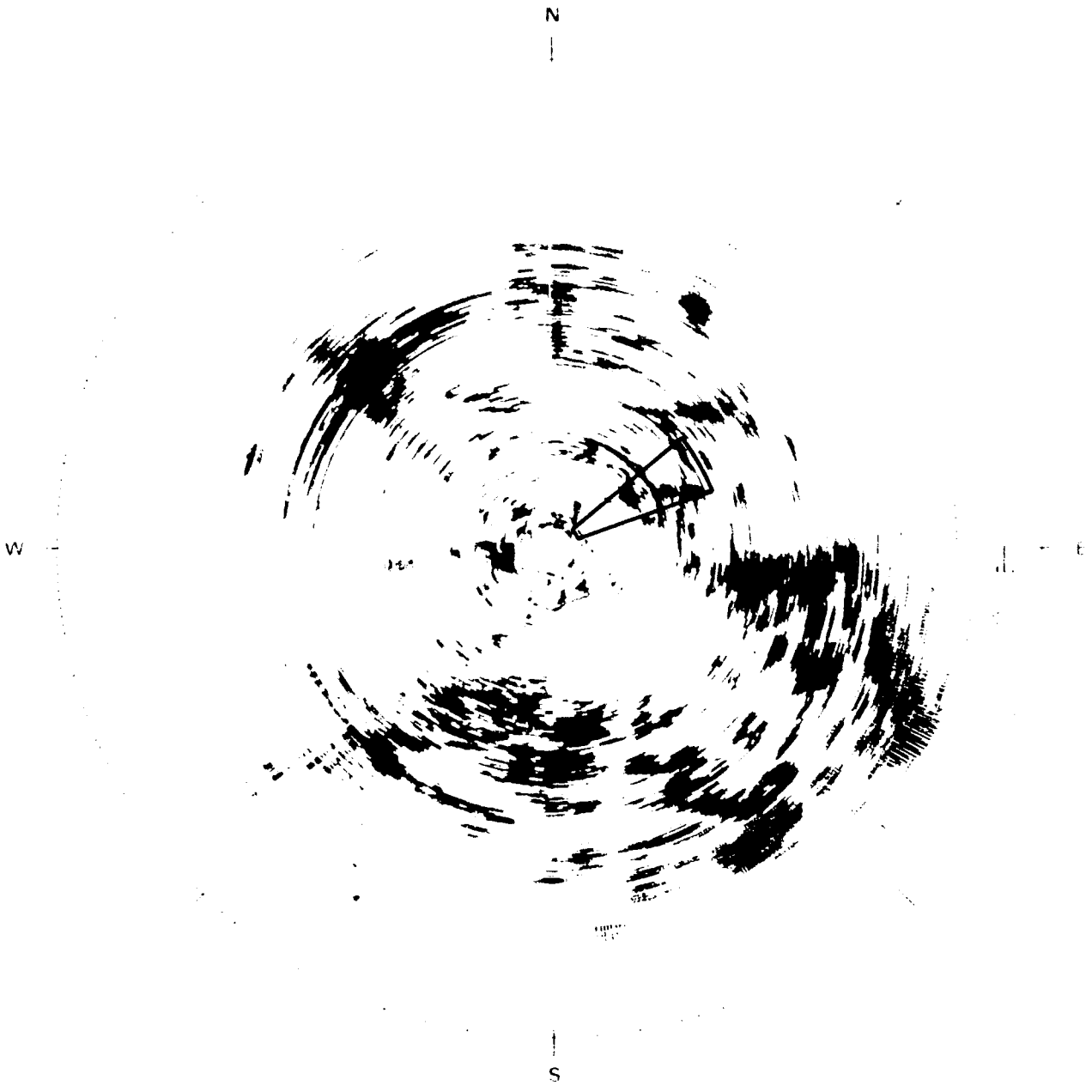

Figure E-111 PPI clutter map and repeat sector at Beulah. Repeat sector is outlined in black. Maximum range = 20 km; UHF, 36-m pulse, horizontal polarization; cells with $\sigma^{\circ}F^{4} \geq 40$ dB are red

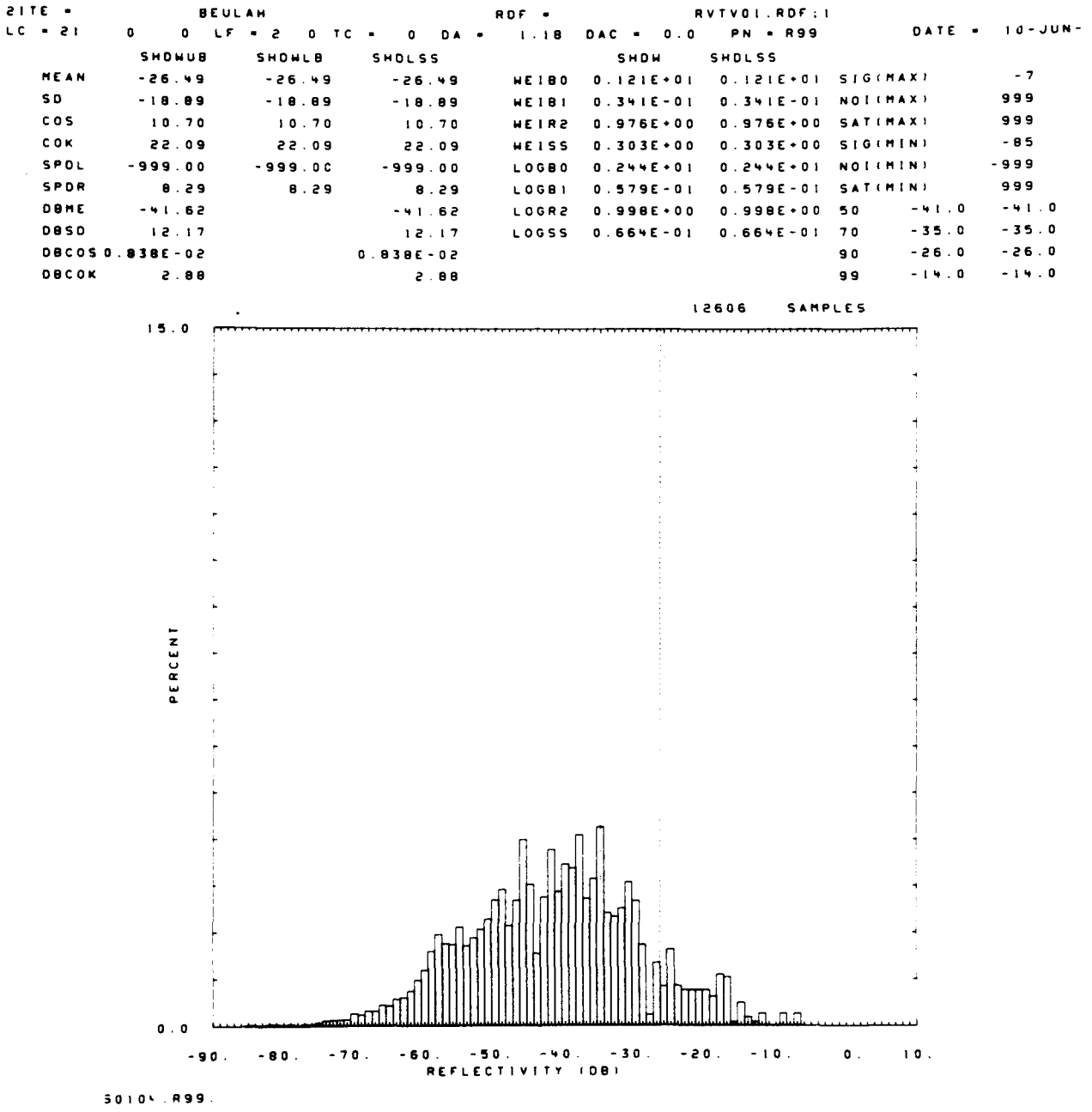

Figure E-112. Clutter strength histogram for Beulah repeat sector. VHF, 36-m pulse, vertical polarization.

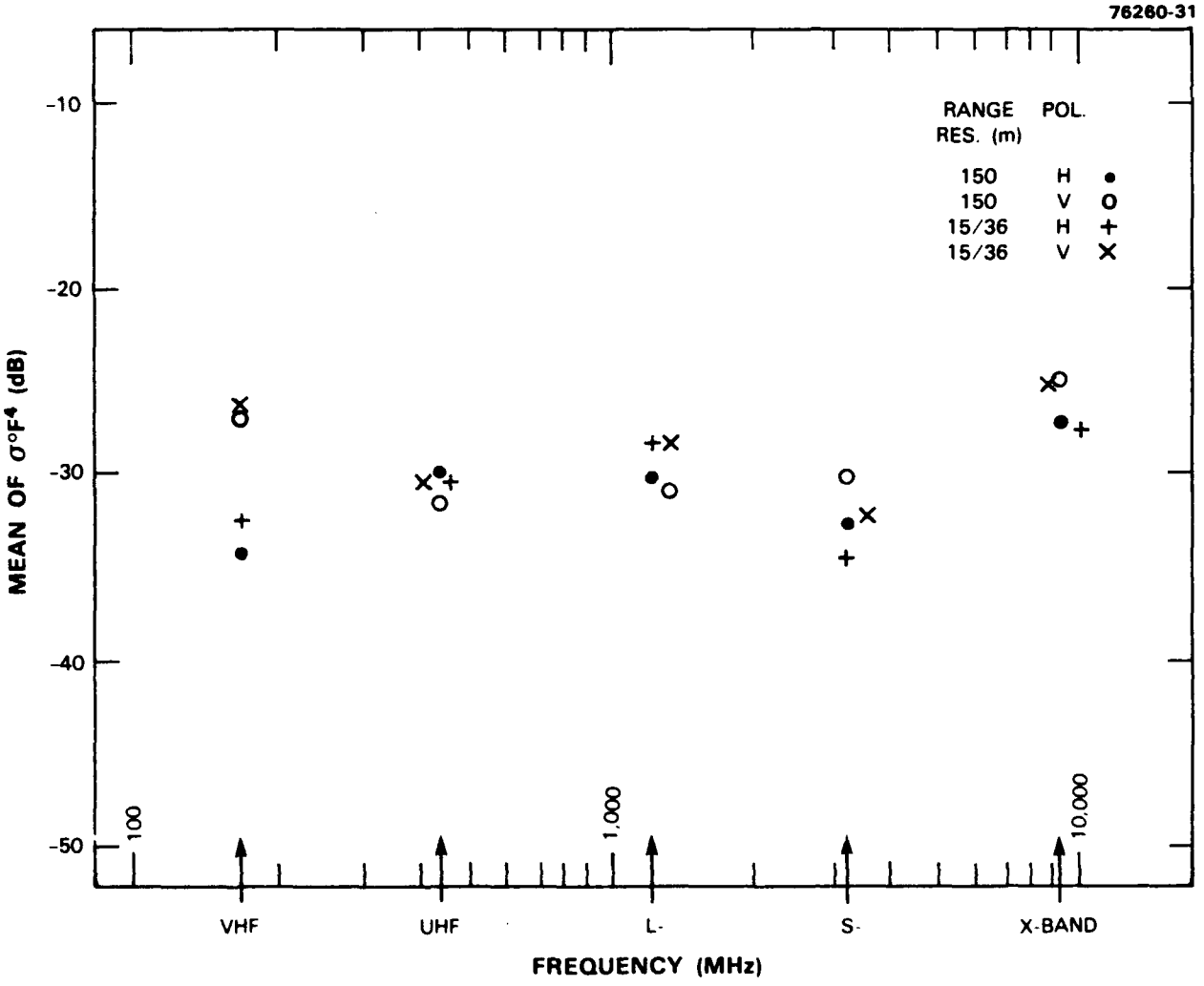

Figure E-113. Mean clutter strength versus frequency at Beulah. For the Beulah repeat sector, depression angle = 1.2 deg, landform = 2, land cover = 21, range = 1 to 6.9 km, azimuth = 50 to 70 deg.

Figure E-114. PPI clutter map and repeat sector at Magrath. Repeat sector is outlined in black. Maximum range = 20 km; X-band, 15-m pulse, horizontal polarization; cells with $\sigma^{\circ}F^4 \geq$ -40 dB are red.

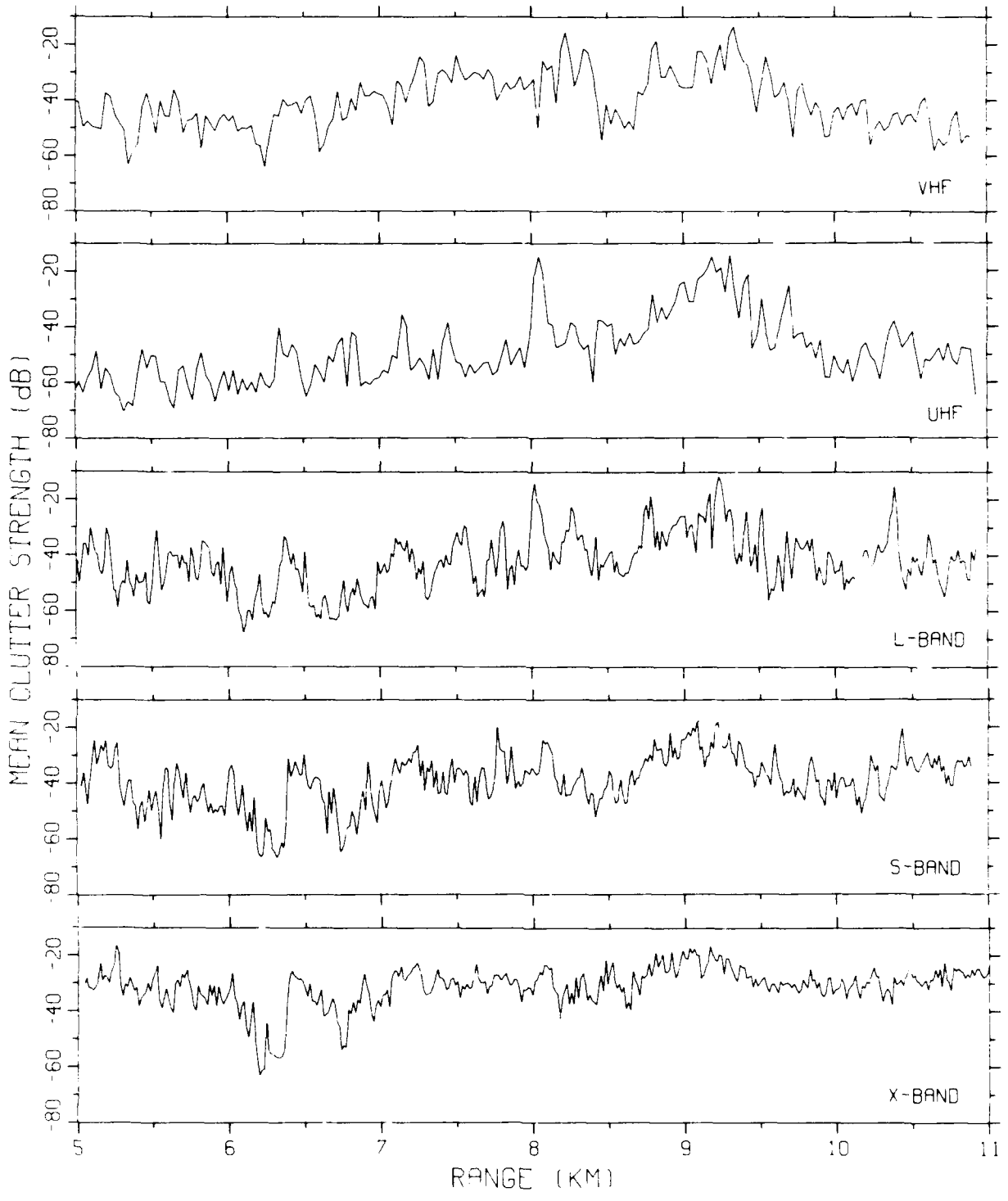

Figure E-115. Mean clutter strength versus range at Magrath. Repeat sector data. Vertical polarization, 15/36-m pulse length. Data shown range gate by range gate, averaged in azimuth over 10 deg.

SITE = MAGRATH RDF = RUFV07.RDF;1

LC = 21 33 0 LF = 3 2 TC = 1 DA = 0.75 DAC = 0.16 PN = R99 DATE = 20-MAY-83

	SHDWUB	SHDWLB	SHDLSS		SHDW	SHDLSS			
MEAN	-28.98	-28.98	-28.97	WEIB0	0.117E+01	0.117E+01	SIG(MAX)		-15
SD	-23.38	-23.38	-23.37	WEIB1	0.274E-01	0.275E-01	NOI(MAX)		-76
COS	6.43	6.43	6.42	WEIR2	0.879E+00	0.878E+00	SAT(MAX)		999
COK	13.47	13.47	13.46	WEISS	0.892E+00	0.907E+00	SIG(MIN)		-76
SPOL	-999.00	-999.00	-999.00	LOGB0	0.228E+01	0.228E+01	NOI(MIN)		-82
SPOR	6.66	6.66	6.65	LOGB1	0.454E-01	0.455E-01	SAT(MIN)		999
DBME	-48.61		-48.54	LOGR2	0.936E+00	0.936E+00	50	-51.0	-51.0
DBSD	12.72		12.65	LOGSS	0.122E+01	0.123E+01	70	-45.0	-45.0
DBCOS	0.88		0.91				90	-26.0	-26.0
DBCOK	3.33		3.32				99	-16.0	-16.0

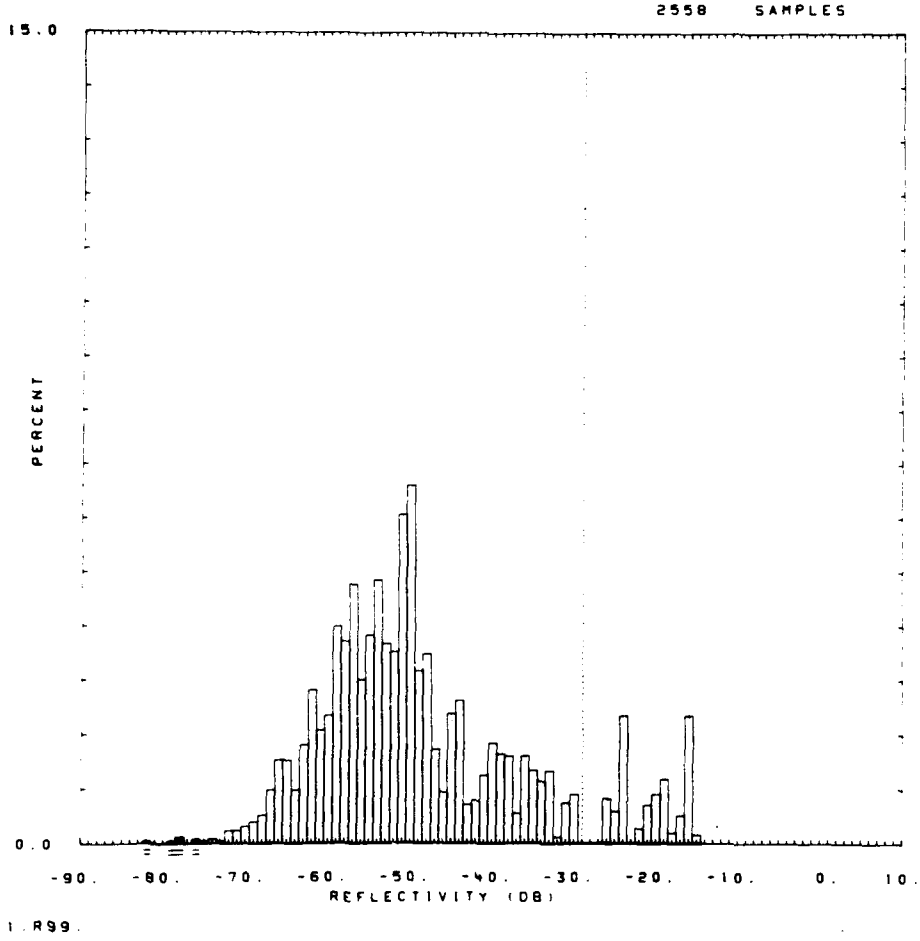

60441.R99.

Figure E-116. Clutter strength histogram for Magrath repeat sector. UHF, 150-m pulse, vertical polarization.

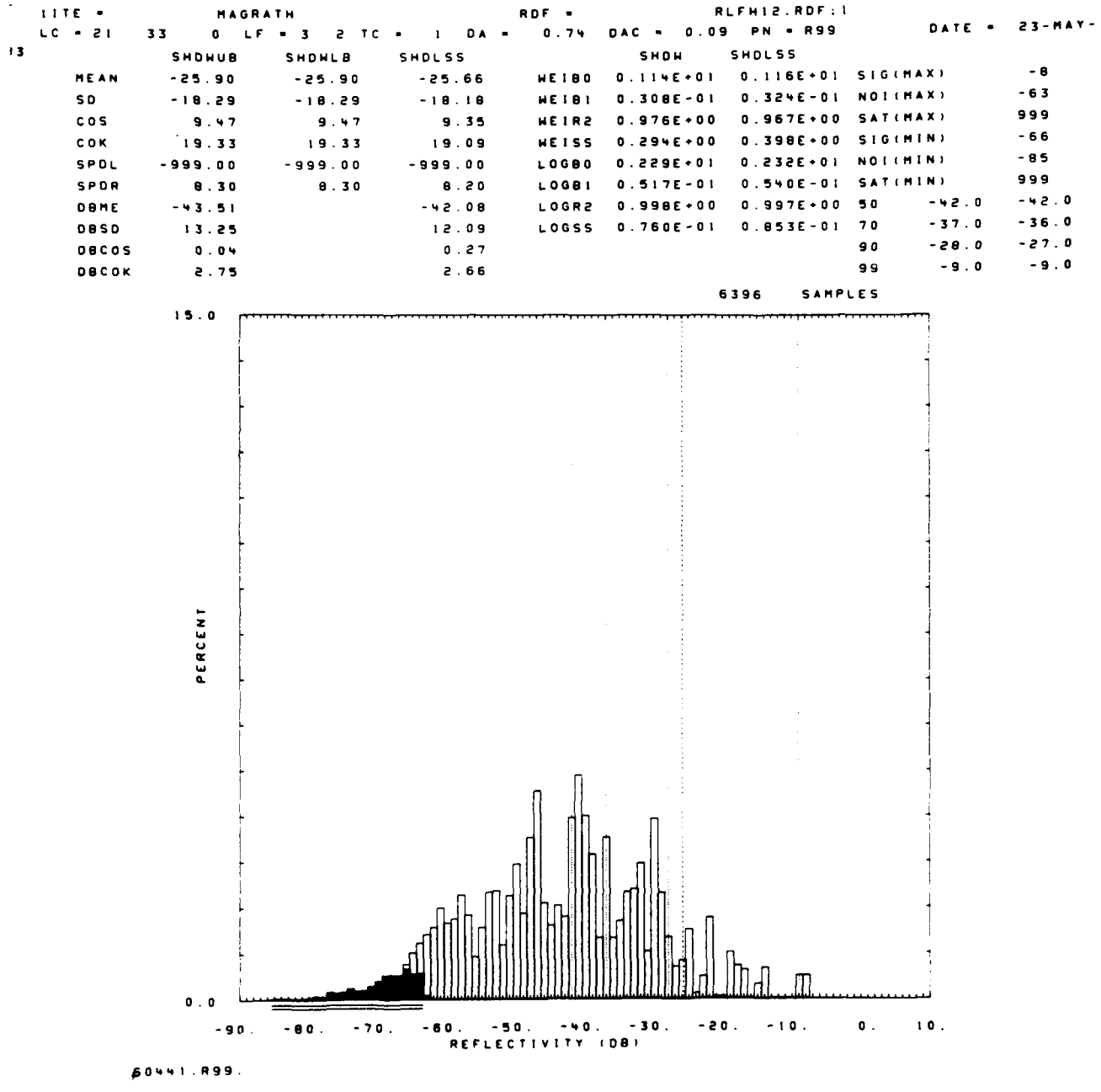

Figure E-117. Clutter strength histogram for Magrath repeat sector. L-band. 150-m pulse. horizontal polarization.

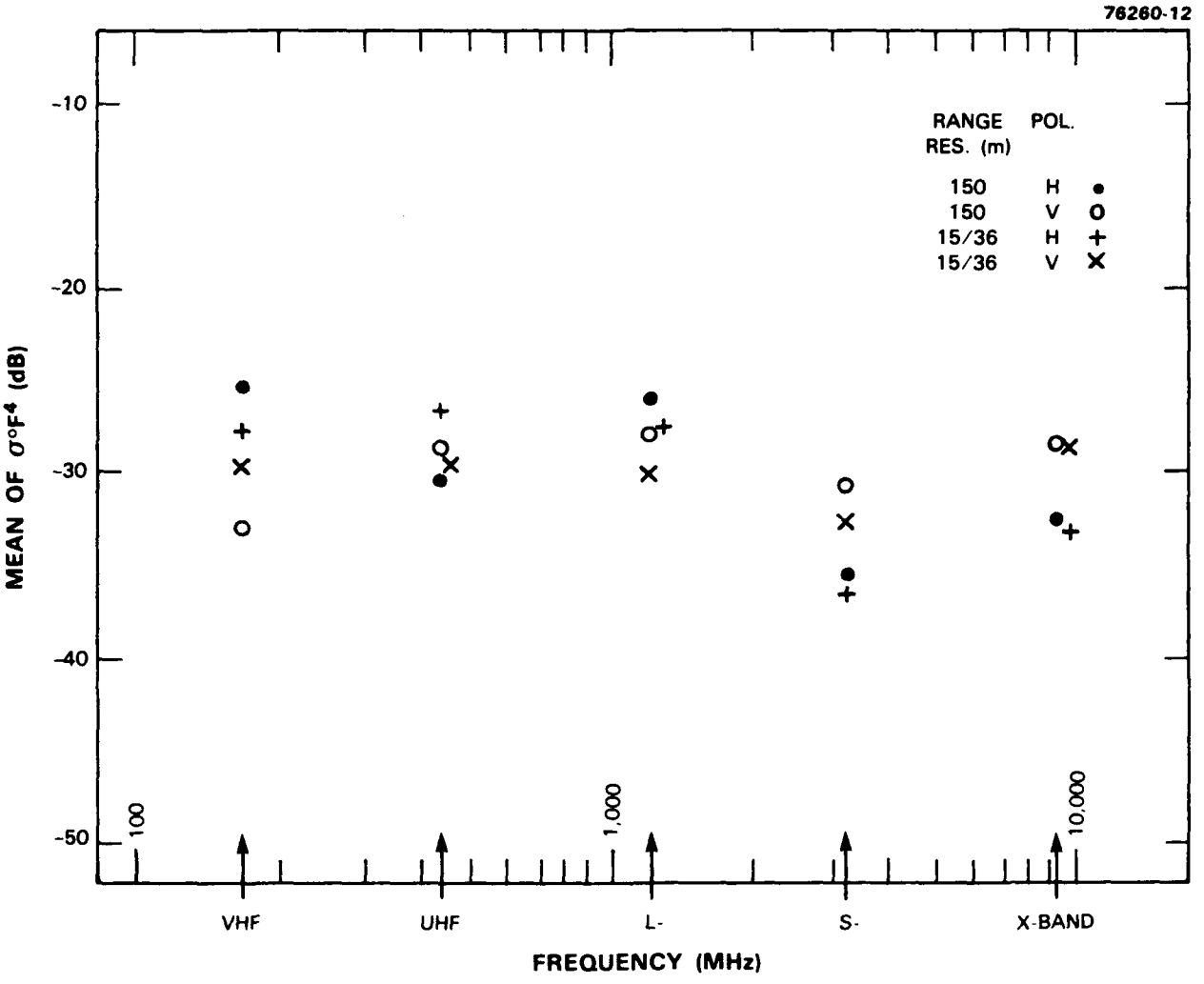

Figure E-118. Mean clutter strength versus frequency at Magrath. For the Magrath repeat sector, depression angle = 0.7 deg, landform = 3-2, land cover = 21-33, range = 5 to 10.9 km, azimuth = 125 to 135 deg.

(a)

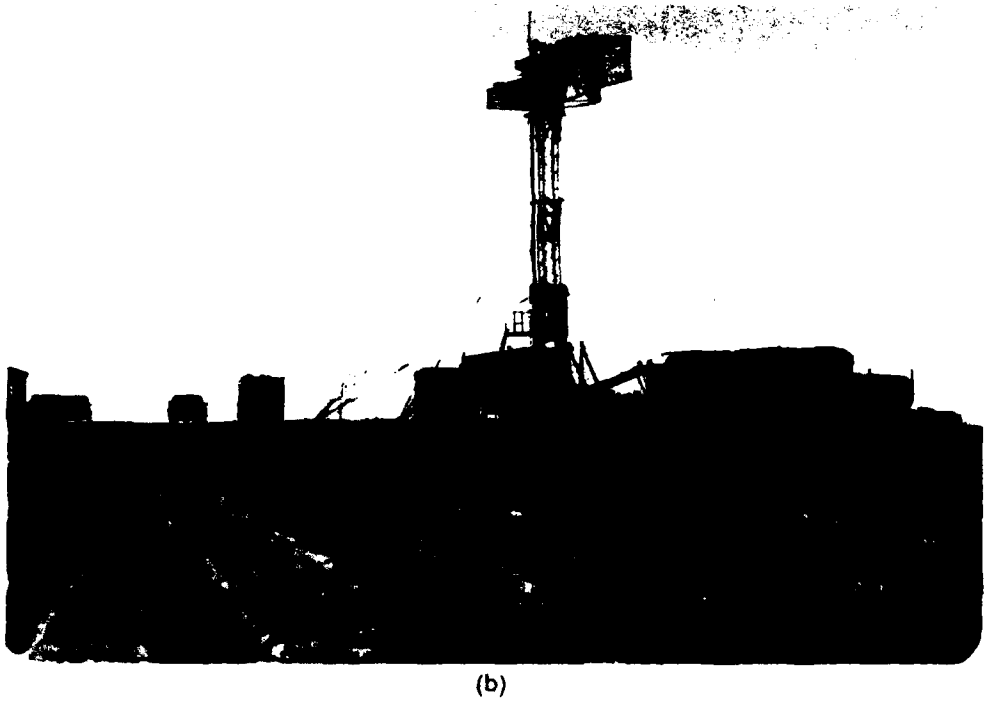

(b)

Figure I-119. Phase One at Berskeville on November 1982 and the February 1983

(c)

SE

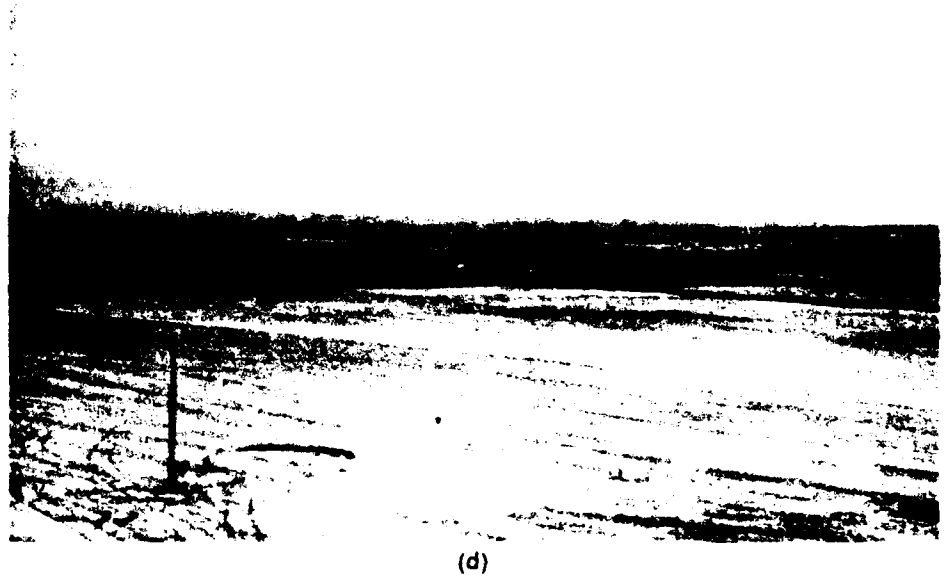

(d)

Figure E-119 (Continued): Phase One at Berseker (c) August 1983. View south from site center and (d) November 1985. Tower top view SE into repeat section.

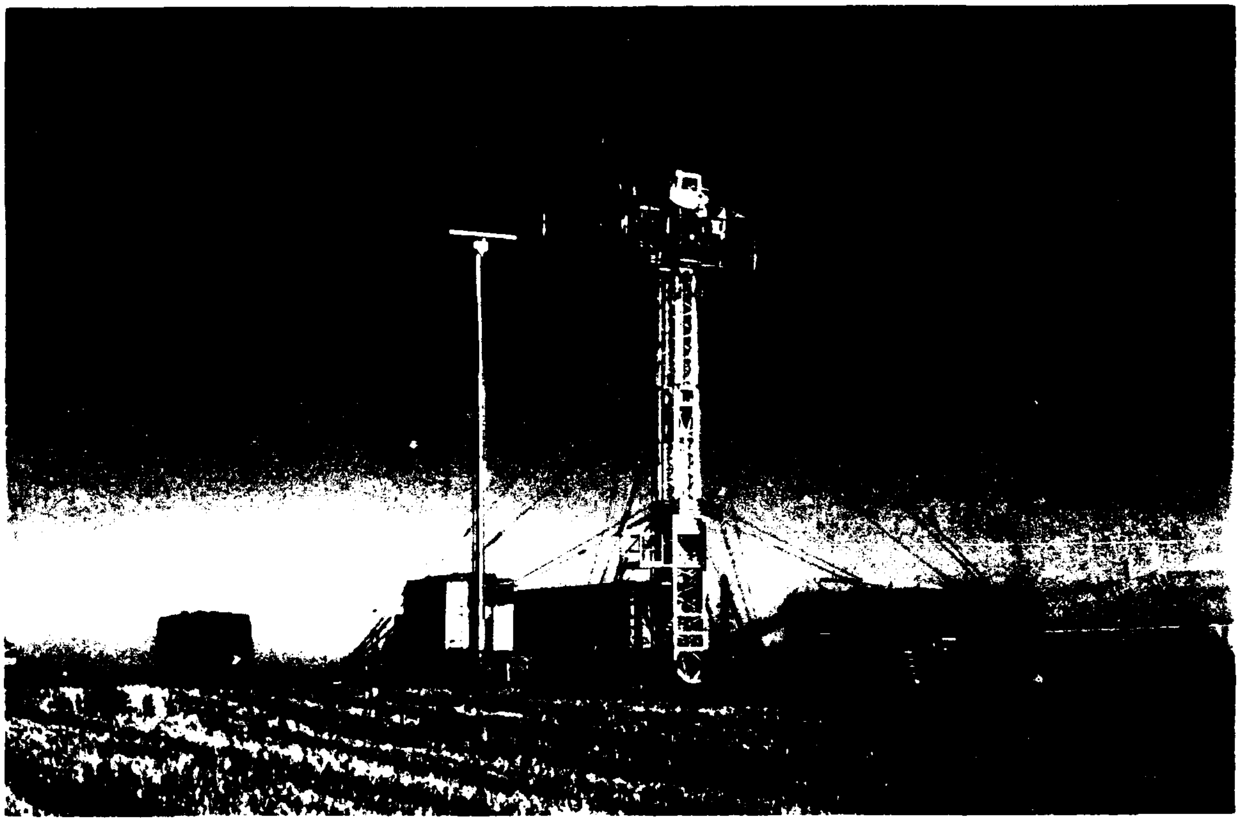

Figure I-[illegible] Phase One Phase Z[illegible] at B[illegible] November 198[illegible]

Figure E-121. PPI clutter map and repeat sector at Beiseker. Repeat sector is outlined in black. Maximum range = 20 km, X-band, 15-m pulse, horizontal polarization; cells with $\sigma^{\circ}F^{4} \geq -40$ dB are red. Fourth visit

SITE = BEISEKER RDF = RVTV01.RDF;1

LC = 21 31 0 LF = 3 2 TC = 0 DA = 0.39 DAC = 0.0 PN = R99 DATE = 17-FEB-83

	SHDWUB	SHDWLB	SHDLSS		SHDW	SHDLSS			
MEAN	-26.48	-26.49	-23.68	WEIB0	0.937E+00	0.962E+00	SIG(MAX)		-5
SD	-17.10	-17.10	-15.72	WEIB1	0.197E-01	0.260E-01	NOI(MAX)		-41
COS	11.62	11.62	10.19	WEIR2	0.989E+00	0.972E+00	SAT(MAX)		999
COK	23.58	23.58	20.76	WEISS	0.156E-01	0.710E-01	SIG(MIN)		-64
SPDL	-999.00	-999.00	-999.00	LOGB0	0.230E+01	0.224E+01	NOI(MIN)		-81
SPDR	9.85	9.86	8.60	LOGB1	0.468E-01	0.551E-01	SAT(MIN)		999
DBME	-44.39		-37.05	LOGR2	0.996E+00	0.993E+00	50	-46.0	-39.0
DBSD	10.84		9.21	LOGSS	0.344E-01	0.751E-01	70	-40.0	-34.0
DBCOS	0.89		0.82				90	-29.0	-24.0
DBCOK	3.62		3.55				99	-14.0	-11.0

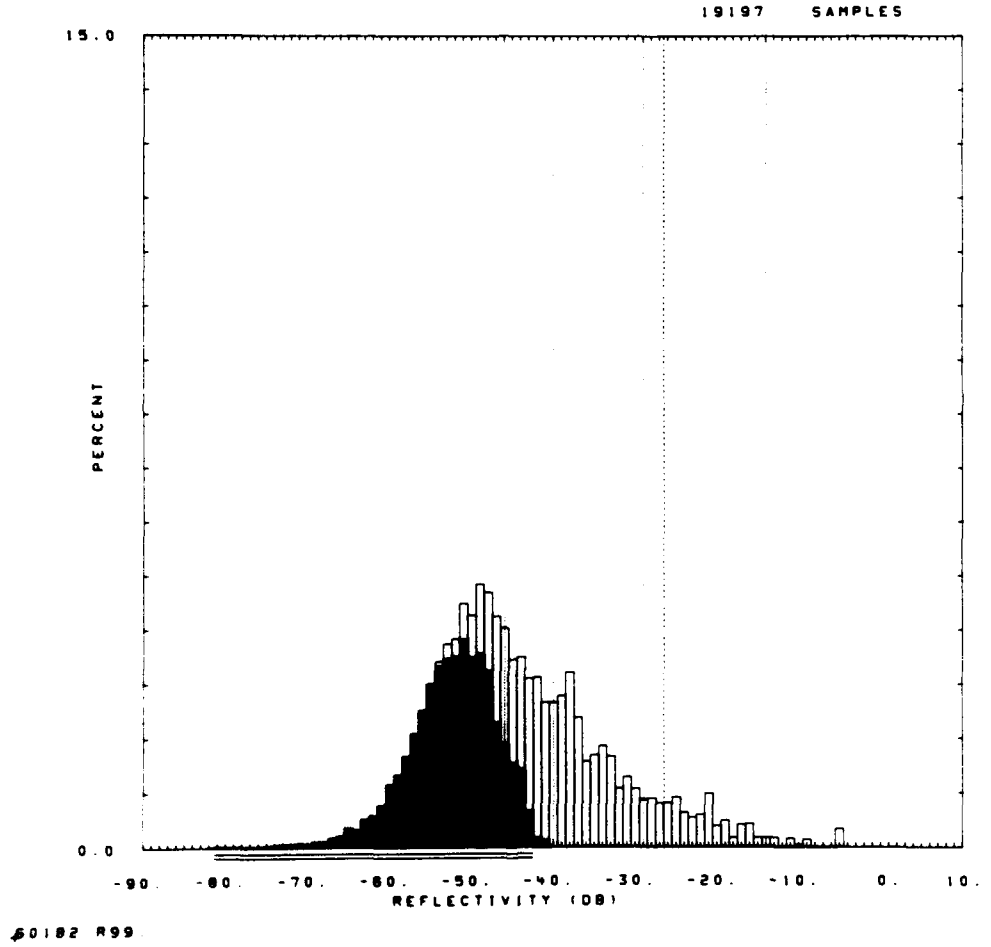

Figure E-122. Clutter strength histogram for Beiseker repeat sector. VHF, 36-m pulse, vertical polarization. Second visit.

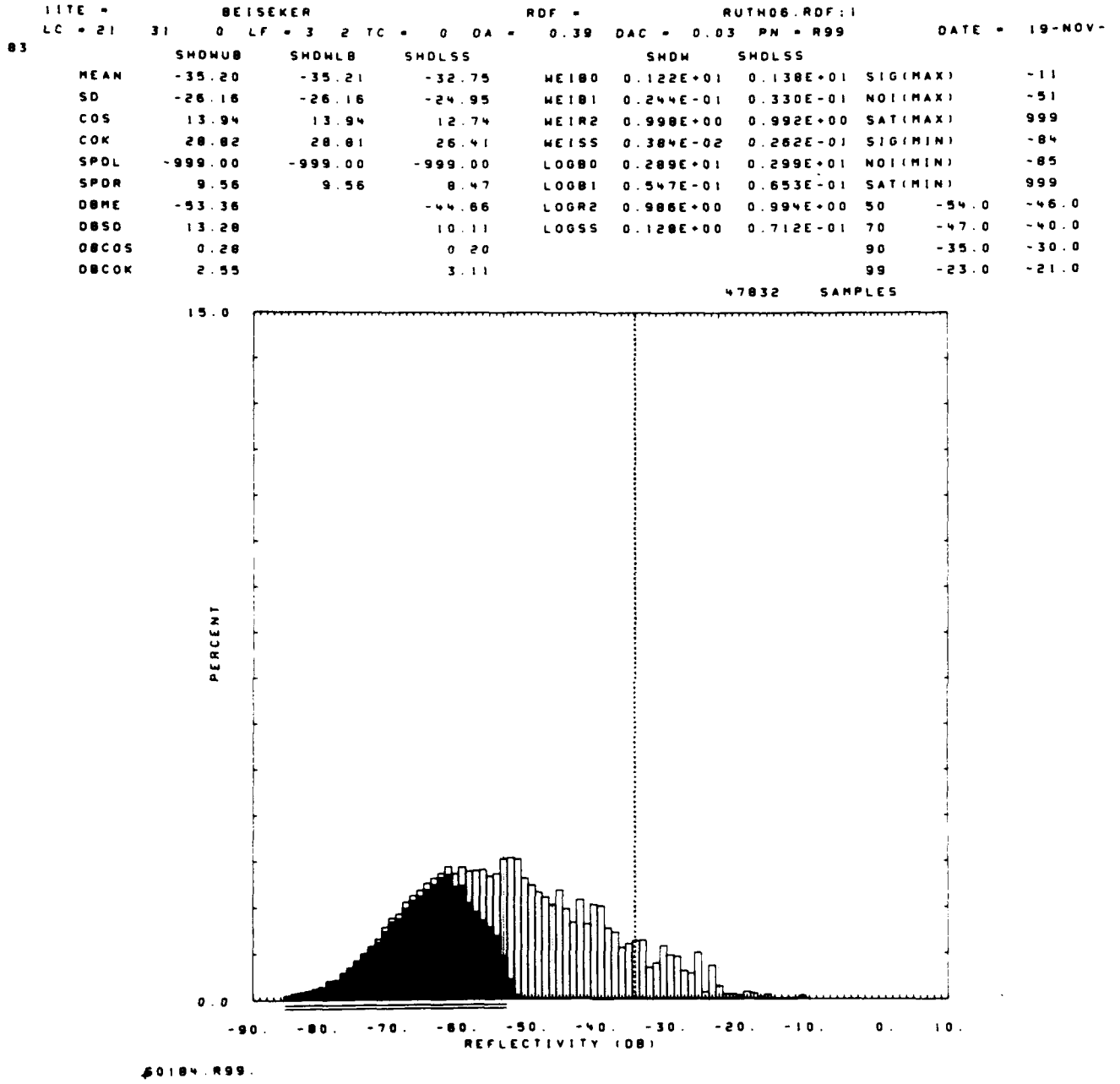

Figure E-123. Clutter strength histogram for Beiseker repeat sector. UHF, 36-m pulse, horizontal polarization. Fourth visit.

SITE = BEISEKER RDF = RLFH12.RDF;1

LC = 21 31 0 LF = 3 2 TC = 0 DA = 0.39 DAC = 0.00 PN = R99 DATE = 19-NOV-83

	SHDWUB	SHDWLB	SHDLSS		SHDW	SHDLSS			
MEAN	-28.24	-28.24	-27.15	WEIB0	0.103E+01	0.114E+01	SIG(MAX)		-9
SD	-21.15	-21.15	-20.63	WEIB1	0.241E-01	0.305E-01	NOI(MAX)		-58
COS	10.20	10.20	9.66	WEIR2	0.998E+00	0.990E+00	SAT(MAX)		999
COK	21.49	21.49	20.43	WEISS	0.755E-02	0.688E-01	SIG(MIN)		-85
SPOL	-999.00	-999.00	-999.00	LOGB0	0.223E+01	0.230E+01	NOI(MIN)		-85
SPDR	7.87	7.87	7.39	LOGB1	0.458E-01	0.525E-01	SAT(MIN)		999
DBME	-48.30		-42.77	LOGR2	0.981E+00	0.991E+00	50	-50.0	-43.0
DBSD	15.70		13.02	LOGSS	0.315E+00	0.187E+00	70	-38.0	-35.0
DBCOS	0.14		0.16				90	-27.0	-25.0
DBCOK	2.17		2.28				99	-14.0	-14.0

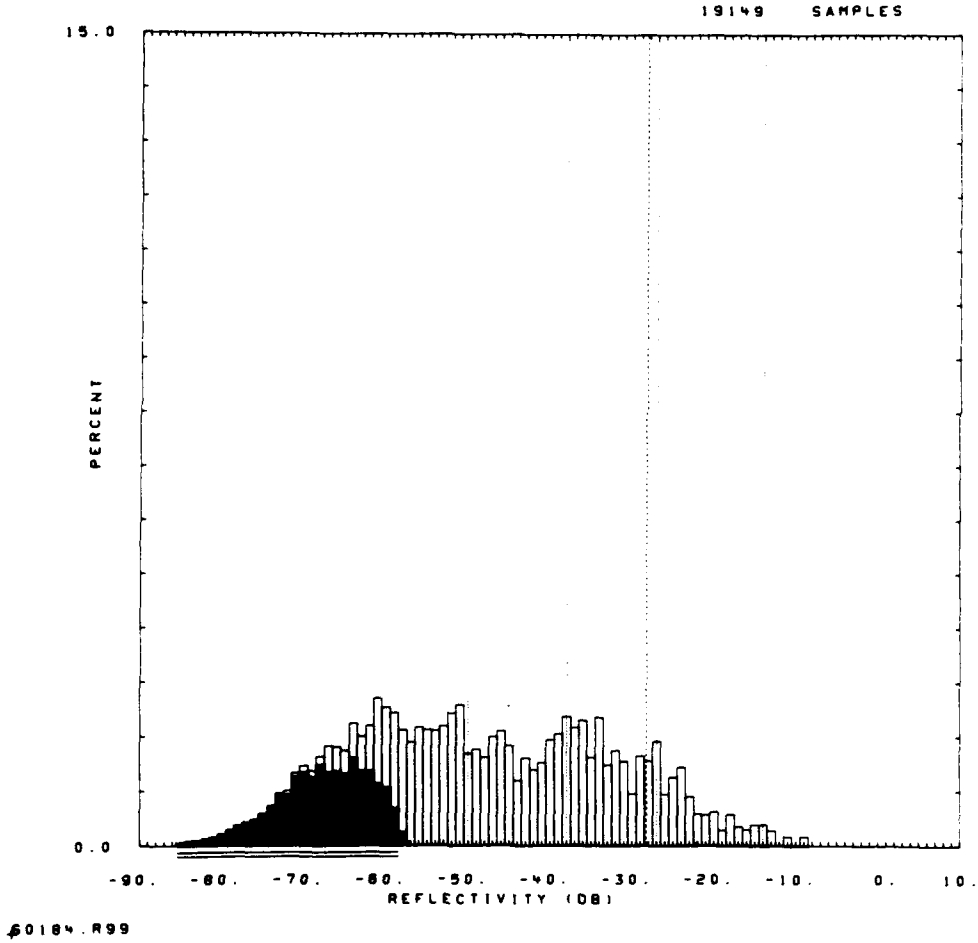

Figure E-124. Clutter strength histogram for Beiseker repeat sector. L-band, 150-m pulse, horizontal polarization. Fourth visit.

SITE = BEISEKER RDF = RSFH16.RDF:1

LC = 21 31 0 LF = 3 2 TC = 0 DA = 0.39 DAC = 0.39 PN = R99 DATE = 21-NOV-83

	SHDWU8	SHDWL8	SHDLSS		SHDW	SHDLSS			
MEAN	-30.59	-30.59	-29.35	WEIB0	0.110E+01	0.126E+01	SIG(MAX)		-6
SD	-20.11	-20.11	-19.50	WEIB1	0.228E-01	0.300E-01	NOI(MAX)		-66
COS	13.45	13.45	12.83	WEIR2	0.999E+00	0.991E+00	SAT(MAX)		999
COK	27.21	27.21	25.97	WEISS	0.517E-02	0.910E-01	SIG(MIN)		-85
SPDL	-999.00	-999.00	-999.00	LOGB0	0.240E+01	0.250E+01	NOI(MIN)		-85
SPDR	10.85	10.85	10.28	LOGB1	0.437E-01	0.512E-01	SAT(MIN)		999
DBME	-55.00		-47.96	LOGR2	0.980E+00	0.994E+00	50	-55.0	-48.0
DBSD	17.30		13.80	LOGSS	0.428E+00	0.179E+00	70	-44.0	-40.0
DBCOS	0.14		0.09				90	-32.0	-30.0
DBCOK	2.01		2.35				99	-19.0	-18.0

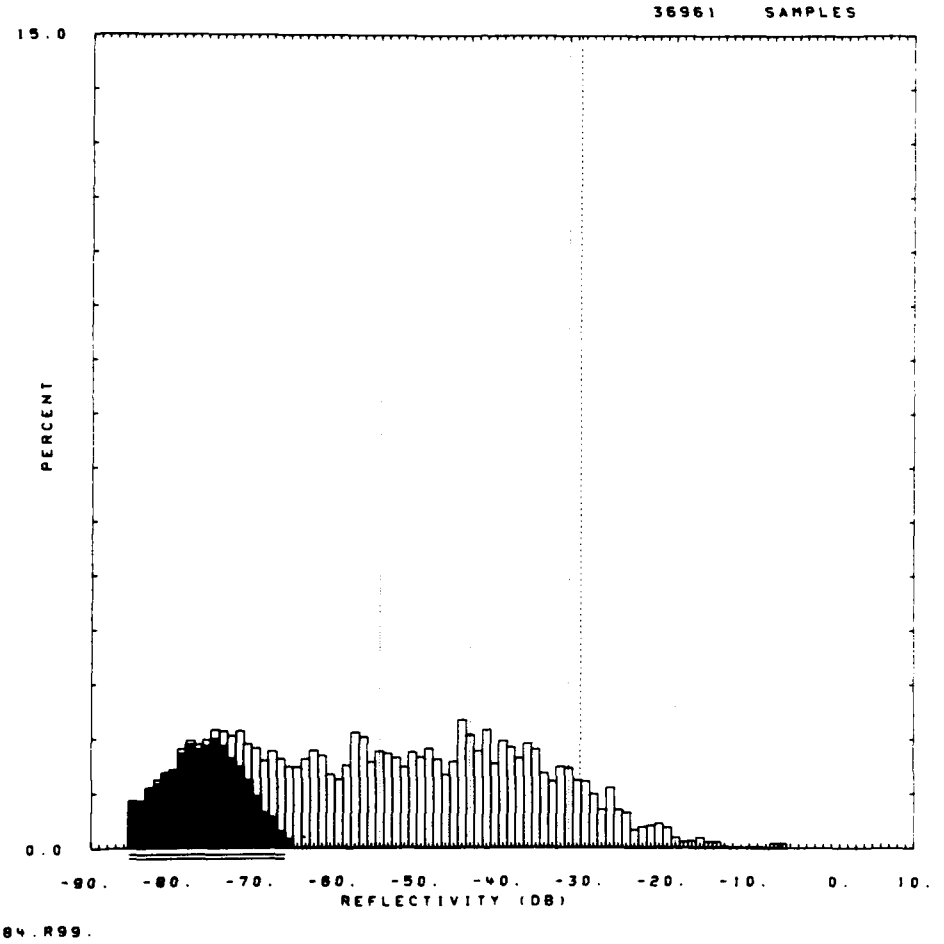

Figure E-125. Clutter strength histogram for Beiseker repeat sector, S-band, 150-m pulse, horizontal polarization. Fourth visit.

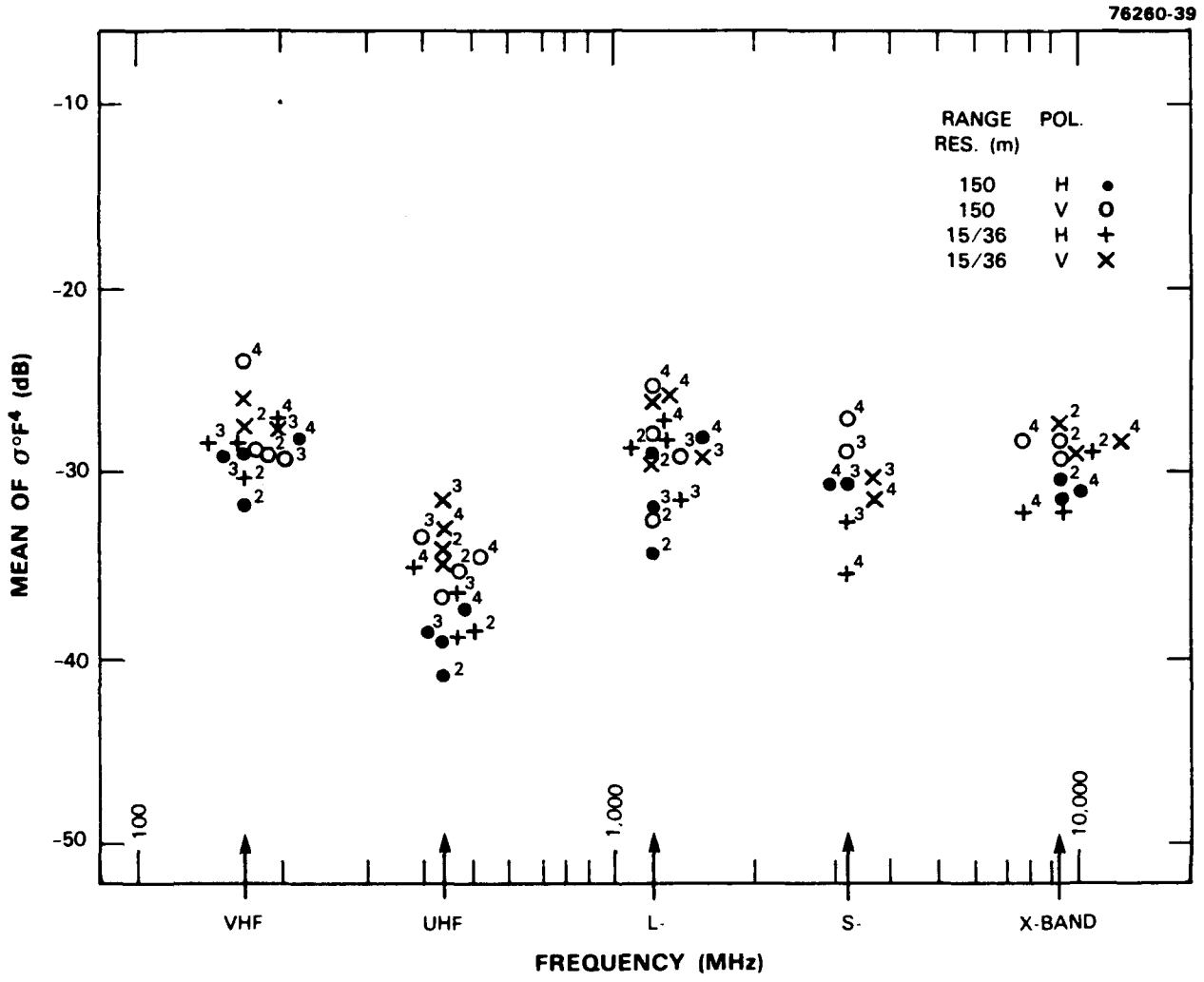

Figure E-126. Mean clutter strength versus frequency at Beiseker. For Beiseker repeat sector, depression angle = 0.4 deg, landform = 3-2, land cover = 21-31, range = 8 to 17 km, azimuth = 150 to 170 deg. Comments: (1) There were four Phase One visits to Beiseker; order of return visits indicated by superscript, e.g., 3's indicate third visit results. (2) During first and second visits, hardware problems at S-band, no useful data acquired. (3) During third visit, hardware problems at X-band, no useful data acquired. (4) At VHF, second visit, interference may have slightly affected high resolution data. (5) At VHF, fourth visit, high resolution/vertical polarization data inadvertently taken at incorrect azimuth; therefore, result omitted. (6) At S-band, third and fourth visits, high resolution range interval (8.0 to 13.9 km) is shorter than for other 18 frequency band/waveform combinations (8.0 to 17.0 km).

Figure F-127. Aerial photo of repeat sector at Orion. Scale = 1:50000. North is up.

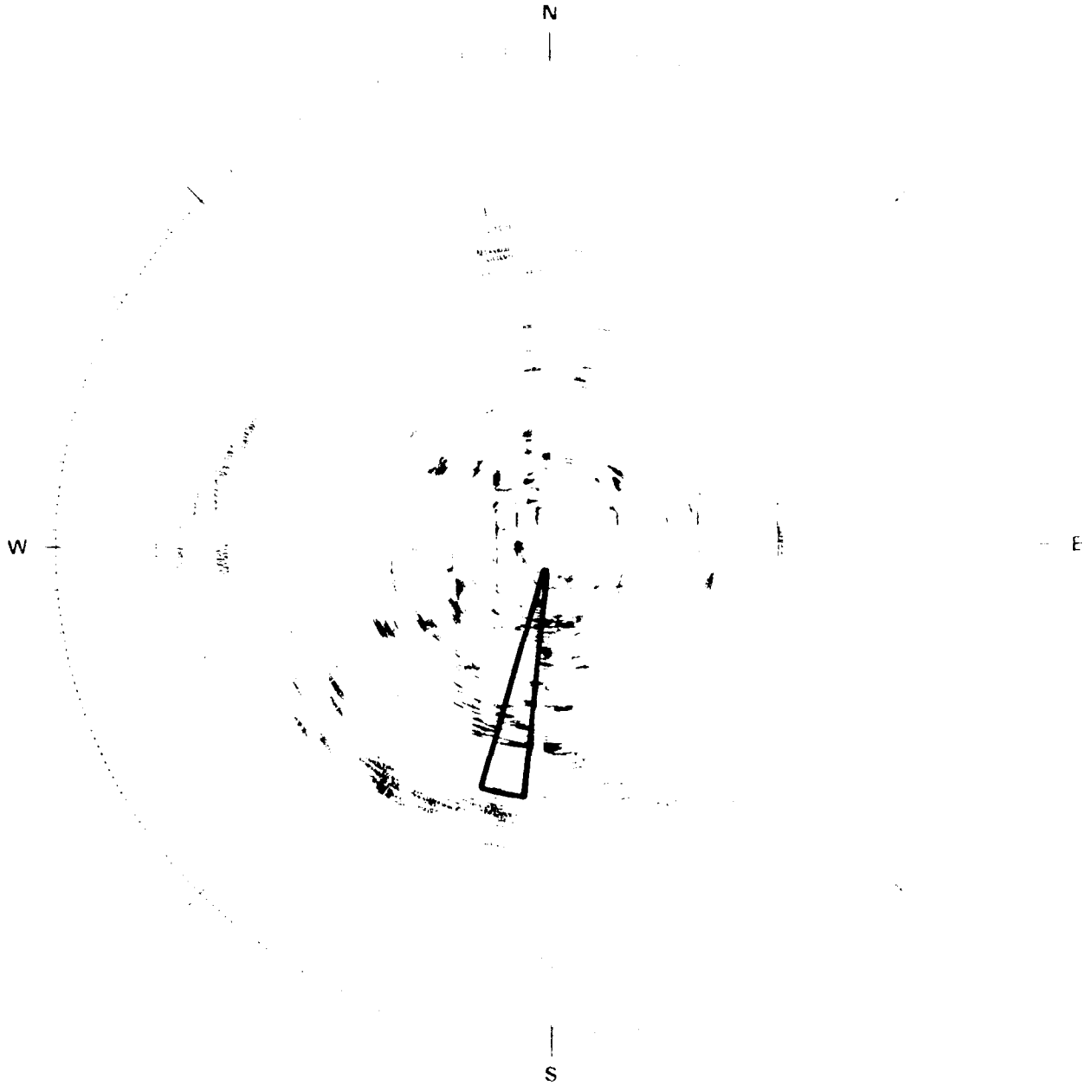

Figure E-128. PPI clutter map and repeat sector at Orion. Repeat sector is outlined in black. Maximum range = 20 km; L-band, 15-m pulse, horizontal polarization; cells with $\sigma^{\circ}F^{4} \geq -40$ dB are red.

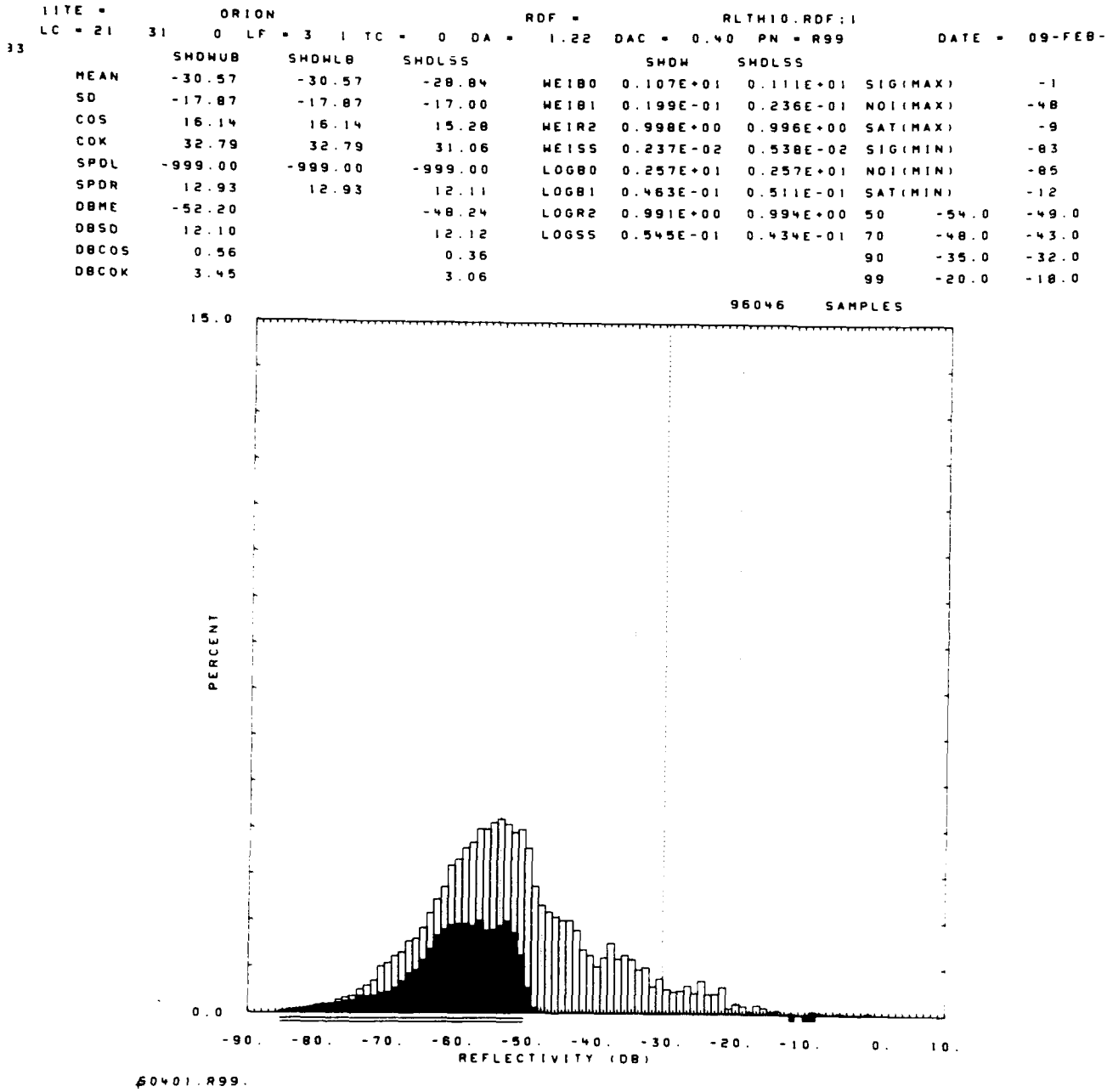

Figure E-129. Clutter strength histogram for Orion repeat sector. L-band, 15-m pulse, horizontal polarization.

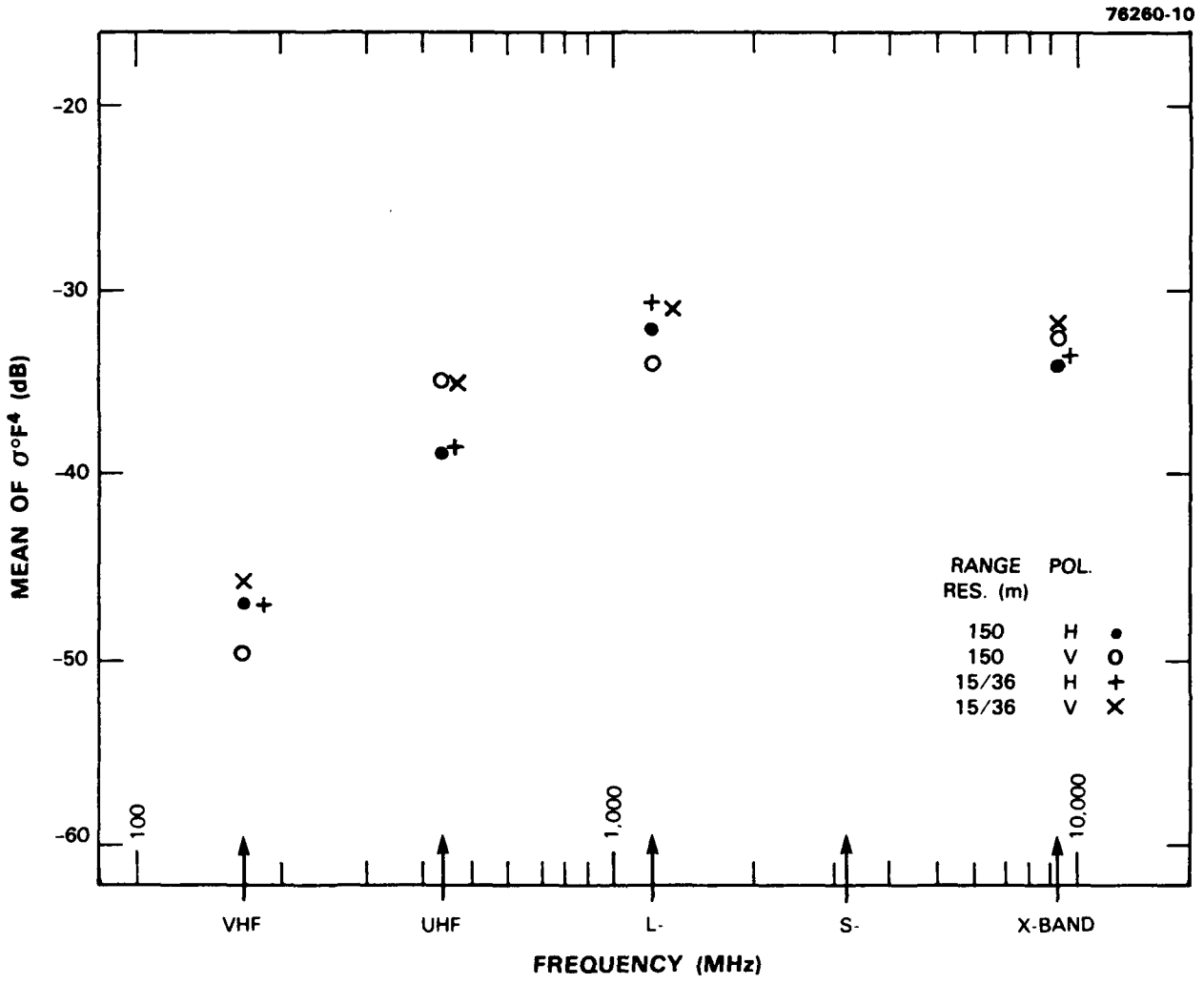

Figure E-130. Mean clutter strength versus frequency at Orion. For the Orion repeat sector, depression angle = 1.2 deg, landform = 3-1, land cover = 21-31, range = 1 to 10 km, azimuth = 186 to 196 deg. Comments: (1) VHF interference may have slightly affected high resolution VHF data. (2) Hardware problems precluded useful data collection at S-band.

Figure E-131 Phase One at Wolseley Looking NW to equipment on site

Figure E-132. PPI clutter map and repeat sector at Wolseley. Repeat sector is outlined in black. Maximum range = 20 km; X-band, 15-m pulse, horizontal polarization; cells with $\sigma^{\circ}F^4 \geq -45$ dB are red.

IITE =   RDF =   RLTHIO.RDF;1

LC = 21   0   0 LF = 3   1 TC = 1 DA = 0.48 DAC = 0.01 PN = R99   DATE = 01-DEC-
3

	SHDHUB	SHDHLB	SHDLSS		SHDH	SHDLSS			
MEAN	-38.28	-38.36	-32.68	WEIBO	0.125E+01	0.153E+01	SIG(MAX)		-18
SD	-30.35	-30.35	-27.66	WEIB1	0.229E-01	0.398E-01	NOI(MAX)		-44
COS	11.09	11.08	8.27	WEIR2	0.998E+00	0.980E+00	SAT(MAX)		999
COK	22.98	22.97	17.42	WEISS	0.155E-02	0.427E-01	SIG(MIN)		-80
SPDL	-999.00	-999.00	-999.00	LOGBO	0.313E+01	0.330E+01	NOI(MIN)		-85
SPDR	8.58	8.65	6.21	LOGB1	0.577E-01	0.797E-01	SAT(MIN)		999
DBME	-53.36		-40.61	LOGR2	0.994E+00	0.997E+00	50	-55.0	-41.0
DBSD	10.50		8.81	LOGSS	0.249E-01	0.237E-01	70	-50.0	-37.0
DBCOS	0.59		-0.40				90	-38.0	-29.0
DBCOK	3.40		4.09				99	-25.0	-21.0

42518 SAMPLES

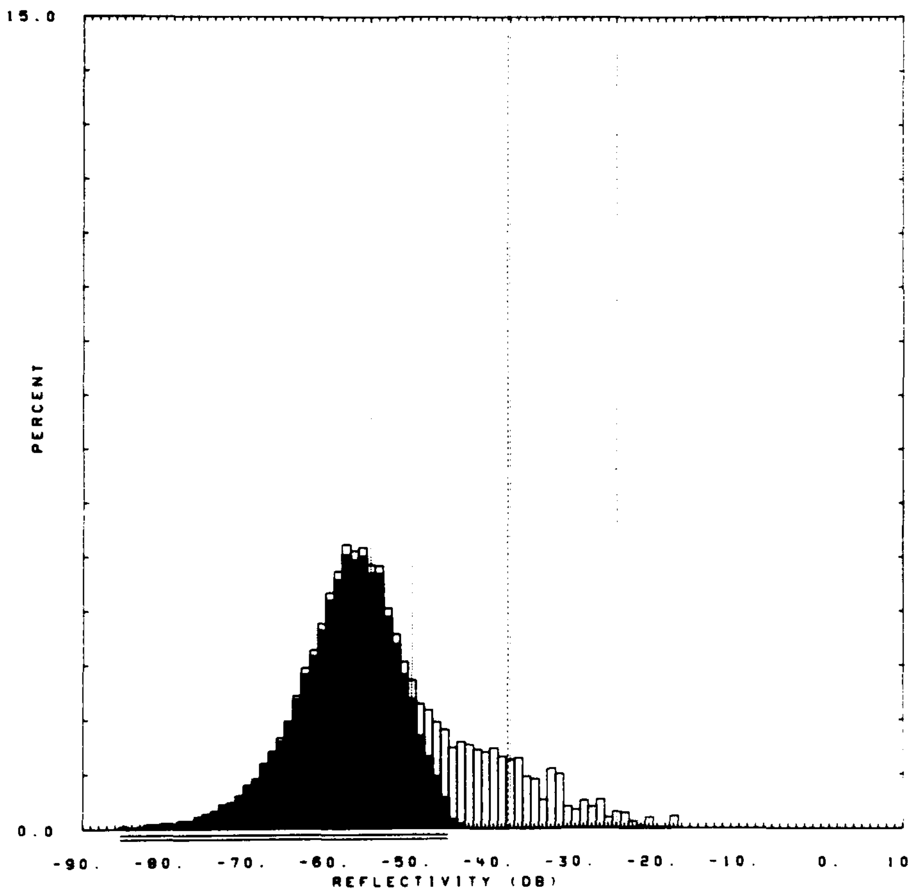

50071.R99.

Figure E-133. Clutter strength histogram for Wolseley repeat sector. L-band, 15-m pulse, horizontal polarization.

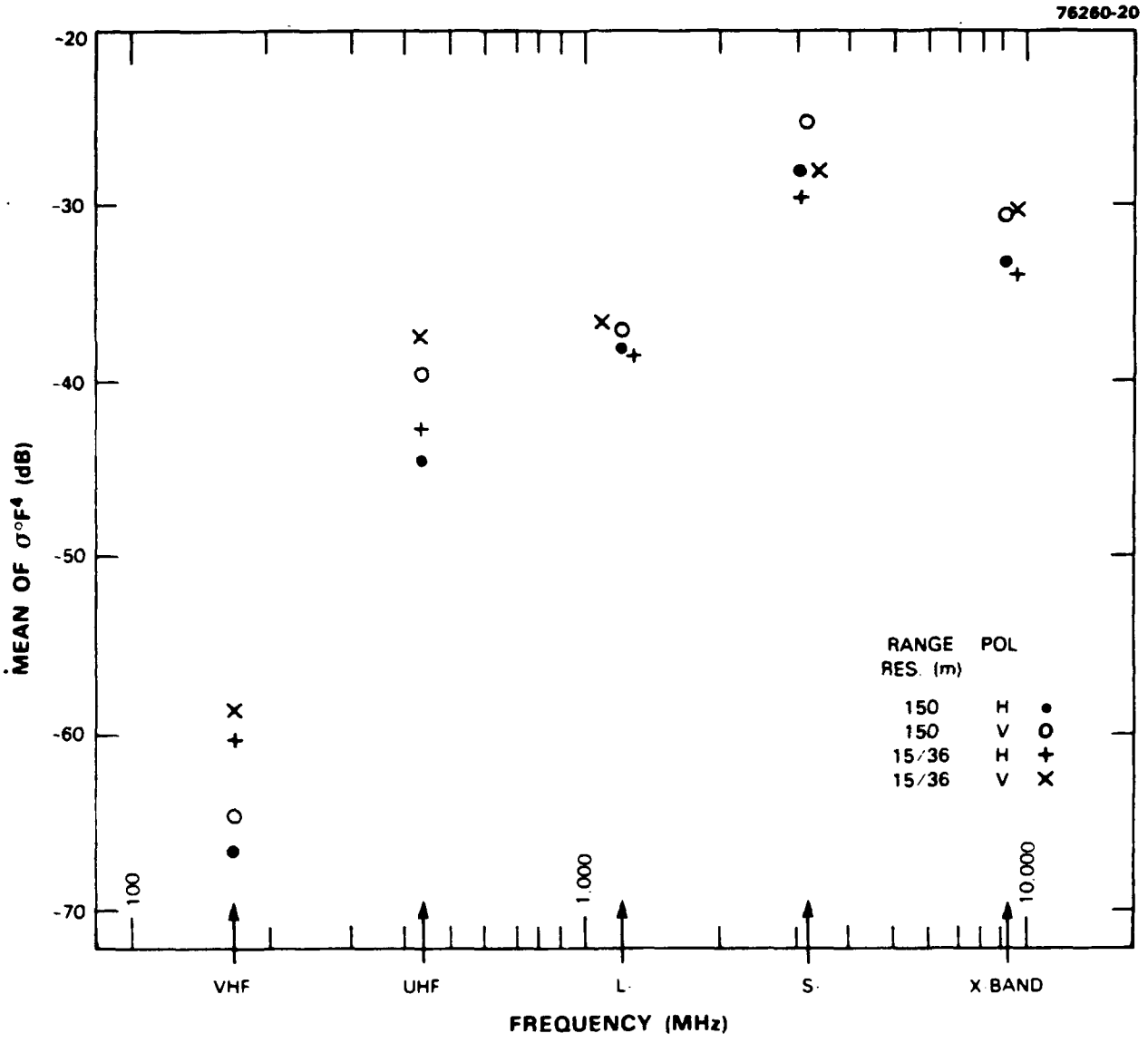

Figure E-134. Mean clutter strength versus frequency at Wolseley. For the Wolseley repeat sector, depression angle = 0.5 deg, landform = 3-1, land cover = 21, range = 6 to 10 km, azimuth = 301 to 311 deg.

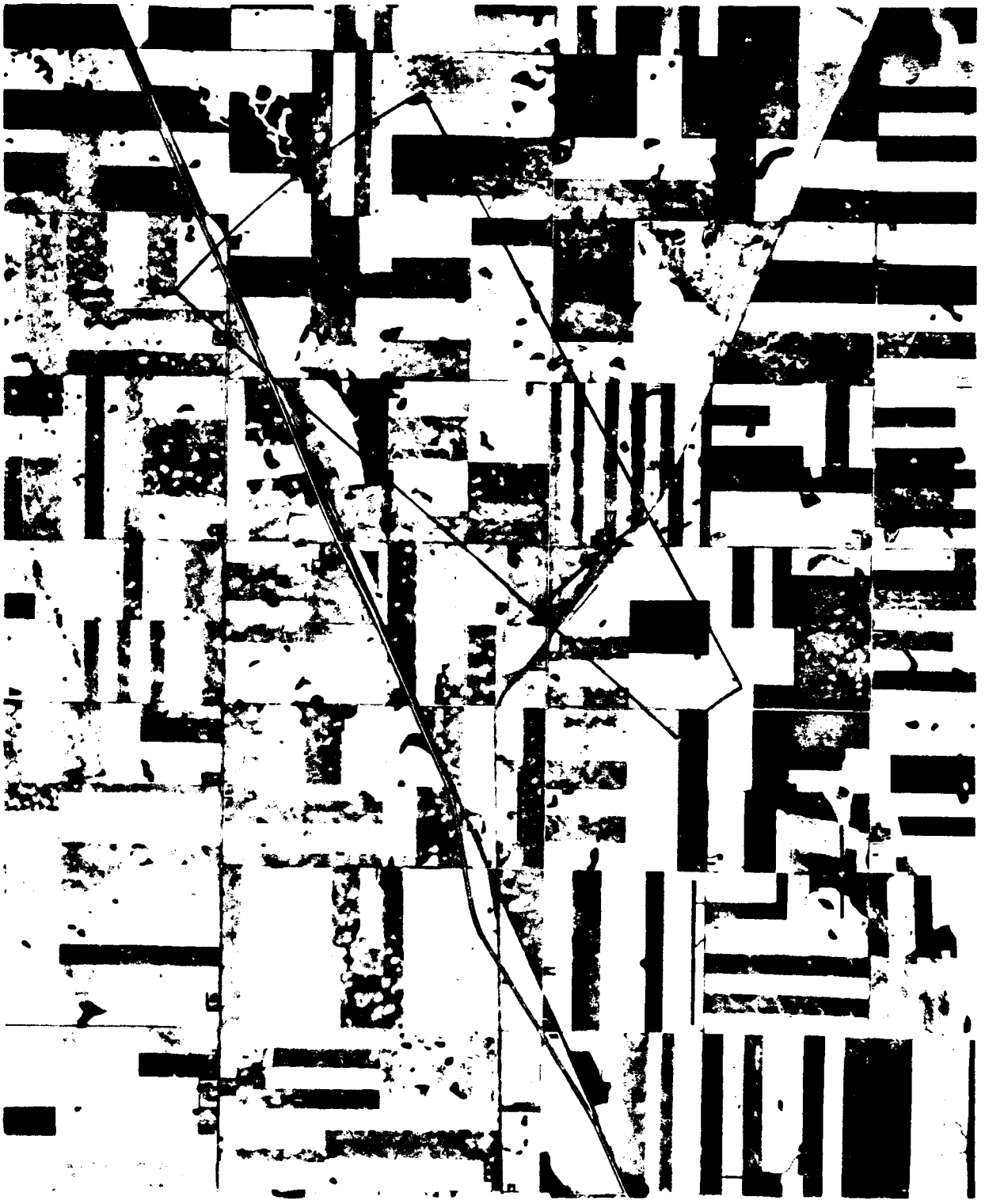

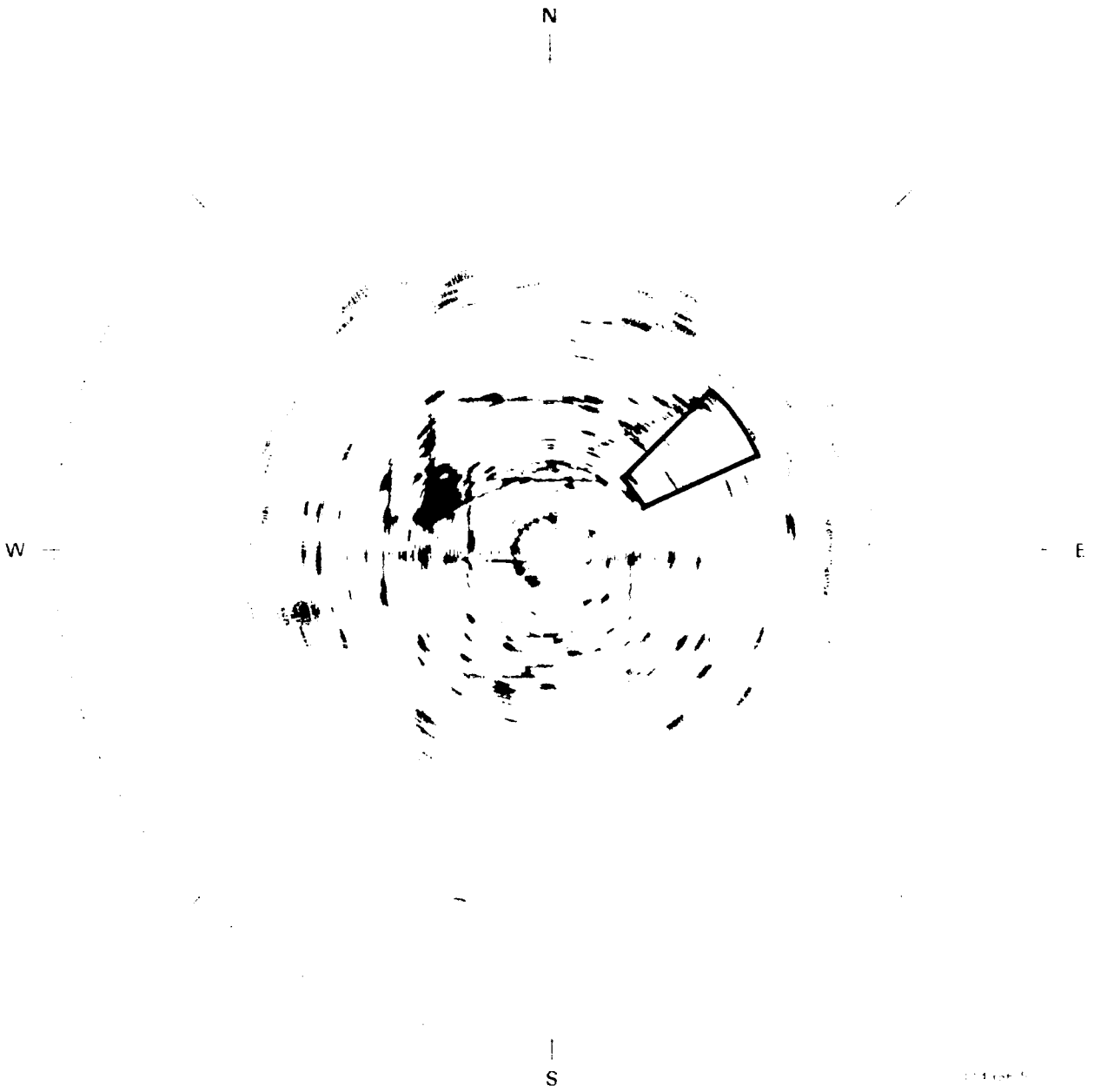

Figure E-137. PPI clutter map and repeat sector at Rosetown Hill. Repeat sector is outlined in black. Maximum range = 20 km; L-band, 15-m pulse, horizontal polarization; cells with $\sigma^{\circ}F^{4} \geq -40$ dB are red.

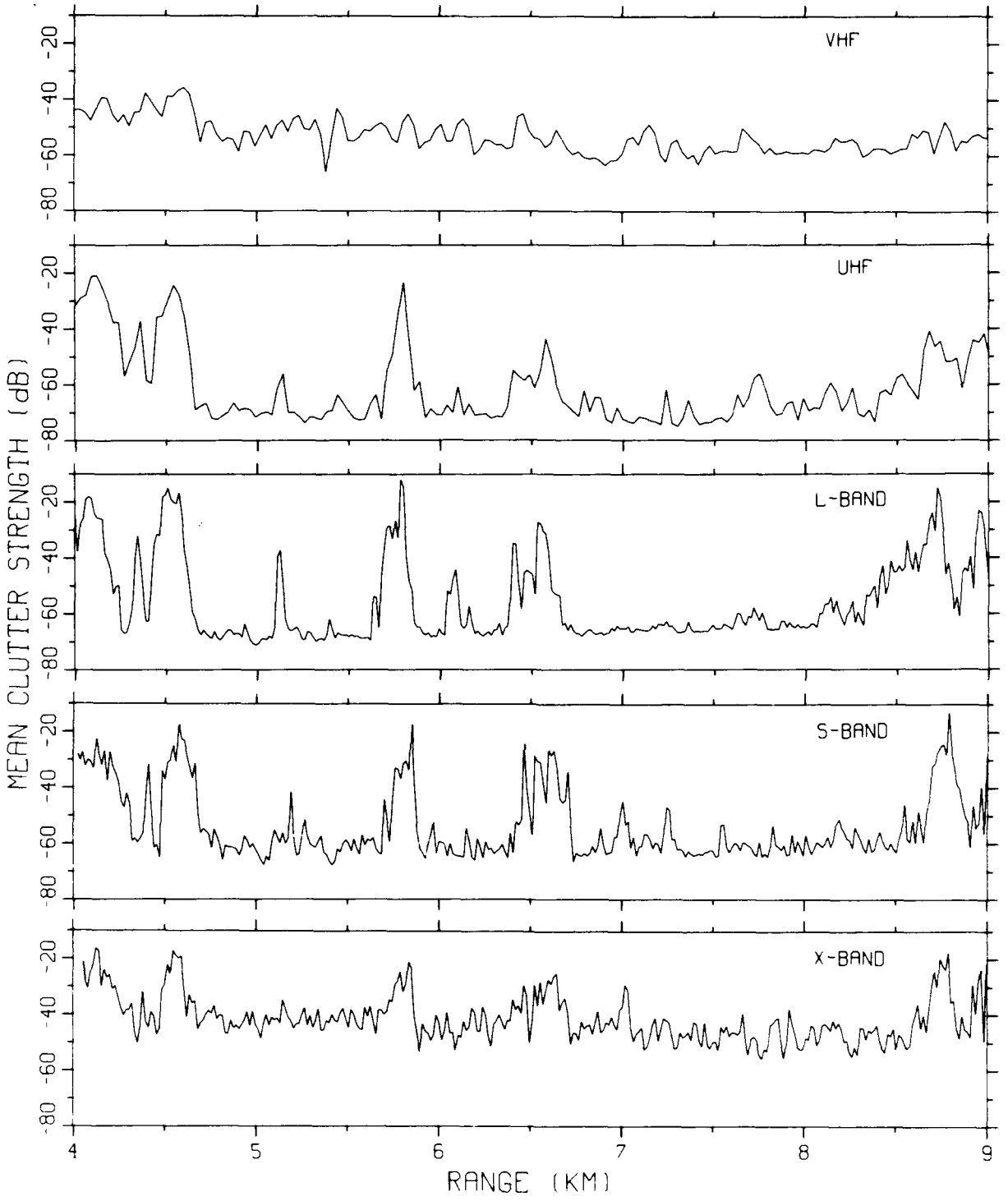

Figure E-138. Mean clutter strength versus range at Rosetown Hill. Repeat sector data. Vertical polarization, 15/36-m pulse length. Data shown range gate by range gate, averaged in azimuth over 20 deg.

SITE = ROSETOWN HILL RDF = RLTH10.RDF;1

LC = 21 0 0 LF = 1 0 TC = 0 DA = 0.39 DAC = 0.00 PN = R99 DATE = 14-MAR-84

	SHDWUB	SHDWLB	SHDLSS		SHDW	SHDLSS			
MEAN	-29.78	-29.78	-22.23	WEIB0	0.882E+00	0.850E+00	SIG(MAX)		-3
SD	-18.45	-18.45	-14.73	WEIB1	0.113E-01	0.212E-01	NOI(MAX)		-47
COS	13.78	13.78	9.98	WEIR2	0.985E+00	0.999E+00	SAT(MAX)		999
COK	28.35	28.35	20.81	WEISS	0.111E-01	0.299E-02	SIG(MIN)		-85
SPDL	-999.00	-999.00	-999.00	LOGB0	0.225E+01	0.197E+01	NOI(MIN)		-85
SPDR	11.63	11.64	8.21	LOGB1	0.301E-01	0.437E-01	SAT(MIN)		999
DBME	-60.64		-44.58	LOGR2	0.988E+00	0.989E+00	50	-62.0	-46.0
DBSD	11.28		15.86	LOGSS	0.172E+00	0.122E+00	70	-59.0	-36.0
DBCOS	1.81		0.23				90	-48.0	-23.0
DBCOK	7.85		2.46				99	-18.0	-8.0

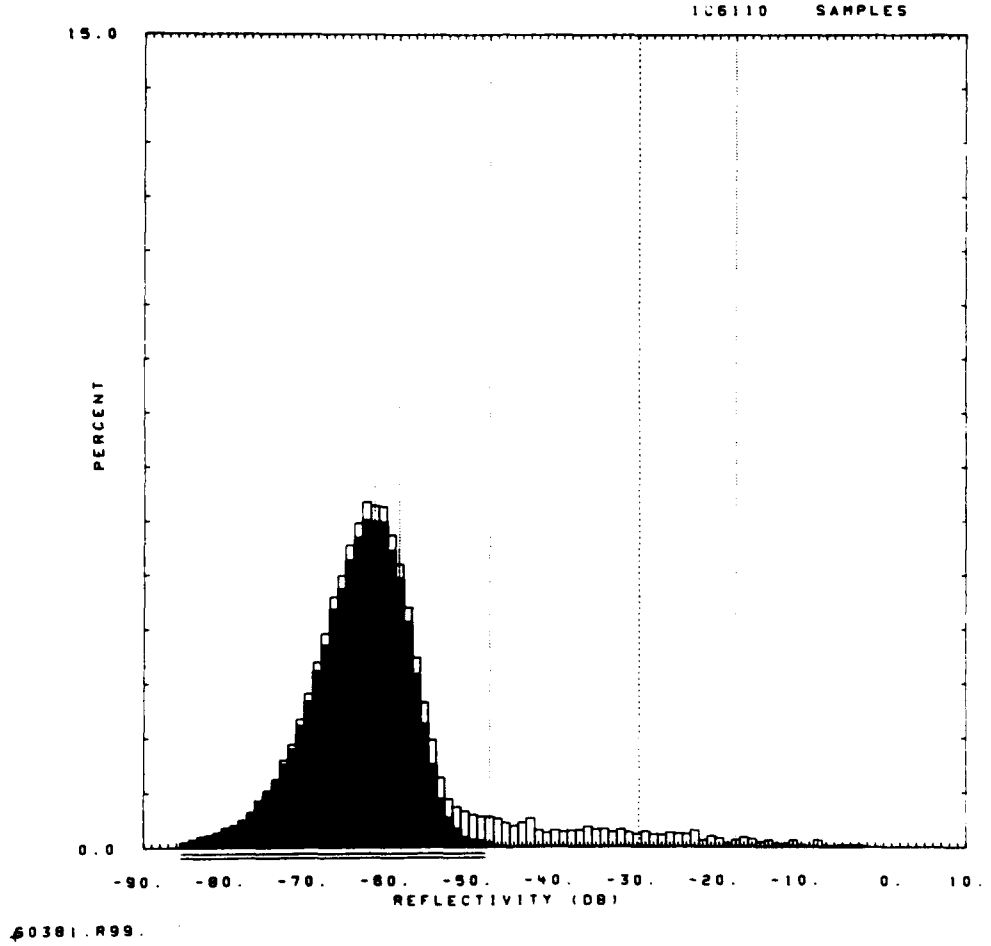

Figure E-139. Clutter strength histogram for Rosetown Hill repeat sector. L-band, 15-m pulse, horizontal polarization.

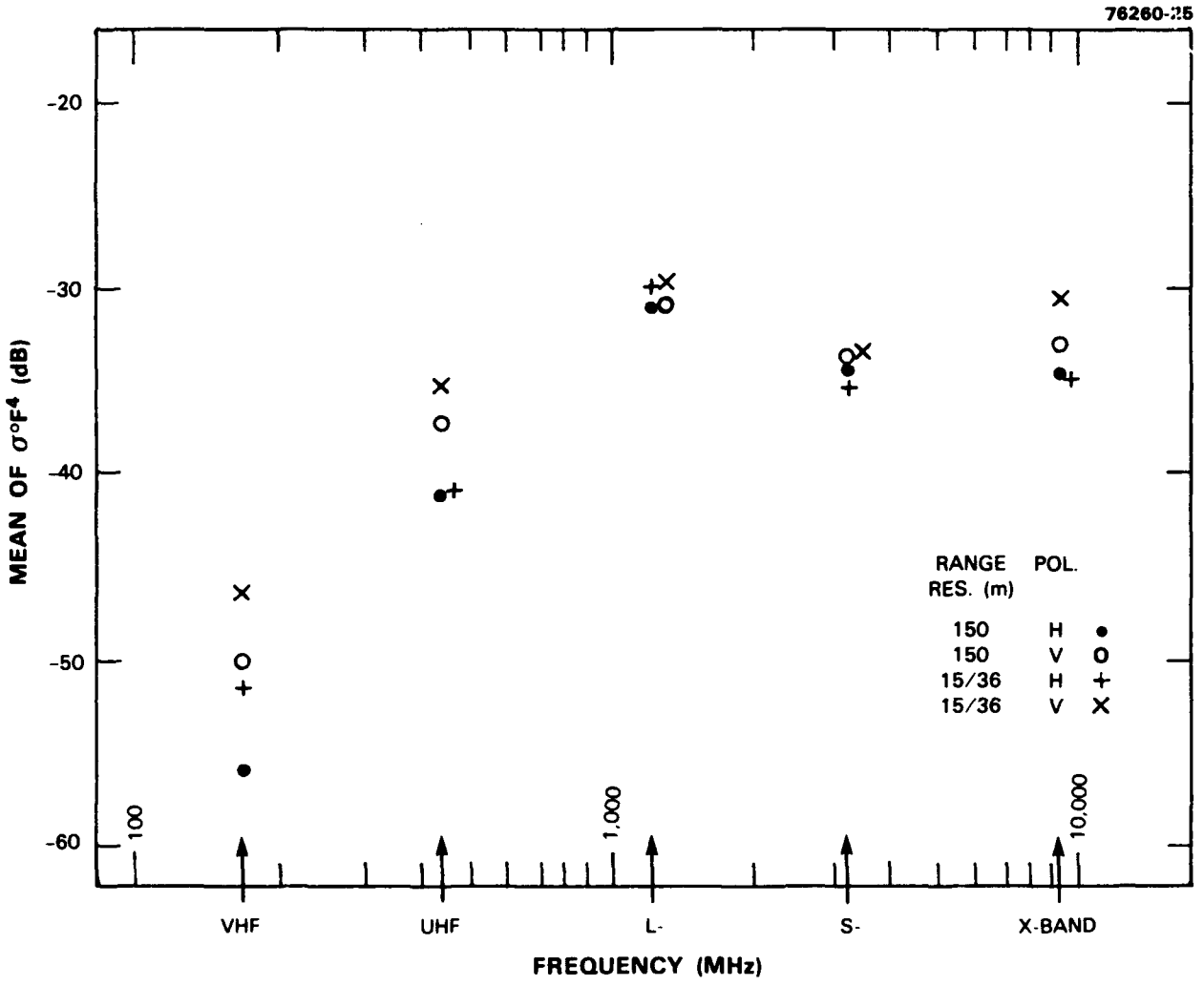

Figure E-140. Mean clutter strength versus frequency at Rosetown Hill. For the Rosetown Hill repeat sector, depression angle = 0.4 deg, landform = 1, land cover = 21, range = 4 to 9 km, azimuth = 45 to 65 deg. Comment: VHF interference may have slightly affected high resolution VHF data.

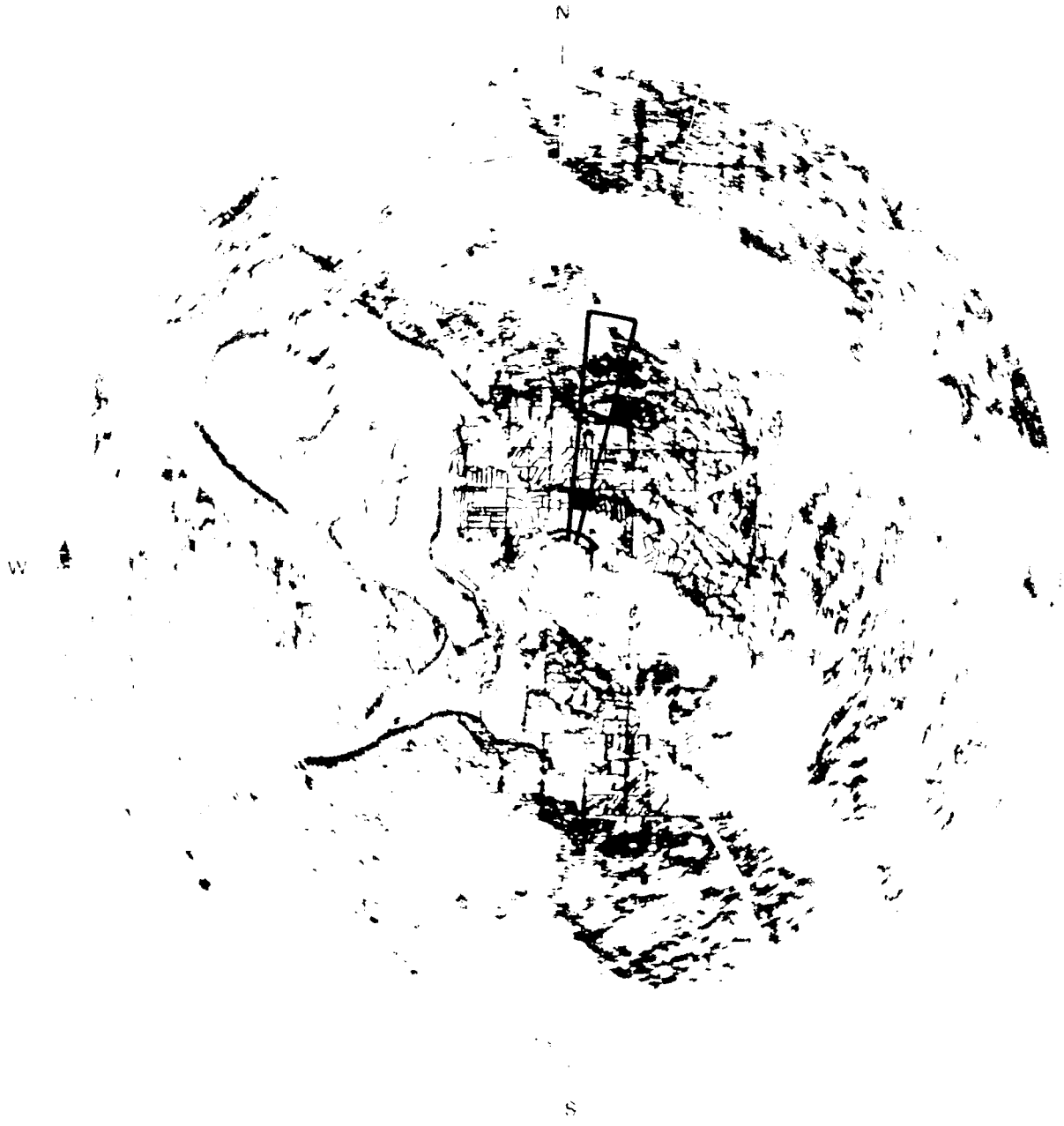

Figure E-141. PPI clutter map and repeat sector at Pakowki Lake. Repeat sector is outlined in black. Maximum range = 20 km; X-band, 15-m pulse, horizontal polarization; cells with $\sigma^{o}F^{4} \geq -40$ dB are red.

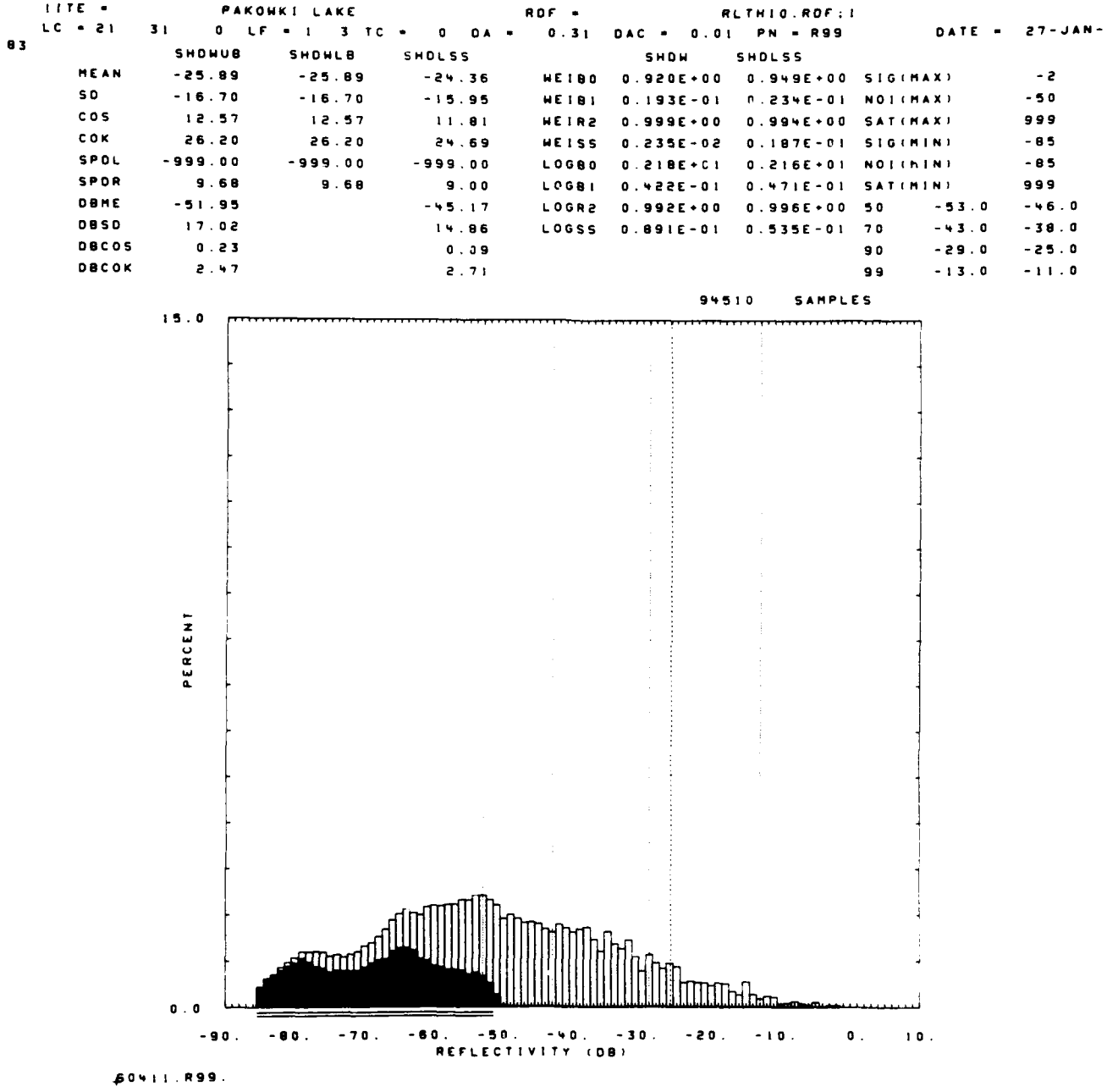

Figure E-142. Clutter strength histogram for Pakowki Lake repeat sector. L-band, 15-m pulse, horizontal polarization.

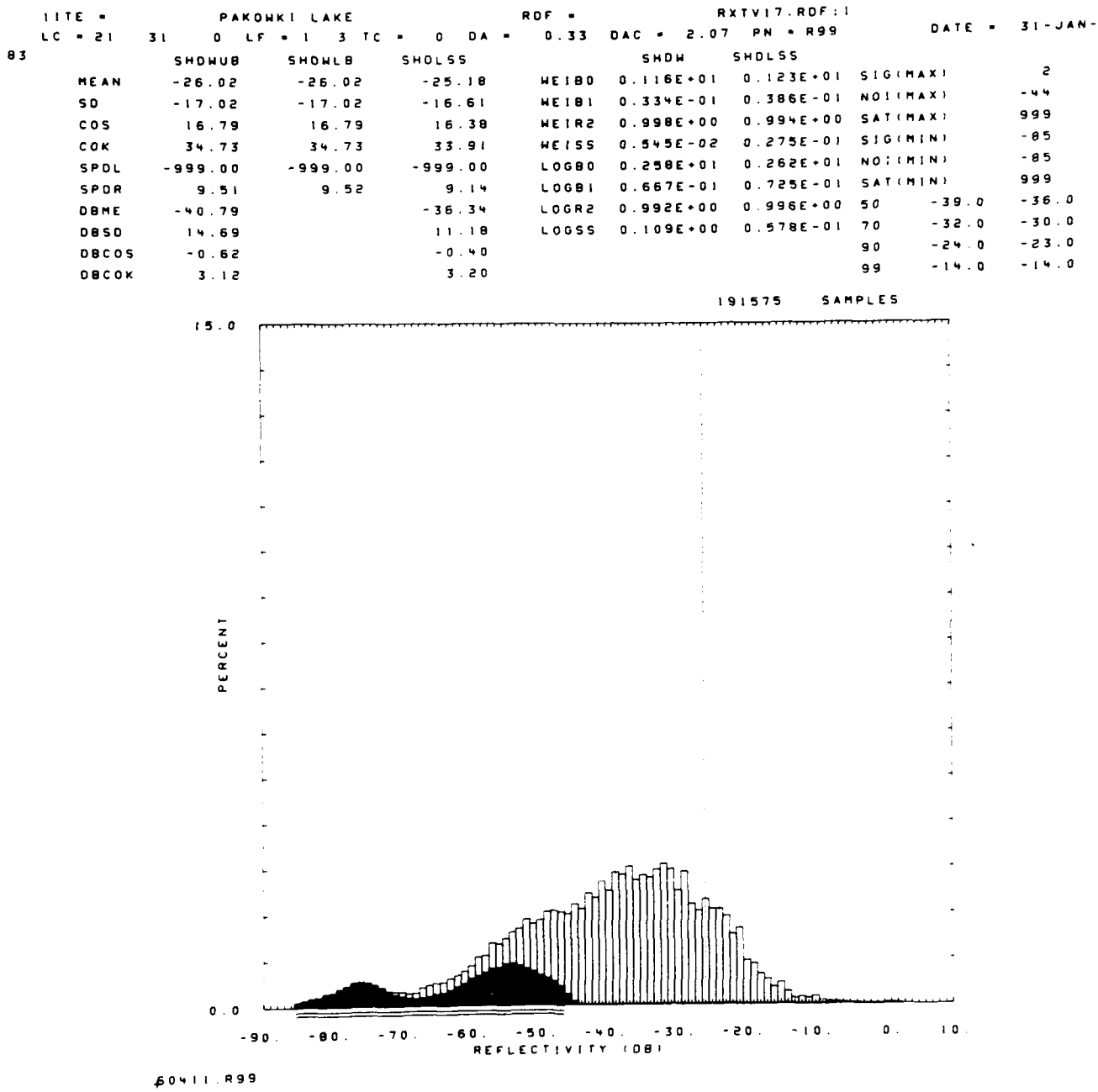

Figure E-143. Clutter strength histogram for Pakowki Lake repeat sector. X-band, 15-m pulse, vertical polarization.

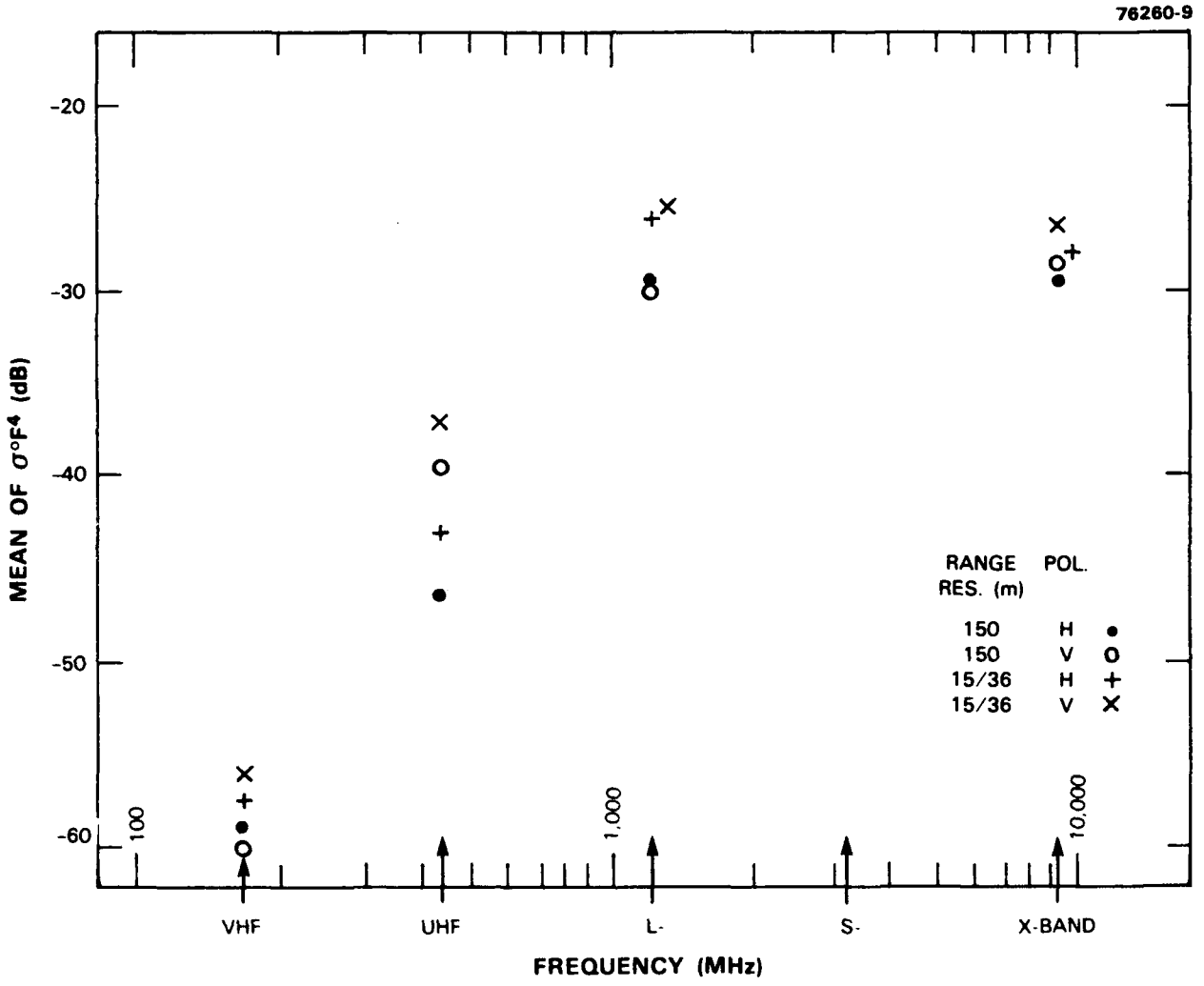

Figure E-144. Mean clutter strength versus frequency at Pakowki Lake. For the Pakowki Lake repeat sector, depression angle = 0.3 deg, landform = 1-3, land cover = 21-31, range = 1 to 10 km, azimuth = 6 to 16 deg. Comments: (1) VHF interference may have slightly affected high resolution VHF data. (2) Hardware problems precluded useful data collection at S-band.

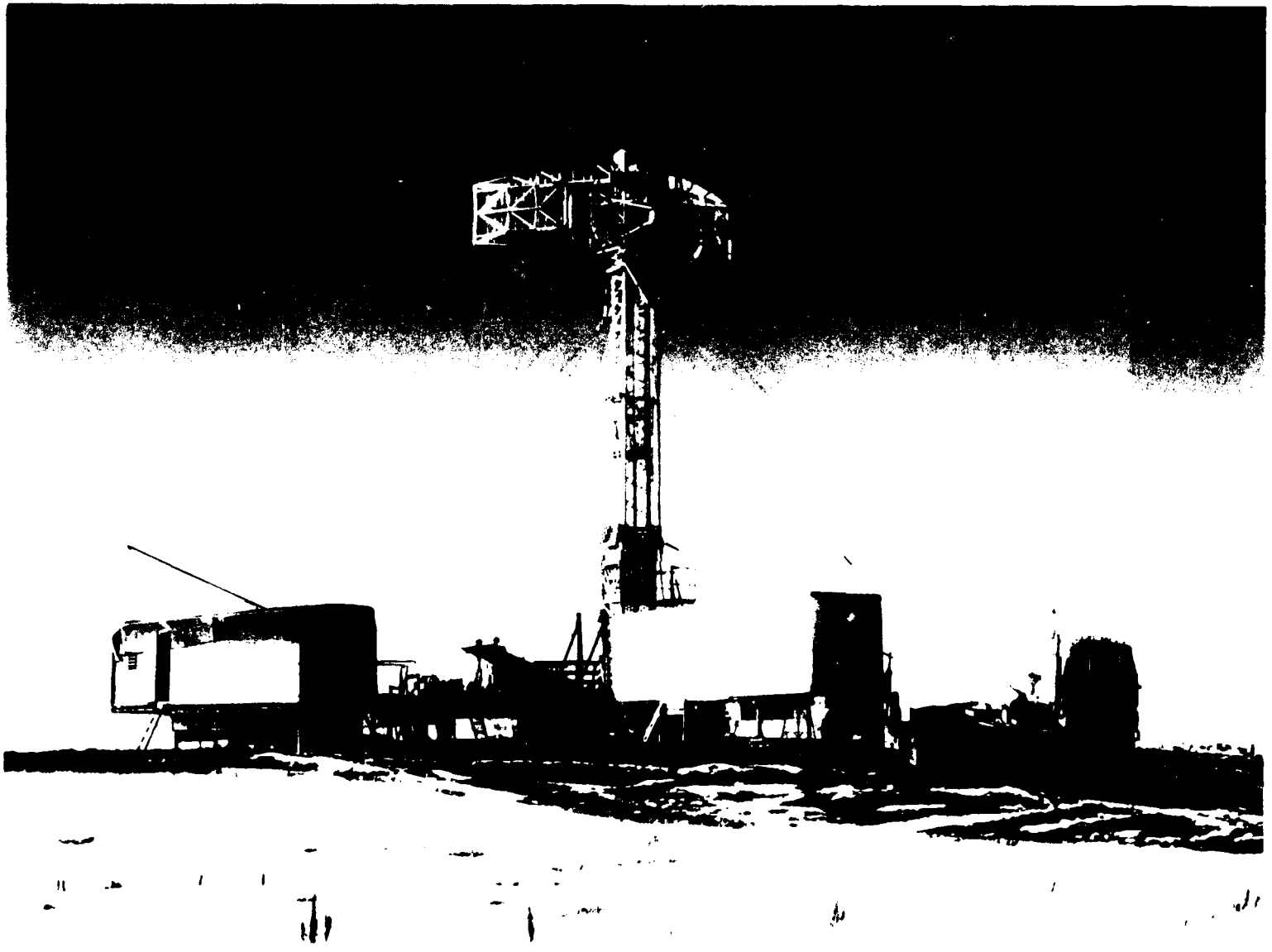

Figure E-145 Phase One equipment at Shilo, Manitoba. Antenna tower is erected to 60 ft February 1982

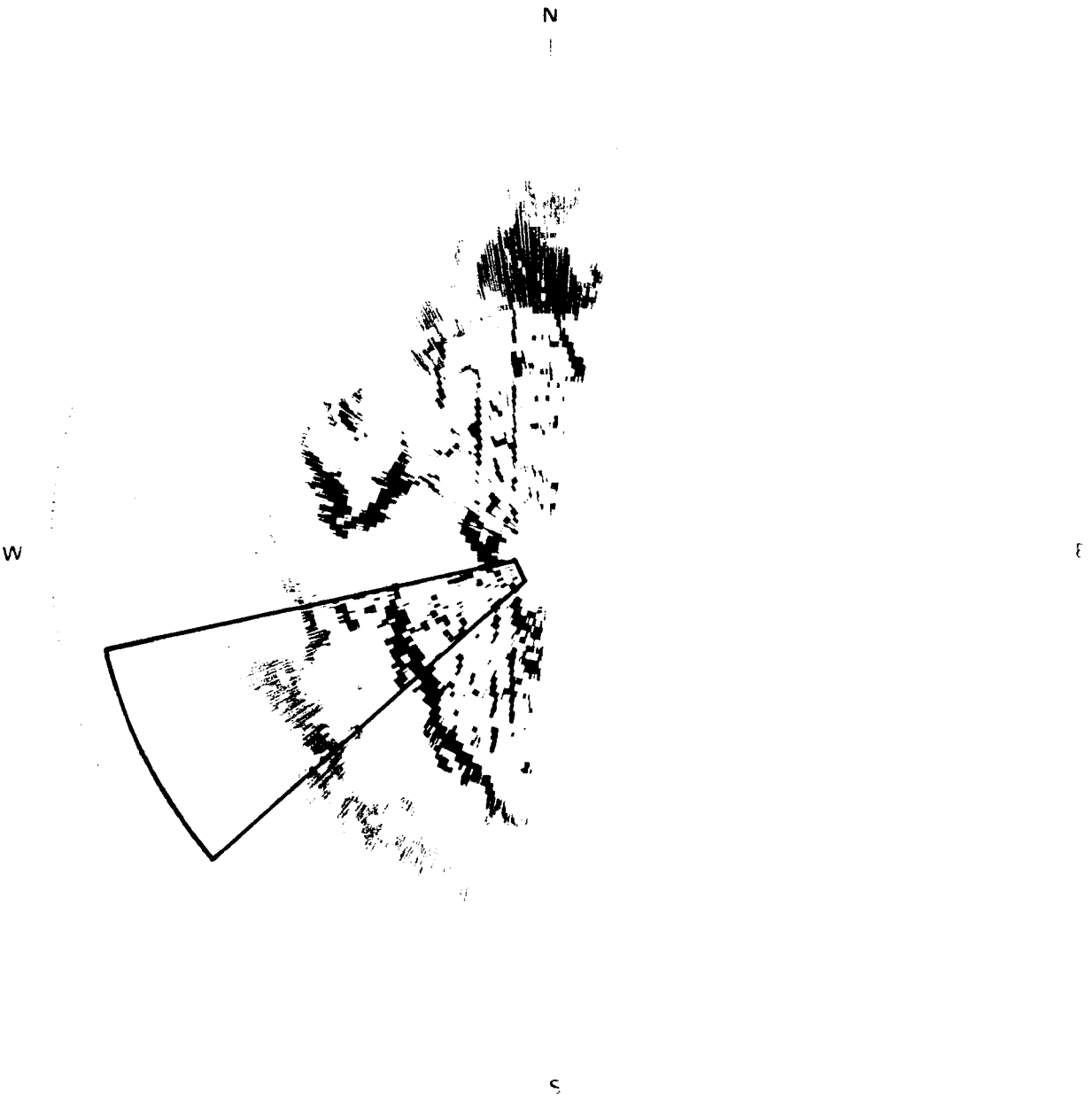

Figure E-146. PPI clutter map and repeat sector at Shilo. Repeat sector is outlined in black. Maximum range = 11 km; X-band, 150-m pulse, horizontal polarization, cells with $\sigma^{o}F^{4} \geq -45$ dB are red.

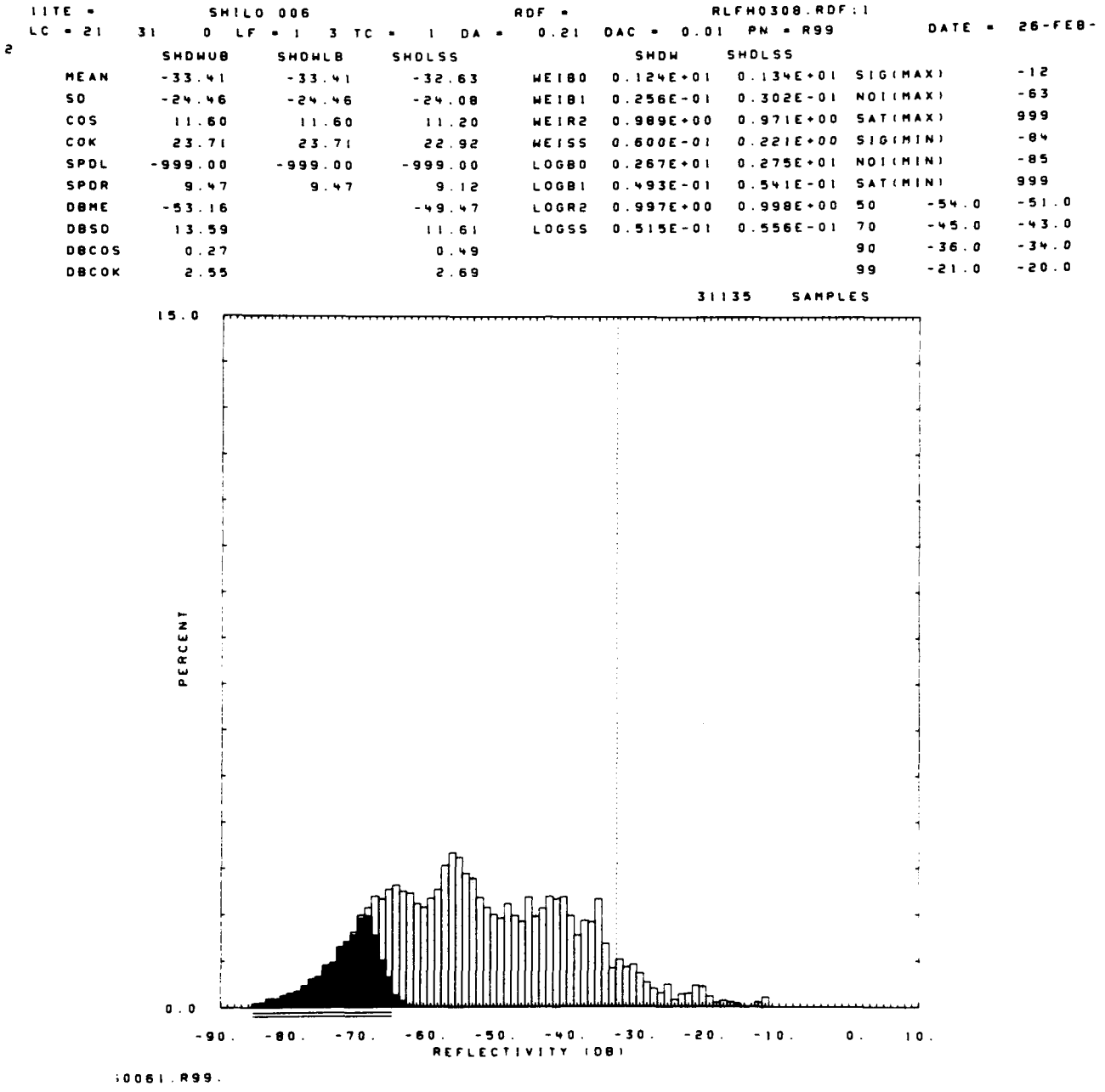

Figure E-147. Clutter strength histogram for Shilo repeat sector. L-band. 150-m pulse. horizontal polarization.

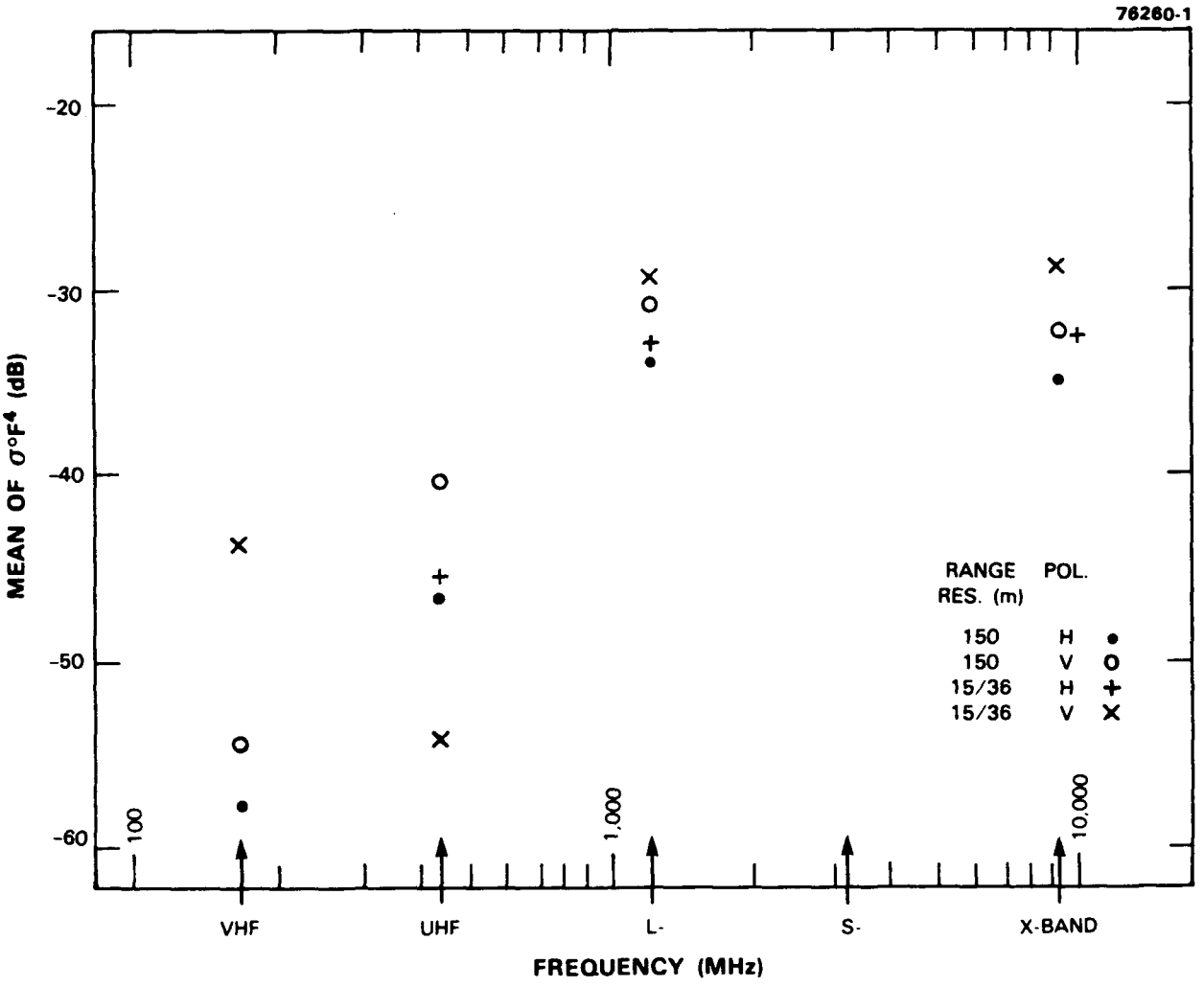

Figure E-148. Mean clutter strength versus frequency at Shilo. For the Shilo repeat sector, depression angle = 0.2 deg, landform = 1-3, land cover = 21-31, range = 1 to 10 km, azimuth = 228 to 258 deg. Comments: (1) At UHF, low resolution/vertical polarization and high resolution/horizontal polarization results shown are from survey data in repeat sector. (2) All VHF results shown are from survey data in repeat sector. (3) S-band was not yet installed at Shilo.

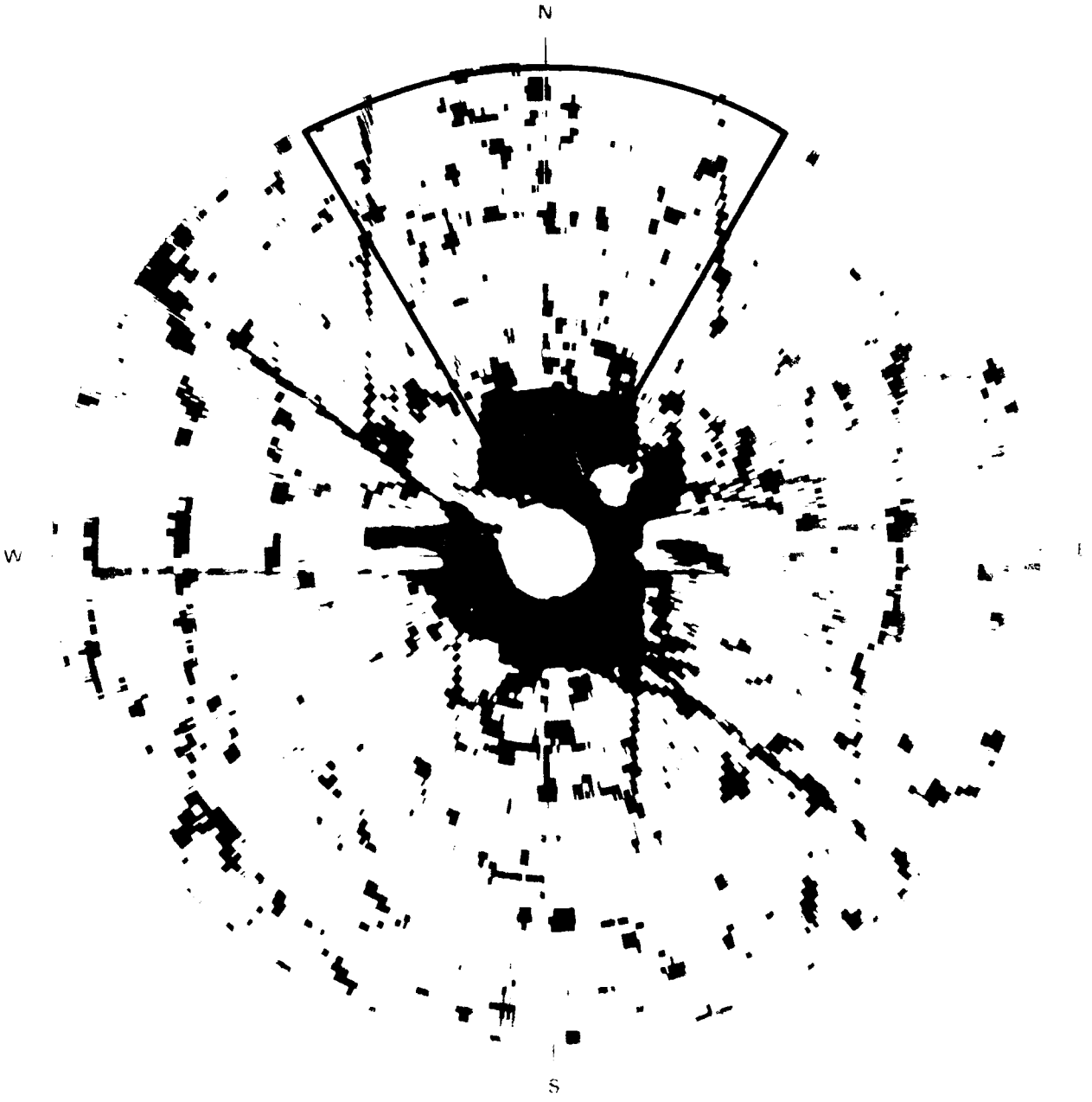

Figure E-149. PPI clutter map and repeat sector at Corinne. Repeat sector is outlined in black. Maximum range = 9 km, X-band, 150-m pulse, horizontal polarization; cells with $\sigma^{o}F^{4} \geq -45$ dB are red.

SITE = CORINNE RDF = RLTH10.RDF;1

LC = 21 0 0 LF = 1 0 TC = 0 DA = 0.14 DAC = 0.01 PN = R99 DATE = 24-APR-

	SHDWUB	SHDWLB	SHDLSS		SHDW	SHDLSS			
MEAN	-32.41	-32.41	-23.57	WEIB0	0.910E+00	0.815E+00	SIG(MAX)		0
SD	-18.49	-18.49	-14.09	WEIB1	0.820E-02	0.138E-01	NOI(MAX)		-44
COS	16.03	16.03	11.59	WEIR2	0.969E+00	0.976E+00	SAT(MAX)		999
COK	33.21	33.21	24.38	WEISS	0.107E-01	0.227E-01	SIG(MIN)		-85
SPOL	-999.00	-999.00	-999.00	LOGB0	0.239E+01	0.200E+01	NOI(MIN)		-85
SPOR	14.09	14.10	9.95	LOGB1	0.244E-01	0.329E-01	SAT(MIN)		999
DBME	-64.93		-54.91	LOGR2	0.955E+00	0.967E+00	50	-65.0	-58.0
DBSD	9.99		15.60	LOGSS	0.137E+00	0.185E+00	70	-61.0	-48.0
DBCOS	1.12		0.81				90	-55.0	-32.0
DBCOK	7.24		3.38				99	-28.0	-7.0

246132 SAMPLES

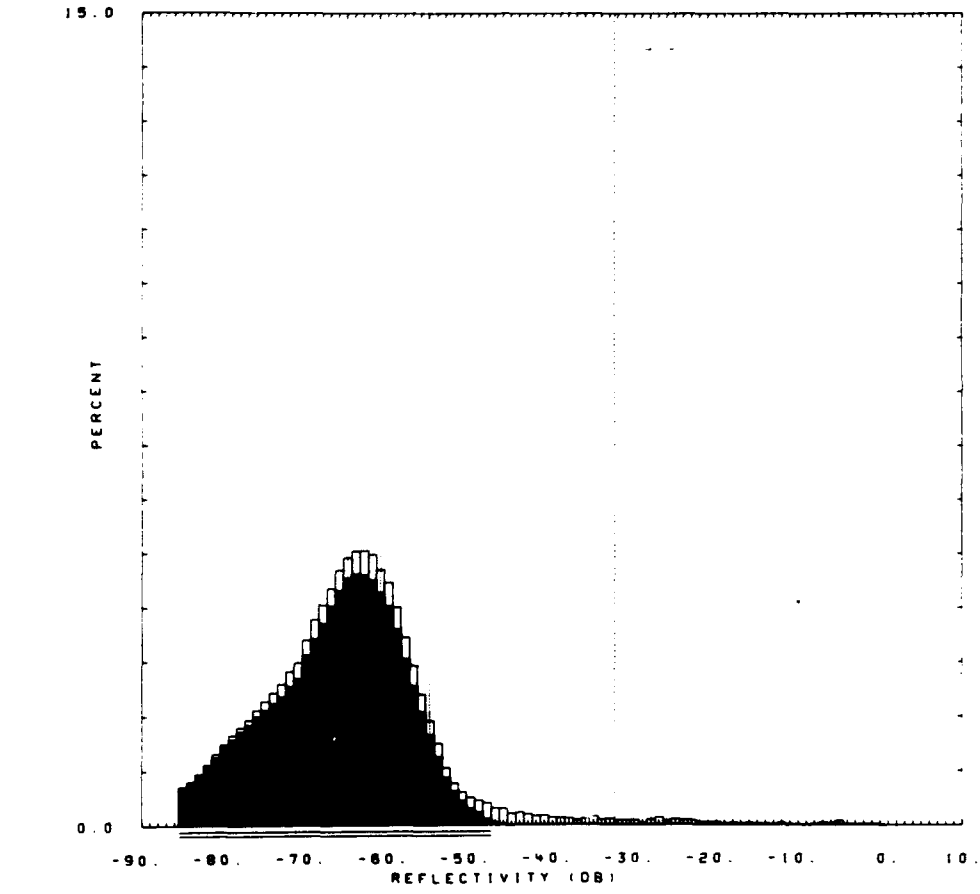

50321.R99.

Figure E-150. Clutter strength histogram for Corinne repeat sector. L-band, 15-m pulse, horizontal polarization.

SITE = CORINNE RDF = RSFV15.RDF;1

LC = 21 0 0 LF = 1 0 TC = 0 DA = 0.14 DAC = 0.03 PN = R99 DATE = 16-APR-84

	SHDWUB	SHDWLB	SHDLSS		SHDW	SHDLSS			
MEAN	-26.07	-26.07	-23.00	WEIB0	0.882E+00	0.882E+00	SIG(MAX)		1
SD	-13.67	-13.67	-12.14	WEIB1	0.119E-01	0.157E-01	NOI(MAX)		-56
COS	13.83	13.83	12.28	WEIR2	0.994E+00	0.983E+00	SAT(MAX)		999
COK	27.98	27.98	24.91	WEISS	0.769E-02	0.392E-01	SIG(MIN)		-85
SPDL	-999.00	-999.00	-999.00	LOGB0	0.218E+01	0.208E+01	NOI(MIN)		-85
SPDR	12.64	12.64	11.20	LOGB1	0.291E-01	0.342E-01	SAT(MIN)		999
DBME	-63.62		-53.33	LOGR2	0.996E+00	0.996E+00	50	-67.0	-56.0
DBSD	14.26		13.43	LOGSS	0.285E-01	0.436E-01	70	-59.0	-49.0
DBCOS	1.28		1.07				90	-44.0	-35.0
DBCOK	4.78		4.36				99	-17.0	-12.0

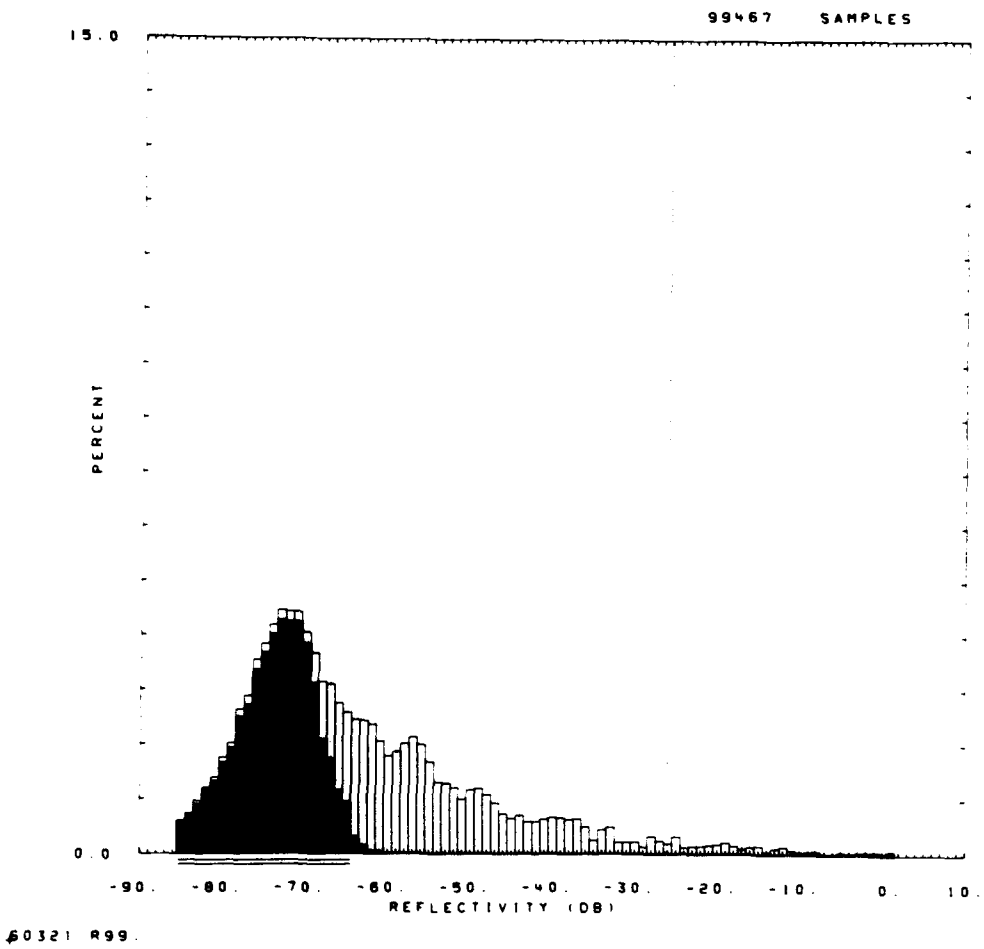

Figure E-151. Clutter strength histogram for Corinne repeat sector, S-band, 150-m pulse, vertical polarization.

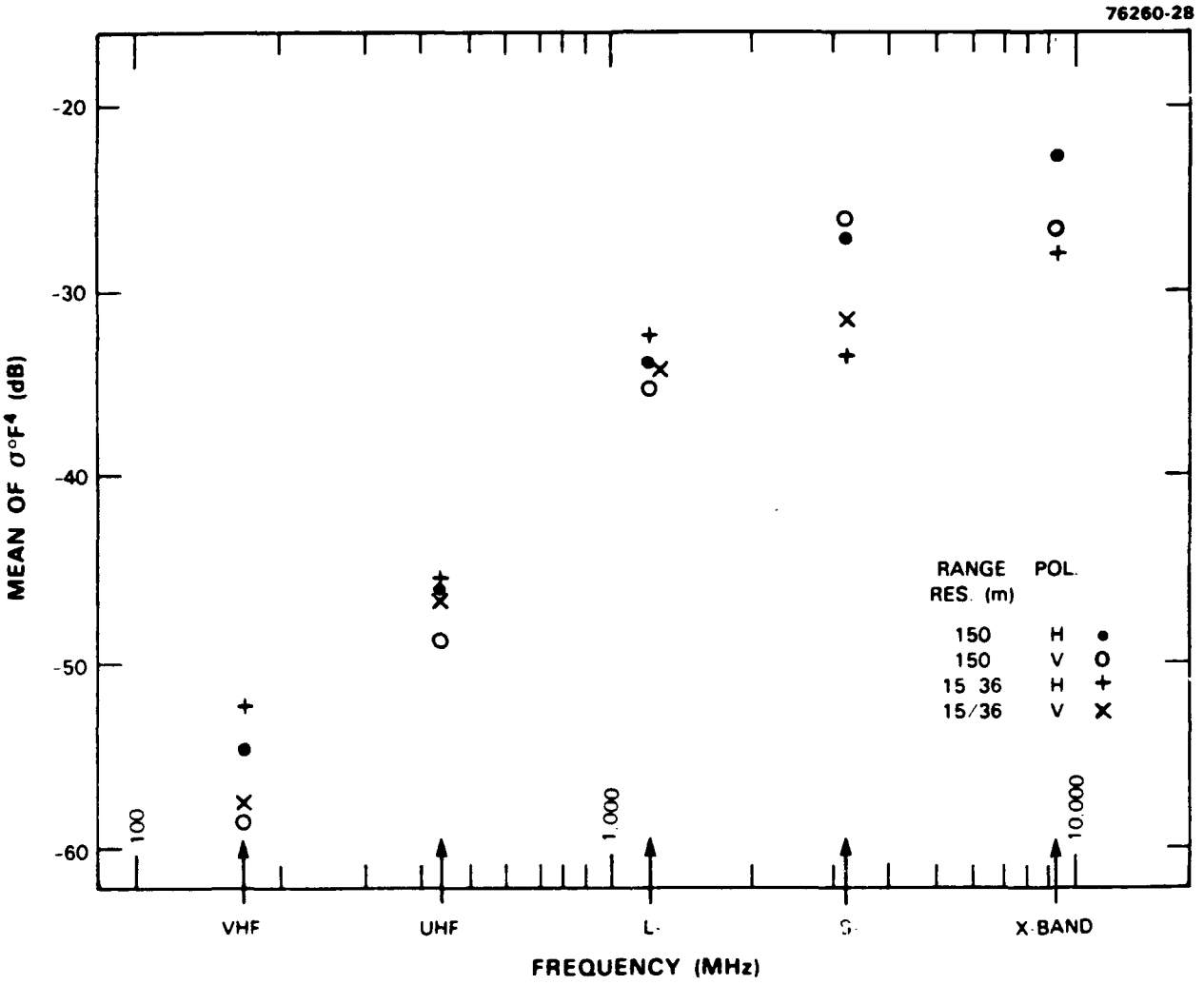

Figure E-152. Mean clutter strength versus frequency at Corinne. For the Corinne repeat sector, depression angle = 0.15 deg, landform = 1, land cover = 21, range = 1 to 8.9 km, azimuth = 330 to 30 deg. Comments: (1) Results shown are for data collected at highest antenna position (three tower sections) at Corinne. (2) At S-band, the high resolution range interval (4.0 to 8.9 km) is shorter than that for the other 18 frequency band/waveform combinations (1.0 to 8.9 km). (3) X-band high resolution/vertical polarization result is deleted because data are questionable.

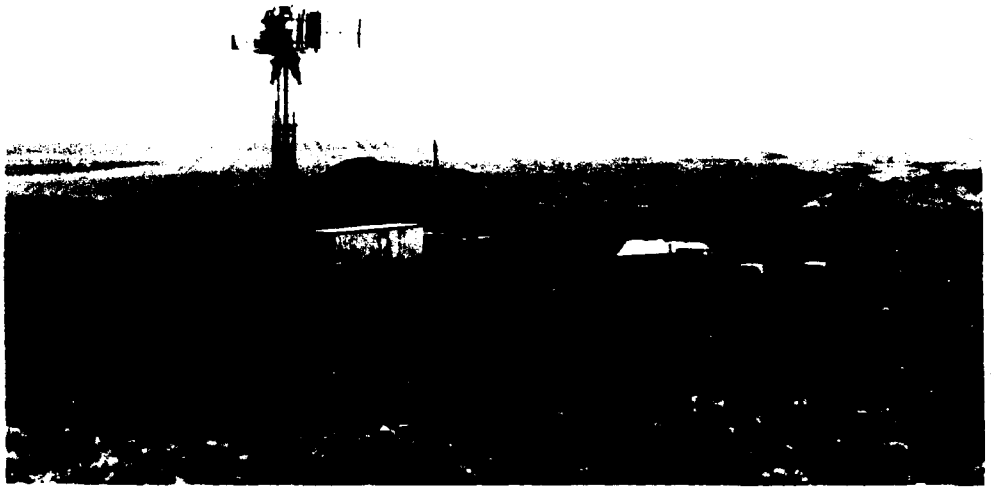

(a)

(b)

Figure E-153. Phase One at Booker Mountain. (a) Looking SE past equipment on site down onto desert floor in repeat sector beyond and (b) looking SE into repeat sector from desert floor at 10-km range.

Figure E-154. PPI clutter map and repeat sector at Booker Mountain. Repeat sector is outlined in black. Maximum range = 48.4 km. X-band, 150-m pulse, horizontal polarization; cells with $\sigma^{\circ}F^{4} \geq -40$ dB are white.

SITE = BOOKER MT. RDF = RUFV07.RDF;1

LC = 70 33 0 LF = 3 0 TC = 0 DA = 1.84 DAC = 0.38 PN = R99 DATE = 24-JUL-

	SHDWUB	SHDWLB	SHDLSS		SHDW	SHDLSS			
MEAN	-38.59	-38.59	-38.19	WEIB0	0.140E+01	0.152E+01	SIG(MAX)		-27
SD	-34.32	-34.32	-34.15	WEIB1	0.292E-01	0.329E-01	NOI(MAX)		-64
COS	5.62	5.62	5.38	WEIR2	0.947E+00	0.921E+00	SAT(MAX)		999
COK	12.19	12.19	11.77	WEISS	0.187E+00	0.360E+00	SIG(MIN)		-70
SPOL	-999.00	-999.00	-999.00	LOGB0	0.265E+01	0.275E+01	NOI(MIN)		-85
SPOR	5.65	5.65	5.49	LOGB1	0.490E-01	0.526E-01	SAT(MIN)		999
DBME	-52.59		-50.82	LOGR2	0.973E+00	0.967E+00	50	-55.0	-54.0
DBSD	12.14		11.15	LOGSS	0.260E+00	0.366E+00	70	-47.0	-45.0
DBCOS	0.40		0.58				90	-34.0	-33.0
DBCOK	2.35		2.16				99	-27.0	-27.0

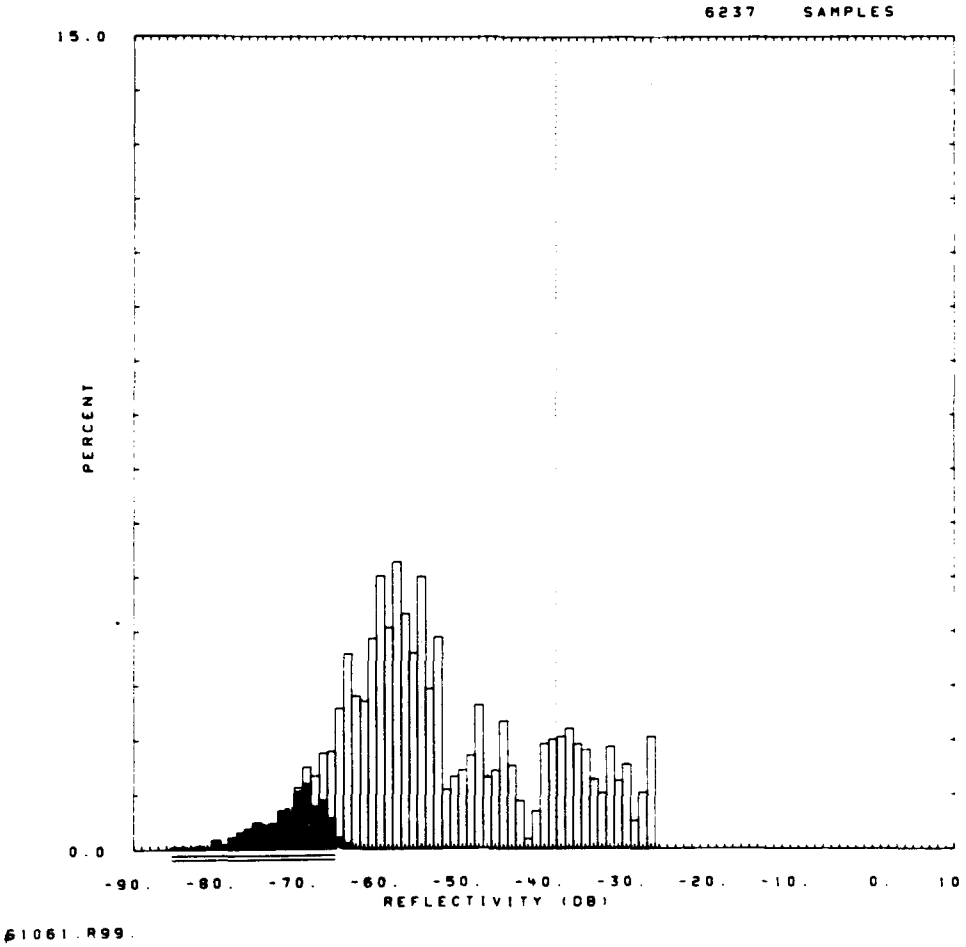

Figure E-155. Clutter strength histogram for Booker Mountain repeat sector. UHF, 150-m pulse, vertical polarization.

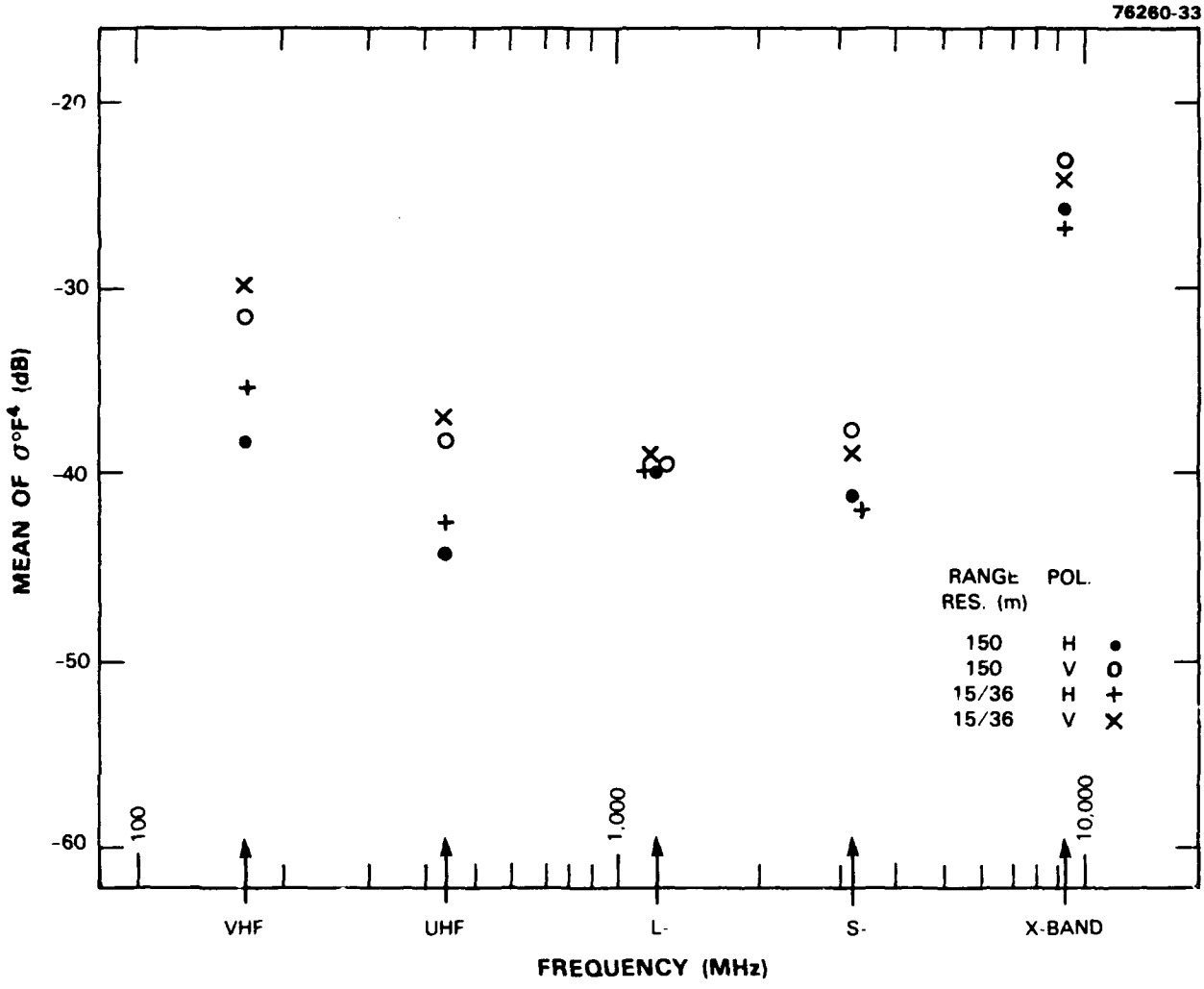

Figure E-156. Mean clutter strength versus frequency at Booker Mountain. For the Booker Mountain repeat sector, depression angle = 1.8 deg, landform = 3, land cover = 7-33, range = 12 to 17.9 km, azimuth = 125 to 145 deg.

(a)

NE

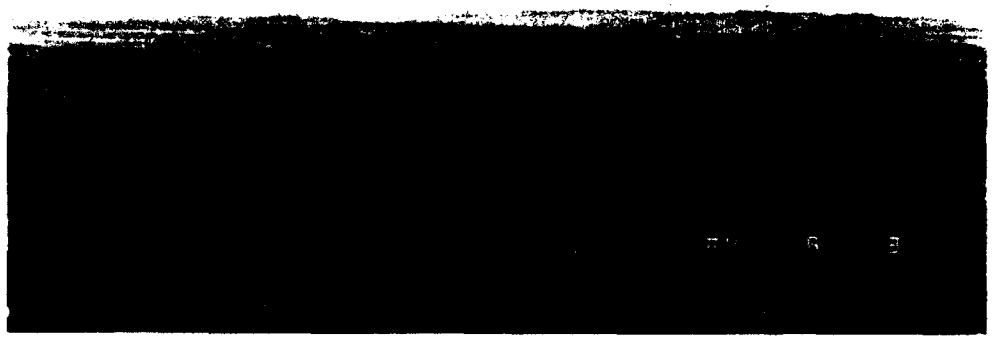

(b)

Figure E-15. Repeat sector at Yamanda East, (a) Looking SW back to Phase One equipment on berm (to center) from a point out in the repeat sector and (b) tower top view NE into repeat sector.

Figure E-158. PPI clutter map and repeat sector at Vananda East. Repeat sector is outlined in black. Maximum range = 20 km; X-band, 15-m pulse, horizontal polarization; cells with $\sigma^{\circ}F^{4} \geq -40$ dB are red.

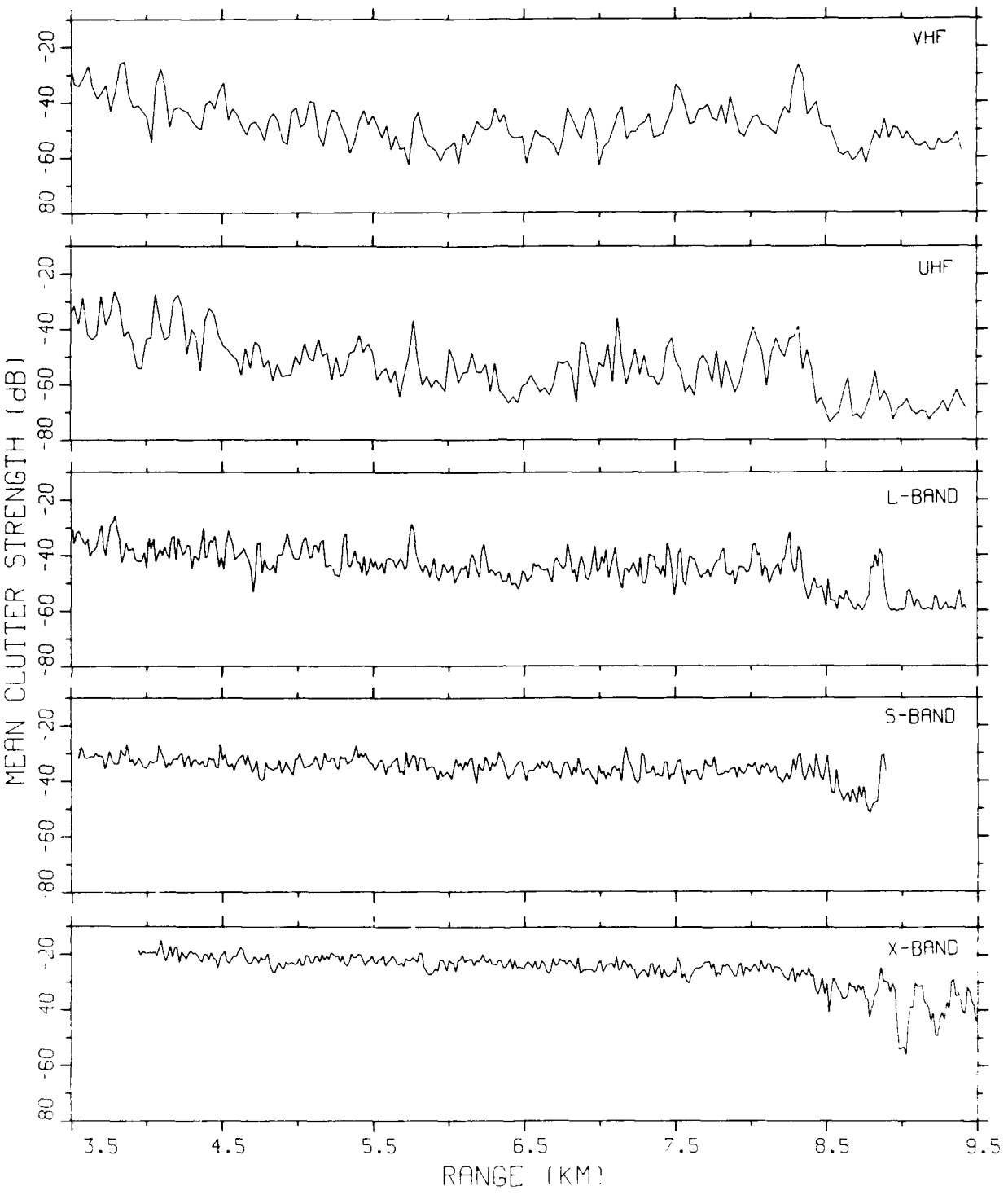

Figure E-159. Mean clutter strength versus range at Vananda East. Repeat sector data. Vertical polarization, 15/36-m pulse length. Data shown range gate by range gate, averaged in azimuth over 20 deg.

SITE = VANANDA EAST RDF = IRUFV07.RDF;1

LC = 31 32 0 LF = 3 4 TC = 0 DA = 1.03 DAC = 0.21 PN = R99 DATE = 02-AUG-84

	SHDWUB	SHDWLB	SHDLSS		SHDW	SHDLSS			
MEAN	-40.27	-40.27	-39.58	WEIB0	0.146E+01	0.161E+01	SIG(MAX)		-24
SD	-33.63	-33.63	-33.31	WEIB1	0.278E-01	0.326E-01	NOI(MAX)		-66
COS	8.18	8.18	7.82	WEIR2	0.956E+00	0.926E+00	SAT(MAX)		999
COK	17.01	17.01	16.31	WEISS	0.204E+00	0.490E+00	SIG(MIN)		-85
SPDL	-999.00	-999.00	-999.00	LOGB0	0.300E+01	0.312E+01	NOI(MIN)		-85
SPDR	7.49	7.49	7.19	LOGB1	0.514E-01	0.564E-01	SAT(MIN)		999
DBME	-56.83		-54.03	LOGR2	0.988E+00	0.980E+00	50	-58.0	-56.0
DBSD	11.76		10.27	LOGSS	0.178E+00	0.365E+00	70	-51.0	-50.0
DBCOS	0.41		0.72				90	-42.0	-40.0
DBCOK	3.06		3.36				99	-25.0	-25.0

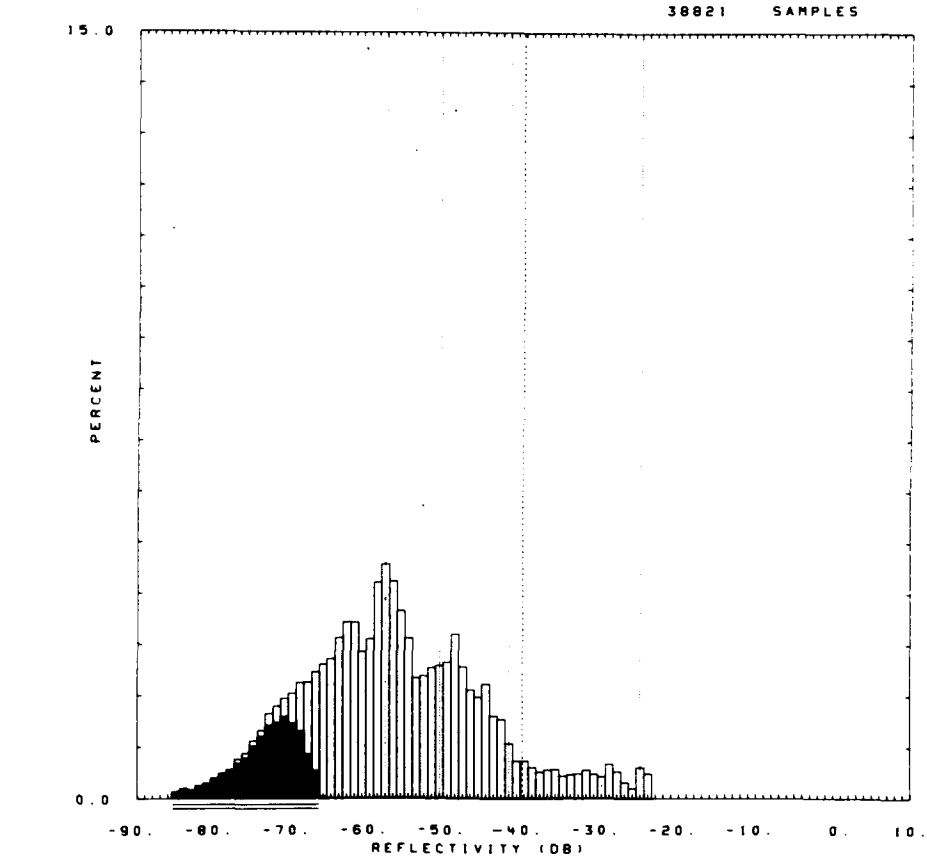

Figure E-160. Clutter strength histogram for Vananda East repeat sector. UHF, 150-m pulse, vertical polarization. Slow scan, 0.125 deg/s, experiment type 3, see Appendix C.

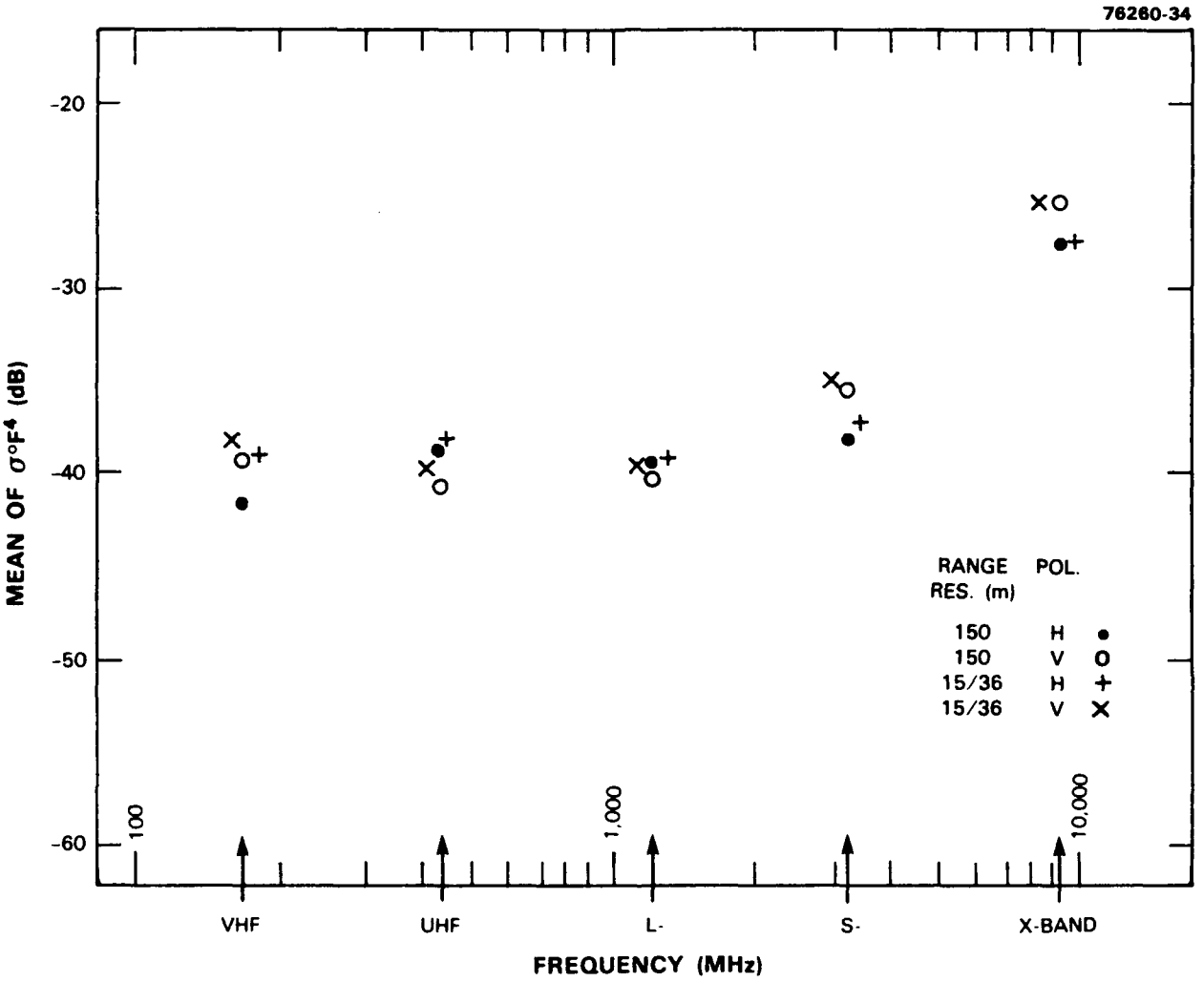

Figure E-161. Mean clutter strength versus frequency at Vananda East. For the Vananda East repeat sector, depression angle = 1.0 deg, landform = 3-5, land cover = 31-32, range = 3.6 to 9.5 km, azimuth = 40 to 60 deg.

Figure E-162. Phase One at Knolls. Looking south to equipment on site.

Figure E-163 PPI clutter map and repeat sector at Knolls. Repeat sector is outlined in black. Maximum range = 7 km, X-band, 15-m pulse, horizontal polarization; cells with $\sigma^{\circ}F^{4} \geq -45$ dB are red.

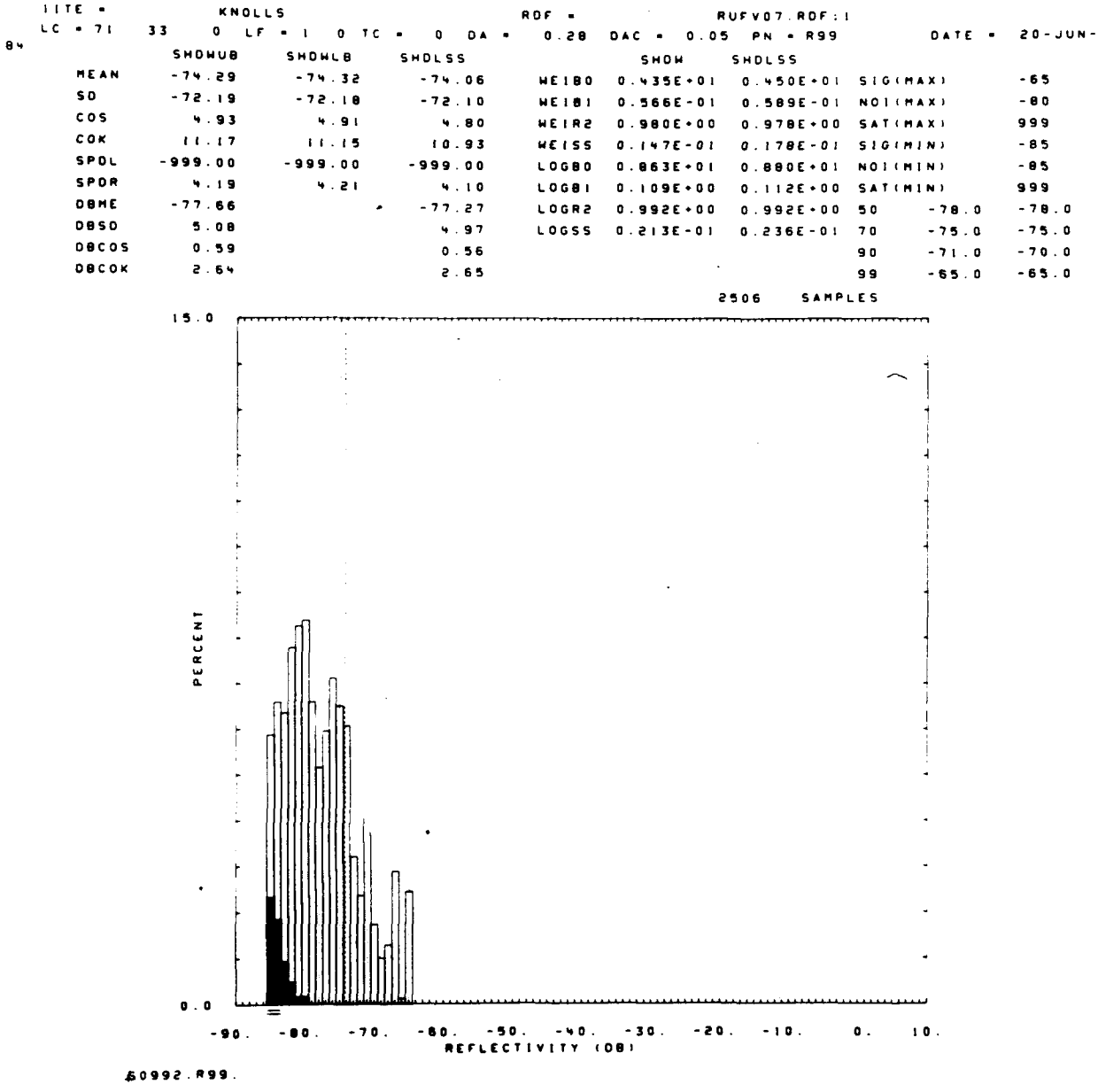

Figure E-164. Clutter strength histogram for Knolls repeat sector. UHF, 150-m pulse, vertical polarization.

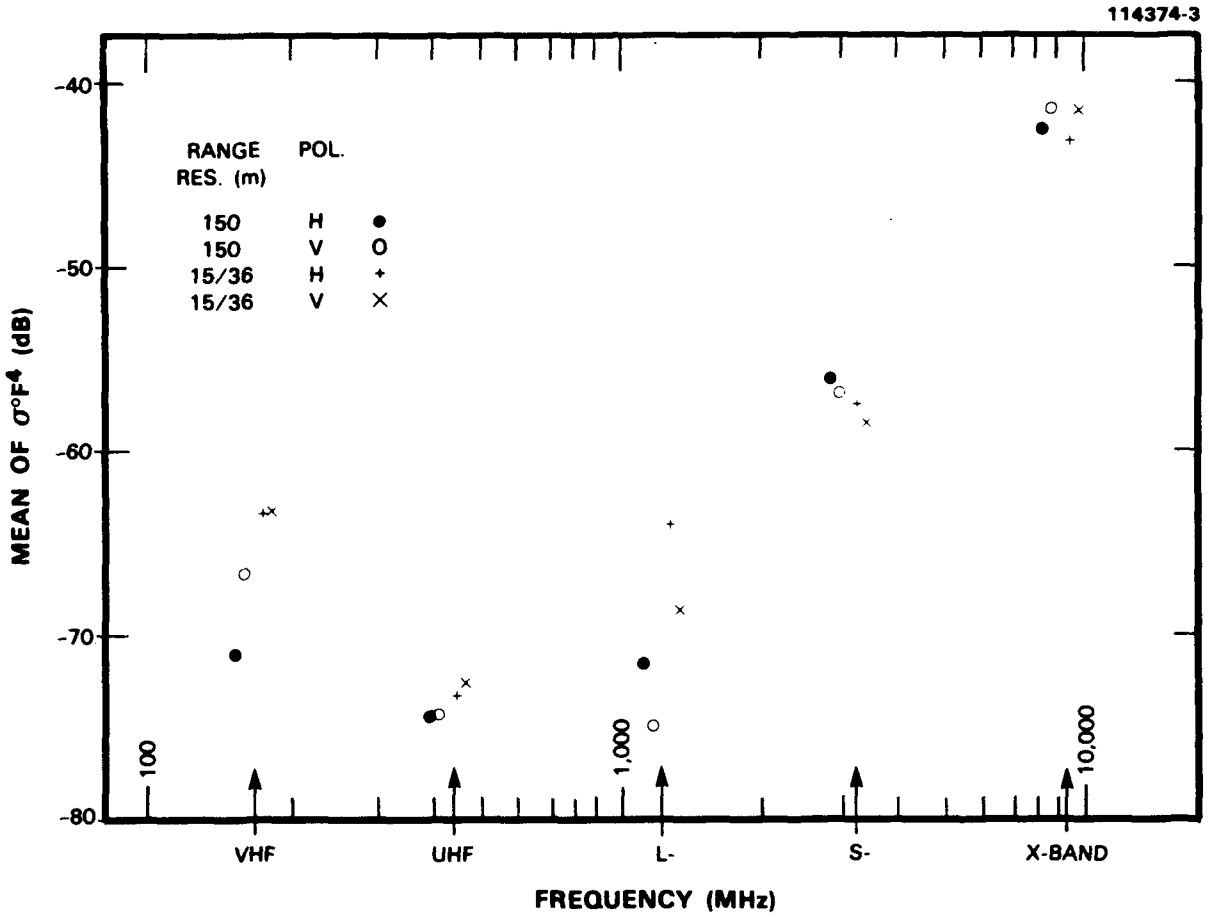

Figure E-165. Mean clutter strength versus frequency at Knolls. For the Knolls repeat sector, depression angle = 0.3 deg, landform = 1, land cover = 7-33, range = 3 to 6.5 km, azimuth = 290 to 307 deg.

Figure F-196. Plant One at Big Grass Marsh. Looking east at equipment on site.

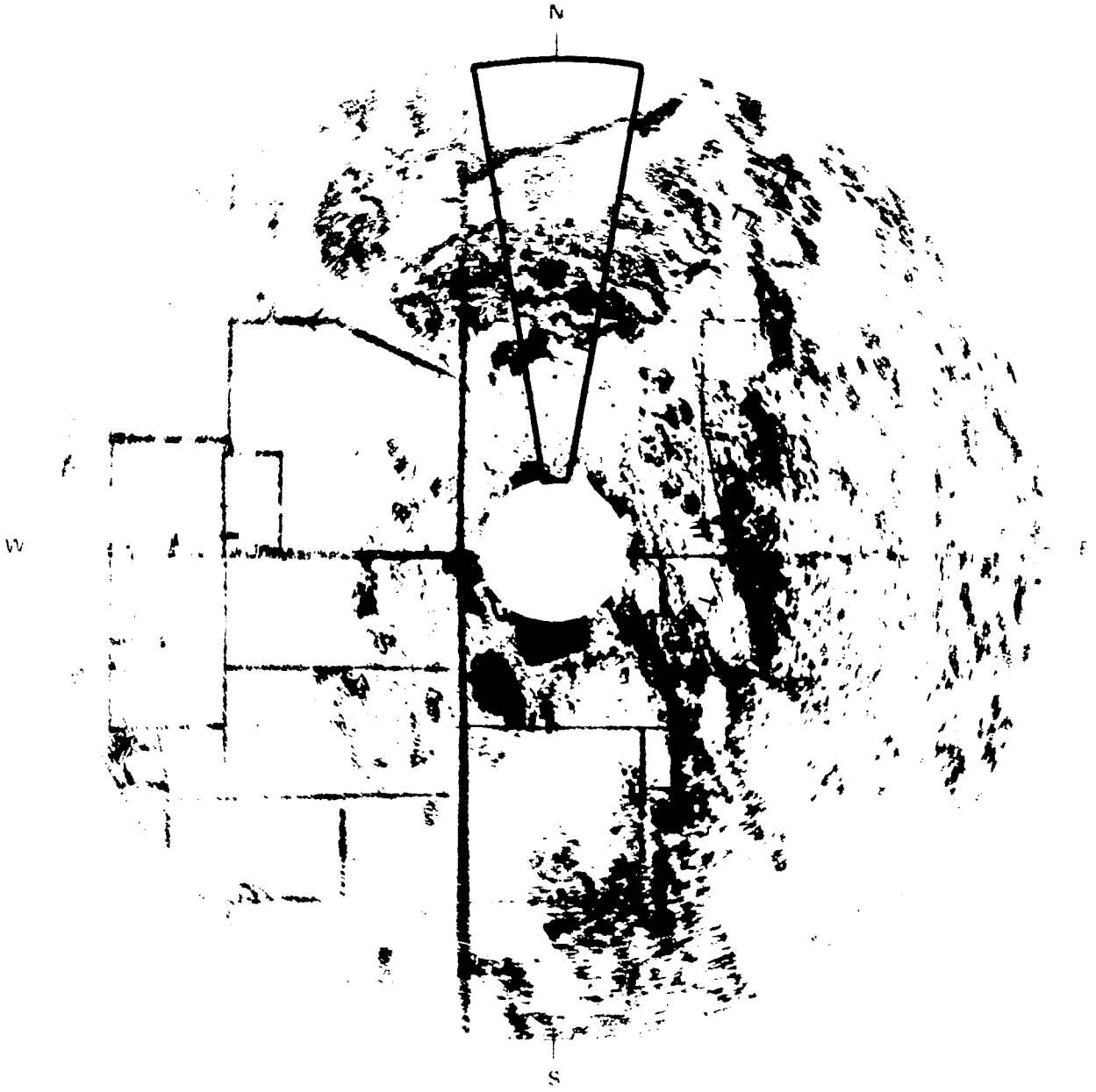

Figure E-167. PPI clutter map and repeat sector at Big Grass Marsh. Repeat sector is outlined in black. Maximum range = 7 km; X-band, 15-m pulse, horizontal polarization; cells with $\sigma^{o}F^{4} \geq -50$ dB are red.

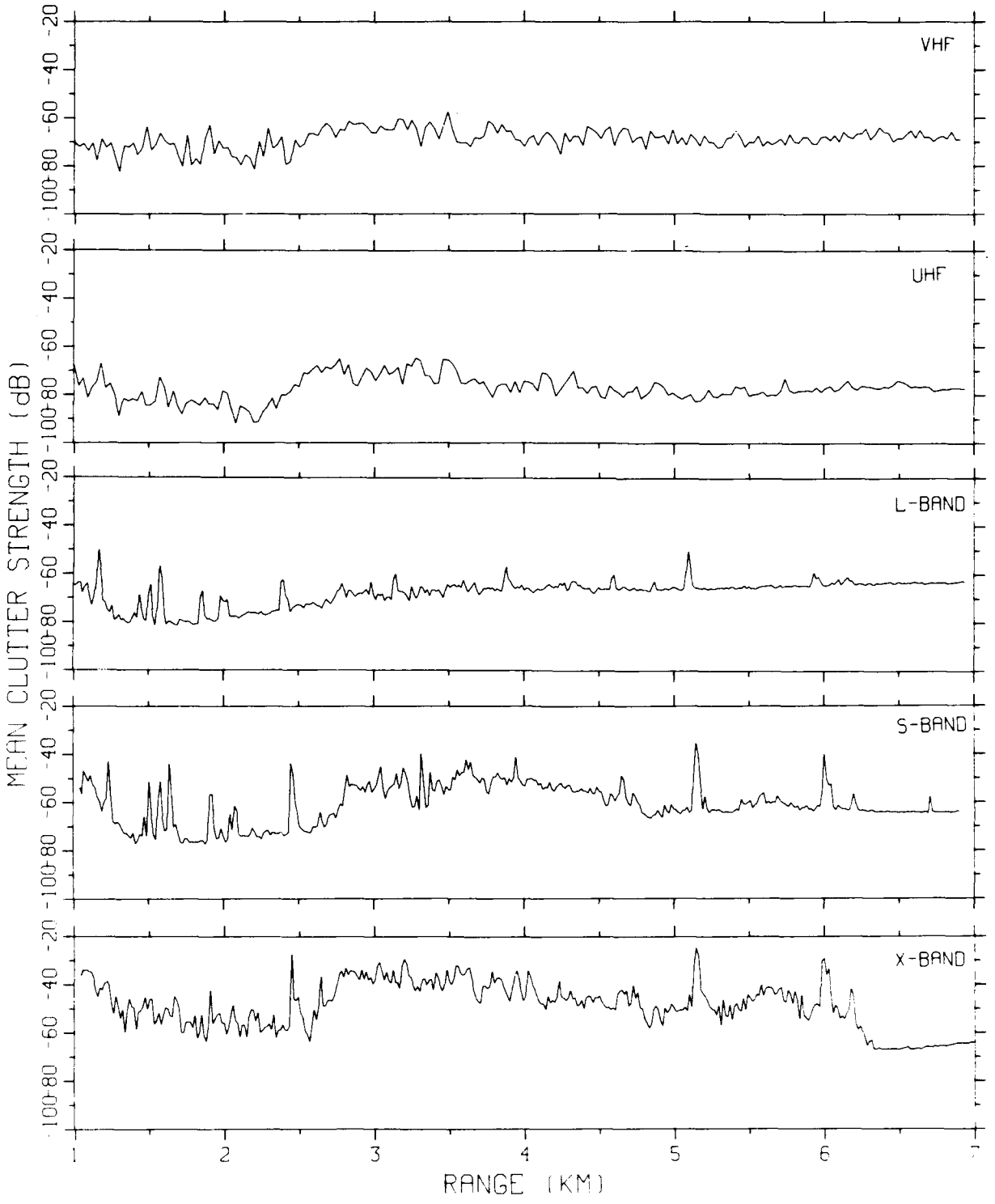

Figure E-168. Mean clutter strength versus range at Big Grass Marsh. Repeat sector data. Vertical polarization. 15/36-m pulse length. Data shown range gate by range gate, averaged in azimuth over 20 deg.

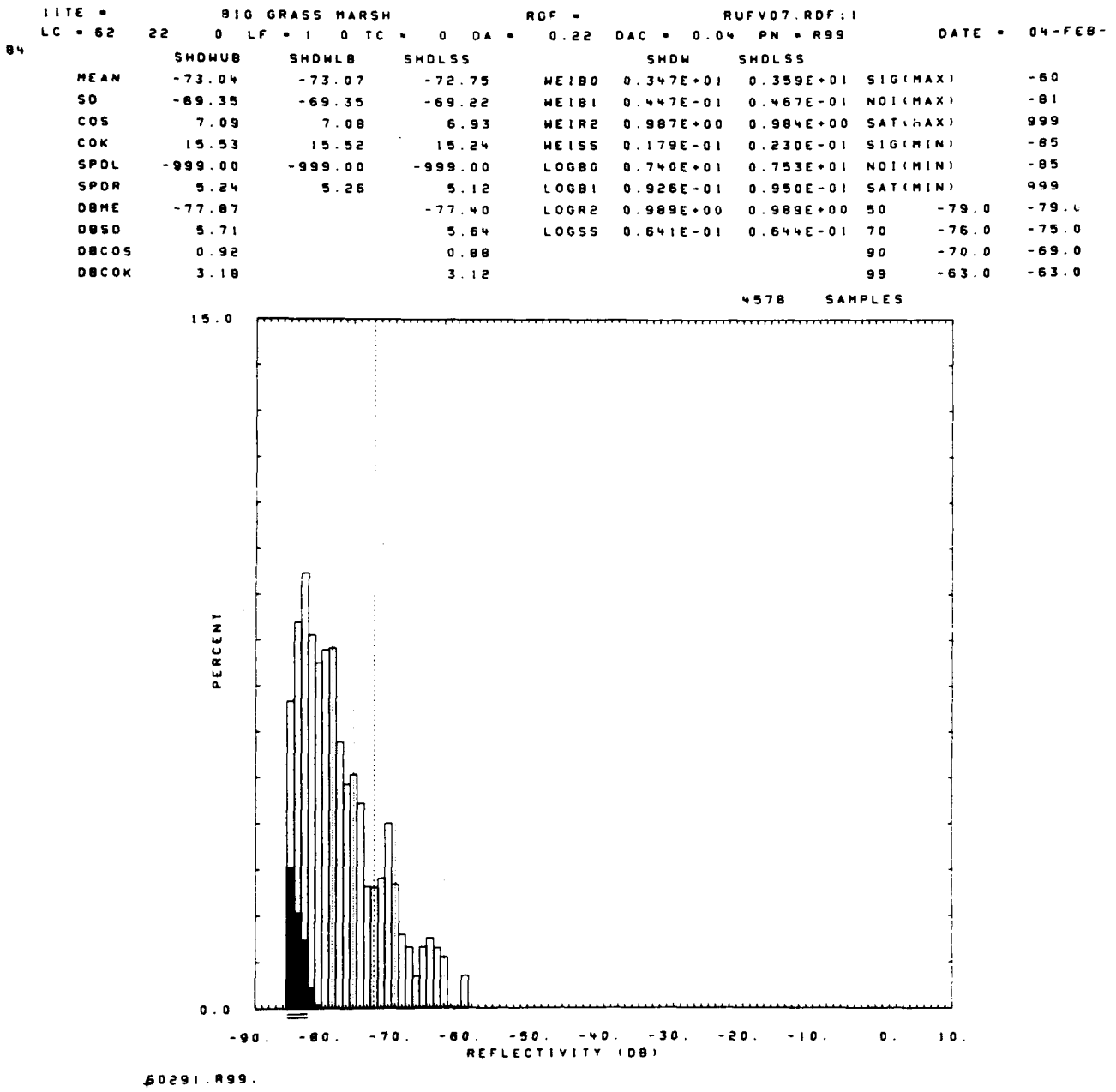

Figure E-169. Clutter strength histogram for Big Grass Marsh repeat sector. UHF, 150-m pulse, vertical polarization.

SITE = BIG GRASS MARSH RDF = RSFH16.RDF;1

LC = 62 22 0 LF = 1 0 TC = 0 DA = 0.21 DAC = 0.19 PN = R99 DATE = 04-FEB-84

	SHDWUB	SHDWLB	SHDLSS		SHDW	SHDLSS			
MEAN	-49.27	-49.27	-48.51	WEIB0	0.168E+01	0.183E+01	SIG(MAX)		-28
SD	-42.60	-42.60	-42.24	WEIB1	0.277E-01	0.316E-01	NOI(MAX)		-71
COS	10.08	10.08	9.71	WEIR2	0.998E+00	0.992E+00	SAT(MAX)		999
COK	21.91	21.91	21.18	WEISS	0.765E-02	0.329E-01	SIG(MIN)		-85
SPDL	-999.00	-999.00	-999.00	LOGB0	0.357E+01	0.370E+01	NOI(MIN)		-85
SPDR	7.52	7.52	7.19	LOGB1	0.545E-01	0.588E-01	SAT(MIN)		999
DBME	-64.82		-62.04	LOGR2	0.992E+00	0.996E+00	50	-65.0	-62.0
DBSD	12.40		11.54	LOGSS	0.953E-01	0.615E-01	70	-58.0	-56.0
DBCOS	0.35		0.22				90	-47.0	-46.0
DBCOK	2.27		2.43				99	-35.0	-35.0

23975 SAMPLES

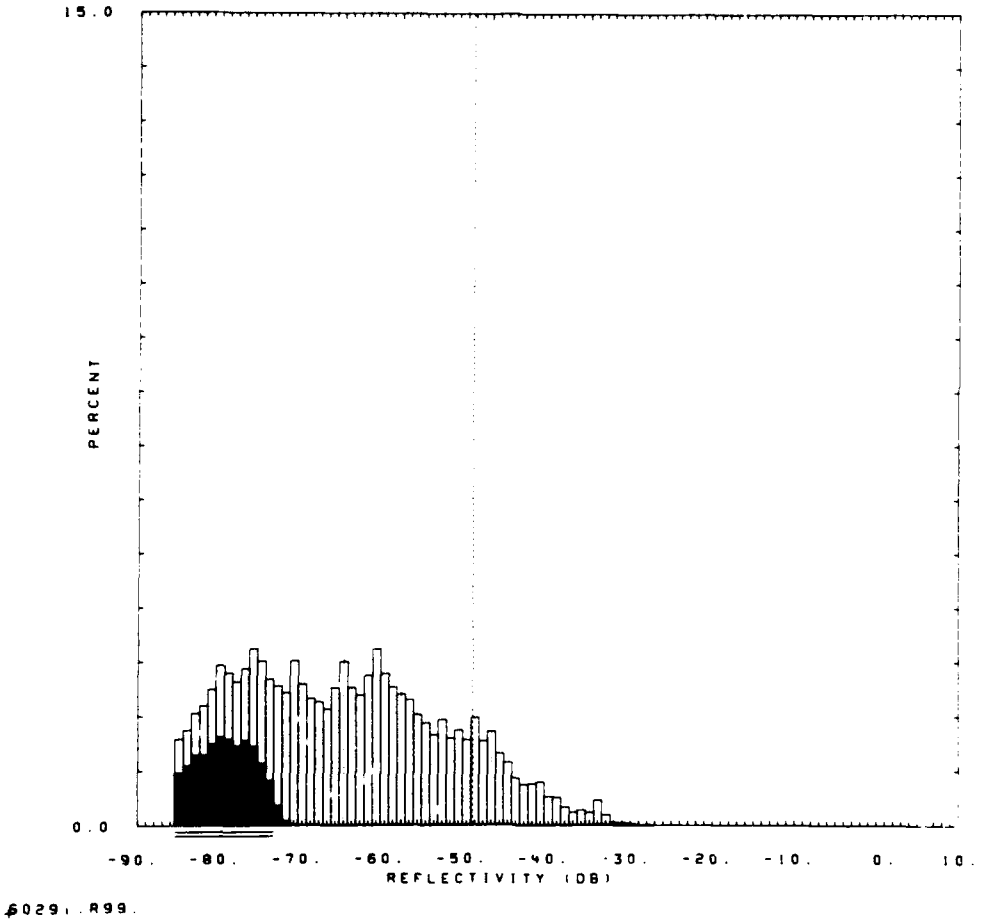

6029I..R99.

Figure E-170. Clutter strength histogram for Big Grass Marsh repeat sector. S-band, 150-m pulse, horizontal polarization.

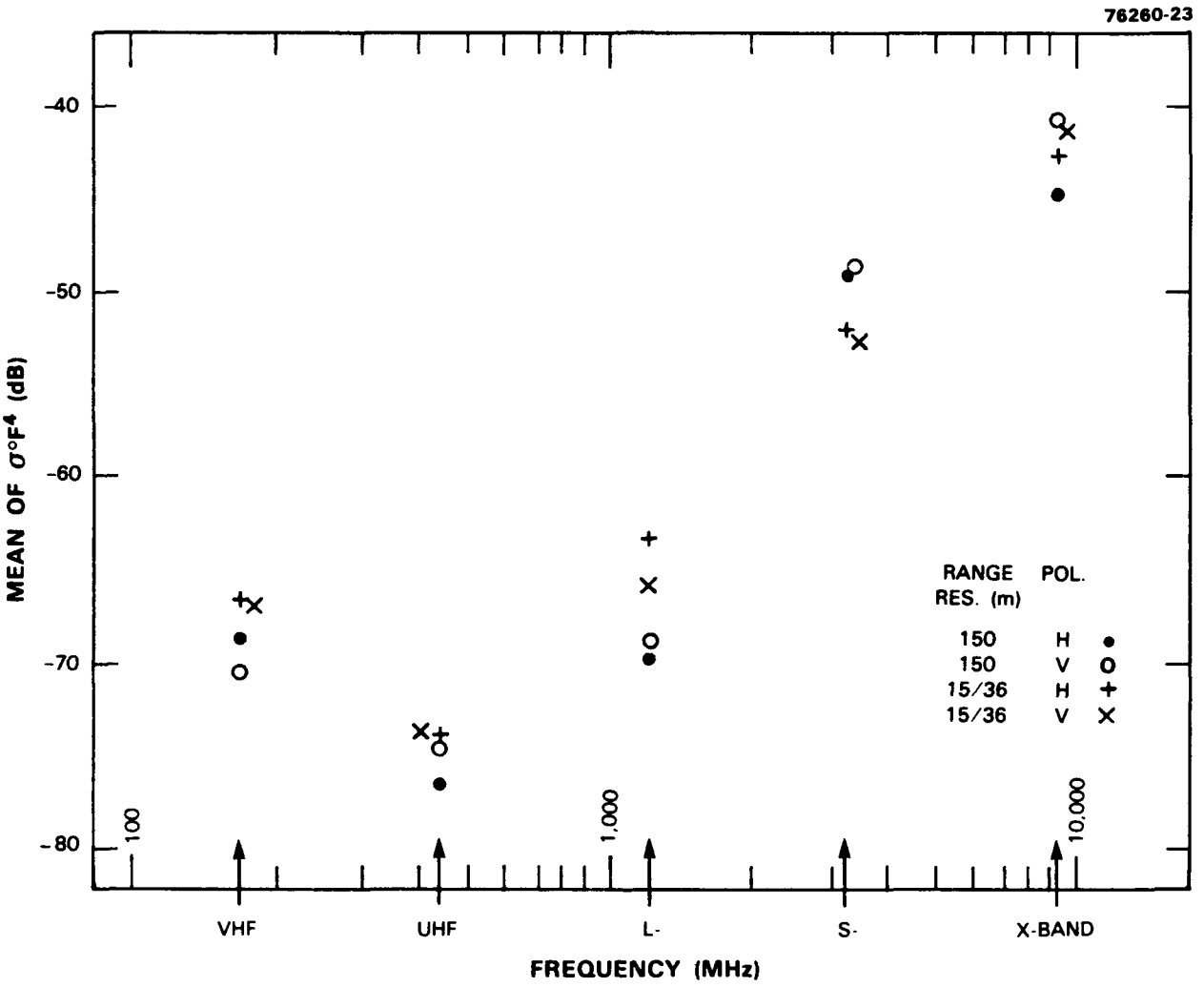

Figure E-171. Mean clutter strength versus frequency at Big Grass Marsh. For the Big Grass Marsh repeat sector, depression angle = 0.2 deg, landform = 1, land cover = 62-22, range = 1 to 6.9 km, azimuth = 350 to 10 deg. Comment: At S-band, intermittent high VSWR levels were measured; however, corrections were made in calibration and data appedr reasonable.

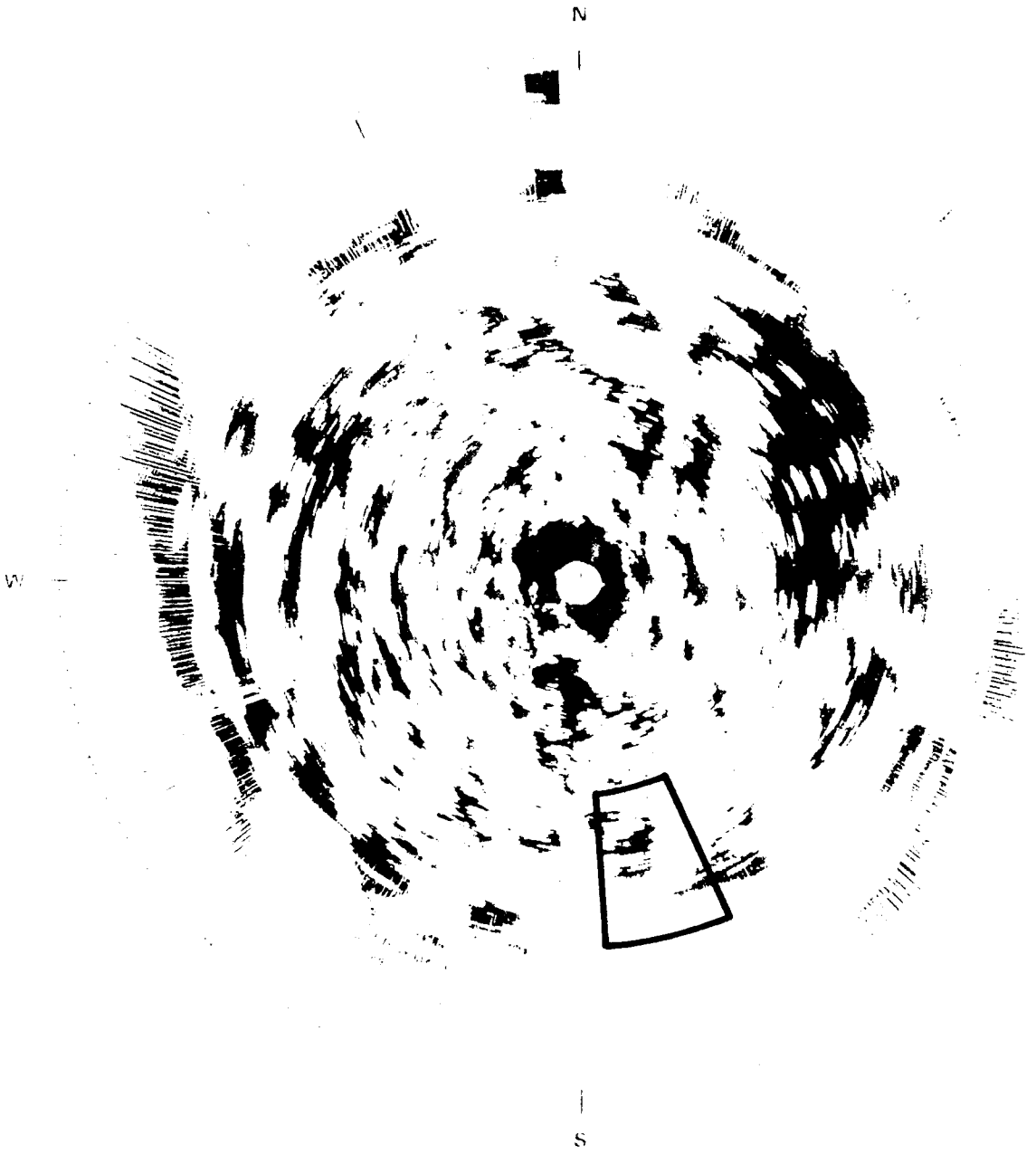

Figure E-172. PPI clutter map and repeat sector at Wachusett Mountain. Repeat sector is outlined in black. Maximum range = 20 km; UHF, 36-m pulse, horizontal polarization; cells with $\sigma^{\circ}F^{4} \geq -40$ dB are white.

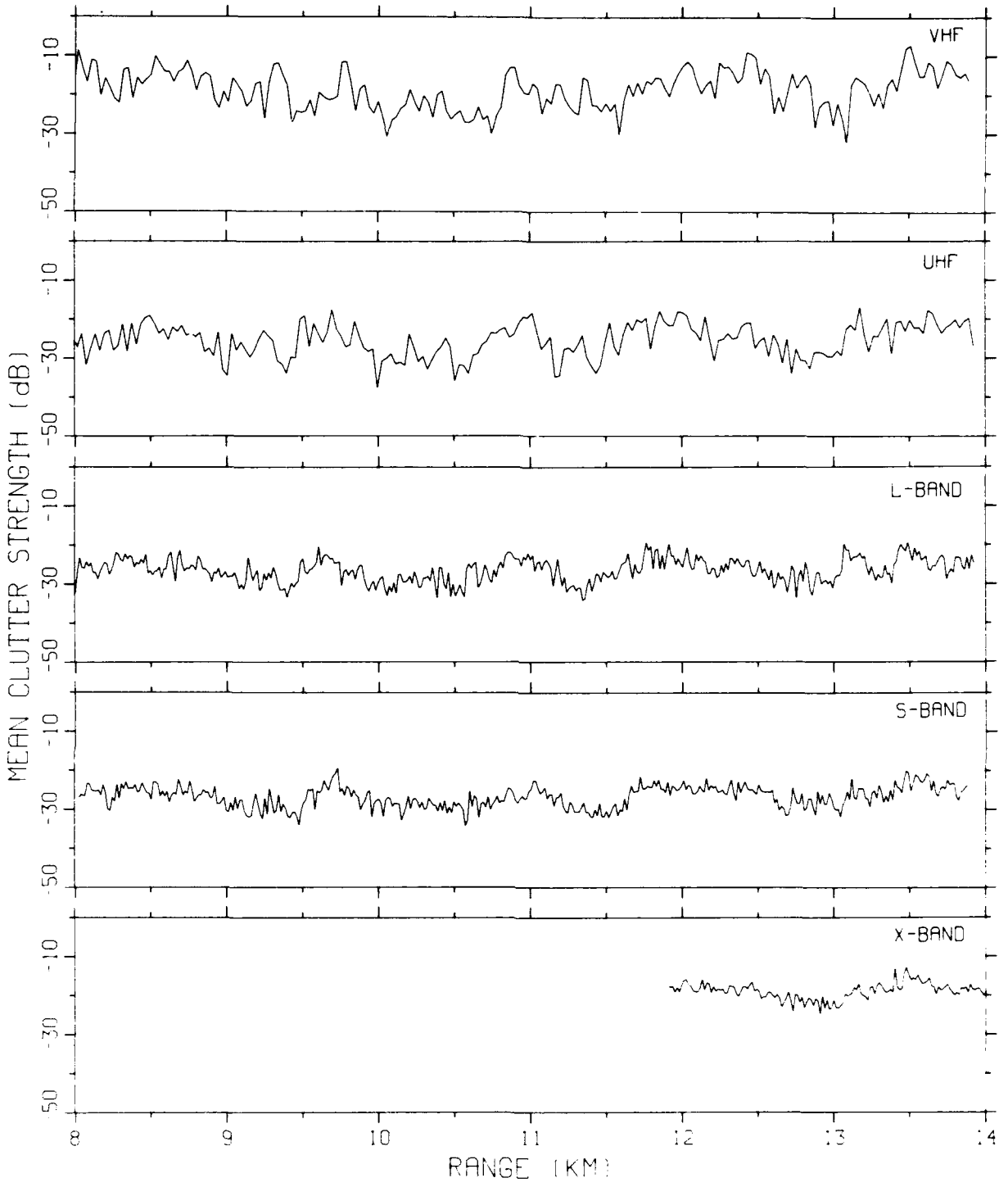

Figure E-173. Mean clutter strength versus range at Wachusett Mountain. Repeat sector data. Vertical polarization, 15/36-m pulse length. Data shown range gate by range gate, averaged in azimuth over 20 deg.

SITE = WACHUSETT MT RDF = RSFH16.RDF;1
LC = 43 21 11 LF = 5 4 TC = 4 DA = 2.04 DAC = 5.32 PN = R99 DATE = 20-AUG-84

	SHDWUB	SHDWLB	SHDLSS		SHDW	SHDLSS			
MEAN	-27.43	-27.43	-27.30	WEIB0	0.141E+01	0.150E+01	SIG(MAX)		-14
SD	-24.73	-24.73	-24.69	WEIB1	0.454E-01	0.492E-01	NOI(MAX)		-58
COS	6.08	6.08	6.02	WEIR2	0.989E+00	0.993E+00	SAT(MAX)		999
COK	14.21	14.21	14.12	WEISS	0.109E+00	0.585E-01	SIG(MIN)		-65
SPDL	-999.00	-999.00	-999.00	LOGB0	0.253E+01	0.269E+01	NOI(MIN)		-84
SPDR	4.56	4.56	4.51	LOGB1	0.689E-01	0.756E-01	SAT(MIN)		999
DBME	-35.54		-34.61	LOGR2	0.930E+00	0.943E+00	50	-33.0	-32.0
DBSD	11.68		10.50	LOGSS	0.163E+01	0.124E+01	70	-28.0	-28.0
DBCOS	-0.91		-0.74				90	-23.0	-23.0
DBCOK	3.28		2.84				99	-18.0	-18.0

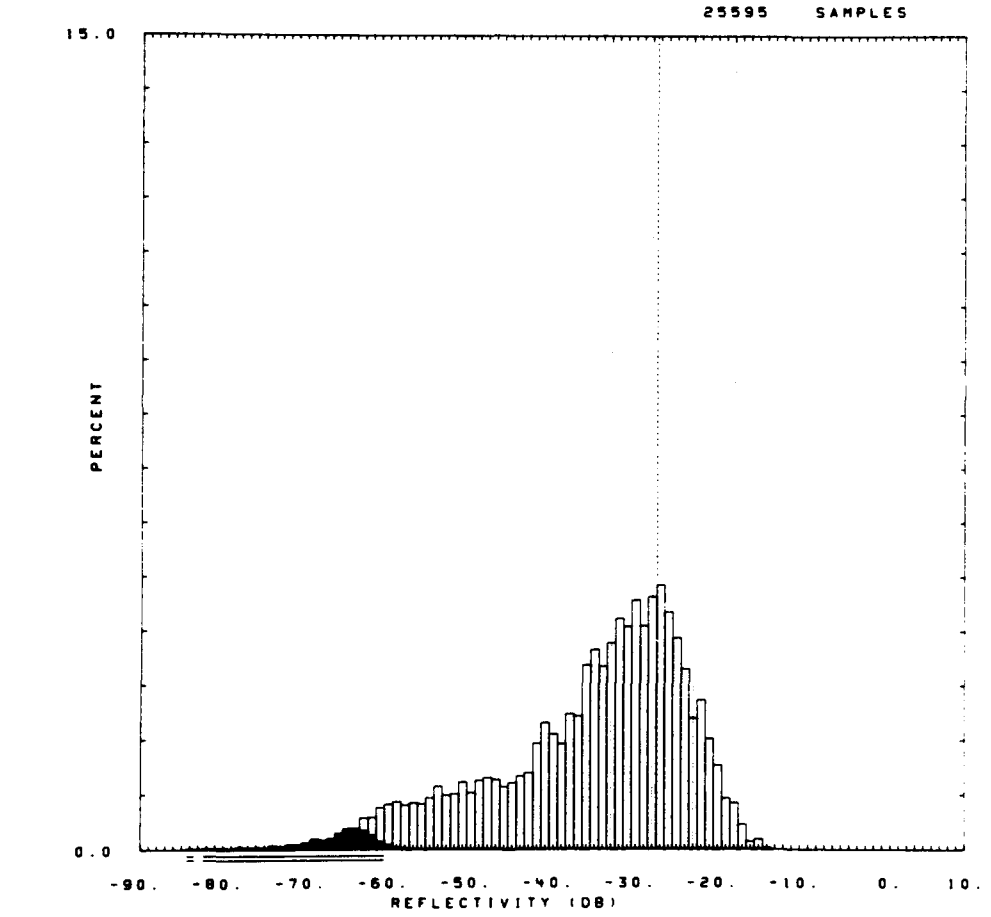

Figure E-174. Clutter strength histogram for Wachusett Mountain repeat sector. S-band, 150-m pulse, horizontal polarization.

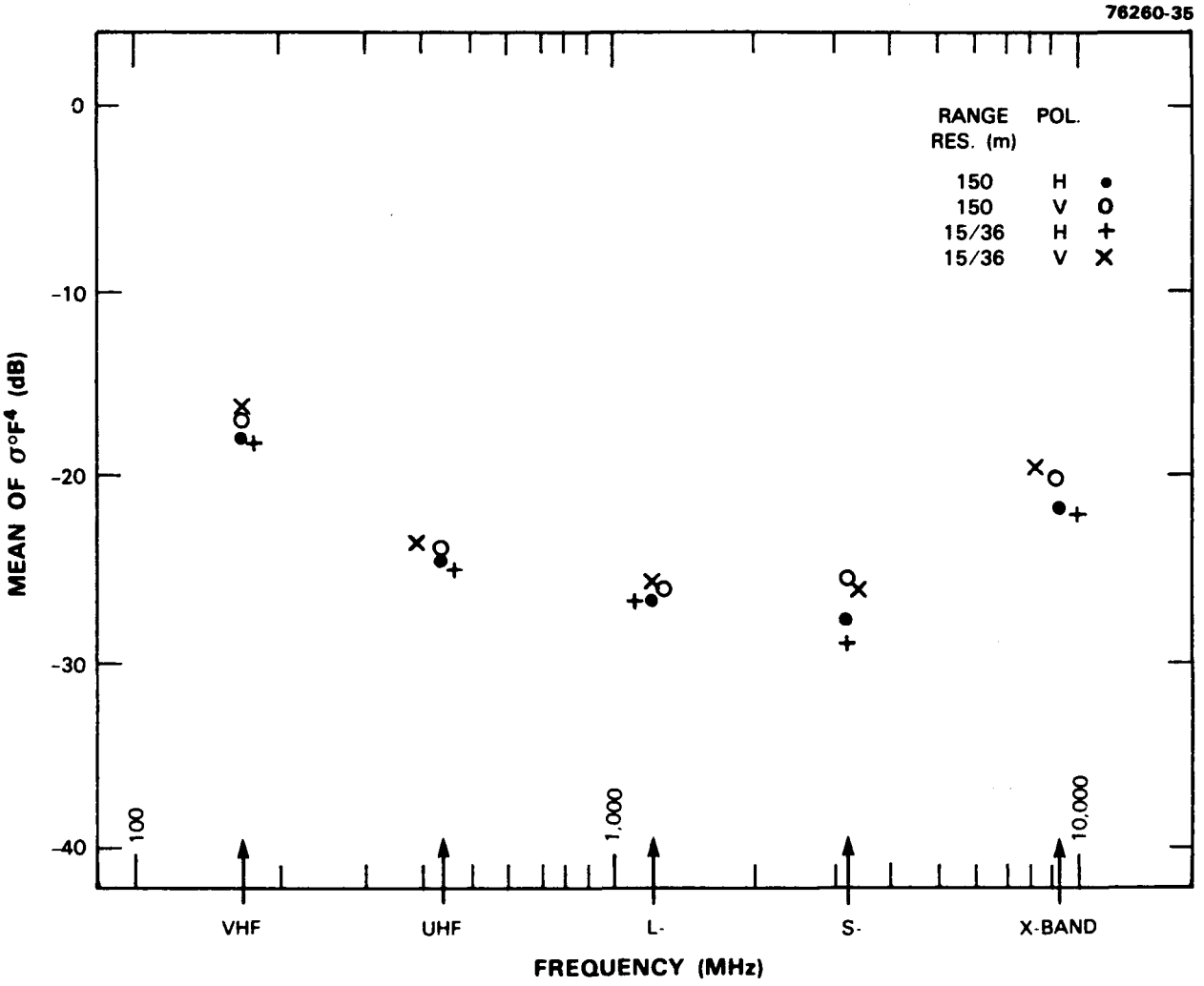

Figure E-175. Mean clutter strength versus frequency at Wachusett Mountain. For the Wachusett Mountain repeat sector, depression angle = 2.1 deg, landform = 5-4, land cover = 43-21-11, range = 8 to 13.9 km, azimuth = 156 to 176 deg. Comment: VHF interference may have slightly affected high resolution VHF data.

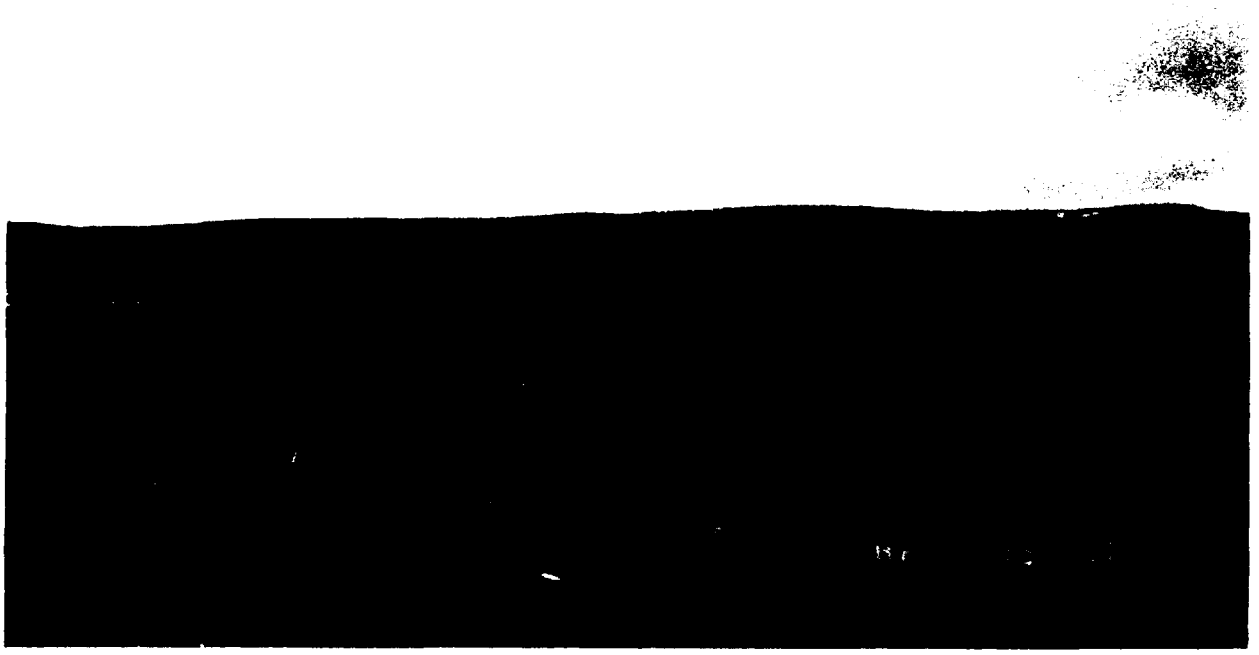

Figure E-176. Cochrane repeat sector. Looking WSW, from a point 9 km out in repeat sector. Primarily rangeland, but note patches of trees on far slopes

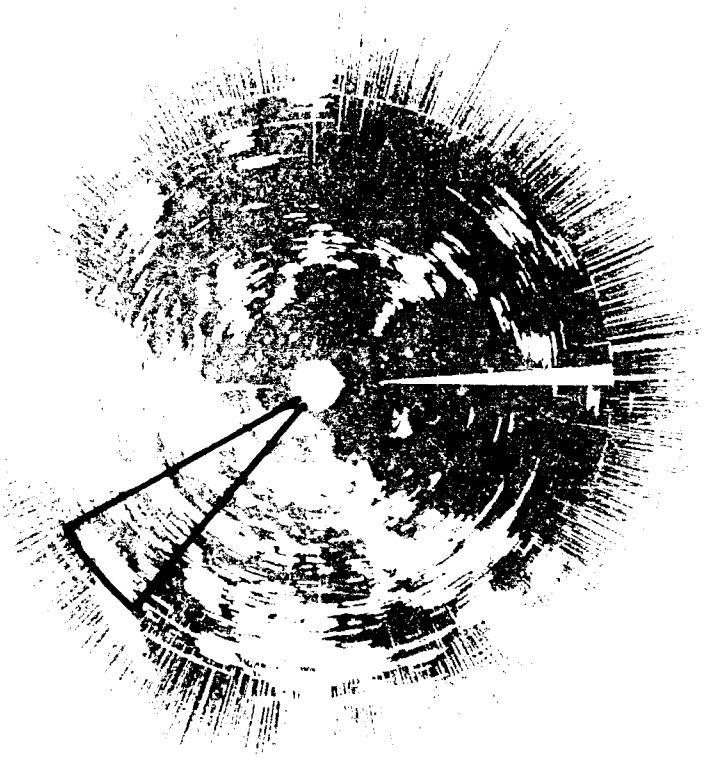

Figure E-177. PPI clutter map and repeat sector at Cochrane. Repeat sector is outlined in black. Maximum range = 20 km; UHF, 36 m pulse, horizontal polarization; cells with $\sigma^{\circ}F^{4} \geq -40$ dB are white. Second visit

SITE = COCHRANE RDF = RLTV09.RDF;1

LC = 31 32 0 LF = 7 2 TC = 2 DA = 1.77 DAC = 0.67 PN = R99 DATE = 12-MAR-33

	SHDWUB	SHDWLB	SHDLSS		SHDW	SHDLSS			
MEAN	-19.32	-19.32	-17.95	WEIB0	0.833E+00	0.848E+00	SIG(MAX)		3
SD	-12.34	-12.34	-11.69	WEIB1	0.259E-01	0.310E-01	NOI(MAX)		-36
COS	11.16	11.16	10.50	WEIR2	0.998E+00	0.100E+01	SAT(MAX)		999
COK	24.04	24.04	22.74	WEISS	0.324E-02	0.112E-02	SIG(MIN)		-83
SPOL	-999.00	-999.00	-999.00	LOGB0	0.196E+01	0.193E+01	NOI(MIN)		-85
SPOR	7.77	7.77	7.18	LOGB1	0.551E-01	0.613E-01	SAT(MIN)		999
DBME	-37.23		-31.26	LOGR2	0.982E+00	0.989E+00	50	-38.0	-32.0
DBSD	14.51		11.81	LOGSS	0.150E+00	0.110E+00	70	-29.0	-24.0
DBCOS	0.12		0.14				90	-17.0	-15.0
DBCOK	2.30		2.39				99	-6.0	-5.0

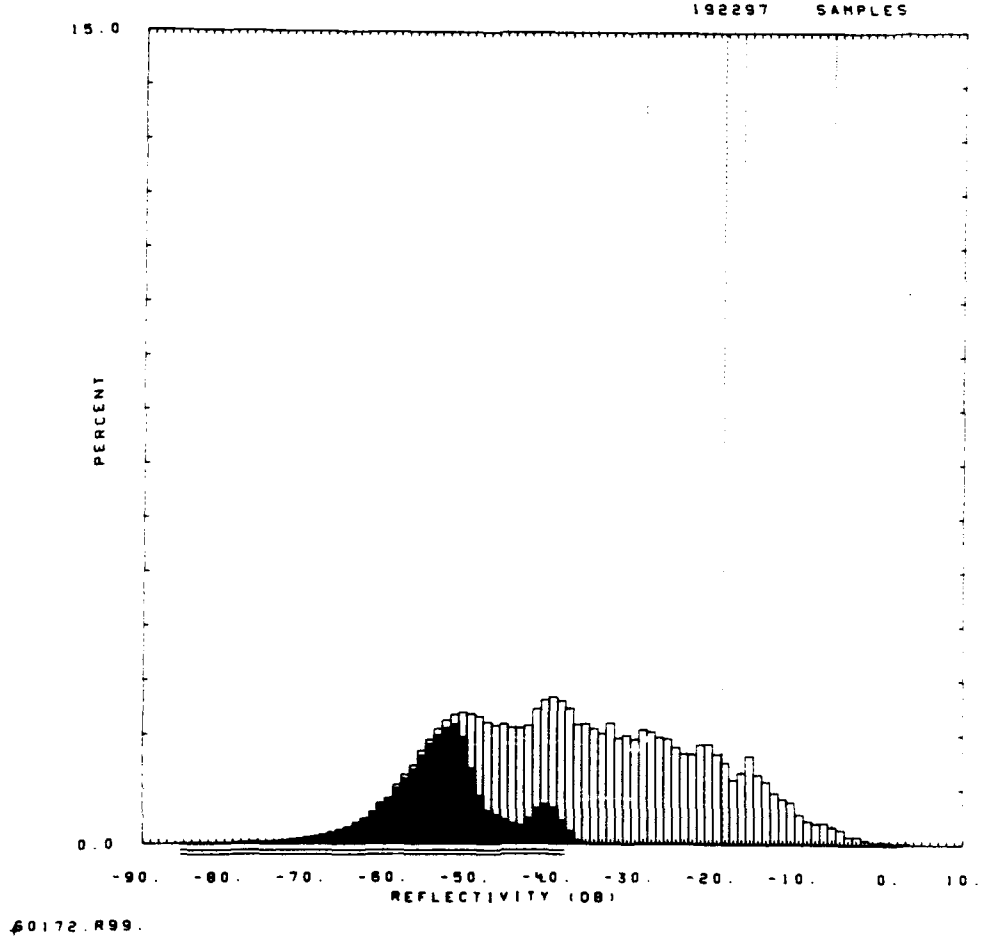

Figure E-178. Clutter strength histogram for Cochrane repeat sector. L-band, 15-m pulse, vertical polarization. Second visit. STC = R^4.

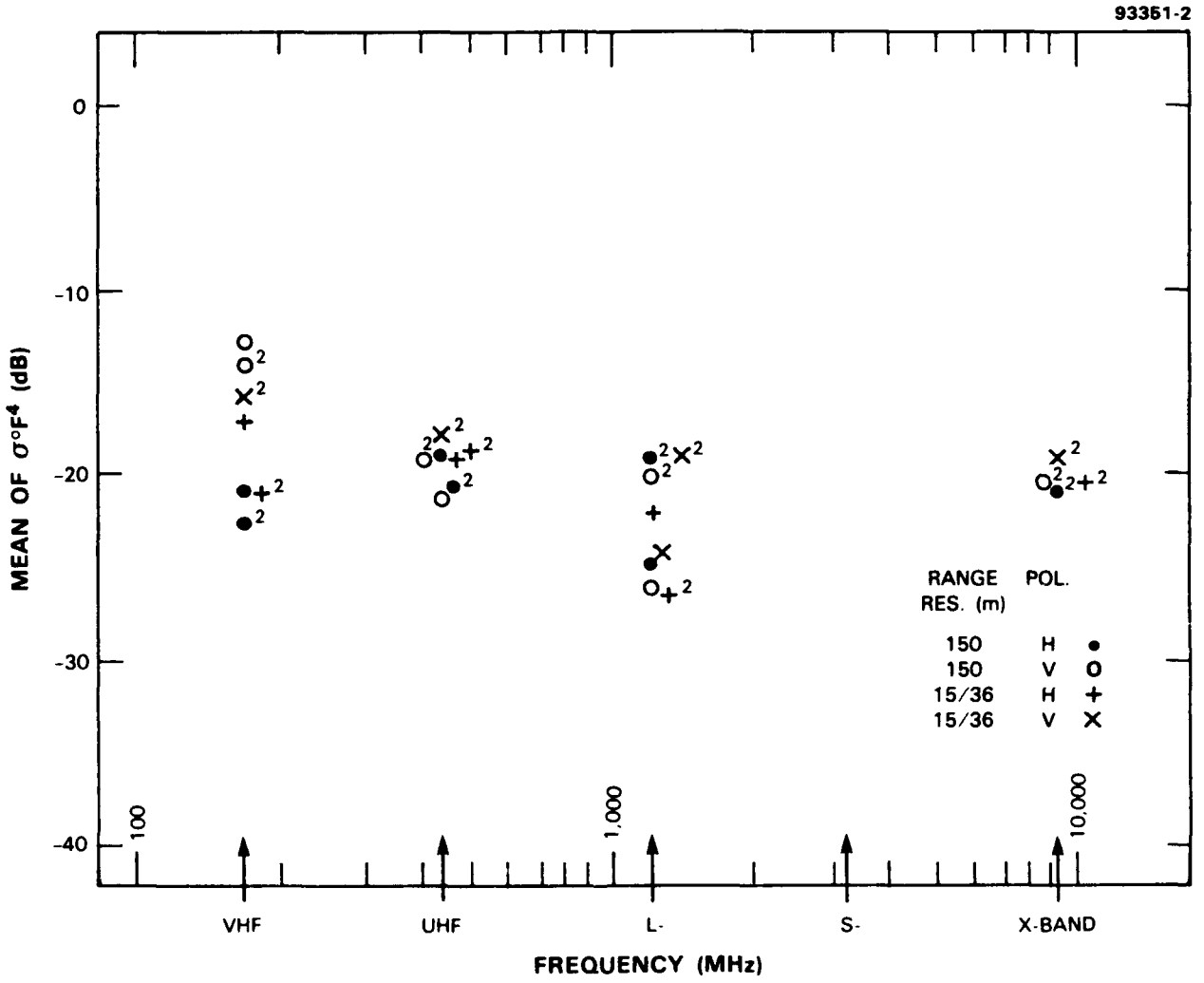

Figure E-179. Mean clutter strength versus frequency at Cochrane. For the Cochrane repeat sector, depression angle = 1.7 deg, landform = 7-2, land cover = 31/32-21/22-41/43-11, range = 1 to 10 km, azimuth = 220 to 240 deg. Comments: (1) There were two Phase One visits to Cochrane, with the second visit results indicated by 2's. (2) For first visit, at both VHF and UHF, low resolution/vertical polarization and high resolution/horizontal polarization results shown are from survey data in repeat sector; ditto for L-band high resolution/horizontal polarization. (3) For both visits, hardware problems precluded useful data collection at S-band. (4) For first visit, hardware problems precluded useful data collection at X-band. (5) For second visit, hardware problem induced high VSWR during L-band high resolution/horizontal polarization experiment, resulting in erroneous data.

(a)

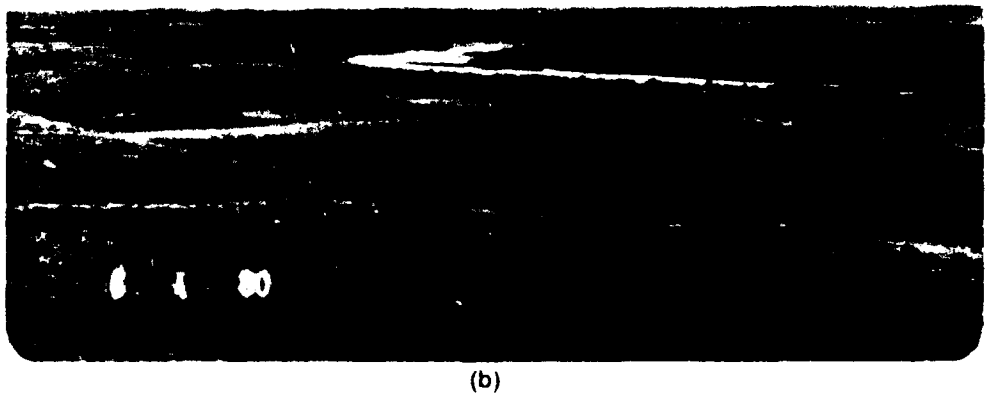

(b)

Figure F-180. Repeat sector at Suffield: (a) View SE into repeat sector and (b) broken terrain further out in repeat sector

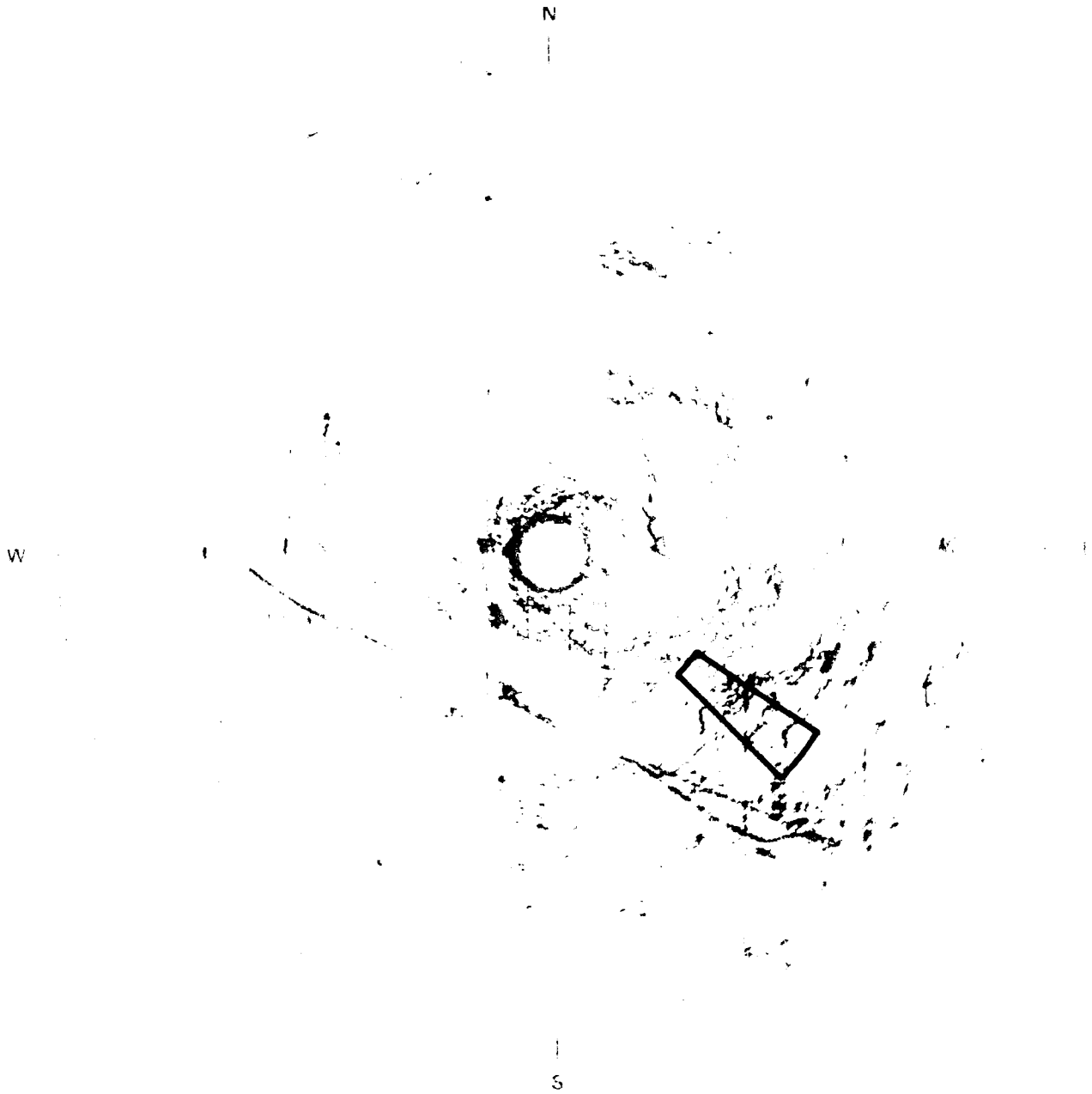

Figure E-181. PPI clutter map and repeat sector at Suffield. Repeat sector is outlined in black. Maximum range = 20 km, X-band, 15-m pulse, horizontal polarization; cells with $\sigma^{\circ}F^{4} \geq -40$ dB are red.

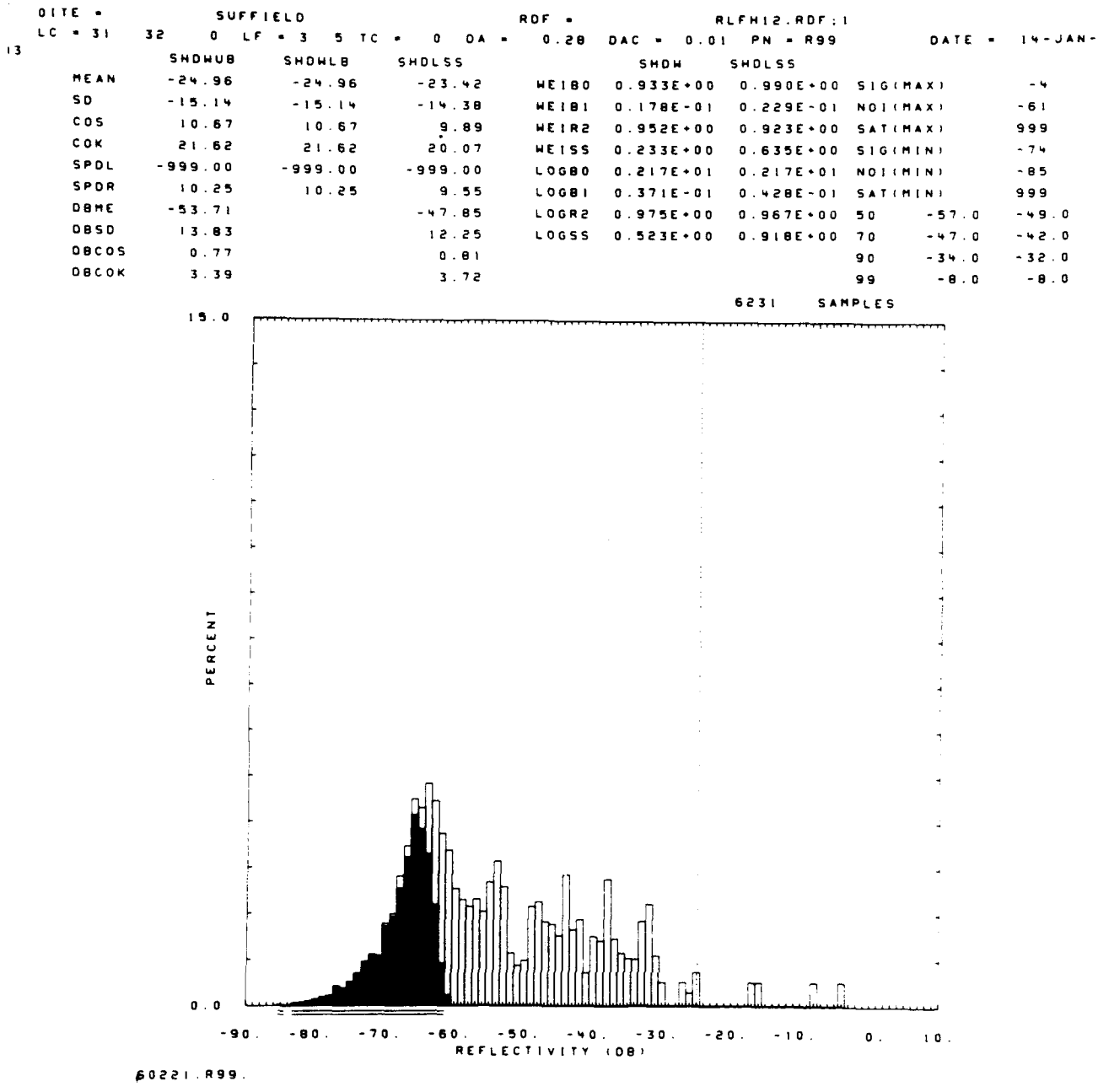

Figure E-182. Clutter strength histogram for Suffield repeat sector. L-band. 150-m pulse. horizontal polarization.

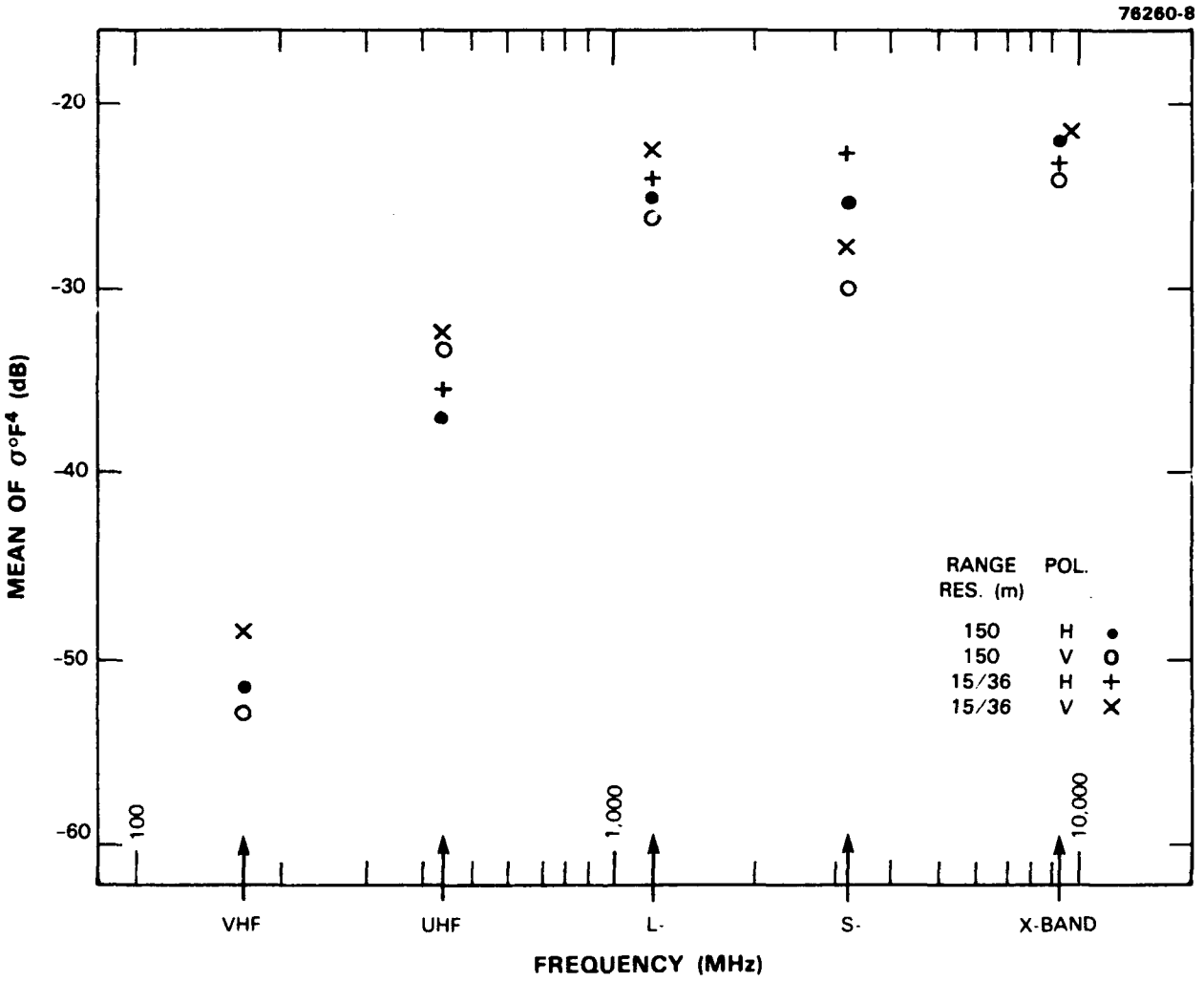

Figure E-183. Mean clutter strength versus frequency at Suffield. For the Suffield repeat sector, depression angle = 0.3 deg, landform = 3-5-9, land cover = 31-62-52-12, range = 7 to 12.9 km, azimuth = 125 to 135 deg. Comments: (1) VHF interference precluded most high resolution data; data shown may have been affected by interference. (2) S-band was repaired and functioned properly for several days before recurrence of failure; data shown are from that portion of visit.

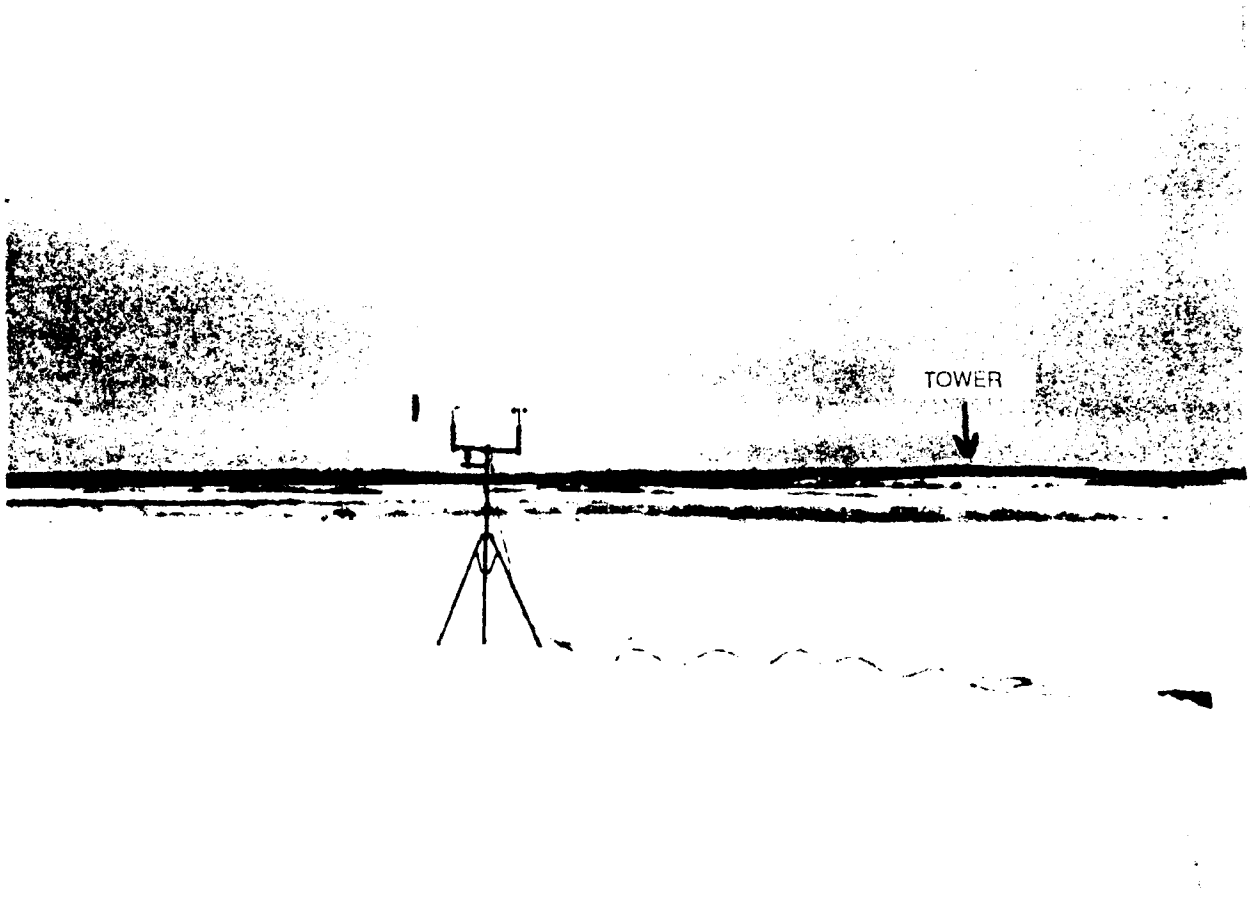

Figure E-184. Repeat sector at Spruce Home. Looking SW past remote weather station located at 6 km range to repeat sector to Phase One tower on horizon beyond.

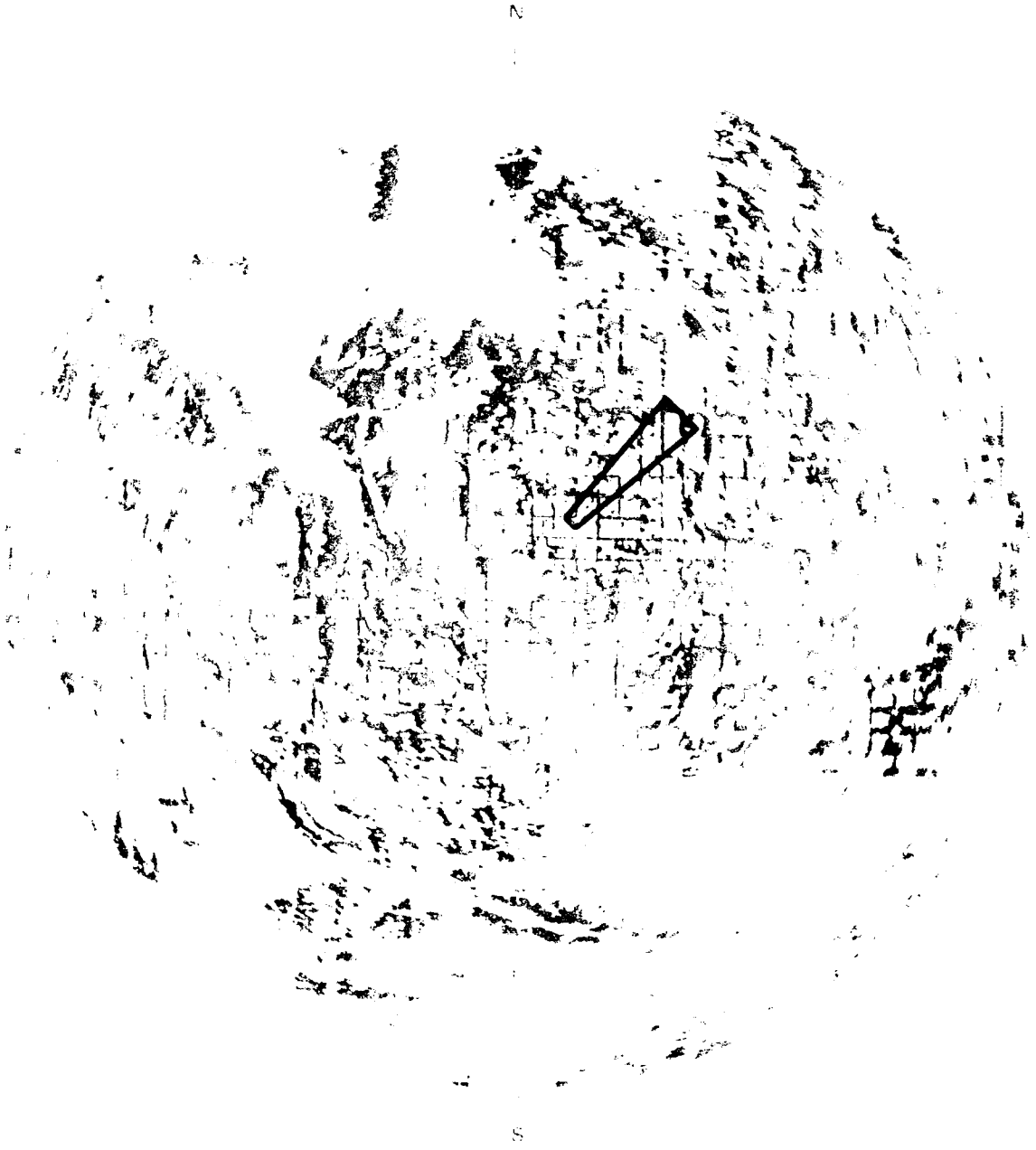

Figure E-185. PPI clutter map and repeat sector at Spruce Home. Repeat sector is outlined in black. Maximum range = 20 km, X-band, 15-m pulse, horizontal polarization; cells with $\sigma^{\circ}F^{4} \geq -40$ dB are red.

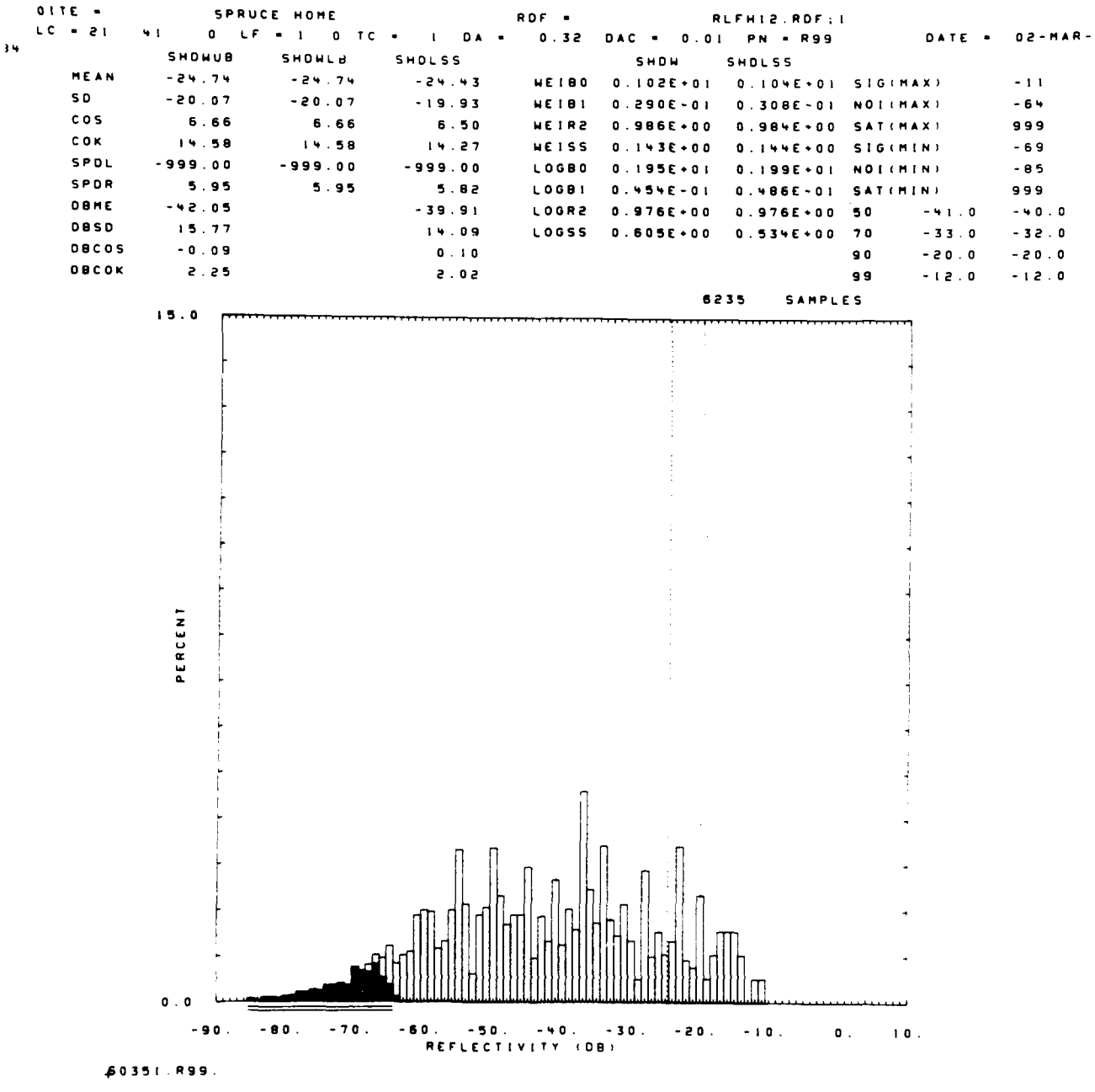

Figure E-186. Clutter strength histogram for Spruce Home repeat sector. L-band. 150-m pulse, horizontal polarization.

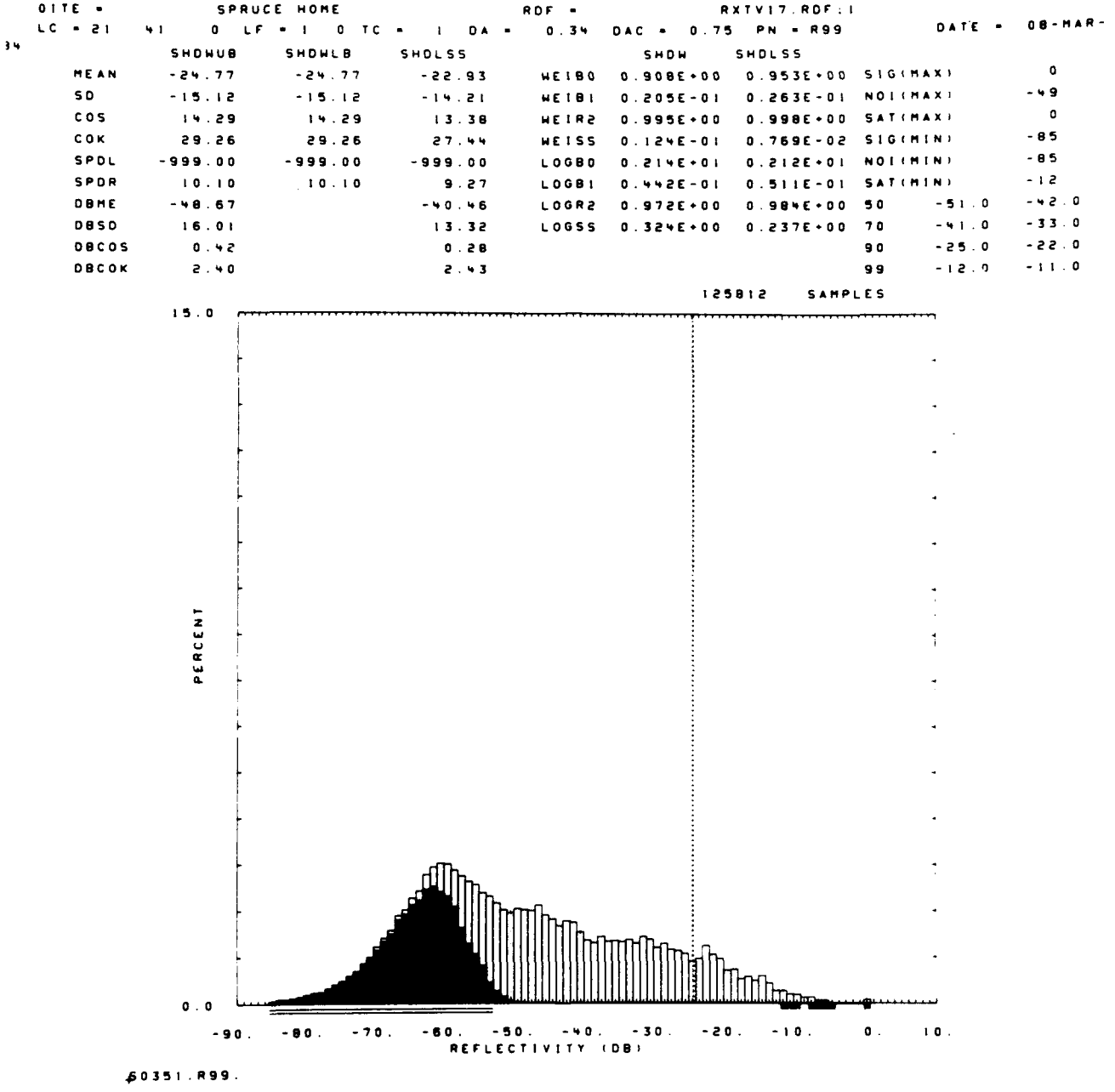

Figure E-187. Clutter strength histogram for Spruce Home repeat sector. X-band. 15-m pulse, vertical polarization.

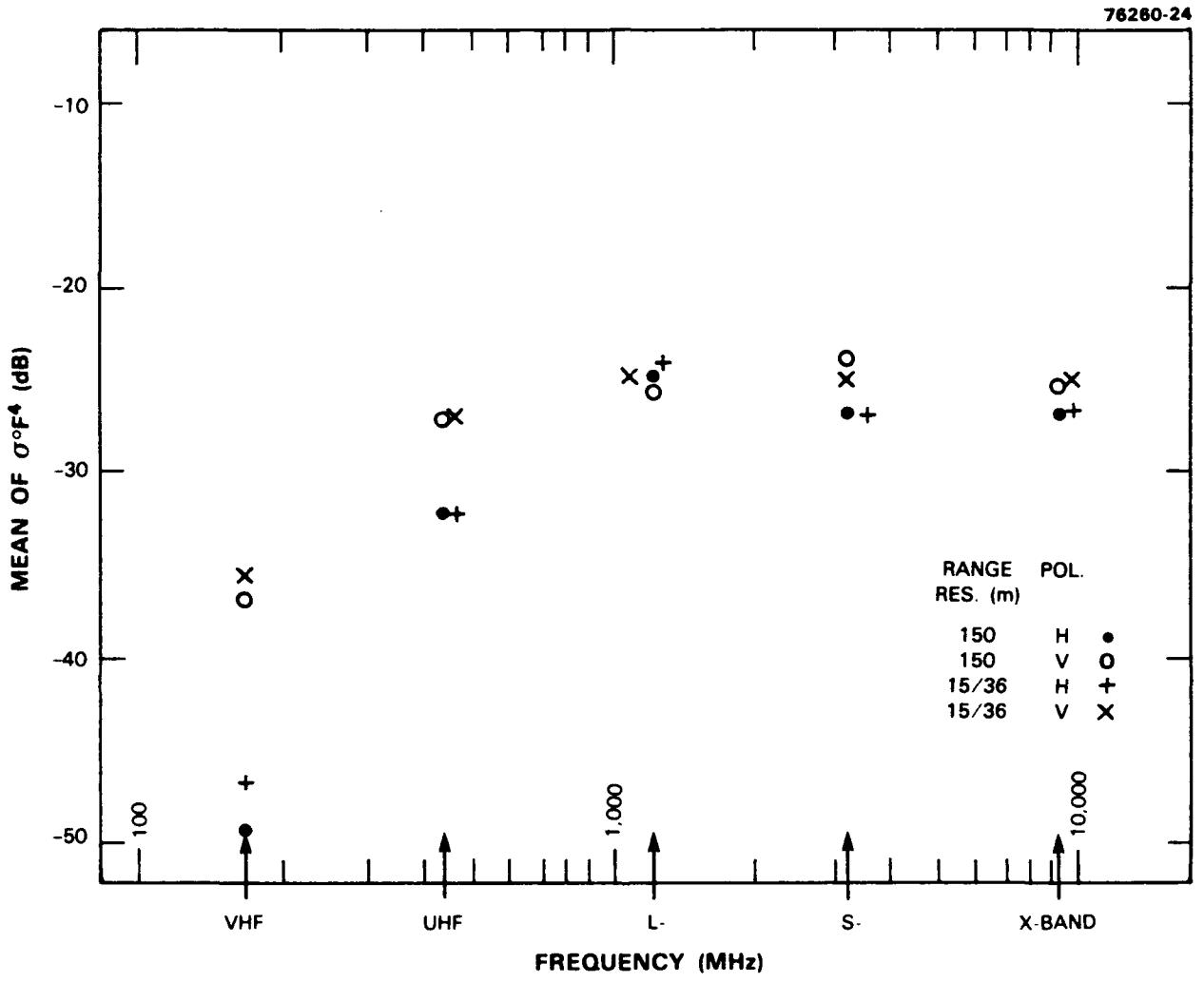

Figure E-188. Mean clutter strength versus frequency at Spruce Home. For the Spruce Home repeat sector, depression angle = 0.3 deg, landform = 1, land cover = 21-41, range = 3 to 8.9 km, azimuth = 40 to 50 deg.

REFERENCES

1. J.B. Billingsley and J.F. Larrabee, "Measured spectral extent of L- and X-band radar reflections from wind-blown trees," MIT Lincoln Laboratory, Lexington, Mass., Project Report CMT-57 (6 February 1987). DTIC AD-A179942/8.

2. S. Ayasli, "Propagation effects on radar ground clutter," *Proc. IEEE National Radar Conference*, IEEE Aerospace and Electronic Systems Society and the IEFE Los Angeles Council, Los Angeles, Calif. (12–13 March 1986).

3. H.C. Chan, "Radar sea-clutter at low grazing angles," *Proc. Inst. Electr. Eng.* **137,** 102–112 (1990).

4. S. Ayasli, (private communication, 1990).

5. E. Jakeman, "On the statistics of K-distributed noise," *J. Phys. A* **13,** 31–48 (1980).

6. S. Watts and K.D. Ward, "Spatial correlation in K-distributed sea clutter," *Proc Inst. Electr. Eng.* **134,** 526–531 (1987).

7. S. Ayasli, "SEKE: A computer model for low-altitude radar propagation over irregular terrain," *IEEE Trans. Antenna Propag.* **AP-34,** 1013–1023 (1986).

REPORT DOCUMENTATION PAGE

Form Approved
OMB No. 0704-0188

1. AGENCY USE ONLY (*Leave blank*)	2. REPORT DATE	3. REPORT TYPE AND DATES COVERED
	15 November 1991	Technical Report

4. TITLE AND SUBTITLE

Multifrequency Measurements of Radar Ground Clutter at 42 Sites

5. FUNDING NUMBERS

C — F19628-90-C-0002

6. AUTHOR(S)

J. Barrie Billingsley and John F. Larrabee

7. PERFORMING ORGANIZATION NAME(S) AND ADDRESS(ES)

Lincoln Laboratory, MIT
P.O. Box 73
Lexington, MA 02173-9108

8. PERFORMING ORGANIZATION REPORT NUMBER

TR-916
Volume 3: Appendix E

9. SPONSORING/MONITORING AGENCY NAME(S) AND ADDRESS(ES)

Department of the Air Force
SAF/AQL
The Pentagon
Washington, D.C. 20330

DARPA
1400 Wilson Blvd.
Arlington, VA 22209

10. SPONSORING/MONITORING AGENCY REPORT NUMBER

ESD-TR-91-176

11. SUPPLEMENTARY NOTES

None

12a. DISTRIBUTION/AVAILABILITY STATEMENT

Approved for public release; distribution is unlimited.

12b. DISTRIBUTION CODE

13. ABSTRACT (*Maximum 200 words*)

This report determines how ground clutter strength varies with RF frequency from VHF to X-band in ground-sited radar. This determination is accomplished by providing extensive empirical results from multifrequency clutter measurements conducted at 42 different sites widely dispersed over the North American continent. These results indicate that the frequency dependence of ground clutter strength depends upon terrain type and can vary, for example, from a strongly decreasing function of frequency in forest to a strongly increasing function of frequency in farmland. Five major terrain categories are defined that encompass this dependence, namely, urban, mountains, forest, farmland, and desert. Within each terrain category, results are also shown to be dependent upon the relief or roughness of the terrain and upon the depression angle at which the terrain is illuminated. The depression angle dependence is important, even for the very low angles (typically within a degree of grazing incidence) and small (typically fractional) variations in angle that occur in ground-sited radar. This report presents specific clutter strength results at each of five frequencies (VHF, UHF, L-, S-, and X-band) from each of the 42 sites at which measurements were conducted. The report then combines results from similar sites to obtain the general dependence of clutter strength versus frequency for each terrain category. Clutter strengths are described in terms of moments (including the mean) and percentile levels (including the median) in measured clutter amplitude distributions resulting from cell-by-cell spatial variation over a selected large kilometer-sized macroregion of terrain at each site called the repeat sector. Measurements over the repeat sector at each site were repeated a number of times to increase the reliability of the results. In addition to determining the frequency dependence of ground clutter strength in various terrain types, this report determines dependencies of clutter strength with radar polarization and resolution and specifies long-term temporal variability of clutter strength with weather and season. The report includes descriptions of the clutter measurement equipment and measurement procedures, provides calibration results, and describes the resultant multifrequency ground clutter measurement data bases that are now maintained at Lincoln Laboratory.

14. SUBJECT TERMS				15. NUMBER OF PAGES
radar ground clutter	terrain reflectivity	land clutter	radar clutter	758
clutter measurements	low-angle	backscatter	electromagnetic propagation	16. PRICE CODE
clutter models	multifrequency	multipath		

17. SECURITY CLASSIFICATION OF REPORT	18. SECURITY CLASSIFICATION OF THIS PAGE	19. SECURITY CLASSIFICATION OF ABSTRACT	20. LIMITATION OF ABSTRACT
Unclassified	Unclassified	Unclassified	None